VNIVERSITAT DE VALÈNCIA

CSIC
CONSEJO SUPERIOR DE INVESTIGACIONES CIENTÍFICAS

DOCTORAT EN ENGINYERIA QUÍMICA, AMBIENTAL I DE PROCESSOS

REGULACIÓ | RD 1393 / 2007

CODI | 3132

TESI DOCTORAL

DESENVOLUPAMENT, CARACTERITZACIÓ, I MODELITZACIÓ DE NOUS MATERIALS POLIMÈRICS DESTINATS A L'ENVASAT ACTIU ALIMENTARI

AUTOR | Josep Pasqual Cerisuelo i Ferriols

DIRECTORS | Dr. Rafael Gavara Clemente

| Dra. Pilar Hernández Muñoz

TUTOR | Dr. Vicent Orchillés Barbastre

CENTRE | Institut d'Agroquímica i Tecnologia d'Aliments

DATA | Juny de 2015

MINISTERIO
DE CIENCIA
E INNOVACIÓN

CSIC
CONSEJO SUPERIOR DE INVESTIGACIONES CIENTÍFICAS

Dr. Rafael Gavara Clemente, Professor d'Investigació de l'Institut d'Agroquímica i Tecnologia d'Aliments del Consell Superior d'Investigacions Científiques, i

Dra. Pilar Hernández Muñoz, Científica Titular de l'Institut d'Agroquímica i Tecnologia d'Aliments del Consell Superior d'Investigacions Científiques,

CERTIFIQUEN:

Que **En Josep Pasqual Cerisuelo i Ferriols**, titulat en Enginyeria Química, ha desenvolupat sota la seva direcció a l'Institut d'Agroquímica i Tecnologia d'Aliments (IATA – CSIC) el treball que, amb el títol de: **"Desenvolupament, caracterització, i modelització de nous materials polimèrics destinats a l'envasat actiu alimentari"**, presenta aquesta memòria i que constitueix la seva tesi per a optar al títol de Doctor per la Universitat de València.

I per a que conste als efectes oportuns signen el present certificat a Paterna, el ____ de _____ de 2015.

Signat: Dr. Rafael Gavara Clemente

Signat: Dra. Pilar Hernández Muñoz

AGRAÏMENTS

Vull expressar el meu agraïment als meus directors de tesi, Rafael Gavara i Pilar Hernández, per haver-me animat a emprendre aquest difícil projecte i, en especial, per la seva ajuda i dedicació durant tot el seu desenvolupament. D'igual manera, agraïsc a Ramon Català el vast coneixement que m'ha transmès, no només científic, així com el temps que ha dedicat a l'acurada revisió d'aquest treball. En general, vull agrair a tots tres el seu constant suport, atenció, paciència, i generositat, tant per haver-me donat la oportunitat de formar part del seu equip, com per haver-me reiterat la seva confiança en aquests darrers anys.

També vull donar les gràcies a tots aquells que m'han acompanyat cada dia al laboratori en aquest llarg període i m'han ofert sempre la seva ajuda quan l'he necessitada. Gràcies a tots ells per la seva bona disposició, voluntat i amistat en tot aquest temps.

Gràcies a tots els estudiants de pràctiques, projectes, o Màster, que han participat o col·laborat activament en aquest treball, i, en general, a tots aquells qui d'una manera o d'una altra, però sempre constructivament, han contribuït a que la present tesi doctoral, i els articles que la componen, hagen esdevingut una realitat.

Gràcies, per últim, a la meva familia i, en especial, a la meva dona, per la seva permanent estima, ajuda, i comprensió en aquesta perllongada etapa que ara es clou.

RESUM

Aquesta tesi tracta del desenvolupament, caracterització, i modelització de nous materials polimèrics destinats a l'envasat actiu alimentari amb capacitat per a exercir una efectiva acció antimicrobiana sobre el producte conservat. Aquests materials es componen fonamentalment de copolímers d'etilè i alcohol vinílic (EVOH) amb carvacrol, citral, o altres olis essencials, com a agents antimicrobians d'origen natural, que, bé en forma de pel·lícules autosostenibles, bé com a recobriments sobre altres polímers convencionals, com polipropilè (PP) o tereftalat de polietilè (PET), permeten l'alliberament dels seus ingredients actius vers l'aliment envasat quan la humitat ambiental generada per aquest és capaç de modificar-los substancialment les característiques barrera. Aquesta relació entre les propietats actives dels nous materials i les condicions ambientals a què es troben sotmesos ha estat estudiada al present treball mitjançant el mesurament dels coeficients de difusió i solubilitat dels esmentats agents a la seva matriu en funció de la temperatura i la humitat relativa. En paral·lel a aquests estudis, s'ha efectuat també una completa caracterització funcional dels nous materials, mitjançant la determinació de les seves principals propietats morfològiques, mecàniques, tèrmiques, òptiques, superficials, i barrera, per tal d'avaluar-ne la possible alteració o deteriorament per causa de les potencials interaccions fisicoquímiques entre els compostos incorporats i llurs matrius portadores.

Amb aquests nous materials s'han construït envasos actius per a la conservació de peix fresc i de productes vegetals mínimament processats, dissenyats per a alliberar els anteriors agents antimicrobians a l'espai de cap en una concentració suficient com per a inhibir el creixement de microorganismes patògens o alterants dels aliments sobre la seva superfície. No obstant això, també s'evidencià al treball que l'activitat exercida per aquests envasos tan sols resultava efectiva durant els tres primers o darrers dies del seu emmagatzemament, en funció de l'emplaçament específic de la seva capa activa dins de l'estructura multicapa característica de les pel·lícules constituents. Per aquest motiu, la present tesi abordà seguidament el potencial millorament del seu rendiment antimicrobià a través de dos enfocaments o estratègies diferents. D'una banda, es desenvoluparen models matemàtics d'ambdós envasos, basats en el mètode dels elements finits (FEM), per tal d'esbrinar, a través de simulacions computacionals, els diversos paràmetres estructurals i / o condicions ambientals que regien en major mesura el seu funcionament, i trobar així, en darrer terme, els camins existents vers la seva optimització. D'una altra, s'introduïren dues noves modificacions químiques i / o estructurals a la matriu del material portador a fi d'augmentar la seva capacitat de retenció per l'agent actiu i controlar en major mesura el seu alliberament. Aquestes consistiren en la incorporació de nanopartícules de bentonita a la matriu polimèrica com a càrrega inorgànica, i en la seva substitució per altres copolímers d'etilè de diferent polaritat en forma de dispersions aquoses (làtex). La millora assolida en el rendiment antimicrobià de l'anterior polímer amb les esmentades modificacions químico-estructurals de la seva matriu s'avaluà de forma experimental amb nous mesuraments de les seves propietats actives i funcionals, si bé, en el cas concret de la incorporació de bentonita, es desenvolupà també un nou model matemàtic per tal d'estimar-la teòricament i poder comparar així els resultats obtinguts per mitjà d'ambdues metodologies.

ABSTRACT

This dissertation deals with the development, characterization, and modelling of new polymeric materials intended for active food packaging applications capable of exerting effective antimicrobial action on the preserved product. These materials are essentially composed of ethylene – vinyl alcohol copolymers (EVOH) with carvacrol, citral or other essential oils functioning as natural antimicrobial agents, which allow the release of their active ingredients towards the packaged foodstuffs when the ambient humidity generated by them is able to substantially modify their barrier characteristics. They are either in the form of stand-alone films or as coatings over other conventional polymers, such as polypropylene (PP) or polyethylene terephthalate (PET). The relation between the active properties of the new materials and the ambient conditions to which they are subjected has been studied in the present work through the measurement of the diffusion and solubility coefficients of the mentioned agents, which were studied in their matrix as a function of the temperature and the relative humidity. In parallel to these studies, a complete functional characterization of the new materials has also been carried out through the determination of their main morphological, mechanical, thermal, optical, surface, and barrier properties in order to evaluate their possible alteration or deterioration due to the potential physicochemical interactions between the incorporated compounds and their carrier matrices.

These new materials were employed in the construction of active packages for the preservation of fresh fish and minimally processed vegetables, designed to release the antimicrobial agents into the headspace in sufficient concentration so as to inhibit the growth of pathogens or food altering microorganisms on their surface. However, it also became evident that the activity exerted by these packages was only effective during the three first or last days of their storage, as a function of the specific location of the active layer within the multilayer structure characteristic of the constituent films. For this reason, the present dissertation subsequently addressed the potential improvement of their antimicrobial performance through two different approaches or strategies. On the one hand, mathematical models of both packages, based on the finite element method (FEM), were developed with the aim of revealing the diverse structural parameters and / or ambient conditions that mostly governed their behavior through computational simulations, and thus ultimately find the existing ways towards their optimization. On the other hand, two new chemical and / or structural modifications were introduced in the matrix of the carrier material with the aim of increasing its retention capacity for the active agent and of further controlling its release. This consisted of the incorporation of bentonite nanoparticles into the polymeric matrix as inorganic loading, and its substitution by other ethylene copolymers of different polarity in the form of aqueous dispersions (latex). The improvement attained in the antimicrobial performance of such a polymer, after these chemo-structural modifications of its matrix, was experimentally evaluated with new measurements of its active and functional properties. In the particular case of bentonite incorporation however, a new mathematical model was also developed in order to theoretically estimate it and thus compare the results found through both methodologies.

RESUMEN

Esta tesis trata del desarrollo, caracterización, y modelización de nuevos materiales poliméricos destinados al envasado activo alimentario con capacidad para ejercer una efectiva acción antimicrobiana sobre el producto conservado. Estos materiales se componen básicamente de copolímeros de etileno y alcohol vinílico (EVOH) con carvacrol, citral, u otros aceites esenciales, como agentes antimicrobianos de origen natural, que, bien en forma de películas autosustentables, bien como recubrimientos sobre otros polímeros convencionales, como polipropileno (PP) o tereftalato de polietileno (PET), permiten la liberación de sus ingredientes activos hacia el alimento envasado cuando la humedad ambiental generada por éste es capaz de modificarles sustancialmente las características barrera. Esta relación entre las propiedades activas de los nuevos materiales y las condiciones ambientales a las que se encuentran sometidos se ha estudiado en el presente trabajo mediante la medición de los coeficientes de difusión y solubilidad de los mencionados agentes en su matriz en función de la temperatura y la humedad relativa. En paralelo a estos estudios, se ha efectuado también una completa caracterización funcional de los nuevos materiales, mediante la determinación de sus principales propiedades morfológicas, mecánicas, térmicas, ópticas, superficiales, y barrera, para evaluar su posible alteración o deterioro por causa de las potenciales interacciones fisicoquímicas entre los compuestos incorporados y sus matrices portadoras.

Con estos nuevos materiales se han construido envases activos para la conservación de pescado fresco y de productos vegetales mínimamente procesados, diseñados para liberar los anteriores agentes antimicrobianos al espacio de cabeza en una concentración suficiente como para inhibir el crecimiento de microorganismos patógenos o alterantes de los alimentos sobre su superficie. No obstante, también se evidenció en el trabajo que la actividad ejercida por estos envases tan sólo resultaba efectiva durante los tres primeros o últimos días de su almacenamiento, en función del emplazamiento específico de su capa activa dentro de la estructura multicapa característica de las películas constituyentes. Por este motivo, la presente tesis abordó seguidamente la potencial mejora de su rendimiento antimicrobiano a través de dos enfoques o estrategias diferentes. Por un lado, se desarrollaron modelos matemáticos de ambos envases, basados en el método de los elementos finitos (FEM), para averiguar, a través de simulaciones computacionales, los diversos parámetros estructurales y / o condiciones ambientales que regían en mayor medida su funcionamiento, y encontrar así, en último término, los caminos existentes hacia su optimización. Por otro lado, se introdujeron dos nuevas modificaciones químicas y / o estructurales en la matriz del material portador con el fin de aumentar su capacidad de retención por el agente activo y controlar en mayor medida su liberación. Éstas consistieron en la incorporación de nanopartículas de bentonita en la matriz polimérica como carga inorgánica, y en su sustitución por otros copolímeros de etileno de diferente polaridad en forma de dispersiones acuosas (látex). La mejora alcanzada en el rendimiento antimicrobiano del anterior polímero con las mencionadas modificaciones químico-estructurales de su matriz se evaluó de forma experimental con nuevas mediciones de sus propiedades activas y funcionales, si bien, en el caso concreto de la incorporación de bentonita, se desarrolló también un nuevo modelo matemático para estimarla teóricamente y poder comparar así los resultados obtenidos mediante ambas metodologías.

CONTINGUTS

1. INTRODUCCIÓ

Des del desenvolupament de l'agricultura i la ramaderia al neolític, els éssers humans han cercat sempre la manera de conservar i transportar l'excedent d'aliments que obtenien en les èpoques de collita i cria. Al llarg de la història, tècniques com l'assecatge, el fumatge, el confitat, la fermentació, o la salaó, han garantit la preservació de la salubritat dels aliments durant el temps suficient per a permetre el seu consum en les èpoques de major escassedat. No obstant això, aquestes tècniques més tradicionals no permetien la correcta conservació de tots els tipus d'aliments, i sovint comportaven una dràstica transformació en la seva aparença, textura, i propietats organolèptiques, a banda de la inevitable pèrdua o alteració d'algunes de les seues principals propietats nutritives. Tots aquests desavantatges van motivar el desenvolupament de noves tècniques de conservació que permeteren allargar la vida útil dels aliments sense comprometre en gran mesura el seu aspecte o característiques originals. Per això, al segle XIX, amb el començament de la revolució industrial, tècniques com la refrigeració, o la pasteurització, van proporcionar a les societats desenvolupades unes noves i millorades formes de preservació dels productes frescos o ja processats, establint, al mateix temps, les bases necessàries per a la futura concepció dels actuals envasos moderns, peça fonamental de quasi tots els sistemes de conservació d'aliments emprats a l'actualitat (Barbosa – Cánovas i Juliano, 2005).

Des de la seva invenció, i fins a l'actualitat, els envasos han representat sempre el punt de trobada entre els interessos dels consumidors i els de les empreses alimentàries. Els motius es troben a doble banda: per un costat, els d'una societat consumidora que es troba cada dia més preocupada per la qualitat i seguretat dels aliments que ingereix, demanant productes més frescos, naturals i saludables, conservats en envasos més segurs, pràctics i ecològics; per un altre, els d'unes companyies distribuïdores que cerquen contínuament la diferenciació dels seus productes i l'allargament de la seva vida útil, per poder aplegar a més i més llunyans consumidors, abaratir els costos, i oferir així millors productes en un món cada cop més competitiu i globalitzat. Aquest creixent interès mostrat per uns i altres fa possible que cada dia es vessen abundants recursos humans i materials per tractar de millorar contínuament les tecnologies d'envasat existents, basades totes en el concepte d'envàs tradicional o passiu (Gerding et al., 1996; Ahvenainen i Hurme, 1997; Fernández, 2000; Lee et al., 2008). Aquest, pot definir-se com aquell recipient o embolcall dissenyat per presentar, contenir, manipular, i distribuir un aliment (Català i Gavara, 2005), protegint-lo al mateix temps de les agressions físiques, químiques, o biològiques derivades de l'ambient que l'envolta, en actuar com una barrera passiva a qualsevol interacció que en puga provenir (llum, gasos, microorganismes, etc.) (Robertson, 1993). Per tant, en el concepte tradicional d'envàs, aquest s'encarrega de protegir el seu contingut tot evitant o retardant

els efectes suposadament adversos que li causarien les interaccions amb l'entorn, i amb una incidència mínima sobre les propietats del producte envasat, garantint així la seva seguretat i qualitat (Català i Gavara, 2001b).

1.1. Envasos actius

Tanmateix, d'unes dècades ençà estan sorgint noves tecnologies de conservació d'aliments basades precisament en la potenciació o aprofitament d'aquestes possibles interaccions entre l'envàs i el producte, i/o el medi ambient (Català i Gavara, 2001b), en les quals l'envàs deixa d'exercir únicament el paper de contenidor passiu del producte envasat per involucrar-se activament en el manteniment o millora de les seves condicions de conservació (Rooney, 1997; López-Rubio et al., 2004). Aquest nou concepte, conegut amb el nom d'"envasat actiu", sol definir-se com aquella tècnica que promou algun tipus d'interacció favorable entre l'envàs i el producte envasat amb l'objectiu de mantenir o millorar la seva qualitat i acceptabilitat (Fernández, 2000). Per la seva banda, l'"envàs actiu" es defineix com aquell sistema aliment/envàs/entorn que funciona de forma coordinada per millorar la salubritat i la qualitat de l'aliment envasat, augmentant així la seva vida útil (Català i Gavara, 2001b; Suppakul et al., 2003) en exercir una protecció activa front als agents responsables de la seva alteració, ja siguen físics, químics, enzimàtics o microbiològics (Fernández, 2000). En aquest sentit, l'envàs actiu és capaç de corregir les deficiències del sistema de conservació actuant en diversos àmbits, com ara en la composició de l'atmosfera interior, mitjançant l'ús de materials permselectius o amb la presència de substàncies que emeten o retenen gasos i vapors, o bé en el propi aliment, modificant la seva composició i/o característiques en alliberar substàncies d'acció positiva o en absorbir compostos indesitjables (López-Rubio et al., 2004).

Totes aquestes interaccions beneficioses creades entre l'aliment i l'envàs solen basar-se en diferents tipus de mecanismes per assolir el seu objectiu, com són: l'alliberament o absorció de gasos (ço és: oxigen, diòxid de carboni, etilè, etc.) per regular-ne el contingut a l'espai de cap de l'envàs, el control de la humitat relativa (mitjançant additius antibaf, absorbents, etc.), l'acció de diferents enzims (com els emprats en el control del colesterol o la lactosa), l'alliberament d'aromatitzants, edulcorants, colorants, nutrients, substàncies antioxidants o antimicrobianes (com ara: etanol, diòxid de sofre, diòxid de clor, àcids orgànics, agents quelants, fungicides, pèptids, enzims, bacteriocines, extractes naturals, etc.), o l'absorció d'aromes indesitjables o, fins i tot, de llum ambiental (Vermeiren et al., 1999; Suppakul et al., 2003; López-Rubio et al., 2004; Ozdemir i Floros, 2004). Així doncs, a diferència

del concepte tradicional d'envàs on els únics canvis observats en el sistema sorgien necessàriament de l'evolució natural del producte, amb el nou concepte d'envàs actiu l'aliment es troba en un entorn modificat expressament per al seu benefici, a través de canvis induïts amb l'ajuda del seu embolcall (Rooney, 1995).

Les tecnologies d'envasat actiu han experimentat una evolució i un creixement molt notables en les dues darreres dècades, tant pel què fa a la investigació i desenvolupament de nous envasos com a la seva producció industrial i comercialització (Restuccia et al., 2010). De fet, a dia d'avui ja són molts i molt diversos els usos comercials de què disposen: absorció d'oxigen a l'envasament de pastes, formatges, fruits secs o productes carnis, control del diòxid de carboni o l'etilè a l'envasat en atmosfera modificada de fruites i hortalisses, control de la humitat en carn o productes vegetals frescos, etc. Aquest ràpid avenç en aquestes noves tecnologies ha estat possible gràcies a la proliferació de materials polimèrics en el disseny fonamental dels nous envasos, atesos els seus grans avantatges respecte als materials convencionals en tant que matrius portadores de substàncies actives (López-Rubio et al., 2004; Singh et al., 2011). No obstant això, el principi de funcionament dels envasos actius no es basa únicament en la introducció de substàncies específiques al si d'una matriu polimèrica, sinó també en les propietats intrínseques del propi polímer emprat com a material d'envàs, ja que aquestes condicionen en gran mesura la forma en què s'ha d'incorporar el compost d'interès (Gontard, 2000).

En efecte, l'agent actiu pot incorporar-se a l'interior del material polimèric o ancorar-se en la seva superfície, o bé introduir-se en estructures multicapa o, fins i tot, en elements individuals associats a l'envàs, com ara bosses, sobres, làmines o etiquetes (Rooney, 1995; Fernández, 2000). Precisament, als primers desenvolupaments d'aquesta tecnologia el citat compost s'hi introduïa contingut en unes bossetes d'un material especial que posseïa una elevada resistència mecànica a l'esquinçament manual, així com una permeabilitat adequada per tal de permetre la lliure actuació del compost actiu, tot impedint, al mateix temps, cap contacte directe amb l'aliment conservat (**Figura 1**). La inserció als envasos d'aquestes xicotetes bosses o sobres contenint el principi actiu constitueix encara el sistema més desenvolupat i utilitzat a l'actualitat (Fernández, 2000; Català i Gavara, 2001b). Darrerament, però, com alternativa a l'ús d'aquests elements, s'estan desenvolupant altres materials d'envasat que ja contenen l'agent actiu integrat a la seva estructura. Els avantatges d'aquesta innovadora tècnica resideixen en la reducció de la mida de l'envàs, la simplificació del procés d'envasat, l'augment de l'efectivitat de la substància activa per la millora del contacte físic amb el producte envasat, la possibilitat d'envasar aliments en fase líquida, i l'obtenció d'envasos d'aparença tradicional, sense la presència d'elements estranys al voltant de l'aliment que puguen ser mal vistos o mal interpretats als

ulls del consumidor, evitant així possibles reticències o confusions per la seva part, com podria ser una ingestió accidental de l'ingredient actiu (López-Rubio et al., 2004). A més a més, atesa la creixent preocupació per part dels consumidors per l'elevada presència d'additius als aliments envasats, resulta molt interessant el desenvolupament d'aquesta tècnica, ja que hi facilita un alliberament gradual dels agents actius, reduint així el seu contingut en el propi aliment (Rooney, 1995). Per tots aquests motius, un dels principals objectius que es proposa assolir la present tesi doctoral és precisament el desenvolupament de nous materials polimèrics destinats a l'envasat actiu alimentari que exhibisquen una efectiva activitat antimicrobiana sobre el producte conservat mitjançant la incorporació de diverses substàncies actives d'origen natural a l'interior de llur matriu polimèrica.

Figura 1. Envasos actius proveïts de sobres permeables farcits amb un absorbidor d'oxigen.

1.1.1. Envasos antimicrobians

D'entre l'ampli ventall de tecnologies d'envasat actiu existents a l'actualitat l'envasat antimicrobià és probablement la més prometedora i innovadora de totes (Floros et al., 1997; Vermeiren et al., 1999). En efecte, la recerca i desenvolupament en aquesta àrea ha experimentat un creixement molt significatiu en les darreres dècades (Collins-Thompson i Hwang, 2000; Cooksey, 2001; Joerger, 2007), degut sobretot al fet d'ésser considerada, tant per part dels productors, com de la industria alimentària, o dels organismes governamentals, com una eina molt valuosa en la lluita front a la majoria d'amenaces potencials vers la seguretat dels aliments, com poden ser les malalties de transmissió alimentària (toxiinfeccions alimentàries), el deteriorament natural dels productes frescos, o la seva adulteració maliciosa, al temps que és capaç de mantenir els creixents estàndards de qualitat i conveniència exigits pels consumidors (Han, 2013). Aquestes qualitats resulten, a més, d'especial

rellevància i interès per al cas de la preservació de productes frescos, mínimament processats, sense additius o conservants, o ja preparats per a menjar (Appendini i Hotchkiss, 2002; Gavara et al., 2009), la demanda dels quals es troba actualment en constant creixement als mercats del món occidental (Collins-Thompson i Hwang, 2000).

A l'igual que la resta d'envasos actius, els envasos antimicrobians tenen per objectiu l'extensió de la vida útil de l'aliment envasat, actuant, en aquest cas, contra els microorganismes patògens o alterants (tals com bacteris, fongs, o llevats) presents originalment en la superfície dels aliments conservats o dels propis materials d'envasat, mitjançant l'endarreriment, la reducció, o la inhibició del seu creixement (Appendini i Hotchkiss, 2002). En concret, el seu mecanisme d'acció es basa en la limitació o impediment de la seva proliferació mitjançant el perllongament de la seva fase de latència, la reducció de la seva taxa de creixement, i / o la reducció dels seus recomptes microbiològics (Han, 2000; Marcos et al., 2007). Aquesta activitat antimicrobiana exercida pels envasos és desenvolupada de forma diferent segons la naturalesa química de l'agent actiu incorporat i la seva disposició física en el material portador, donant lloc així a diferents sistemes d'envasat antimicrobià caracteritzats fonamentalment pel seu disseny estructural i mode de funcionament (Vermeiren et al., 2002; Han, 2013). Segons això, l'ingredient actiu pot trobar-se, bé integrat a l'estructura interna dels materials que conformen l'envàs, bé ancorat, adsorbit, o recobrint la seva superfície, o bé, en el cas d'un compost volàtil, contingut dins d'elements independents de l'envàs, com les xicotetes bosses, sobres, làmines, o etiquetes esmentades a la secció anterior (Cooksey, 2001; Appendini i Hotchkiss, 2002; Suppakul et al., 2003; Han, 2013). A més a més, també existeix la possibilitat de conformar l'envàs a partir de polímers inherentment antimicrobians (Appendini i Hotchkiss, 2002), o, fins i tot, de substituir-lo per un recobriment comestible aplicat directament sobre l'aliment conservat i constituït per un biopolímer antimicrobià (Cuq et al., 1995; Cha i Chinnan, 2004).

Com que la major part de la contaminació i creixement microbians que malmeten els aliments envasats s'origina en la seva superfície, especialment en aquelles àrees en contacte amb l'envàs on sol formar-se una capa d'humitat entre ambdós, és en aquestes zones on es deu exercir principalment l'activitat antimicrobiana (Collins-Thompson i Hwang, 2000; Brody et al., 2001; Appendini i Hotchkiss, 2002). En aquest context, l'envasat antimicrobià constitueix una tecnologia molt avantatjosa en comparació amb altres tècniques més tradicionals, com són l'addició directa de conservants al cos dels aliments, o la seva impregnació superficial per polvorització o immersió, ja que no requereix la incorporació de grans quantitats de compost actiu a la matriu alimentària en no trobar-se afectat pels fenòmens de dilució o inactivació associats a la seva difusió cap a l'interior de l'aliment (Vermeiren et al., 2002; Appendini

i Hotchkiss, 2002; López-Rubio et al., 2004; Marcos et al., 2007). També per aquesta raó, d'entre tots els sistemes d'envasat antimicrobià desenvolupats fins al moment el més avantatjós és aquell que integra una substància volàtil en la matriu polimèrica de la seva pel·lícula o recobriment actiu, ja que és l'únic capaç de proporcionar una activitat uniforme i constant en tota la superfície de l'aliment sense requerir altes concentracions de l'agent actiu, ni tan sols el seu contacte directe amb el producte envasat. Aquesta major efectivitat és possible gràcies a la seva capacitat per a alliberar el compost antimicrobià a un ritme lent i constant, permetent així una activitat contínua sobre la membrana cel·lular dels microorganismes, bé directament a través de la pròpia fase vapor, o bé indirectament mitjançant la seva prèvia sorció i concentració en la superfície de l'aliment, al temps que evita també possibles problemes organolèptics o elevats costos d'implementació (Cooksey, 2001; Appendini i Hotchkiss, 2002; Han, 2013).

En aquest darrer cas, l'eficiència de l'envàs es troba estretament relacionada amb el balanç entre la velocitat d'alliberament de l'agent actiu des del material portador a l'espai de cap de l'envàs, l'abast de la seva sorció a la matriu alimentària, la velocitat de la seva difusió a través d'aquesta, i la cinètica del creixement microbià. Al seu torn, el primer paràmetre és funció, entre d'altres, de la naturalesa d'ambdues substàncies involucrades i de les interaccions existents entre elles (Han, 2013). Per aquest motiu, cal que el compost antimicrobià seleccionat siga compatible amb el material portador i no interactue amb ell, especialment durant l'etapa de formació de l'envàs, on les altes pressions i temperatures poden facilitar-ne la degradació o la reacció química (Suppakul et al., 2003). D'aquesta manera, les molècules de l'agent actiu queden simplement atrapades en els espais existents entre les cadenes polimèriques i no interfereixen ni creen lligams amb elles que puguen dificultar la seva migració a través de l'estructura interna del material o, fins i tot, malmetre-li les propietats funcionals, ço és, les mecàniques, tèrmiques, òptiques, superficials o barrera (Cooksey, 2001; Han, 2013).

Pel què fa a la naturalesa química de l'agent antimicrobià, els compostos més utilitzats fins al moment en la recerca i desenvolupament de nous envasos actius per a aliments són: àcids, sals i anhídrids orgànics, sulfits, nitrats, alcohols, metalls, enzims, pèptids, bacteriocines, polisacàrids, antibiòtics, antioxidants, agents quelants, gasos desinfectants, i extractes naturals de plantes (Suppakul et al., 2003; Cha i Chinnan, 2004; Joerger, 2007; Han, 2013). La selecció del compost concret a incorporar deu efectuar-se segons diversos criteris, fonamentalment, atenent al seu espectre d'activitat i mecanisme d'acció, a la composició fisicoquímica de l'aliment conservat, i a l'índex de creixement o estat fisiològic de la població microbiana que es pretén combatre (Appendini i Hotchkiss, 2002). No obstant això, en aquesta selecció també s'han de considerar altres factors importants, com són la

compatibilitat química i sensorial del compost actiu amb el producte envasat, la seva seguretat i estabilitat en el sistema de conservació elegit, i la seva relació cost - efectivitat (Wagner i Moberg, 1989). Ara bé, cal tenir també en compte que totes aquelles substàncies antimicrobianes d'origen no natural que puguen constituir migrants potencials vers l'aliment envasat prenen la consideració legal d'additius alimentaris (Reglament (CE) 450/2009 de la Comissió de les Comunitats Europees), per la qual cosa la seva utilització deu complir en tot moment la legislació vigent (Reial Decret 142/2002).

1.1.1.1. Agents antimicrobians d'origen natural

Les noves demandes de la societat envers productes més frescos, naturals i saludables, unides a la seva creixent preocupació per la presència d'additius artificials als aliments envasats, i a l'estricta regulació legal que comporten aquests, està esperonant els investigadors cap al desenvolupament de nous envasos antimicrobians basats en substàncies actives d'origen natural, com poden ser els extractes vegetals i, en especial, els olis essencials d'espècies o herbes aromàtiques i els seus compostos constituents (Tuley de Silva, 1996; Collins-Thompson i Hwang, 2000; Smid i Gorris, 2007; Tyagi et al., 2012). Certament, la procedència natural d'aquestes substàncies, i el fet que durant segles hagen estat emprades per la medicina popular per a la curació de malalties infeccioses o el tractament dels seus símptomes (Ríos et al., 1987; Burt, 2004), fa que actualment siguen percebudes pels consumidors com a ingredients totalment acceptables de la composició dels aliments, i, per tant, suficientment segurs com per a ser-hi incorporats deliberadament (Suppakul et al., 2003; Holley i Patel, 2005; Sadaka et al., 2014). Com a conseqüència, el seu ús hegemònic i tradicional en farmacologia i cosmètica, per les seves propietats fragants i funcionals, està essent desplaçat als darrers temps per un consum creixent en la indústria alimentària (Burt, 2004), on, a dia d'avui, ja gaudeixen d'un important reconeixement legal, tant per part de la EFSA (European Food Safety Authority), en tant que aromatitzants alimentaris, com per la US FDA (United States Food and Drug Administration), en tant que substàncies GRAS (Generally Recognized As Safe) (Suppakul et al., 2003).

1.1.1.1.1. Olis essencials

Els olis essencials d'origen vegetal són líquids aromàtics d'aparença oleaginosa que poden obtenir-se de matèria vegetal diversa, tal com plantes herbàcies (herbes) o llenyoses (productores d'espècies) (Burt, 2004) generalment procedents de països càlids o temperats, com els tropicals o mediterranis, on representen una part molt important de la farmacopea tradicional (Bakkali et al., 2008). L'obtenció de l'oli essencial pot realitzar-se partint de qualsevol part de la planta, ço és: arrels, fusta, branques, tiges, capolls, flors, fruites i llavors (Burt, 2004), mitjançant l'aplicació de diferents tècniques d'extracció, com poden ser la destil·lació al vapor o fraccionada, l'enfloratge, la maceració o enfloratge en calent, l'espressió o premsat en fred, la fermentació, la percolació, l'extracció per dissolvents, per fluids supercrítics, o assistida per microones, i el procés fitònic (Tuley de Silva, 1996; Sadaka et al., 2014), essent la primera la més utilitzada a nivell comercial (Van de Braak i Leijten, 1999; Burt, 2004; Bakkali et al., 2008). La substància resultant d'aquests processos de separació consisteix en una mescla molt complexa i variable que pot incloure fins a diversos centenars de compostos químics diferents (Burt, 2004; Sadaka et al., 2014), els quals solen pertànyer fonamentalment a dos grups químics caracteritzats pels seus diferents orígens biogenètics: el grup dels terpens i terpenoides, d'una banda, i el dels alifàtics i aromàtics derivats del fenilpropà, d'una altra (Bruneton, 2001; Bakkali et al., 2008). El primer grup inclou majoritàriament monoterpens (C_{10}) i sesquiterpens (C_{15}), encara que els diterpens (C_{20}) també poden ser-hi presents en quantitats apreciables. El segon, en canvi, inclou una gran varietat d'hidrocarburs alifàtics de baixa massa molecular (lineals, ramificats, saturats o insaturats), àcids, alcohols, aldehids, esters acíclics, lactones, i també, excepcionalment, compostos sulfurats o nitrogenats, cumarines i altres homòlegs dels fenilpropanoides (Dorman i Deans, 2000).

Tot i aquesta àmplia diversitat, els olis essencials solen caracteritzar-se pels seus dos o tres compostos més abundants, presents en concentracions relativament altes, d'entre el 20 i el 70 % (Bakkali et al., 2008), per bé que, en alguns casos, poden arribar a constituir fins el 85 % de la seva massa total (Burt, 2004). En canvi, d'altres compostos menors poden trobar-se desenes, o, fins i tot, centenars, presents únicament en forma de traces (Burt, 2004; Bakkali et al., 2008; Sadaka et al., 2014). Addicionalment, els olis essencials també poden contenir diversos components menors que són producte dels processos de degradació que afecten als compostos constituents de menor volatilitat (Bruneton, 2001). En qualsevol cas, la composició química final de l'oli essencial obtingut, així com la seva puresa, pot variar qualitativa i quantitativament en funció de la part de la planta utilitzada, de la seva subespècie, de l'edat o estadi del cicle vegetatiu en què es troba, del lloc geogràfic de cultiu i el seu biòtop (clima, composició del sol, etc.), de l'estació de cultiu o de collita, i del mètode d'extracció elegit

(Bakkali et al., 2008; Kuorwel et al., 2011; Sadaka et al., 2014), i és aquesta, al seu temps, la que li confereix les principals propietats organolèptiques, físiques, i funcionals (Burt, 2004).

Respecte a llurs propietats físiques, la majoria d'olis essencials són líquids a temperatura ambient i mostren una densitat inferior a la de l'aigua (Bruneton, 2001). També solen presentar una alta volatilitat (Tyagi et al., 2012), que és la responsable del seu accentuat aroma (Bakkali et al., 2008) i, en general, de les seves principals característiques organolèptiques (Burt, 2004) i microbiològiques (Kuorwel et al., 2011). A més a més, també són liposolubles, pel que es dissolen bé en els dissolvents orgànics habituals (Bruneton, 2001; Bakkali et al., 2008). Des del punt de vista òptic, solen ser transparents i poc colorits (Bakkali et al., 2008). No obstant això, solen presentar un índex de refracció elevat i la majoria d'ells desvien la llum polaritzada (Bruneton, 2001). Pel que fa a les propietats funcionals, molts olis essencials i els seus components principals han demostrat posseir altes capacitats antibacterianes, antifúngiques, antivíriques, antiparasitàries, insecticides, antimutagèniques i antioxidants (Burt, 2004; Bakkali et al., 2008; Sadaka et al., 2014). Totes aquestes propietats antisèptiques formen part de l'estratègia d'autodefensa d'algunes plantes, les quals sintetitzen els olis essencials com a metabolits secundaris, sia de forma constitutiva, sia a partir de precursors inactius com a resposta a una situació d'estrès, amb l'objectiu de fer front als organismes patògens que les afecten o, fins i tot, a l'atac d'algun herbívor (Holley i Patel, 2005). Al mateix temps, aquestes substàncies també poden jugar un paper important en el seu cicle reproductiu, en exercir un efecte d'atracció o repulsió selectiva sobre els insectes responsables de la disseminació del seu polen o de les seves llavors (Bakkali et al., 2008).

Malgrat que l'activitat antimicrobiana dels olis essencials és ben coneguda des de l'antiguitat (Bakkali et al., 2008; Sadaka et al., 2014), i ha estat àmpliament estudiada i demostrada als nostres temps front a un vast espectre de microorganismes patògens o alterants dels aliments, com són els bacteris Gram-positius o Gram-negatius, els fongs, i els llevats (Holley i Patel, 2005; Kuorwel et al., 2011), el seu mecanisme d'acció no ha pogut definir-se mai amb total claredat, i a dia d'avui encara requereix de major estudi (Burt, 2004; Han, 2013, Sadaka et al., 2014). No obstant això, existeix actualment un cert consens entre els investigadors sobre la relació d'aquesta activitat antimicrobiana amb la presència de compostos fenòlics a l'oli essencial, i amb llur lipofilicitat (Burt, 2004; Holley i Patel, 2005; Kuorwel et al., 2011) i volatilitat (Tyagi et al., 2012). Segons aquesta teoria, els esmentats compostos podrien atacar els microorganismes nocius provocant una disrupció de la membrana cel·lular, que conduiria a la seva expansió, a l'increment de la seva fluïdesa i permeabilitat, al deteriorament de les proteïnes que hi té integrades, a l'alteració dels processos de transport iònic, i a la inhibició de la respiració

cel·lular (Sadaka et al., 2014). Tanmateix, atesa la gran diversitat de compostos químics amb diferents grups funcionals que constitueixen els olis essencials, llur activitat antimicrobiana sol atribuir-se més bé a l'efecte de tot un rang de mecanismes diferents que actuen de forma sinèrgica (Burt, 2004; Bakkali et al., 2008), tals com la degradació de la paret cel·lular, la disrupció de la membrana citoplasmàtica, el deteriorament de les proteïnes de membrana o la inhibició de la seva síntesi, la fuita de components intracel·lulars (com ions o metabolits), la coagulació del citoplasma, l'alteració de la quimiosmosi (per col·lapse de la bomba de protons), l'exhauriment de les reserves d'ATP, i l'alteració de la síntesi d'ARN o ADN (Burt, 2004; Holley i Patel, 2005; Bakkali et al., 2008; Kuorwel et al., 2011; Sadaka et al., 2014).

En l'actualitat es coneixen més de 3 000 olis essencials diferents, dels quals només uns 300 gaudeixen d'una certa importància a nivell comercial, fonamentalment per les seves propietats funcionals i organolèptiques (Bakkali et al., 2008). Respecte a les propietats antimicrobianes, els olis que han demostrat posseir una major activitat o efectivitat són els de romer, timó, sajolida, orenga, alfàbega, sàlvia, clau, llorer, pebre de Jamaica, canyella, vainilla, gerani, citronella, all, ceba, rave i mostassa, tots ells d'elevat contingut en timol, carvacrol, eugenol, cinamaldehid i citral, així com en altres compostos fenòlics, terpènics, al·lílics i isotiocianats volàtils. La presència d'aquestes substàncies actives també s'ha detectat als olis de menta, herba-sana, majorana, anet, coriandre, comí, api, anís, sèsam, estragó, fenigrec, xili, gingebre, cardamom, càmfora, botja, pebre (blanc, negre o roig), nou moscada, oliva, ginebre, eucaliptus, arbre del té, pi i avet, si bé en concentracions més baixes i, per tant, amb capacitats antimicrobianes més limitades (Burt, 2004; Cha i Chinnan, 2004; Holley i Patel, 2005; Bakkali et al., 2008; Kuorwel et al., 2011; Sadaka et al., 2014).

1.1.1.1.2. Carvacrol

Es coneix pel nom tradicional de carvacrol, cimofenol, o isotimol, el compost químic anomenat sistemàticament: 2 – metil – 5 – (1 – metiletil) fenol o 5 – isopropil – 2 – metilfenol, segons la nomenclatura IUPAC, de fórmula empírica: $C_{10}H_{14}O$, massa molecular relativa: 150.21 g/mol, i que presenta l'estructura detallada a la **Figura 2** (ChemSpider; PubChem).

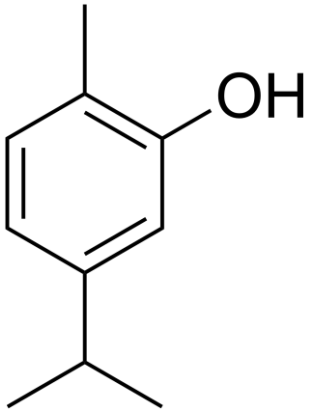

Figura 2. Estructura molecular del carvacrol.

Aquest compost es tracta d'un fenol monoterpenoide, biosintetitzat a partir del γ-terpinè, via el p-cimè (Nostro i Papalia, 2012), pels òrgans secretors de nombroses plantes aromàtiques autòctones del Mediterrani (Bakkali et al., 2008), junt amb la resta de constituents orgànics del seu oli essencial. De fet, el carvacrol sol representar el component principal d'aquest oli en diverses espècies vegetals de la família *Labiatae*, com ara les pertanyents als gèneres *Thymus*, *Satureja*, *Origanum*, *Thymbra* i *Corydothymus* (De Vincenzi et al., 2004; Nostro i Papalia, 2012). A manera d'exemple, s'han recollit a la **Taula 1** els intervals de concentració de carvacrol més habituals als olis essencials d'algunes espècies conegudes de plantes aromàtiques.

Taula 1. Presència del carvacrol en olis essencials de plantes aromàtiques.

Nom comú	Nom científic	Riquesa en carvacrol (%)
Timó, timonet, farigola	Thymus vulgaris	9 – 60
Timó blanc o capitat	Thymus capitatus	12.7 – 74.4
Timó negre, farigola de muntanya, serpoll	Thymus serpyllum	12.0 – 36.9
Timó roig o gràcil	Thymus zygis	4.8 – 25
Sajolida de jardí	Satureja hortensis	1.2 – 44.0
Sajolida de bosc o muntanya, herba d'olives	Satureja montana	30 – 40
Dictam o marduix de Creta	Origanum dictamnus	58.8 – 82.3
Marduix, amàrac, majorana	Origanum majorana	48.7
Orenga, marduix bord	Origanum vulgare	90

Font: De Vincenzi et al., 2004.

Des del punt de vista fisicoquímic, el carvacrol pren l'aparença, a temperatura ambient, d'un líquid oleaginós, dens, viscós i transparent, de color variable entre groguenc i rogenc pàl·lid, i olor càlid, especiat o medicinal, i pungent. D'altra banda, mostra una baixa volatilitat (T_B = 236 – 238 °C, p_v = 3 –

5 Pa), y una alta solubilitat en dissolvents orgànics habituals (Log $P_{o/w}$ = 3.64), com ara: alcohols, èters i cetones (ChemSpider; PubChem), si bé la presència del grup OH li confereix també una certa solubilitat en aigua (0.8 – 1.3 g/L) i, per tant, un lleuger caràcter amfifílic (Peltzer et al., 2009). A més a més, atès el seu origen natural i baixa toxicitat (LD_{50} = 810 mg/kg, oral en rates) ha estat aprovat per la US FDA (United States Food and Drug Administration) com a substància GRAS (Generally Recognized As Safe) i inclòs per la EFSA (European Food Safety Authority) en la llista d'aromatitzants químics alimentaris de categoria B, a l'igual que els olis essencials dels què procedeix, per la qual cosa està autoritzada la seva incorporació als aliments en concentracions d'entre 2 i 25 ppm, en funció del producte a envasar (De Vincenzi et al., 2004; Nostro i Papalia, 2012). Sota aquest context legal, el carvacrol ha estat emprant-se fins l'actualitat en la preparació de nombrosos productes alimentaris, com ara: sopes, salses, productes càrnics, condiments, begudes, gelats, caramels, púdings, gelatines, i articles de forn i sucreria (De Vincenzi et al., 2004; Chalier et al., 2007).

Pel que fa a les propietats funcionals i biològiques de la molècula, el carvacrol ha demostrat tenir capacitats antiinflamatòries, antioxidants, antitumorals, antimutagèniques, inhibitòries de l'acetilcolinesterasa, analgèsiques, antihepatotòxiques, antiparasítiques, insecticides, i antimicrobianes, tal i com han evidenciat nombrosos estudis als darrers anys (Davidson i Naidu, 2000; Nostro i Papalia, 2012). D'entre elles, la darrera és probablement la més rellevant, ja que és la que possibilita la seva aplicació com a conservant natural dels aliments envasats (Burt, 2004). En aquest sentit, el carvacrol ha demostrat la seva eficàcia contra un ampli espectre de microorganismes patògens i alterants dels aliments, com són els bacteris Gram-positius dels gèneres: *Bacillus*, *Carnobacterium*, *Enterococcus*, *Lactobacillus*, *Listeria*, *Pediococcus* o *Staphylococcus*, els bacteris Gram-negatius dels gèneres: *Enterobacter*, *Escherichia*, *Proteus*, *Pseudomonas*, *Salmonella*, *Shigella*, *Vibrio* o *Yersinia*, els fongs dels gèneres: *Alternaria*, *Aspergillus*, *Botrytis*, *Eurotium* o *Penicillium*, i els llevats dels gèneres: *Candida*, *Debaryomyces*, *Saccharomyces* o *Zygosaccharomyces*, incloent-hi espècies tan pernicioses com la *Candida albicans*, l'*Escherichia coli*, la *Listeria monocytogenes*, o l'*Staphylococcus aureus* (Davidson i Naidu, 2000; Chalier et al., 2007; Kuorwel et al., 2011; Nostro i Papalia, 2012).

Aquesta potent activitat antimicrobiana sol relacionar-se amb les característiques estructurals de la molècula, ço és, amb la presència simultània d'un grup hidroxil lliure, un sistema d'electrons deslocalitzat, i un fort caràcter hidrofòbic (Nostro i Papalia, 2012). No obstant això, i a l'igual que ocorre en la majoria de compostos antimicrobians d'origen natural, el seu mecanisme específic d'acció encara no es coneix completament (Chalier et al., 2007). Segons les darreres recerques, el carvacrol podria

exercir un efecte considerable sobre les propietats estructurals i funcionals de la membrana citoplasmàtica. Degut a la seva naturalesa hidrofòbica, interaccionaria amb la bicapa lipídica de la membrana, alineant-se entremig de les cadenes d'àcids grassos, i ocasionaria l'expansió i desestabilització de la seva estructura, tot incrementant la seva fluïdesa i permeabilitat en formar canals per al transport de ions, material cel·lular, àcid nucleic i ATP. Aquest darrer component, a més, seria també exhaurit seguint mecanismes paral·lels, com són la reducció de la seva síntesi o l'augment de la seva hidròlisi (Burt, 2004; Chalier et al., 2007; Nostro i Papalia, 2012).

1.1.2. Materials polimèrics d'envasat actiu

Els primers materials polimèrics foren ja desenvolupats a mitjan segle XIX, però no fou fins a principis del XX, amb la intensificació de la recerca sobre la seva naturalesa i propietats químiques, quan el seu nombre i diversitat experimentaren un major creixement. Gràcies a aquesta investigació fonamental, avui dia existeixen desenes de polímers sintètics diferents, d'estructura i característiques fisicoquímiques ben conegudes, que abasten una gran multitud d'aplicacions comercials, tot copsant els mercats dels principals productes. Una d'aquestes aplicacions és precisament l'envasat alimentari, on els avantatges intrínsecs dels materials polimèrics, units a la millora constant de llurs processos de fabricació, els han permès de desplaçar els materials tradicionals, com la fusta, el paper, la llauna, la ceràmica, o el vidre, de la seva hegemonia al sector fins a dècades recents. L'èxit i la idoneïtat d'aquests nous materials per a l'envasat d'aliments s'ha posat també de manifest amb altres fets similars, com ara, que tan bon punt foren descoberts, ja foren reeixidament provats com a substituents del paper encerat en bosses i embolcalls per a productes de forn (Hanle et al., 1966), o què la seva destinació final en l'esmentat mercat no haja deixat de créixer fins a l'actualitat, moment en que ja representa més d'una tercera part de la seva producció i consum global (WPO, 1998; Hernández et al., 2000).

Els motius d'aquesta progressiva migració de la indústria alimentària envers els materials polimèrics resideixen en les seves excel·lents característiques i propietats fisicoquímiques, ço és, la seva lleugeresa, bona termosoldabilitat, processabilitat i imprimibilitat, alta resistència tèrmica i química, excel·lents propietats mecàniques i òptiques, bona compatibilitat amb microones, gran versatilitat de formes i presentacions, baixos costos de fabricació i transformació, baix consum energètic durant el termoconformat, segellat, i transport dels envasos finals, possibilitat d'ésser incorporats en sistemes de producció integrats, etc. (Hernández et al., 2000; Català i Gavara, 2001b; López-Rubio et al., 2004). En general, la característica més apreciada d'aquests materials és la seva disponibilitat en un ampli

ventall de composicions químiques diferents, així com la seva notable capacitat per a combinar-se entre ells, i/o amb altres materials (com paper, cartró, o alumini) i additius sintètics (com colorants, estabilitzants, plastificants, etc.). D'aquesta manera, els polímers poden donar lloc a tota una nova gamma de materials amb composició i estructura variable, i, en conseqüència, amb propietats mecàniques, tèrmiques, òptiques, i barrera variables, les quals poden ser, a més a més, fàcilment modificades o regulades per tal d'ajustar-se exactament als requeriments específics del producte a envasar (Català i Gavara, 2001b; López-Rubio et al., 2004).

Com a conseqüència de tots aquests avantatges, i segons s'ha esmentat més amunt, l'ús de materials polimèrics per al disseny d'envasos alimentaris ha experimentat un fort creixement en les últimes dècades (Català i Gavara, 2005). En concret, han estat el polietilè (PE), el polipropilè (PP), el poliestirè (PS), el clorur de polivinil (PVC), el tereftalat de polietilè (PET), i el copolímer d'etilè i alcohol vinílic (EVOH) els polímers que han assolit una major implantació industrial i abast comercial als darrers temps. Així, per exemple, el polietilè ha estat molt utilitzat en la fabricació de bosses, ampolles, barquetes, recipients d'ús general, i pel·lícules d'embolcallar, degut fonamentalment al seu baix cost, però també a la seva alta hidrofobicitat, termosoldabilitat, tenacitat, i flexibilitat, fins i tot a temperatures de congelació. En canvi, el polipropilè ha demostrat la seva idoneïtat per a l'envasat en calent i la fabricació de contenidors i pel·lícules aptes per a microones, gràcies a la seva notable resistència mecànica, tèrmica, i química a altes temperatures, tot mantenint unes característiques òptiques i barrera millorades respecte al polietilè. Per la seva banda, el tereftalat de polietilè està esdevenint actualment el polímer d'elecció per a l'envasat general de nombrosos productes, en especial, d'aigües minerals i begudes carbonatades, degut a les seves excel·lents propietats mecàniques, òptiques, i barrera, així com a la seva considerable resistència tèrmica i química als àcids, dissolvents, i olis naturals. Finalment, el copolímer d'etilè i alcohol vinílic, component fonamental de quasi tots els materials actius desenvolupats en aquesta tesi doctoral, també està incrementant la seva presència en pel·lícules i làmines multicapa destinades a la fabricació d'envasos alimentaris amb capacitats d'alta barrera front a gasos permanents i compostos orgànics volàtils, com ara les bosses, sobres, barquetes o terrines destinades a contenir salses, condiments o menjars precuinats (Català i Gavara, 2005; Arora i Padua, 2010).

Malgrat tot, els materials polimèrics encara presenten algunes limitacions respecte a altres materials d'envasat més tradicionals, com són el vidre o la llauna, derivades de llurs interaccions fisicoquímiques en el sistema aliment / envàs / entorn. En efecte, els polímers no són totalment inerts, sinó que permeten el desenvolupament de determinats fenòmens de transferència de matèria entre llur matriu

i l'aliment o l'entorn, com ara el transport de gasos (oxigen, diòxid de carboni, etilè, etc.), de vapors (aigua, compostos aromàtics, etc.), i d'altres molècules de baixa massa molecular, els quals, al seu torn, poden manifestar-se al sistema d'envasat de tres formes diferents (Hernández i Gavara, 1999):

- Permeació: transferència de substàncies volàtils a través de la matriu polimèrica.
- Sorció: retenció a la matriu polimèrica de substàncies procedents de l'aliment envasat.
- Migració: alliberament a l'aliment envasat de substàncies procedents de la matriu polimèrica.

Tots aquests mecanismes de transferència de matèria són possibles gràcies a la particular estructura interna dels materials polimèrics, caracteritzada habitualment per la presència de nombroses zones amorfes formades per cabdells desordenats de cadenes polimèriques. Aquesta estructura permet a les molècules del polímer de configurar una extensa xarxa de buits, coneguda com a volum lliure, on poden accedir-hi i desplaçar-se les molècules d'altres compostos si són suficientment xicotetes. D'aquesta manera, el transport de massa a través del polímer es desenvolupa mitjançant una successió d'etapes de sorció i difusió, l'extensió i característiques de les quals es troben determinades per la naturalesa i composició del polímer, per les característiques del producte envasat i per les condicions ambientals del sistema (Hernández i Gavara, 1999; Lagaron et al., 2004).

Així doncs, i en conseqüència de tot l'anterior, la principal limitació dels polímers respecte a llur aplicació en l'envasat alimentari resideix en els importants canvis químics, nutricionals i sensorials que aquests poden infligir als aliments conservats per efecte dels esmentats fenòmens de transport, arribant fins i tot a comprometre llur seguretat i qualitat quan els materials escollits per a la construcció dels envasos no presenten les característiques d'interacció adequades (ço és: composició química, estructura interna, nivell d'additius, etc.) per a la particular naturalesa i propietats fisicoquímiques del producte a envasar (Català i Gavara, 2005). Tanmateix, totes aquestes interaccions també poden ser utilitzades positivament per a millorar la qualitat i perllongar la vida útil de l'aliment conservat, en la mesura que permeten el desenvolupament de noves tecnologies de conservació, com l'envasat en atmosfera modificada o l'envasat actiu, que es basen precisament en l'aprofitament de les inferiors i variables capacitats barrera d'aquests materials, les quals, a més a més, i segons s'ha esmentat adés, poden ser fàcilment modificades o regulades per tal d'ajustar-se exactament als requeriments específics del producte a envasar (Català i Gavara, 2001b; López-Rubio et al., 2004).

1.1.2.1. Copolímer d'etilè i alcohol vinílic (EVOH)

A l'hora d'afrontar el disseny d'un envàs actiu basat en l'ús de materials polimèrics per a la seva construcció resulta molt convenient la inclusió d'algun mecanisme que mantinga els materials inactius durant el seu procés de fabricació, transport, i emmagatzemament, així com durant les etapes de termoconformat, ompliment, i segellat dels envasos finals, però que permeta llur activació en el moment adient, ço és, a l'inici del període de conservació de l'aliment, per tal què es puga evitar efectivament l'exhauriment prematur, total o parcial, de l'activitat de l'envàs. Un dels materials polimèrics que, a banda de permetre la conformació d'envasos, és capaç també de desenvolupar aquesta funció és el copolímer d'etilè i alcohol vinílic (EVOH), que pot fer ús del seu fort comportament hidròfil per romandre inactiu fins el moment en què es requereix l'acció de l'agent que incorpora.

L'EVOH és un polímer semicristal·lí desenvolupat al Japó el 1970, obtingut mitjançant una hidròlisi controlada del copolímer d'etilè i acetat vinílic (EVA) per transformar el grup VA ~~(~~CH_2–$CHOC(CH_3)O$~~)~~ en VOH ~~(~~CH_2–$CHOH$~~)~~, donant lloc així a l'estructura molecular representada a la **Figura 3**. Aquest copolímer es caracteritza fonamentalment per la seva baixa permeabilitat als gasos permanents i compostos aromàtics, la seva elevada resistència tèrmica i química als olis i dissolvents orgànics, i les seves excel·lents propietats mecàniques i òptiques (Hernández et al., 2000), si bé l'accentuat comportament hidròfil que el caracteritza fa també que les seves propietats barrera resulten molt sensibles a la humitat ambiental (Aucejo et al., 1999 i 2000). A més a més, malgrat ser un material sintètic i procedent del petroli té l'avantatge de ser biocompatible i reciclable (Oyane et al., 2006).

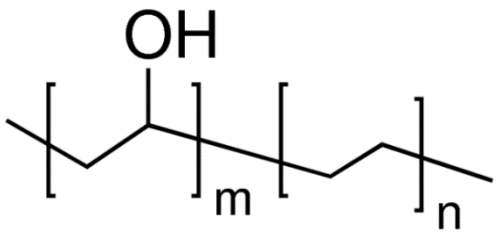

Figura 3. Estructura molecular del copolímer d'etilè i alcohol vinílic (EVOH).

En efecte, la incorporació de grups hidroxil a l'esquelet de carbonis del PE, en substitució d'un determinat nombre d'hidrògens, provoca una profunda modificació de les seves propietats fisicoquímiques. Per un costat, l'elevada polaritat d'aquest grup fa augmentar les forces intermoleculars i incrementa considerablement el seu caràcter hidròfil, en comparació amb el PE. Per un altre, el grup OH^- resulta isomorf amb els àtoms d'hidrogen i, per tant, suficientment xicotet com

per a proporcionar a les cadenes polimèriques la estereoregularitat necessària per a formar un polímer amb un alt nivell de cristal·linitat, malgrat, fins i tot, l'aleatòria distribució de les seves unitats constituents, d'etilè i alcohol vinílic, al llarg de les esmentades cadenes. Aquesta característica microestructural de l'EVOH és precisament la responsable de les seves excel·lents propietats físiques i, en especial, de la seva alta capacitat barrera a les molècules permeants (Hernández et al., 2000).

Així doncs, quan el percentatge de grups OH^- a l'esquelet olefínic és zero, el producte resultant és el polietilè (PE), mentre que en assolir el 100 %, el polímer esdevé l'alcohol polivinílic (PVOH). Aquest darrer, al contrari que el PE, gaudeix d'unes propietats barrera excepcionalment bones per als gasos i aromes (les millors d'entre tots els polímers existents, sobretot amb els compostos de baixa polaritat), però resulta molt difícil de processar i es dissol fàcilment en aigua. Llavors, el fet què l'EVOH siga un copolímer d'etilè i alcohol vinílic fa que combine encertadament el caràcter hidròfob del primer amb el comportament hidròfil del segon, de tal manera que, quan el percentatge d'etilè oscil·la entre el 26 i el 48 %, aquests copolímers exhibeixen simultàniament la resistència a l'aigua i la processabilitat del PE junt amb les característiques barrera als gasos i aromes del PVOH. En canvi, quan el percentatge d'etilè s'aproxima al 26 %, les propietats barrera als gasos i vapors orgànics són excepcionalment elevades però la resistència a l'aigua es redueix considerablement i les condicions de processament es dificulten en gran mesura (Aucejo, 2000; Hernández et al., 2000; Català i Gavara, 2001a).

La majoria de copolímers d'EVOH, fins a un 20 % en contingut d'etilè, han estat reconeguts i acceptats per la US FDA (United States Food and Drug Administration) (Code of Federal Regulations, títol 21, capítol I, subcapítol B, part 177, subpart B, secció 1360) i han rebut una opinió científica positiva per part de la EFSA (European Food Safety Authority) (Scientific opinion on 26th list of substances for food contact materials, EFSA Journal 2009, 7 (10): 1324) per al seu ús en aplicacions de contacte amb aliments. Algunes de les aplicacions més habituals en l'envasat alimentari inclouen els contenidors rígids i flexibles, com ara les ampolles de salses i sucs, les conserves de confitura, els envasos de carn, formatges i iogurts, els paquets d'aperitius, cereals, condiments i infusions, les terrines i barquetes de menjars precuinats, etc. (Osborn i Jenkins, 1992; Hernández et al., 2000).

1.1.2.2. Nanocompòsits polimèrics

Tradicionalment, els materials polimèrics s'han farcit amb substàncies inorgàniques de diversa naturalesa, y en grans concentracions (> 20 %), com una manera de reciclar residus i / o de reduir costos de producció (Rhim i Ng, 2007; Pavlidou i Papaspyrides, 2008). Aquesta pràctica, però, conferia importants desavantatges als materials compostos resultants (compòsits), com ara l'increment del seu pes, fragilitat i opacitat (Pavlidou i Papaspyrides, 2008), al temps que comportava una pitjor processabilitat i unes majors velocitats de desgast a les instal·lacions de processament (Tjong, 2006). Tanmateix, la situació va canviar el 1986, quan un grup d'investigadors de Toyota va sintetitzar reeixidament un nanocompòsit de nylon-6 i montmoril·lonita per mitjà de polimerització in situ (Rhim et al., 2013), atenyent unes grans millores en les propietats tèrmiques, mecàniques, i barrera respecte al polímer pur, en afegir només una baixa quantitat de la càrrega argilosa (< 5 %) (Pavlidou i Papaspyrides, 2008). Aquesta troballa, entre d'altres, fou la que centrà la atenció i els esforços dels científics envers el desenvolupament de nous materials híbrids d'estructura anàloga, així com envers l'estudi de les seves propietats i aplicacions potencials (Rhim i Ng, 2007). Actualment, fruit d'aquesta recerca, es coneix que els nanocompòsits polimèrics experimenten millores dramàtiques en multitud de propietats fisicoquímiques, concretament, en la resistència a la tracció i a l'impacte, el mòdul de Young, la deformació al trencament, la temperatura de transició vítria i de distorsió per calor, l'estabilitat tèrmica i dimensional, la permeabilitat a l'aigua i als gasos (oxigen i diòxid de carboni), la resistència a l'abrasió i al rascat, el retardament de flama, la conductivitat iònica i elèctrica, l'angle de contacte, la resistència a l'oxidació i als dissolvents, la reciclabilitat, i la biodegradabilitat, sense malmetre llur densitat, característiques òptiques i fluïdesa en fos (Sorrentino et al., 2007; Pavlidou i Papaspyrides, 2008; Kiliaris i Papaspyrides, 2010; Cushen et al., 2012; Rhim et al., 2013). D'entre totes aquestes propietats, les primeres són les que resulten de major importància per a les aplicacions d'envasat alimentari, motiu pel qual són discutides més profundament a les línies següents.

1.1.2.2.1. Propietats mecàniques

La raó principal per a incorporar nanopartícules en matrius polimèriques resideix en incrementar llur mòdul o rigidesa a través dels mecanismes de reforçament que descriuen les teories de mecànica de compòsits convencionals (Tjong, 2006; Paul i Robeson, 2008; Kumar et al., 2011). En efecte, aquestes teories prediuen grans millores en el mòdul de Young dels nanocompòsits resultants realitzant només xicotetes addicions de nanopartícules correctament dispersades i alineades (Paul i Robeson, 2008), que són naturalment resistents a la deformació degut al seu elevat mòdul (Pavlidou i Papaspyrides, 2008). Aquests milloraments teòrics han estat àmpliament demostrats per les dades i tendències experimentals, i els resultats reportats per ambdós han atribuït habitualment un major reforçament mecànic a les estructures laminars que a les fibroses, degut a la seva naturalesa i efectes físics bidimensionals (Paul i Robeson, 2008). En aquest sentit, les làmines són capaces de desviar la propagació de les microclivelles en camins tortuosos (Tjong, 2006) que evolucionen en totes direccions dins el pla de la mostra (Paul i Robeson, 2008), quan es troben alineades amb ella, al temps que ofereixen una gran àrea superficial que facilita la transferència i concentració de l'esforç a la fase reforçant (Tjong, 2006; Pavlidou i Papaspyrides, 2008).

Pel que fa a la resistència a la tracció, aquesta pot resultar millorada o empitjorada respecte al polímer pur en funció del nivell d'adhesió interficial del farciment inorgànic a la matriu polimèrica (Paul i Robeson, 2008). Per tant, si ambdues fases materials es troben fortament enllaçades poden obtenir-se nanocompòsits d'alta resistència, mentre que la seva incompatibilitat química sol traslladar-se en una major fragilitat i fallada precoç (Paul i Robeson, 2008; Pavlidou i Papaspyrides, 2008). Malauradament, encara no existeix cap mètode en l'actualitat que permeta mesurar o millorar efectivament aqueix nivell d'adhesió (Paul i Robeson, 2008). Finalment, respecte a la deformació al trencament, les nanopartícules solen disminuir generalment la ductilitat dels polímers, i, en conseqüència, l'energia absorbida per a trencar-se, estretament relacionada amb llur resistència a l'impacte (Paul i Robeson, 2008). Aquest comportament és probablement degut a la formació de microbuits coalescents provocats pel desenganxament de grans aglomerats de partícules de la matriu polimèrica durant la fallida del material (Pavlidou i Papaspyrides, 2008). Tanmateix, aquesta reducció és habitualment més severa per davall de la temperatura de transició vítria de la matriu polimèrica, mentre que per damunt d'aquest punt pot no ser tan dramàtica i, en alguns casos, pot trobar-se, fins i tot, sobradament compensada amb un increment en la resistència a la tracció per mitjà dels mecanismes de reforçament esmentats anteriorment (Paul i Robeson, 2008).

1.1.2.2.2. Propietats tèrmiques

Les propietats tèrmiques són molt rellevants en el cas dels nanocompòsits polimèrics dissenyats per a aplicacions d'envasat alimentari que impliquen l'ús d'envasos esterilitzables, aptes per microones, d'ompliment en calent o de cocció en bossa. Durant el refredament del polímer fos, les nanopartícules poden actuar com a agents nucleants per als seus cristalls i esferulites, reduint així la seva mida considerablement i augmentant, al mateix temps, el seu nombre i irregularitat (Tjong, 2006; Pavlidou i Papaspyrides, 2008; Paul i Robeson, 2008). En aquestes condicions, i a baixos nivells de càrrega (< 5 %), les nanopartícules poden accelerar la velocitat de cristal·lització del polímer mentre disminueixen el seu punt de fusió (Tjong, 2006; Pavlidou i Papaspyrides, 2008), la qual cosa permet reduir el temps del cicle de màquina, i, en conseqüència, millorar la productivitat del procés de fabricació (Tjong, 2006; Silvestre et al., 2011). A més a més, les nanopartícules amb una gran àrea superficial també poden interactuar amb les cadenes polimèriques per a estabilitzar fases metastables, induint així un cert grau de polimorfisme cristal·lí al polímer (Tjong, 2006), el qual pot contribuir també a millorar les propietats mecàniques dels nanocompòsits resultants (Yuan et al., 2005).

Un cop format l'envàs, les nanopartícules tendeixen a incrementar la temperatura de transició vítria (punt de transició de l'estat vitri a l'estat gomós) (Rhim i Ng, 2007; Paul i Robeson, 2008), i la temperatura de distorsió per calor (punt de deformació sota una càrrega especificada) (Sinha Ray i Okamoto, 2003; Pavlidou i Papaspyrides, 2008) de la matriu polimèrica, degut a la formació d'una estructura intercalada que restringeix el moviment segmental de les cadenes polimèriques (Rhim i Ng, 2007), i millora així llur estabilitat mecànica (Sinha Ray i Okamoto, 2003). Malgrat tot, en alguns casos també s'ha reportat la disminució del primer paràmetre, bé atribuïda als efectes de plastificació induïts per la fracció orgànica d'algunes argiles organomodificades, o bé al deficient mullament de les partícules encastades amb la superfície interficial del polímer (Paul i Robeson, 2008). En qualsevol cas, la millorada estabilitat mecànica dels nanocompòsits polimèrics sempre es trasllada en un increment de llur coeficient d'expansió tèrmica, el qual resulta de gran importància per a l'estabilitat dimensional dels envasos formats. Com que les fibres i làmines inorgàniques solen posseir un major mòdul i un menor coeficient d'expansió tèrmica que la matriu polimèrica, poden resistir els seus canvis dimensionals creant esforços oposats en ambdues fases materials (Paul i Robeson, 2008).

1.1.2.2.3. Propietats barrera

El tercer major avantatge dels nanocompòsits polimèrics en les aplicacions d'envasat alimentari resideix en les seves millorades propietats barrera al vapor d'aigua, gasos permanents (nitrogen, oxigen i diòxid de carboni), i compostos aromàtics (Choudalakis i Gotsis, 2009). Aquestes millores són conseqüència de la reducció en la solubilitat, difusivitat, i, per tant, permeabilitat, de les molècules de gas en migrar per l'interior de la matriu nanocomposta, assolides amb la incorporació de farciments impermeables al polímer pur. Aquestes nanopartícules encastades a la matriu del material poden afectar la tortuositat del camí de forma directa, quan les molècules penetrants són forçades a viatjar al seu voltant (**Figura 4**), i de forma indirecta, quan indueixen l'alineament de les cadenes polimèriques, o l'alineament i modificació dels seus cristalls (Manias et al., 2007). En el primer cas, a banda de la resistència a la difusió causada per l'increment de la distància del camí tortuós al voltant de les partícules, i per la reducció de l'àrea transversal entre elles, alguns autors també consideren significativa la resistència causada pel desplaçament del solut a través de les escletxes formades entre partícules adjacents en el mateix pla horitzontal, i per la seva constricció o estrenyiment en entrar o eixir d'aquelles més angostes (Falla, 1996).

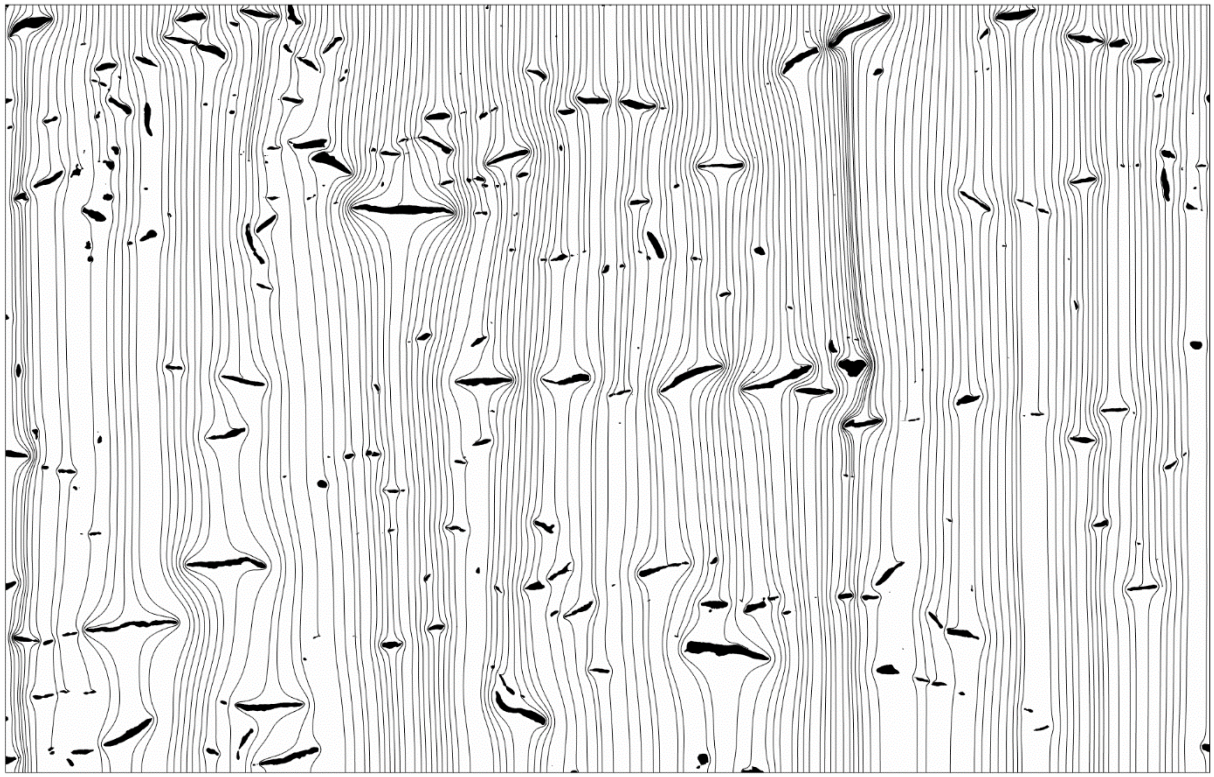

Figura 4. Línies de corrent del flux de solut a través de la matriu d'un nanocompòsit polimèric revelant les trajectòries tortuoses de les molècules al voltant de les nanopartícules encastades.

Atesos tots aquests mecanismes de retenció, les nanopartícules laminars, per la seva naturalesa bidimensional, resulten d'especial efectivitat en la millora de les propietats barrera del nanocompòsits polimèrics, podent-se millorar encara més el seu rendiment amb l'augment del seu grau d'exfoliació i alineament, així com de la seva relació d'aspecte (Feldman, 2013). De fet, sota aquestes condicions ideals, s'ha reportat que les nanopartícules poden reduir la permeabilitat a gasos en unes 50 – 500 voltes, fins i tot a baixos nivells de càrrega (Choudalakis i Gotsis, 2009). Malgrat tot, el grau de millora finalment assolit en aquests materials és molt variable i dependent de les seves principals característiques geomètriques (mida i forma de les partícules, concentració, distribució, orientació, etc.). Per aquesta raó, des del segle XIX s'han portat a terme diversos intents de modelitzar-la teòricament i d'estimar-la matemàticament, encara que amb diferents graus d'èxit (Choudalakis i Gotsis, 2009; Kumar et al., 2011). El motiu d'aquesta situació és que la majoria d'enfocaments teòrics no assumeixen canvis de permeabilitat en la matriu polimèrica, i consideren els farciments com a partícules totalment impermeables, pseudo-bidimensionals i no superposades, de forma uniforme i regular (rectangular, hexagonal, o circular), distribució regular o aleatòria en la matriu del polímer, i orientació paral·lela o perpendicular respecte a la direcció de la difusió molecular (Manias, 2007; Choudalakis i Gotsis, 2009), mentre que la microestructura dels nanocompòsits reals està molt allunyada d'aquestes característiques idealitzades. Altres models, en canvi, estan esdevenint cada cop més complexos en el seu intent per millorar llur simulació i trobar resultats més propers a les dades experimentals, requerint així cada volta més paràmetres i de més difícil estimació.

1.1.2.2.4. Nanopartícules laminars: argiles

Quan les partícules d'un material tenen només una dimensió en l'escala nanomètrica, essent les altres dues molt majors, formen estructures amb aspecte de làmina, fulla, disc o plaqueta (Pavlidou i Papaspyrides, 2008). No obstant, en la natura, aquestes estructures laminars rarament es troben de forma individual, a causa de les potents forces atractives de caràcter electrostàtic, d'enllaços de van der Waals, o d'enllaços per pont d'hidrogen, que s'estableixen al voltant de la seva superfície (Kumar et al., 2011). Així doncs, les esmentades partícules tendeixen més bé a apilar-se per desenes, formant grans aglomerats laminars semblants a baralles de cartes (tactoides) (Paul i Robeson, 2008; Pavlidou i Papaspyrides, 2008), dels quals prenen nom aquests materials. D'aquest tipus de substàncies en són exemples el grafè (fulla monocapa de carboni de grossària monoatòmica) i els seus derivats, alguns òxids, halurs, o calcogenurs metàl·lics, i la major part de miques i argiles (Naffakh et al., 2013; Nicolosi

et al., 2013). D'entre ells, els darrers materials són actualment els més rellevants per a la producció de nanocompòsits polimèrics, abastant la major part de recerques i desenvolupaments comercials fins al moment, especialment en aplicacions d'envasat alimentari (Pavlidou i Papaspyrides, 2008). Aquest fet és degut principalment al seu relatiu baix preu, gran abundància natural, característiques químiques ben conegudes, i aprovació legal com a additius alimentaris per la EFSA i com a substàncies GRAS (Generally Regarded as Safe) per la US FDA (Tjong, 2006; Pavlidou i Papaspyrides, 2008).

Les argiles són fil·losilicats alumínics hidratats, constituïts per fines làmines hexagonals (o fibres en alguns casos) de mida molt reduïda (< 10 µm de diàmetre) que exhibeixen una estructura interna en forma de sandvitx, composta per capes tetraèdriques de silicats ($Si_2O_5^{2-}$) i capes octaèdriques de naturalesa gibbsítica ($Al_2(OH)_4^{2+}$) disposades espacialment en diferents combinacions (t-o o 1:1, t-o-t o 2:1, t-o-t-o o 2:2, etc.), a l'igual que altres minerals de la mateixa família. No obstant això, ambdós tipus de capes experimenten freqüentment determinats fenòmens de substitució isomòrfica, on els cations tetravalents de silici que ocupen posicions tetraèdriques són habitualment reemplaçats per cations trivalents d'alumini, transformant així els silicats en aluminats ($Al_2O_5^{4-}$), mentre que els cations d'alumini que ocupen posicions tetraèdriques són habitualment reemplaçats per cations bivalents de magnesi (i, en alguns casos, per cations de ferro), transformant així les capes gibbsítiques en brucítiques ($Mg_2(OH)_4$) (Amorós et al., 1994; Barba et al., 2002). Com a resultat d'ambdós tipus de substitució, s'indueixen algunes càrregues negatives en l'estructura cristal·lina que es distribueixen homogèniament en el pla de les làmines i s'equilibren elèctricament amb l'absorció de contraions positius externs, usualment sodi, potassi, i calci. Aquests contraions solen localitzar-se entre les làmines i formar enllaços iònics amb els anions òxid externs de les capes de silicats, essent llavors responsables de mantenir les làmines unides en forma de pileres o tactoides, la forma natural en què es troben les argiles, i, en conseqüència, de complicar llur exfoliació (Paul i Robeson, 2008).

Com que les argiles constitueixen una de les famílies de minerals més abundants de la Terra, on s'inclouen desenes de substàncies amb diferent composició i propietats químiques, solen ser generalment classificades per grups d'acord amb, entre altres, les tres característiques esmentades anteriorment, ço és, l'estructura interna de les làmines, el tipus de contraions integrats entre elles, i el tipus i proporció de substituents dels cations alumini (Amorós et al., 1994; Barba et al., 2002). En aquest context, les argiles pertanyents al grup dels 2:1 fil·losilicats substituïts amb magnesi i equilibrats amb sodi, també coneguts com a esmectites, com ara la bentonita, la montmoril·lonita, l'hectorita, i la saponita sòdiques, comprenen els materials més comunament inclosos com a farciments inorgànics en la composició química dels nanocompòsits polimèrics (Sinha Ray i Okamoto, 2003; Pavlidou i

Papaspyrides, 2008). Aquest fet és fonamentalment degut als seus majors avantatges en matèria de grandària de partícula (< 1 μm diàmetre), relació d'aspecte (diàmetre / grossària en l'ordre de 10 – 1000) i comportament hidròfil (Pavlidou i Papaspyrides, 2008; Barba et al., 2002). Tanmateix, altres grups d'argiles de naturalesa similar, com la caolinita, l'hal·loysita, la vermiculita, o el talc, també estan atraient actualment l'atenció dels investigadors per motiu de les seves particulars propietats, com són la capacitat de formació de tubs de l'hal·loysita en condicions de sequedat (Du et al., 2010) o les bones característiques òptiques de la caolinita. A la **Figura 5** es mostren les micrografies de rastreig d'alguns exemples característics d'aquestes argiles.

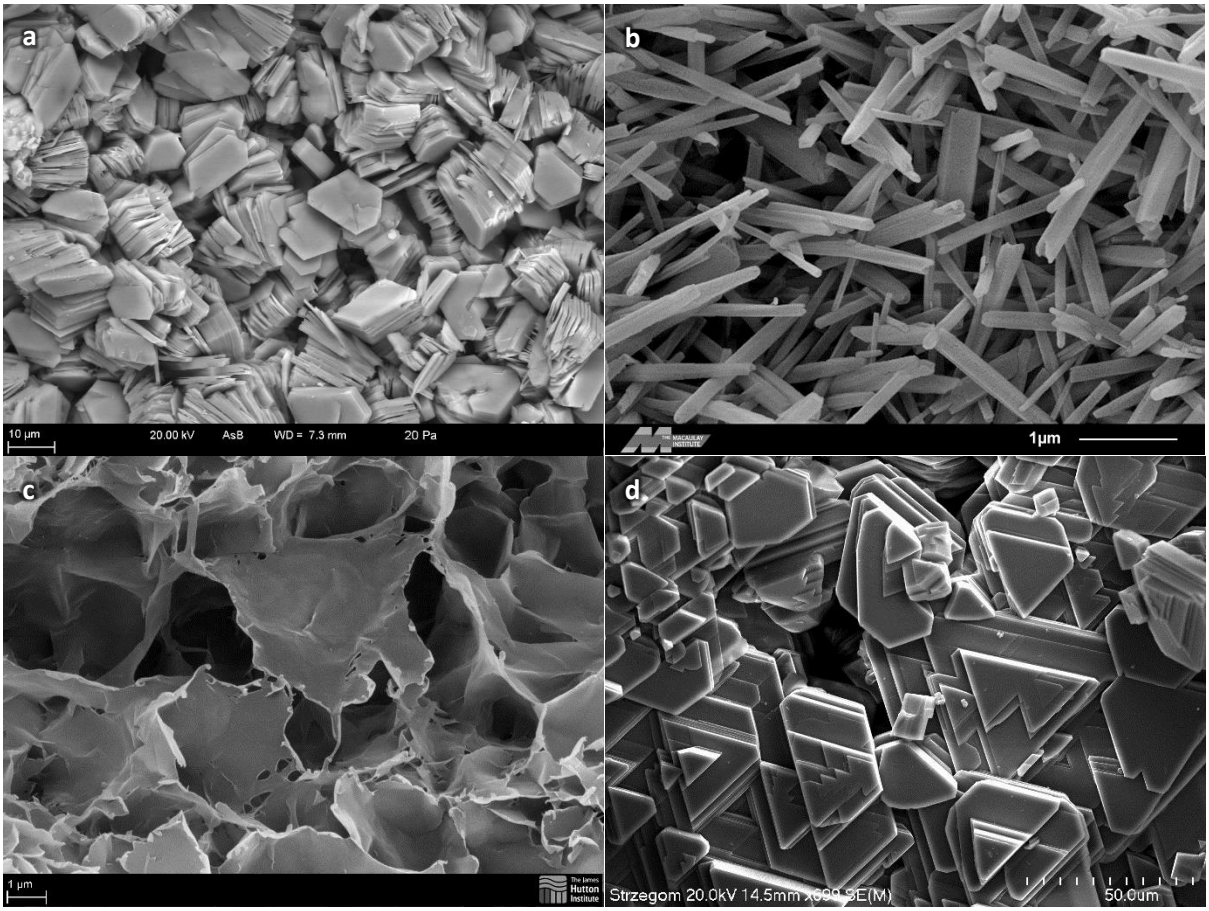

Figura 5. Imatges de microscòpia electrònica de rastreig (SEM) de cristalls apilats d'argiles amb diferent estructura laminar: (a) dickita (1:1), (b) hal·loysita (1:1), (c) esmectita (2:1) i (d) clorita (2:2)

A l'igual que els altres materials laminars, i segons s'ha explanat adés, les argiles són habitualment incorporades a les matrius polimèriques per a millorar llurs propietats físiques (Rhim i Ng, 2007). Malgrat tot, per tal de desenvolupar tot el seu potencial, les argiles deuen ser completament exfoliades, i les seves làmines individuals acuradament integrades en l'estructura interna del material (Pavlidou i Papaspyrides, 2008; Nicolosi et al., 2013). Com que la major part de les argiles són altament

hidròfiles (algunes d'elles poden absorbir fins i tot diverses voltes el seu pes en aigua) tenen tendència a absorbir molècules d'aigua i a coordinar-les entre les seves fulles, on solen localitzar-se habitualment els contraions positius. Aquesta aigua interestratificada es capaç de solvatar aqueixos cations i reduir així les seves interaccions electrostàtiques amb els oxianions silicat de les fulles, provocant, com a resultat, un increment de la distància interlaminar, i, en conseqüència, un inflament dels tactoides argilosos fins a la seva completa exfoliació (Amorós et al., 1994). Aquesta característica de les argiles els permet generar bones estructures nanocompostes en polímers altament hidròfils, com són l'òxid de polietilè (PEO) o l'alcohol polivinílic (PVOH) (Pavlidou i Papaspyrides, 2008), mitjançant mètodes de dissolució. Malauradament, també suposa una barrera per a produir bons nanocompòsits a partir de polímers hidròfobs convencionals, com són el polietilè (PE), el polipropilè (PP), o el tereftalat de polietilè (PET), i deuen emprar-se altres tècniques diferents, com ara el processat en fos, la mòlta combinada en molí de boles, la síntesi amb plantilla, la polimerització in situ, o els mètodes de làtex, en el seu lloc (Sinha Ray i Okamoto, 2003; Sorrentino et al., 2007; Pavlidou i Papaspyrides, 2008). Malgrat tot, aquestes tècniques tampoc no són completament efectives, i, de fet, com a resultat de la seva aplicació, i de la particular naturalesa o característiques fisicoquímiques dels materials de partida, poden obtenir-se en última instància tres estructures nanocompostes molt diferents, en funció del grau de dispersió de les partícules finalment atès en la matriu polimèrica (**Figura 6**): immiscible o tactoide, intercalada, i miscible o exfoliada (Sinha Ray i Okamoto, 2003; Paul i Robeson, 2008).

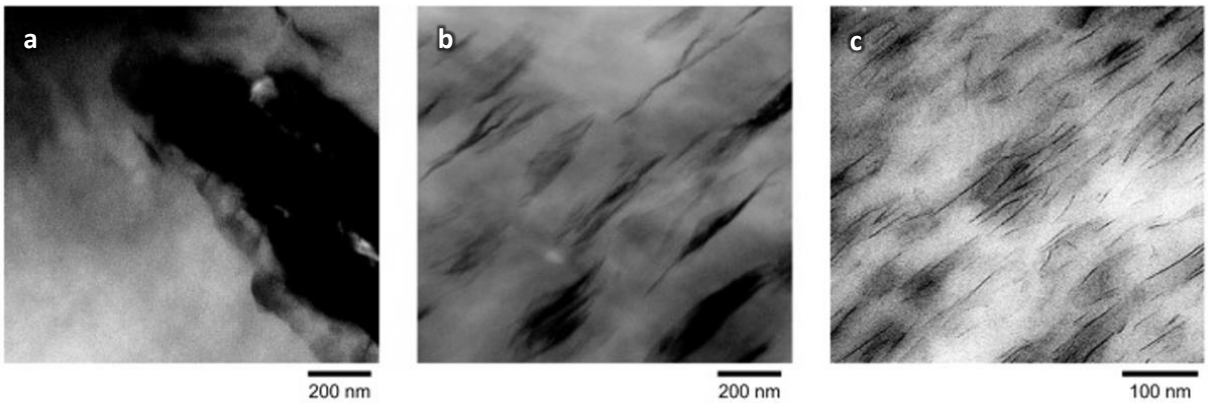

Figura 6. Estructures nanocompostes: (a) immiscible o tactoide, (b) intercalada, i (c) exfoliada.

Així doncs, per tal de millorar el grau d'exfoliació i dispersió de les nanopartícules argiloses en aquests casos, s'ha desenvolupat una estratègia diferent basada en l'aprofitament de la seva elevada capacitat d'intercanvi catiònic. En concret, les argiles son modificades superficialment per esdevenir organòfiles (organoargiles), i, per tant, químicament compatibles amb els polímers apolars, en reemplaçar els seus

contraions externs alcalins o alcalinoterris per grans cations orgànics. Amb aquest objectiu, els materials són sotmesos a reaccions d'intercanvi iònic amb surfactants catiònic – orgànics, com les sals d'alquilamoni, sulfoni, i fosfoni amb substituents de llarga cadena, d'almenys 12 àtoms de carboni, o altres compostos anàlegs de tipus "oni". Aquestes substàncies amfifíliques són capaces de reduir l'energia superficial de les partícules, millorar les característiques de mullabilitat de la matriu polimèrica, i incrementar la distància interlaminar, promovent així l'inflament dels tactoides argilosos, la difusió de les cadenes polimèriques al seu interior, i la seva exfoliació final en partícules individuals. Addicionalment, els modificadors orgànics també poden proporcionar grups funcionals que reaccionen amb la matriu polimèrica i, en alguns casos, poden, fins i tot, iniciar la polimerització de monòmers per a formar el polímer in situ. En qualsevol cas, i en últim terme, aquestes substàncies donen suport a la correcta formació d'estructures nanocompostes en servir de compatibilitzants entre les argiles hidròfiles i els polímers organòfils (Pavlidou i Papaspyrides, 2008).

1.2. Fenòmens de transferència de matèria

La transferència de matèria és un fenomen que es desenvolupa com a conseqüència de la tendència natural que mostren tots els sistemes químics d'avançar vers un estat d'equilibri termodinàmic. En la majoria d'aplicacions dels materials polimèrics aquests solen, bé exposar-se a un sistema químic diferent del de la seva obtenció, com ara un canvi de temperatura o humitat ambiental, o bé trobar-se separant diferents components o sistemes químics, com per exemple, un aliment del seu entorn, o les atmosferes exterior i interior d'un envàs.

En aquest darrer cas, el d'un aliment conservat a l'interior d'un envàs actiu, com pot ser l'exemple representat a la següent **Figura 7**, el sistema químic sol comprendre com a mínim quatre fases: l'atmosfera externa (AE), el propi envàs polimèric (E), l'atmosfera interna (AI) i l'aliment, que al seu temps pot consistir d'una o diverses fases (F).

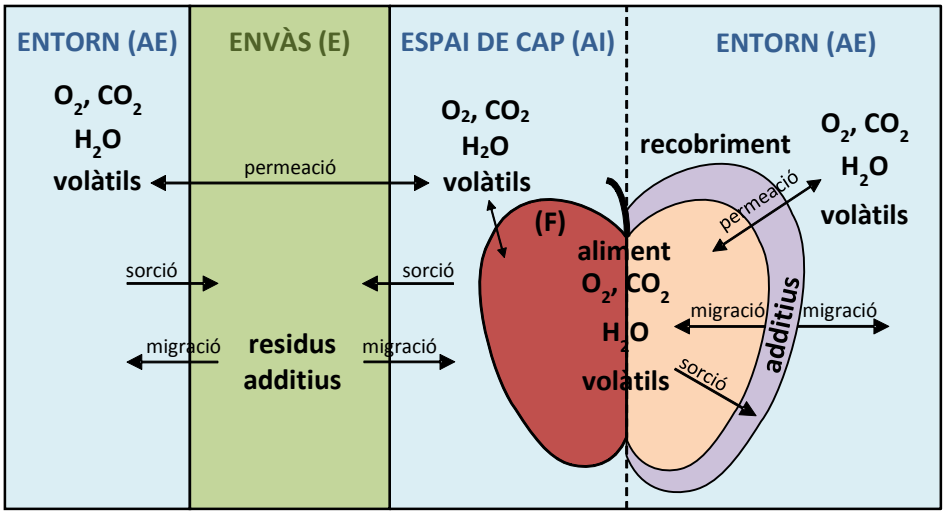

Figura 7. Esquema de les fases i els processos de transferència de matèria a dos sistemes de conservació d'aliments: un envàs actiu (esquerra) i un recobriment actiu comestible (dreta).

Cada fase, per la seva banda, pot trobar-se constituïda per nombrosos components, molts d'ells de baixa massa molecular i elevada mobilitat, com ara l'oxigen, el diòxid de carboni, el vapor d'aigua, els components dels aromes alimentaris o de les olors externes, els agents actius incorporats a l'envàs, etc. Existeixen altres substàncies, en canvi, que poden considerar-se més bé immòbils, com ara les macromolècules que conformen la matriu alimentària o la matriu polimèrica de l'envàs actiu. Com és lògic, els components mòbils poden desplaçar-se lliurement dins de cada fase i entre les diverses fases,

a través de les corresponents interfases, fins ocupar totes les fases que componen el sistema, assolint així finalment l'estat d'equilibri.

1.2.1. Equilibri químic. Coeficients de solubilitat i repartiment

Com s'acaba d'explicar, cada component d'un sistema químic sol transferir-se des d'una fase inicial vers les seves fases adjacents fins assolir un estat d'equilibri químic. Segons les lleis de la termodinàmica, es pot afirmar que un sistema químic es troba en equilibri quan s'assoleix la identitat de potencials químics per a tots els components *i* que es troben presents al sistema, i en cadascuna de les fases *α* que el conformen (Hernández i Gavara, 1999), així doncs:

$$\mu_i^{\alpha} = \mu_i^{AE} = \mu_i^{AI} = \mu_i^{E} = \mu_i^{F1} = \mu_i^{F2} = \ldots \quad (1)$$

No obstant això, resulta poc pràctic descriure els equilibris químics en funció del potencial químic de llurs components, motiu pel qual es preferible expressar-los com a proporcions entre les concentracions i/o pressions parcials de cada component entre un determinat parell de fases del sistema. L'elecció depèn fonamentalment del tipus de fases entre les quals esdevé l'intercanvi. Per exemple, en els intercanvis de massa entre l'envàs i l'atmosfera externa, l'equilibri pot expressar-se com la relació entre la concentració de cada component *i* en la fase condensada (l'envàs) i la corresponent pressió parcial en la fase gasosa (l'ambient extern).

Experimentalment, aquest equilibri sol representar-se mitjançant una isoterma de sorció, la qual, en funció del seu perfil, pot trobar-se descrita per algun dels diversos models matemàtics disponibles, com ara les equacions de Langmuir, Flory – Huggins, B.E.T., G.A.B., Freundlich o la llei de Henry. De fet, aquesta última es tracta del model més simple existent, i descriu que la pressió parcial d'un component *i* al si d'un medi gasós (AE o AI, per exemple) és directament proporcional a la concentració del citat component al medi condensat amb què es troba en contacte (E o F, per exemple), essent la constant de proporcionalitat, H_i, l'anomenada constant de Henry, segons es mostra a la següent equació:

$$p_i^{AE\ o\ AI} = H_i \cdot C_i^{E\ o\ F} \quad (2)$$

Aquest paràmetre H_i, per la seva part, es considera constant per a un determinat component *i* repartit entre un parell de fases concretes, si bé pot variar en funció de la temperatura segons la coneguda llei de Van't Hoff:

$$H_i = H_i^0 \cdot e^{\frac{\Delta H_S}{R \cdot T}} \qquad (3)$$

on ΔH_S representa l'entalpia de solubilització del component *i*, H_i^0 el valor d'H_i a 0 K, *T* la temperatura ambiental, i *R* es tracta de la constant universal dels gasos ideals.

D'altra banda, cal comentar també que la inversa de la constant de Henry, coneguda com a coeficient de solubilitat, S_i, és un paràmetre àmpliament utilitzat en la descripció de la retenció de gasos permanents en polímers sintètics, on la llei de Henry es compleix de forma raonable dins d'un determinat interval de pressions parcials. A més a més, també sol aplicar-se en la descripció de la sorció de compostos orgànics molt volàtils en polímers, malgrat que, en aquests sistemes, la llei de Henry sol presentar desviacions importants com a conseqüència de les interaccions existents entre el polímer i la molècula penetrant.

En polímers hidrofílics, per exemple, la isoterma de sorció de l'aigua sol desviar-se notablement de la linearitat, presentant, en general, un perfil de tipus II segons la classificació de la IUPAC, detallada esquemàticament a la **Figura 8**. Si, a més a més, en aquests materials es detecten també fenòmens d'histèresi, la descripció de llurs isotermes pot resultar de tipus III o IV. Com a conseqüència, en els sistemes constituïts per aquests polímers (com els envasos actius) no es habitual descriure la sorció de vapors, i especialment la del vapor d'aigua, mitjançant el citat coeficient de solubilitat (Gavara i Hernández, 1994; Aucejo et al., 2000).

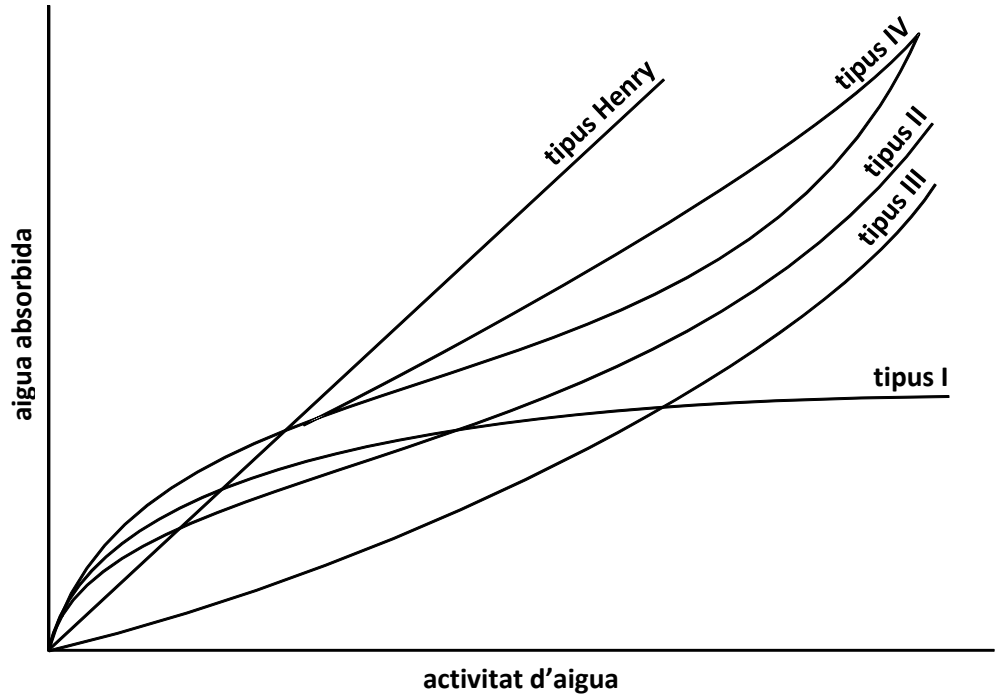

Figura 8. Classificació de les isotermes d'adsorció segons la IUPAC.

Per una altra banda, quan l'equilibri s'estableix entre dues fases condensades, com ara l'envàs (E) i l'aliment (F), s'utilitza un nou paràmetre anomenat constant de repartiment, o coeficient de partició, K_i, per descriure la distribució del component *i* entre ambdues fases, segons:

$$C_i^E = K_i \cdot C_i^F \qquad (4)$$

el qual, al seu temps, varia en funció de la temperatura segons l'anterior llei de Van't Hoff (3).

La utilitat de paràmetres com S_i o K_i resideix en la possibilitat d'estimar l'extensió dels processos de transferència de matèria en el cas hipotètic d'assolir l'estat d'equilibri. Així doncs, valors elevats d'aquests paràmetres indiquen que els components romanen retinguts principalment en les fases condensades (com ara l'envàs o l'aliment), mentre que valors reduïts dels mateixos impliquen un major grau d'alliberament dels compostos vers les fases gasoses (com són l'atmosfera interna o externa de l'envàs). Per contra, aquests paràmetres no proporcionen cap informació sobre la celeritat de l'avanç del sistema vers l'equilibri, ja que aquest fenomen depèn de la cinètica del procés i dels seus paràmetres corresponents.

1.2.2. Cinètica química. Coeficients de difusió i permeabilitat

És un fet comprovable que a l'interior de cadascuna de les fases que componen un sistema les substàncies poden desplaçar-se amb cinètiques diferents. Així doncs, mentre que a les fases fluides, líquides o gasoses, la cinètica és tan ràpida que habitualment es considera que els soluts es troben sempre distribuïts de forma homogènia, a les fases sòlides, o líquides d'elevada viscositat, les substàncies solen difondre's tan lentament que, en general, es considera que la seva cinètica segueix les lleis de Fick (Crank, 1975). Segons aquestes lleis, el flux d'un component penetrant *i*, a través de la paret d'un envàs polimèric (E), i en la direcció de la seva grossària *z*, $J_{i\,z}^{E}$, és proporcional al gradient de concentració del component *i* al llarg d'aquesta direcció, $\frac{\partial C_i^E}{\partial z}$, de tal manera que:

$$J_{i\,z}^{E} = \frac{q_{i\,z}^{E}}{A \cdot t} = -D_i^E \cdot \frac{\partial C_i^E}{\partial z} \quad ; \quad \frac{\partial C_i^E}{\partial t} = D_i^E \cdot \frac{\partial^2 C_i^E}{\partial z^2} \tag{5}$$

En aquest cas, la constant de proporcionalitat és el coeficient de difusió o difusivitat, D_i^E, que normalment es considera constant per a un determinat solut que es transfereix a través d'una matriu polimèrica concreta, depenent únicament de la temperatura segons la llei d'Arrhenius:

$$D_i = D_i^0 \cdot e^{\frac{-E_D}{R \cdot T}} \tag{6}$$

on E_D representa l'energia d'activació del procés de difusió del component *i*, i D_i^0 el valor del coeficient D_i a 0 K.

No obstant això, s'ha observat que el valor d'aquest coeficient també pot variar en funció d'altres factors, com ara les condicions mecàniques o tèrmiques en què s'ha obtingut l'envàs, la grossària de la seva paret polimèrica, o la presència d'altres molècules permeants, molt especialment la de l'aigua. Com és evident, valors elevats de D_i^E indiquen processos de difusió molt ràpids, mentre que valors reduïts impliquen sistemes químics que avancen molt lentament vers el seu estat d'equilibri.

La majoria d'aplicacions dels envasos polimèrics estan relacionades amb el control dels processos de transferència de massa que esdevenen al si dels aliments des de la seva producció fins el moment de consum, entre els quals es troben: la reducció de la pèrdua d'aigua de l'aliment, l'intercanvi de gasos atmosfèrics (oxigen, diòxid de carboni, etc.), la reducció de les pèrdues de components aromàtics o la seva incorporació, etc. En totes elles, la funció de l'envàs consisteix en alentir el procés natural de

transport de massa, interposant-se entre l'aliment i el medi exterior per evitar que el sistema arribe a l'equilibri. En aquestes condicions, el procés assoleix un estat estacionari en el qual el gradient de concentració del component *i* a la paret de l'envàs roman constant, de tal forma que la primera llei de Fick pot reescriure's de la següent manera:

$$J_{i\,z}^{E} = \frac{q_{i\,z}^{E}}{A \cdot t} = -D_i^E \cdot \frac{\partial C_i^E}{\partial z} = -D_i^E \cdot \frac{C_i^{E\,i} - C_i^{E\,e}}{L} \tag{7}$$

on $C_i^{E\,i}$ i $C_i^{E\,e}$ representen les concentracions del component *i* als extrems interior i exterior de la paret de l'envàs, respectivament, i *L* la seva grossària.

En aquest punt, aplicant la llei de Henry a l'equació (7) s'obté l'expressió del flux $J_{i\,z}^{E}$ en funció de les pressions parcials del component *i* als ambients interior i exterior del sistema, $p_i^{E\,i}$ i $p_i^{E\,e}$:

$$J_{i\,z}^{E} = \frac{q_{i\,z}^{E}}{A \cdot t} = -D_i^E \cdot \frac{S_i^E \cdot p_i^{E\,i} - S_i^E \cdot p_i^{E\,e}}{L} = -D_i^E \cdot S_i^E \cdot \frac{\Delta p^E}{L} \tag{8}$$

Finalment, al producte dels coeficients de solubilitat i de difusió se'l coneix com a coeficient de permeabilitat, i reescrivint l'anterior equació (8) s'obté així la seva definició:

$$P_i^E = D_i^E \cdot S_i^E = \frac{q_{i\,z}^{E} \cdot L}{A \cdot t \cdot \Delta p^E} \tag{9}$$

on la permeabilitat, P_i^E , representa la quantitat de component *i* que travessa la paret d'un envàs (E) de grossària *L* en la direcció *z*, per unitat d'àrea, de temps i de gradient de pressió.

Aquest coeficient es tracta d'una magnitud intensiva per a un polímer i un permeant concrets, que resta independent de la forma o volum de l'envàs en conjunt, si bé es considera funció exclusiva de la temperatura segons la llei d'Arrhenius. Malgrat tot, cal recordar que en la definició de la permeabilitat s'ha considerat el compliment de la llei de Henry i la constància del coeficient de difusió en la llei de Fick, així com que en determinats sistemes polímer/permeant, especialment en aquells on el polímer posseeix un marcat caràcter hidròfil, s'observen importants desviacions d'aquestes lleis, motiu pel qual, en general, es mesuren els valors de les permeabilitats efectives enlloc de calcular-los a partir dels seus paràmetres.

1.2.3. Simulació i predicció dels fenòmens de transferència de matèria

Si bé les pel·lícules polimèriques que constitueixen les parets dels envasos actius representen un dels sistemes físics més senzills d'estudiar des del punt de vista dels fenòmens del transport, la gran varietat i complexitat dels mecanismes de transferència de massa que solen involucrar impedeix conèixer amb exactitud el comportament d'aquests sistemes en situacions reals amb la simple realització d'assajos experimentals.

Així doncs, l'interès en la realització de simulacions matemàtiques d'aquests fenòmens de transport resideix fonamentalment en l'obtenció de descripcions exhaustives de tots els processos fisicoquímics involucrats, a través de càlculs computeritzats i alimentats per un inventari mínim de dades experimentals, amb el conseqüent estalvi en costos i recursos humans o materials.

A més a més d'un major aprofundiment en els coneixements fisicoquímics del sistema en estudi, aquestes simulacions també permeten assolir un doble objectiu:

- La predicció amb exactitud raonable de la seva evolució a llarg termini quan es troba sotmès a diferents accions externes.
- El disseny de nous sistemes, l'evolució dels quals a llarg termini puga ser ajustada per tal d'acomplir un determinat objectiu.

Malgrat tots aquests avantatges, la simulació matemàtica té una capacitat limitada per a representar els processos de transferència de massa que esdevenen en sistemes reals. D'una banda, es troba el clàssic dilema "exactitud – rapidesa", atès que, a mesura que s'augmenta el nombre de variables i equacions que les relacionen, amb la intenció de reduir el nombre d'hipòtesis i obtenir així una major exactitud de resultats, s'incrementa també de forma exponencial el temps necessari per a la seva computació. D'una altra, aquest augment de complexitat també incrementa la necessitat de disposar de suficients coeficients i paràmetres fonamentals que satisfacen totes les equacions integrades al model. Atesa l'escassesa de referències bibliogràfiques sobre multitud d'aquests paràmetres, així com de mètodes d'estimació suficientment fiables, amb freqüència deuen determinar-se a través d'assajos experimentals, per la qual cosa, a l'hora d'afrontar la simulació matemàtica de qualsevol procés de transferència de matèria sempre deu trobar-se el correcte compromís entre la seva exactitud, la rapidesa de resposta i la mida mínima del seu inventari de dades experimentals.

1.2.3.1. Modelització d'envasos actius

El primer pas per a simular un sistema real consisteix en la construcció d'un model d'aquest sistema, amb unes característiques geomètriques i propietats fisicoquímiques tan aproximades com siga possible, però mantenint, al mateix temps, una senzillesa suficient com per a poder tractar-lo matemàticament assolint el compromís "exactitud – rapidesa" adés esmentat.

En el cas dels models de sistemes d'envasat actiu constituïts per pel·lícules de materials polimèrics, les característiques i propietats que solen aproximar-se més freqüentment són:

- Geometria de "làmina infinita", ço és, cos simètric paral·lelepipèdic de grossària finita i llargària i amplària infinites.
- Propietats fisicoquímiques isotròpiques i constants a tot el sistema.

Amb aquestes premisses, el model matemàtic per a la transferència de, per exemple, un component *i*, a través d'una pel·lícula polimèrica de grossària *2L* vers, o des, del medi format per les fases físiques confrontants, es representa esquemàticament a la **Figura 9**:

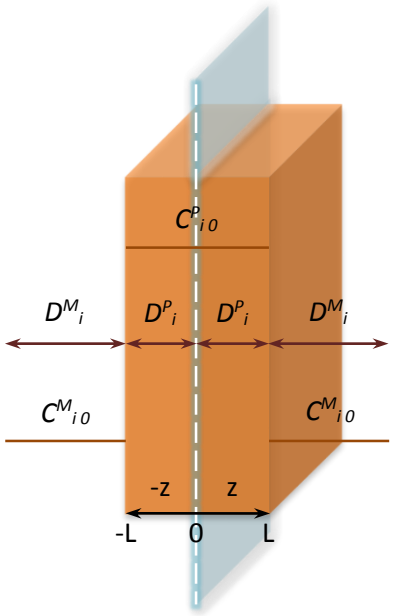

Figura 9. Model matemàtic per a la transferència d'un component *i* des del si d'una pel·lícula polimèrica de grossària *2L* vers el medi format les fases físiques confrontants.

on:

C_{i0}^{P} : concentració inicial del component *i* al si de la pel·lícula

C_{i0}^{M} : concentració inicial del component *i* al si del medi exterior

D_{i}^{P} : coeficient de difusió del component *i* a través de la pel·lícula

D_{i}^{M} : coeficient de difusió del component *i* a través del medi exterior

1.2.3.2. Hipòtesis i equació general

Amb l'objectiu de plantejar correctament el balanç general de matèria sobre el volum de control de la pel·lícula estudiada és necessari detallar de bestreta totes les hipòtesis fonamentals del model que seran preses en consideració:

- Fases sòlides, i fluïdes en repòs, estàtiques (absència de flux net de matèria en qualsevol direcció) i homogènies (identitat de propietats en qualsevol punt).
- Fases fluïdes en agitació, dinàmiques però perfectament agitades i, per tant, homogènies.
- Interfases en equilibri termodinàmic (en conseqüència, identitat de potencials químics en sengles llindars de fase).
- Volum interfacial nul (en conseqüència, identitat de densitats de flux de matèria en sengles llindars de fase).
- Temperatura i pressió uniformes i constants a tot el sistema.
- Concentració total d'espècies químiques constant a tot el sistema (absència de generació o desaparició global de matèria).
- Estat no estacionari (evolució del sistema amb el temps fins assolir un estat d'equilibri) amb absència de període d'inducció.
- Transferència de matèria unidireccional i de tipus molecular o difusiu, regentada sempre per la llei de Fick.

Tenint en compte totes les característiques i propietats del model construït, així com les hipòtesis formulades, i combinant la llei de conservació de la matèria amb la llei de continuïtat de Fick, es dedueix l'equació general del balanç microscòpic de matèria aplicat al component *i*:

$$\frac{\partial C_i^P}{\partial t} = D_i^P \frac{\partial^2 C_i^P}{\partial z^2} \tag{10}$$

Aquesta expressió matemàtica és una equació diferencial en derivades parcials (PDE) de tipus parabòlic. La seva resolució permet conèixer el perfil de concentració del component *i*, $C_i^P(z,t)$, en cada punt de l'interior de la pel·lícula i per a cada instant del temps transcorregut.

1.2.3.3. Resolució de l'equació del balanç general de matèria

Malauradament, l'anterior equació diferencial en derivades parcials només pot resoldre's analíticament per a sistemes simplificats i en aquelles situacions en què es puguen aplicar condicions d'integració molt concretes i senzilles. Per a la resta de circumstàncies més generals deuen emprar-se obligatòriament mètodes alternatius d'aproximació, com són els mètodes gràfics o els numèrics.

En qualsevol dels casos, tant la resolució analítica com la numèrica requereixen l'ajuda d'avançats sistemes de computació per a trobar i representar les solucions amb una exactitud suficient, i sempre dins d'un interval de temps raonable. En funció del mètode finalment elegit, el nombre i complexitat dels càlculs a efectuar serà diferent i, en conseqüència, els requisits mínims en programari i maquinari del sistema computador també ho seran. Pel que fa a les solucions de programari disponibles en l'actualitat, les suites de càlcul i programació com MATLAB (The MathWorks Inc., Natick, MA, EEUU) o COMSOL Multiphysics (COMSOL AB, Estocolm, Suècia) són, en general, les aplicacions més utilitzades i recomanables per la seva potència i versatilitat.

1.2.3.3.1. Solució analítica de l'equació general

En la literatura de càlcul matemàtic es poden trobar nombrosos mètodes analítics per a resoldre equacions diferencials en derivades parcials. D'entre tots ells, els més utilitzats per la seva senzillesa i aplicabilitat són: la separació de variables, el canvi de variables i la transformada integral (habitualment de Fourier o de Laplace). L'aplicabilitat de cada mètode al model en estudi estarà sempre condicionada al compliment, per part d'aquest, d'uns determinats requeriments matemàtics, ço és: la "separabilitat" de les variables de la PDE, l'existència d'una funció bijectiva entre les variables a intercanviar, o l'existència d'una transformada inversa de Fourier o Laplace, respectivament. En cas que siguen aplicables simultàniament més d'un mètode analític es recomana escollir sempre el més senzill de desenvolupar, si bé amb qualsevol d'ells el resultat deu romandre invariable.

Per aplicar el mètode seleccionat a l'anterior equació diferencial deuen fixar-se prèviament totes les condicions d'integració del model, de manera que les solucions de la integral resultant queden així correctament definides. Aquestes condicions emanen de les característiques i propietats del model en estudi, i/o de les hipòtesis fonamentals fixades anteriorment, i solen ser de dos tipus:

- Condicions inicials: estableixen la distribució del component *i* a totes les fases del sistema i per a l'instant inicial del procés de transport.
- Condicions de contorn, frontera o límit: estableixen l'evolució del component *i* amb el temps per a cada punt frontera o límit del sistema.

En el cas de la pel·lícula polimèrica que s'ha utilitzat com a exemple de model matemàtic en aquesta secció, s'ha considerat que es troba immersa en un medi infinit constituït per una fase fluida agitada, de tal manera que, inicialment, les concentracions del component *i* a la pel·lícula i al medi són C_{i0}^{P} i C_{i0}^{M} respectivament. Pel que fa a les condicions de contorn, al present cas existeix una condició "de simetria" a l'origen de coordenades, on es compleix que: $\partial C_i^P / \partial z = 0$ i una altra condició "de frontera" a $z = L$, on es troba la interfase entre la pel·lícula polimèrica i el medi fluid, l'expressió de la qual serà funció del nivell d'agitació d'aquest últim, entre d'altres factors.

Si s'admet que es compleixen les hipòtesis descrites anteriorment de què la fase fluida és infinita i que es troba sempre perfectament agitada, es pot inferir que la concentració del component *i* al seu si, $C_i^M(t)$ és uniforme en l'espai i constant en el temps, i per tant de valor conegut. Així doncs, la segona

condició de contorn a $z = L$ serà: $C_i^P = K_i \cdot C_i^M$, on K_i fa referència a la constant de repartiment o de Henry, segons si la fase fluïda és líquida o gasosa.

Finalment, integrant l'equació diferencial en derivades parcials amb totes les condicions inicials i de contorn ja descrites, mitjançant l'aplicació d'algun dels mètodes analítics exposats adés, s'obté l'expressió general del balanç macroscòpic de matèria aplicat al component *i* (Crank, 1975):

$$C_i^P = K_i \cdot C_i^M + \frac{2\left(C_{i0}^P - K_i \cdot C_i^M\right)}{\pi} \sum_{\nu=1}^{\infty} \frac{(-1)^{\nu-1}}{\nu - \frac{1}{2}} \cdot e^{\frac{-\pi^2 \cdot \left(\nu - \frac{1}{2}\right)^2 \cdot D_i^P \cdot t}{L^2}} \cdot \cos\left(\frac{z \cdot \pi}{L}\left(\nu - \frac{1}{2}\right)\right) \qquad (11)$$

1.2.3.3.2. Solució numèrica de l'equació general

En càlcul matemàtic es defineixen els mètodes numèrics com aquells algoritmes d'aproximació numèrica que permeten simular processos matemàtics molt més complexos, i que es troben associats a la resolució de funcions contínues del món real. En altres paraules, l'anàlisi numèrica d'una funció contínua, com és la funció diferencial en derivades parcials plantejada a l'apartat 1.2.3.2, permet sempre la seva resolució matemàtica en tots aquells casos en què, per la complexitat dels sistemes físics o de les seves condicions d'integració, aquesta resulta impossible d'assolir o computacionalment molt costosa.

No obstant això, atesa la complexitat de la majoria d'algoritmes, o l'elevat nombre d'iteracions necessàries per aconseguir la seva convergència, la utilització d'aquests mètodes sempre requereix la disposició d'avançats sistemes de computació per a trobar i representar les solucions amb una exactitud i un temps raonables. En aquest sentit, com que, a diferència dels mètodes analítics, aquests algoritmes només presenten un interval de valors que engloba la solució en lloc d'un valor exacte, resulta molt important definir adequadament la magnitud d'aquest interval, en funció de la precisió requerida, per poder controlar així el nombre d'iteracions necessàries per assolir la convergència i, per tant, el temps total de computació.

En el cas de la pel·lícula polimèrica utilitzada com a exemple de model matemàtic a l'apartat anterior, la solució analítica desenvolupada podria haver-se assolit de forma molt més ràpida i senzilla mitjançant qualsevol procediment d'anàlisi numèrica assistida per ordinador. A més a més, aquesta anàlisi també resultaria útil en altres casos molt més complexos (i més reals), on el sistema adquirira

diferents geometries o propietats anisotròpiques, o bé allà on resultara impossible l'admissió d'algunes hipòtesis. Són exemples d'aquests casos les pel·lícules multicapa, les pel·lícules utilitzades en la construcció d'envasos o embolcalls de dimensions reduïdes o irregulars (on la transferència de matèria pot ser multidireccional), els materials amb propietats no uniformes ni constants, els fenòmens de transport multicomponent, o no regits per la segona llei de Fick, o bé aquells que inclouen turbulències o altres fluxos advectius de matèria a banda del transport molecular per difusió, o aquells sistemes en què la transferència de massa d'un component es troba lligada a la d'un altre compost o al transport simultani d'energia, o bé, en definitiva, qualsevol combinació possible de tots ells.

D'entre els abundants algoritmes numèrics que es recullen a la bibliografia els més destacables per la seva raonable senzillesa, al mateix temps que per la seva demostrada eficàcia, són: el mètode de les diferències finites, el mètode dels volums finits i el mètode dels elements finits. Tots ells resolen les equacions diferencials en derivades parcials discretitzant-les prèviament en subespais finits, per a reduir així els problemes a sistemes simples d'equacions algebraiques o diferencials fàcilment resolubles mitjançant els mètodes analítics convencionals.

En el mètode dels elements finits, per exemple, el producte de la discretització del domini de la PDE es tracta d'una multitud de nodes de malla i xicotets subdominis de mida finita, anomenats "elements", que es troben completament interconnectats i permeten ser tractats matemàticament un per un conformant un conjunt interrelacionat de models molt senzills i fàcils d'analitzar. Així doncs, aplicant l'anàlisi dels elements finits a aquests subdominis s'obté un valor aproximat de la solució real per a cada node, que serà tant més exacta quan més densa siga la malla generada en el domini de la funció que es pretén simular.

El procediment habitual per a resoldre una PDE mitjançant aquest mètode numèric segueix fonamentalment aquestes etapes (Beers, 2007):

- Expressió de la PDE en la seva forma feble (forma integral), tot separant les condicions de contorn de Dirichlet (les relacionades amb la concentració de propietat, C_i^P) i de Neumann (les relacionades amb el flux de propietat, $\frac{\partial C_i^P}{\partial z}$).

- Discretització del domini en elements finits, tot generant una malla de nodes interconnectats en forma poligonal (habitualment tetraedres o hexaedres en 3D, i quadrilàters o triangles no solapats en 2D).

- Aproximació de les funcions com a interpolació de valors nodals amb funcions de forma, normalment n-lineals o n-quadràtiques.
- Selecció de les funcions de test per a la verificació de la forma feble (per exemple, les definides en el mètode de Galerkin, basat en l'expressió de la funció de test de la solució com una combinació lineal del producte del valor de cada node per la corresponent funció de forma global).
- Obtenció del sistema lineal corresponent (amb una matriu no regular obtinguda a partir de l'assemblatge de les matrius associades a cada element).
- Imposició de les condicions de contorn (amb l'ajuda de diversos mètodes).
- Resolució de la matriu del sistema lineal mitjançant els mètodes convencionals de l'àlgebra lineal en espais de dimensió finita.

Els principals avantatges que presenta el mètode dels elements finits en comparació amb el mètode de les diferències o dels volums finits resideixen en la possibilitat d'utilitzar malles irregulars i/o desestructurades (ço és, d'elements finits amb mida i forma variables), en la possibilitat d'imposar condicions de contorn de forma sistemàtica (sense casuística), i en la seva creixent convergència per a divisions dels elements finits successivament més fines.

2. MARC DE LA RECERCA

2.1. Temàtica i fonaments

L'envasat actiu és una innovadora tecnologia de conservació dels aliments que, al llarg d'aquestes darreres dècades, ha demostrat reiteradament la seva capacitat per, no només mantenir i millorar la qualitat i salubritat dels aliments envasats, augmentant-ne així la vida útil, sinó també per millorar-ne, fins i tot, les característiques organolèptiques i nutritives originals, esdevenint en conseqüència un important punt de trobada entre els interessos dels consumidors i els de les empreses alimentàries. Dins d'aquesta nova tecnologia, l'envasat antimicrobià és el sistema que ha despertat un major interès als darrers temps, atesa la seva provada eficàcia contra la contaminació i proliferació de microorganismes patògens o alterants dels aliments, i, molt especialment, per la seva possibilitat d'incorporar ingredients actius d'origen natural, com són els olis essencials d'espècies o herbes aromàtiques, en la composició química dels materials d'envasat.

En aquest context, són nombroses les investigacions realitzades en temps recents que han tractat de desenvolupar i caracteritzar nous materials d'envasat actiu amb capacitats antimicrobianes, així com d'avaluar la seva efectivitat biostàtica o biocida contra determinats microorganismes nocius de presència habitual en aliments, tals com bacteris, fongs, i llevats. No obstant això, són escassos els treballs que han considerat l'estudi d'envasos complets, incloent-hi tant els materials d'envasat, com l'atmosfera externa, l'espai de cap, i el propi aliment, així com els diversos compostos químics que hi participen en els processos associats de transferència de matèria, i les possibles interaccions entre ells. Precisament, i en aquest sentit, també han estat poc estudiades les interaccions fisicoquímiques entre l'agent antimicrobià i la matriu portadora, així com els seus potencials efectes adversos sobre les propietats funcionals del polímer actiu en tant que material d'envasat, ço és, respecte de les seves propietats mecàniques, tèrmiques, òptiques, superficials, i barrera.

D'altra banda, un dels principals obstacles encara a vèncer per a l'extensiva implantació de l'envàs antimicrobià a nivell comercial rau en el control i manteniment de la seva activitat al llarg de tot el període de conservació de l'aliment. Aquest problema ha estat tractat freqüentment a la literatura i generalment abordat amb la introducció de modificacions químiques i/o estructurals a la matriu portadora de l'agent actiu, si bé amb uns enfocaments i resultats finals molt diferents.

Una de les possibilitats consisteix en la utilització de polímers hidròfils per a exercir aquesta funció, atesa llur capacitat per a variar les propietats funcionals, en especial la permeabilitat, en funció de la

humitat relativa, constituent així uns materials idonis per a l'envasat actiu de productes alimentaris amb elevada activitat d'aigua. No obstant això, la major part dels polímers hidròfils provats a la literatura com a materials portadors d'activitat no són polímers habituals d'envasat, sinó biopolímers d'origen natural que es troben encara sota intensa recerca per esdevenir-ne els materials substitutius en un pròxim futur. Aquest fet es deu, d'una banda, a l'escassedat de polímers convencionals amb caràcter significativament hidròfil, i, d'una altra, a les dificultats per a incorporar-los el compost actiu de forma eficient, així com per a fabricar els envasos finals sense provocar-los degradacions o induir possibles interaccions entre els materials que els componen, especialment a escala industrial.

Una altra possibilitat consisteix en la modificació de la morfologia microestructural de la matriu polimèrica per tal d'adaptar-la als requeriments imposats per l'envàs objectiu, mitjançant la utilització de dispersions polimèriques (làtex) sotmeses a diferents condicions tèrmiques de processament. Aquesta solució és una via innovadora, i quasi inexplorada, de fabricar envasos actius amb propietats fàcilment controlables i adaptables als requeriments específics del producte conservat, no existint encara a la literatura cap publicació científica on s'haja utilitzat aquesta tecnologia per al desenvolupament de materials d'envasat actiu amb capacitats antimicrobianes.

Per últim, una tercera possibilitat consisteix en l'emprament de nanocompòsits polimèrics com a matrius portadores de substàncies actives, per tal de controlar-ne la difusió vers l'aliment conservat, i, per tant, l'acció antimicrobiana finalment exercida, a través de la forma, mida, càrrega, distribució, i orientació, de les nanopartícules encastades. En aquest cas, si bé la literatura recull alguns treballs on es desenvolupa aquest tipus de materials i s'avalua llur eficàcia contra el creixement microbià, són escassos els estudis existents on se'ls efectua una caracterització completa, tant des del punt de vista de la millora assolida en les propietats actives com en les propietats funcionals, i molt especialment en el cas dels polímers hidròfils esmentats anteriorment.

Una de les ferramentes que pot contribuir en major mesura a la comprensió de l'activitat d'aquests envasos, a la predicció del seva evolució amb el temps sota diferents condicions de treball, i a la modificació del seu disseny fonamental per tal d'ajustar-ne el comportament a la consecució d'un determinat objectiu, és la modelització i simulació matemàtica dels fenòmens de transferència de matèria associats al seu funcionament. En aquest sentit, els models matemàtics constitueixen una eina molt valuosa per a l'obtenció de descripcions exhaustives de tots els processos fisicoquímics involucrats al sistema d'envasat sense la necessitat de realitzar assajos experimentals, sinó únicament a través de l'execució de càlculs computeritzats, amb el conseqüent estalvi en costos i recursos humans o materials. Tanmateix, d'entre els pocs treballs existents a la literatura on es desenvolupen models

matemàtics per a envasos actius, la major part tan sols estudia el transport de matèria a través dels materials d'envasat i, més concretament, dels agents actius a través de llur matriu portadora, menystenint així els altres compostos o dominis materials que configuren en conjunt el sistema complet d'envasat actiu, com poden ser l'espai de cap o el propi aliment, a l'igual que les diverses possibles interaccions entre ells.

En canvi, en el cas concret del transport d'un solut a través de la matriu d'un nanocompòsit polimèric, la literatura conté desenes de treballs publicats des de finals del segle XIX, atesa la importància i interès suscitats per aquests materials d'ençà de la seva invenció. Malgrat tot, encara no es disposa en l'actualitat de cap model d'aquest tipus que reunisca tant les qualitats de senzillesa i facilitat d'ús, característiques dels primers enfocaments teòrics, com les d'exactitud i universalitat, pròpies dels desenvolupaments més recents. En aquest sentit, s'ha constatat àmpliament que els primers models proposats no resulten de total aplicabilitat, ni permeten assolir uns nivells de precisió acceptables, en tot l'ampli ventall d'estructures nanocompostes existents a l'actualitat, mentre que els models més recents estan atenyent cada cop més extensió i complexitat, requerint cada volta més paràmetres i de més difícil estimació, i dificultant així, en definitiva, la seva usabilitat real.

2.2. Objectius

Atesos els fonaments anteriors, l'objectiu general que es proposa assolir la present tesi doctoral consisteix en el desenvolupament de nous materials polimèrics destinats a l'envasat actiu alimentari amb capacitat per a exercir una efectiva acció antimicrobiana sobre el producte conservat, mitjançant la incorporació de diverses substàncies actives d'origen natural, així com de diversos mecanismes de control i manteniment de la seva activitat, la caracterització de llurs propietats actives i funcionals, i l'optimització del disseny fonamental dels envasos finals a través de la modelització i simulació matemàtica de tots els processos de transferència de matèria associats al seu funcionament.

Per a la consecució d'aquest objectiu general s'han plantejat de bestreta tota una sèrie d'objectius parcials o específics:

- Desenvolupament de pel·lícules i recobriments d'envasat actiu amb capacitat antimicrobiana mitjançant la incorporació de diverses substàncies actives d'origen natural a l'interior de llur matriu polimèrica.
- Desenvolupament de pel·lícules i recobriments d'envasat actiu amb capacitat de retenció de compostos volàtils i de control del seu alliberament a l'aliment conservat.
- Caracterització de les propietats actives dels materials desenvolupats mitjançant la determinació dels coeficients de solubilitat i difusió dels agents actius a través de llur matriu polimèrica en funció de la temperatura i la humitat relativa.
- Caracterització de les propietats funcionals dels materials desenvolupats, ço és, morfològiques, mecàniques, tèrmiques, òptiques, superficials, i barrera, i de la seva relació amb les possibles interaccions fisicoquímiques entre els compostos actius i llurs matrius portadores.
- Proposició de models matemàtics basats en el mètode dels elements finits (FEM) que descriguen adequadament tots els processos de transferència de matèria associats al funcionament d'envasos actius construïts amb els materials desenvolupats.
- Avaluació de la capacitat descriptiva dels models proposats mitjançant la simulació del comportament de diversos sistemes complets d'envasat actiu, estudiats en condicions habituals de conservació dels aliments, i la comparació de les seves prediccions teòriques amb els resultats experimentals obtinguts d'assajos amb envasos reals.
- Optimització del disseny fonamental dels envasos estudiats, i, en conseqüència, del seu rendiment antimicrobià, mitjançant la simulació i predicció de llur comportament a llarg termini, i sota diferents condicions de treball, amb l'ajut dels models proposats.

2.3. Desenvolupament

La present tesi doctoral està composta per sis treballs originals d'investigació, el títol, referència i contingut dels quals es detallen a continuació:

I. **Cerisuelo, J. P., Muriel – Galet, V., Bermúdez, J. M., Aucejo, S., Català, R., Gavara, R., Hernández – Muñoz, P. (2012). Mathematical model to describe the release of an antimicrobial agent from an active package constituted by carvacrol in a hydrophilic EVOH coating on a PP film. *Journal of Food Engineering*, 110 (1), 26 – 37.**

En aquest treball s'han desenvolupat pel·lícules d'envasat actiu amb capacitat antimicrobiana destinades a la conservació de productes de IV gamma, compostes per una capa funcional de polipropilè (PP) finament recoberta amb un copolímer hidròfil d'etilè i alcohol vinílic (EVOH) que contenia un 5 % de carvacrol com a agent antimicrobià d'origen natural. Tot seguit, s'han caracteritzat les propietats actives del nou material mitjançant la determinació dels coeficients de solubilitat i difusió del compost actiu a través d'ambdós polímers, PP i EVOH, en funció de la temperatura i la humitat relativa. A continuació, s'ha proposat un model matemàtic del sistema complet d'envasat actiu basat en el mètode dels elements finits, amb l'objectiu d'obtenir una descripció exhaustiva de tots els processos de transferència de matèria associats a l'envàs, així com de simular el seu comportament en condicions reals de treball. Finalment, s'ha efectuat la validació del model desenvolupat mitjançant la comparació de les seves prediccions teòriques amb els resultats experimentals obtinguts d'assajos amb envasos reals, i s'han portat a terme diverses simulacions addicionals per tal d'optimitzar-ne el disseny i millorar-ne així el rendiment antimicrobià.

II. **Cerisuelo, J. P., Bermúdez, J. M., Aucejo, S., Català, R., Gavara, R., Hernández – Muñoz, P. (2013). Describing and modeling the release of an antimicrobial agent from an active PP / EVOH / PP package for salmon. *Journal of Food Engineering*, 116 (2), 352 – 361.**

En aquest treball s'han desenvolupat pel·lícules d'envasat actiu amb capacitat antimicrobiana destinades a la conservació de peix fresc, compostes per dues capes exteriors i funcionals de polipropilè (PP) i una capa interior activa d'un copolímer hidròfil d'etilè i alcohol vinílic (EVOH) que contenia un 6.5 % de carvacrol com a agent antimicrobià d'origen natural. Tot seguit, s'han

caracteritzat les propietats actives del nou material mitjançant la determinació dels coeficients de solubilitat i difusió del compost actiu a través d'ambdós polímers, PP i EVOH, així com de l'aliment conservat, un filet de salmó, en funció de la temperatura i la humitat relativa. A continuació, s'ha proposat un model matemàtic del sistema complet d'envasat actiu basat en el mètode dels elements finits, amb l'objectiu d'obtenir una descripció exhaustiva de tots els processos de transferència de matèria associats a l'envàs, així com de simular el seu comportament en condicions reals de treball. Finalment, s'ha efectuat la validació del model desenvolupat mitjançant la comparació de les seves prediccions teòriques amb els resultats experimentals obtinguts d'assajos amb envasos reals, i s'han portat a terme diverses simulacions addicionals per tal d'optimitzar-ne el disseny i millorar-ne així el rendiment antimicrobià.

III. **Cerisuelo, J. P., Gavara, R., Hernández – Muñoz, P. (2015). Diffusion modeling in polymer – clay nanocomposites for food packaging applications through finite element analysis of TEM images. *Journal of Membrane Science*, 482, 92 – 102.**

En aquest treball s'han desenvolupat pel·lícules d'envasat alimentari constituïdes per tres nanocompòsits hidròfils de zeïna (prolamina del panís) i d'un copolímer d'etilè i alcohol vinílic (EVOH) que contenien un 2 – 4 % de bentonita sòdica com a càrrega inorgànica. Tot seguit, s'ha avaluat llur morfologia microestructural a través de microscòpia electrònica de transmissió (TEM), i s'ha desenvolupat un procediment alternatiu i innovador per a estimar el grau de millora assolit en les seves propietats barrera o de retenció, basat en la modelització i simulació matemàtica dels processos de difusió que esdevenen al seu interior, mitjançant el tractament gràfic i subsegüent anàlisi pel mètode dels elements finits (FEM) de les micrografies electròniques adés adquirides. Per últim, s'ha efectuat la validació del nou model mitjançant la comparació de les seves prediccions teòriques amb les dades obtingudes en assajos de permeació a l'oxigen, amb altres valors experimentals reportats en un treball previ, i amb els resultats teòrics predits per 18 models anteriors recollits a la literatura.

IV. **Cerisuelo, J. P., Alonso, J., Aucejo, S., Gavara, R., Hernández – Muñoz, P. (2012). Modifications induced by the addition of a nanoclay in the functional and active properties of an EVOH film containing carvacrol for food packaging. *Journal of Membrane Science*, 423 – 424, 247 – 256.**

En aquest treball s'han desenvolupat pel·lícules d'envasat actiu amb capacitat antimicrobiana, constituïdes per un nanocompòsit hidròfil d'un copolímer d'etilè i alcohol vinílic (EVOH) que contenia un 2 % de bentonita sòdica com a càrrega inorgànica i un 5 % de carvacrol com a agent antimicrobià d'origen natural. A continuació, se n'ha avaluat l'aparença macroscòpica i la morfologia microestructural, a través de microscòpia electrònica de rastreig (SEM) i de transmissió (TEM). Finalment, s'han determinat les isotermes d'absorció d'aigua, i s'han caracteritzat la resta de propietats actives i funcionals del nou material amb el mesurament dels seus coeficients de solubilitat, difusió, i permeabilitat a l'oxigen i diòxid de carboni, dels coeficients de solubilitat i difusió del compost actiu, i de les temperatures de fusió i transició vítria, en funció de la humitat relativa, tot comparant els resultats obtinguts amb els derivats del polímer original.

V. **Cerisuelo, J. P., Gavara, R., Hernández – Muñoz, P. (2014). Natural antimicrobial – containing EVOH coatings on PP and PET films: Functional and active property characterization. *Packaging Technology and Science*, 27 (11), 901 – 920.**

En aquest treball algunes pel·lícules seleccionades d'entre les desenvolupades en treballs anteriors han estat sotmeses a diverses anàlisis fisicoquímiques per tal d'avaluar-ne la idoneïtat en tant que materials actius d'envasat alimentari. En concret, s'han fabricat pel·lícules actives amb capacitat antimicrobiana, tant a escala de laboratori com a escala industrial, compostes per una capa funcional de polipropilè (PP) o tereftalat de polietilè (PET) finament recoberta amb un copolímer hidròfil d'etilè i alcohol vinílic (EVOH) que contenia un 7.5 – 10 % de carvacrol, citral, oli essencial de timó, o oli essencial de canonet de canyella, com a agent antimicrobià d'origen natural, junt amb, segons el cas, un 2 % de bentonita sòdica com a càrrega inorgànica. Tot seguit, s'ha avaluat l'estabilitat dels esmentats recobriments sobre diversos substrats de PP i PET pretractats amb irradiació UV, descàrrega d'efecte corona, o imprimacions basades en poliuretà (PU) i polietilenimina (PEI), mitjançant assajos d'adhesió i de soldadura tèrmica. A continuació, s'han determinat les propietats funcionals de les pel·lícules resultants, ço és, mecàniques, òptiques, superficials, i barrera, i s'han caracteritzat llurs propietats actives amb el mesurament dels coeficients de partició del compost actiu entre els polímers

constituents, així com de l'eficiència de la seva incorporació a la matriu portadora. Finalment, s'han avaluat els efectes de la modificació microestructural d'aquesta capa material, basada en la incorporació de nanopartícules de bentonita sòdica a la seva matriu polimèrica, sobre el rendiment antimicrobià d'envasos actius conformats amb les esmentades pel·lícules i estudiats en condicions reals de treball i, més concretament, sobre la seva capacitat de retenció per l'agent actiu i de control del seu alliberament a l'aliment conservat.

VI. **Cerisuelo, J. P., Gavara, R., Hernández – Muñoz, P. (2015). Antimicrobial films and coatings for food packages based on carvacrol and latex dispersions of ethylene copolymers: Study of the matrix effects on their active and functional properties. *Polymer International*, (en revisió).**

En aquest treball s'han desenvolupat pel·lícules i recobriments d'envasat actiu amb capacitat antimicrobiana, constituïts per copolímers d'etilè de diversa polaritat (poli(etilè – co – octè) (LLDPE), poli(etilè – co – acetat vinílic) (EVA), poli(etilè – co – àcid metacrílic) (EMA), i poli(etilè – co – metacrilat alcalí) (ION)), en forma de dispersions aquoses (làtex), que contenien un 5 % de carvacrol com a agent antimicrobià d'origen natural. A continuació, s'ha avaluat la morfologia microestructural dels nous materials per mitjà de microscòpia electrònica de rastreig (SEM), se'ls han determinat les propietats funcionals, ço és, mecàniques, tèrmiques, òptiques, superficials, i barrera, i s'han caracteritzat llurs propietats actives amb el mesurament dels coeficients de solubilitat i difusió del compost actiu a través del seu si. Finalment, s'han relacionat els resultats obtinguts en les anteriors anàlisis amb les modificacions introduïdes en llur matriu polimèrica en termes de polaritat i estructura interna.

3. RESULTATS I DISCUSSIÓ

3.1. Materials actius basats en matrius hidròfiles de copolímer d'etilè i alcohol vinílic

Per tal de donar compliment als objectius proposats en aquesta tesi doctoral, els dos primers treballs desenvolupats foren fonamentalment enfocats a l'estudi de l'EVOH com a nou material d'envasat actiu. En efecte, i tal i com s'ha explicat a la secció 1.1.2.1, l'EVOH és un copolímer d'etilè i alcohol vinílic emprat habitualment en la industria alimentària per a l'envasat de productes sensibles a l'oxidació o al deteriorament aromàtic, degut a les seves excel·lents característiques barrera en condicions de sequedat. No obstant això, el seu marcat caràcter hidròfil el fa especialment vulnerable en condicions d'alta humitat ambiental, com són les generades pels aliments d'elevada activitat d'aigua, deteriorant així de forma considerable la seva resistència al transport de permeants, al temps que les seves notables propietats mecàniques. Aquest desavantatge, junt amb el fet que la seva incorporació als materials d'envasat sol encarir-ne el preu, limita el seu ús a les pel·lícules multicapa, on pot trobar-se, tant en forma de recobriment sobre substrats funcionals d'altres materials, com, més habitualment, inserit entre capes de polímers hidròfobs que l'aïllen i protegeixen de l'exterior. Tanmateix, és precisament aquesta propietat la que el fa especialment adient per a l'envasat actiu de productes alimentaris d'elevada activitat d'aigua, atesa la seva capacitat per a retenir i preservar els compostos actius durant les etapes d'emmagatzemament dels materials d'envasat, així com de termoconformat, ompliment i segellat dels envasos finals, per a, tot seguit, permetre el seu alliberament a l'aliment conservat tant bon punt la humitat ambiental generada per aquest és capaç de modificar-li substancialment les característiques barrera.

Així doncs, al primer treball constituent d'aquesta tesi doctoral (**Treball I**) es van avaluar les propietats actives de l'EVOH en tant que material portador de carvacrol, un agent antimicrobià d'origen natural, mitjançant la determinació dels coeficients de difusió i solubilitat del compost actiu en funció de la concentració d'aigua a la matriu polimèrica. Com a resultat, es va observar que el valor de la constant de Henry del carvacrol (inversa del coeficient de solubilitat) creixia sigmoïdalment amb la concentració d'aigua al polímer, augmentant fins a dos ordres de magnitud quan la humitat relativa ambiental passava del 40 al 100 %. Aquesta evolució s'ajustava correctament al model de Peleg, una equació sigmoïdal de 3 paràmetres basada en la forma matemàtica de la funció de distribució de Fermi, i podia explicar-se en termes de polaritat i estructura de la matriu polimèrica. Així, amb l'extensiva captació de molècules d'aigua, la matriu de l'EVOH hauria experimentat un augment de polaritat, i/o uns fenòmens de relaxació polimèrica, que haurien permès o promogut l'alliberament de llurs molècules

de carvacrol al medi circumdant. En contrast, el valor d'aquest paràmetre al polipropilè (PP), molt superior al de l'EVOH, no variava significativament amb la humitat relativa, d'acord amb la hidrofòbia característica d'aquest material. Tanmateix, la distància que separava aquest valor de l'obtingut a l'EVOH evidenciava una major solubilitat de les molècules de carvacrol en aquest darrer polímer, que podria estar estretament relacionada amb la naturalesa amfifílica d'ambdós materials.

Pel que fa a la difusivitat del carvacrol, es va observar que el valor del coeficient de difusió a l'EVOH creixia linealment amb la seva concentració d'aigua, augmentant fins a quatre ordres de magnitud en passar la humitat relativa del 0 al 100 %. En canvi, i a l'igual que adés, el valor d'aquest paràmetre al PP romania constant i de magnitud superior sota qualsevol condició ambiental. Novament, l'efecte combinat de la relaxació estructural del polímer i la menor solubilitat del compost actiu a la seva matriu podrien estar darrere d'aquesta evolució amb el contingut en humitat del material. D'altra banda, ateses les dificultats trobades per a mesurar experimentalment el valor d'aquest paràmetre en condicions de sequedat i a temperatura ambiental, es va emprendre un estudi paral·lel enfocat a avaluar la seva variació amb la temperatura en absència d'humitat relativa, i a calcular així finalment el valor cercat per simple extrapolació de la funció obtinguda. Com a resultat d'aquest, es va observar que el valor del coeficient de difusió augmentava un ordre de magnitud en passar la temperatura de 42 a 77 °C, i exhibia una evolució amb aquesta que s'ajustava correctament a la llei d'Arrhenius.

Un cop avaluades les propietats actives de l'EVOH amb carvacrol, i confirmada la seva capacitat per a retenir el compost actiu i controlar-ne l'alliberament amb la humitat relativa, es va fer ús del nou material en la construcció d'envasos antimicrobians per a la conservació de peix fresc (**Treball II**) i de productes de IV gamma (**Treball I**). En el primer cas, es fabricaren pel·lícules multicapa per coextrusió, compostes per una capa central activa d'EVOH amb un 6.5 % de carvacrol, dues capes externes funcionals de PP, i dues capes intermèdies adhesives de PP empeltat amb anhídrid maleic, i s'empraren en el tancament de barquetes rígides de PP / EVOH / PP destinades a la conservació de salmó fresc. En el segon cas, es fabricaren pel·lícules bicapa per càsting, compostes per un recobriment actiu d'EVOH amb un 5 % de carvacrol sobre un substrat funcional de PP, i s'empraren en la confecció de bosses flexibles destinades a la conservació d'amanida a punt per consumir. En ambdós casos, les pel·lícules elaborades presentaren un aspecte homogeni i una estructura uniforme, i atenyeren una concentració final del compost actiu propera al 70 – 80 % del seu valor nominal.

Pel que fa als envasos construïts amb aquestes, les barquetes allotjaren un filet de salmó fresc, mentre que les bosses d'amanida es farciren amb diverses porcions d'aigua gelificada en tant que simulant alimentari dels seus principals ingredients. Un cop omplerts i hermèticament tancats, els envasos foren

emmagatzemats en cambres climàtiques durant una setmana, i la concentració de carvacrol atesa al seu espai de cap fou regularment monitoritzada en el decurs del temps. Com a resultat, s'observà que les bosses d'amanida alliberaren molt ràpidament el compost actiu durant els primers minuts de conservació de l'aliment, generant així un acusat pic de concentració a l'atmosfera interior dels envasos abans de la primera hora posterior al seu tancament. Tanmateix, passat aquest sobtat pic, la concentració de carvacrol començà a experimentar de nou un pronunciat i continu decreixement, que es perllongà durant els dies subsegüents fins a assolir valors inferiors a la concentració mínima inhibitòria d'algunes bactèries nocives, com l'*Escherichia coli*, la *Listeria monocytogenes*, o la *Salmonella enterica*, al cap de tan sols 72 h de l'inici de l'experiment. Contràriament, a les barquetes de salmó, la concentració de compost actiu present a la superfície de l'aliment romangué quasi indetectable durant les 8 primeres hores de conservació del producte, rere les quals experimentà un sobtat creixement de progressió sigmoïdal que es perllongà fins el quart dia d'emmagatzematge, moment en què ja quedà definitivament estabilitzada entorn al seu valor màxim.

Dels resultats anteriors, obtinguts amb l'estudi dels envasos actius, s'evidencià la necessitat de millorar-ne el rendiment antimicrobià, i, en conseqüència, les propietats actives dels materials que els componen. En aquest sentit, l'estudi posà de manifest les limitacions d'aquests materials a l'hora de controlar l'alliberament de l'agent incorporat, i, en particular, llur vulnerabilitat front als seus pics o caigudes de concentració, així com al seu retard en l'assoliment d'uns nivells estables. Per aquest motiu, als dos treballs presentats adés es va emprendre també la modelització matemàtica d'ambdós sistemes d'envasat actiu, mitjançant el conegut mètode dels elements finits (FEM), per tal d'esbrinar els paràmetres estructurals i/o condicions ambientals que regien en major mesura el seu comportament, i poder trobar així, en última instància, els camins existents vers la seva optimització.

Així doncs, en el cas de les bosses d'amanida, el model inclogué l'estudi del transport per difusió de les molècules d'aigua i de carvacrol a través dels diferents dominis materials que componien el sistema, ço és, l'atmosfera externa, el substrat funcional de PP, el recobriment actiu d'EVOH, i l'espai de cap de l'envàs, així com l'acoblament multifísic entre ambdós, derivat de la dependència del coeficient de difusió del carvacrol amb la humitat relativa. Pel què fa a les barquetes de salmó, a banda de tots els processos i dominis ja esmentats, també es va incloure el transport de carvacrol a través de la matriu interna del propi aliment, i l'inflament de la capa central d'EVOH per efecte de l'absorció d'aigua. En ambdós casos els models proposats foren validats experimentalment en confrontar llurs prediccions teòriques amb les dades empíriques recollides a l'estudi anterior, permetent així de comprovar llur capacitat descriptiva respecte d'aquests dos sistemes d'envasat actiu.

Com a resultat de l'avaluació, es constatà que les corbes teòriques d'alliberament o acumulació de carvacrol a l'aliment conservat s'ajustaven satisfactòriament als valors mesurats adés de forma experimental, inferint-se, en conseqüència, que els models desenvolupats per als citats envasos devien descriure correctament tots els processos de transferència de matèria associats al seu funcionament. Amb la reeixida validació dels models matemàtics, aquests possibilitaren l'execució de noves simulacions encaminades a determinar els valors de les variables estructurals i/o ambientals que minimitzaven les pèrdues d'activitat dels envasos, maximitzant així llur rendiment antimicrobià. D'aquestes anàlisis de sensibilitat i optimització es conclogué que, des del punt de vista del manteniment dels nivells d'activitat, l'estructura òptima de les pel·lícules bicapa amb què es conformaren les bosses d'amanida devia ser aproximadament: PP (30 µm) / EVOH (10 µm), mentre que l'estructura idònia per a les pel·lícules multicapa amb què es tancaren les barquetes de salmó devia apropar-se a: PP (20 µm) / EVOH (20 µm) / PP (2 µm). A més a més, dels resultats d'aquestes simulacions també es va desprendre que la humitat ambiental podia arribar a afectar molt greument el rendiment actiu dels envasos i, per consegüent, que devia evitar-se, en la mesura del possible, la seva exposició prolongada a humitats relatives superiors al 60 %.

Després del desenvolupament d'aquests nous materials, i en paral·lel a l'estudi de les seves propietats actives, s'abordà l'avaluació de la seva idoneïtat funcional en tant que materials d'envasat alimentari, així com la implementació de la seva producció a nivell industrial. Així doncs, al **Treball V** de la present tesi doctoral es seleccionaren algunes pel·lícules actives d'entre els materials estudiats als treballs anteriors, es desenvoluparen algunes altres d'estructura i característiques anàlogues, i es portà llur fabricació a escala industrial per tal de comprovar la reproductibilitat dels resultats obtinguts al laboratori i determinar-los les propietats actives i funcionals més rellevants. Concretament, es fabricaren cinc pel·lícules bicapa per rotogravat, compostes per un substrat funcional de PP o PET finament recobert amb una capa d'EVOH que contenia un 7.5 – 10 % de carvacrol, citral, oli essencial de timó o oli essencial de canonet de canyella com a agent antimicrobià d'origen natural.

Respecte a les esmentades propietats funcionals, en primer lloc s'avaluà l'estabilitat dels recobriments d'EVOH sobre els substrats de PP i PET mitjançant assajos d'adhesió i de termosegellabilitat. Aquest estudi preliminar fou motivat pels resultats obtinguts al **Treball I** d'aquesta tesi doctoral, on diversos substrats de PP foren sotmesos a un tractament superficial amb irradiació UV, previ a l'aplicació del recobriment actiu d'EVOH, amb l'objectiu d'augmentar la força d'adhesió entre ambdós polímers, tot millorant els mecanismes d'ancoratge desenvolupats en llur interfície. No obstant això, aquest pretractament s'evidencià insuficient durant el desenvolupament experimental de l'anterior treball,

atès què tan sols aconseguí de generar una feble adhesió entre ambdós materials, no arribant a conferir-los l'estabilitat necessària com per a mantenir la integritat estructural de les pel·lícules conformades fins a les darreres anàlisis del citat estudi.

Per aquests motius, l'efecte compatibilitzador d'aquest tractament superficial es comparà al **Treball V** amb el d'altres tècniques semblants, com són la descàrrega d'efecte corona, o les imprimacions basades en poliuretà (PU) i polietilenimina (PEI). D'aquest estudi previ es constatà que l'aplicació d'una imprimació de PEI sobre les superfícies dels substrats de PP i PET sotmeses prèviament a una descàrrega d'efecte corona constituïa la millor tècnica d'ancoratge disponible per als recobriments actius d'EVOH, atès que la forta adhesió generada entre ambdues capes materials n'impedia la separació física per mitjans convencionals, al temps que permetia millorar les característiques de termosegellabilitat exhibides pels substrats originals, arribant, fins i tot, a duplicar-ne els valors de la resistència a l'obertura per tracció dels segells formats. Així doncs, fruit d'aquests resultats, es convingué d'implementar l'anterior pretractament en la producció industrial de les cinc pel·lícules desenvolupades, per tal de garantir així llur estabilitat estructural durant tota la resta d'anàlisis fisicoquímiques previstes seguidament en aquest treball.

Pel que fa a aquestes anàlisis, un cop es disposà de les esmentades pel·lícules a escala industrial es procedí a determinar-los la resta de propietats funcionals de rellevància per a l'envasat alimentari, ço és, mecàniques, òptiques, superficials, i barrera. Així doncs, mecànicament, tots els materials actius mostraren un lleuger, però significatiu, empitjorament de llur resistència a la tracció, deformació al trencament, i mòdul de Young, respecte als valors assolits pels substrats originals. Malgrat que les diferències observades restaven inferiors al 15 % en tots els casos, sí que resultaven indicatives d'unes deficients propietats mecàniques dels recobriments dipositats, i/o d'un lleuger deteriorament de llur matriu substrat per mecanismes de reacció o de plastificació amb els compostos actius.

D'altra banda, des del punt de vista òptic, tant les pel·lícules passives estudiades com els corresponents polímers substrat mostraren una tènue coloració (C^*_{ab} = 0.13 – 0.73) i una elevada lluminositat (L^* = 97 – 99). Tanmateix, amb la presència de compostos actius al seu si, el valor d'ambdós paràmetres empitjorà significativament a tots els materials (augmentant fins a un punt el primer i disminuint fins a dos el segon), si bé de forma molt lleugera i, per tant, no perceptible a ull nu.

En quant a les propietats superficials, s'observà que, sota les condicions experimentals assajades en aquest estudi, la mullabilitat de l'EVOH blanc resultava molt baixa i semblant a la del PP. No obstant això, amb la incorporació de qualsevol agent actiu a la seva matriu, l'esmentada propietat millorava

considerablement, atenyent reduccions d'entre el 33 i el 46 % en el valor de l'angle de contacte de l'aigua pura sobre la seva superfície.

Finalment, respecte a les característiques barrera, ambdós substrats, de PP i PET, exhibiren una permeància a l'oxigen de valor elevat i invariable amb la humitat relativa, que encara es multiplicava per 10 en el cas de la transmissió del diòxid de carboni, en correspondència amb els nombrosos resultats de permeació reportats a la literatura. En canvi, quan aquests materials es recobriren amb una fina capa d'EVOH la permeància de les pel·lícules formades quedà reduïda a una petita fracció del seu valor original (1/160 en PP i 1/6 en PET) sota condicions de sequedat. Tanmateix, degut a la marcada naturalesa hidròfila d'aquest polímer, l'efecte barrera aconseguit als materials tornava a dissipar-se gradualment amb l'augment de la humitat relativa, recuperant les permeàncies llur magnitud anterior fins a atènyer el 70 – 80 % del valor inicial assolit pels materials de substrat.

Així doncs, a partir d'aquests resultats, es va concloure que la incorporació d'agents actius als nous materials desenvolupats permetia millorar considerablement les seves propietats superficials sense deteriorar de forma important o apreciable les seves propietats mecàniques, òptiques, i barrera, resultant, en conseqüència, funcionalment idonis per a qualsevol aplicació d'envasat alimentari.

A banda de totes aquestes propietats funcionals, les anàlisis fisicoquímiques adés esmentades també inclogueren la caracterització d'altres propietats d'interès per al seu emprament en l'envasat actiu, fonamentalment, de llur capacitat de retenció pels compostos incorporats. Aquesta propietat activa es determinà mitjançant el mesurament dels coeficients de partició d'aquelles substàncies entre els polímers constituents, així com de l'eficiència de la seva incorporació a la matriu portadora. Respecte a aquest darrer paràmetre, al treball s'observà que, en termes generals, la concentració d'agent actiu romanent a les pel·lícules finals tan sols atenyia entre el 40 i el 60 % del seu valor nominal, fet que els suposava unes importants pèrdues d'activitat en funció de la volatilitat pròpia de cada molècula. Pel que fa als coeficients de partició, es constatà que totes les substàncies actives resultaven generalment molt més solubles o afins pels seus recobriments portadors d'EVOH que pels corresponents substrats, si bé, en alguns casos, com ara el citral en PP/EVOH o l'oli de canonet de canyella en PET/EVOH, la migració del compost vers la matriu de substrat podia esdevenir molt significativa.

3.2. Materials actius basats en matrius hidròfiles i nanocompostes d'EVOH i bentonita

D'aquests darrers resultats i, en general, de tots aquells obtinguts als tres primers treballs que componen la present tesi doctoral, es pogué constatar la notable capacitat de l'EVOH per a retenir, preservar i alliberar diferents tipus de substàncies actives, i, per tant, la seva idoneïtat com a material portador d'activitat per a la construcció d'envasos alimentaris. Tanmateix, tots aquests treballs també posaren de manifest la seva feblesa a l'hora de controlar, per si sol, l'extensió i velocitat dels processos esmentats i, en conseqüència, el comportament i rendiment actiu dels envasos finals. Per aquesta raó, als **Treballs III**, **IV,** i **V** d'aquesta tesi s'abordà el potencial millorament de les seves característiques actives i funcionals mitjançant la modificació estructural de la seva matriu polimèrica, amb la incorporació d'una càrrega inorgànica i nanomètrica al seu interior. D'aquesta manera, i segons recull l'extensa literatura revisada, esperava obtenir-se un nou material nanocompost amb major capacitat de retenció de compostos actius, tant respecte a llur pèrdua per evaporació durant la fabricació dels materials com respecte a llur alliberament per difusió durant la conservació dels aliments.

Com ja s'ha esmentat anteriorment, a l'apartat 1.1.2.2.3, aquesta millora en la retenibilitat del nou material és sempre conseqüència de la reducció en la difusivitat, solubilitat, i, per tant, permeabilitat, de les molècules de solut en migrar pel seu interior, resultant així el seu abast d'una magnitud molt variable i dependent de les seves principals característiques geomètriques (mida i forma de les partícules, concentració, distribució, orientació, etc.). Aquesta dependència es formula habitualment a través d'equacions teòriques, que relacionen aquestes variables microestructurals del material amb la reducció en la difusivitat experimentada pels soluts a la seva matriu, també coneguda com difusivitat relativa. Les esmentades equacions permeten doncs, mitjançant l'estimació d'aquest paràmetre, quantificar aproximadament el grau de millora assolit als nanocompòsits respecte dels polímers originals, fet que ha convertit llur deducció analítica en l'objectiu principal de nombrosos models teòrics desenvolupats d'ençà del segle XIX.

Amb tot, malgrat el gran nombre de models matemàtics disponibles a la literatura, i la seva repetida validació experimental en el temps, cap d'ells no ha demostrat reunir les qualitats necessàries de fiabilitat, precisió, i simplicitat, o facilitat d'ús, per a garantir la seva total aplicabilitat a l'ampli ventall d'estructures nanocompostes existents a l'actualitat. En aquest sentit, s'ha constatat que els algorismes més antics i senzills tendeixen a generar resultats dispars i d'escassa exactitud quan s'empren en la modelització de nanocompòsits polimèrics de baixa fracció volumètrica i relació d'aspecte de les partícules, objecte habitual de la major part d'estudis científics realitzats als darrers

temps, mentre que aquells més recents i complexos solen requerir la resolució de diverses i/o extenses equacions, així com la incorporació d'alguns paràmetres addicionals de difícil estimació, dificultant així, en definitiva, la seva usabilitat real.

Per aquest motiu, al **Treball III** de la present tesi doctoral s'ha proposat un procediment nou i alternatiu per a estimar el valor de la difusivitat relativa als nous materials nanocompostos, basat en la modelització i simulació matemàtica dels principals processos de difusió de matèria que esdevenen al seu interior. A diferència dels models anteriors recollits a la literatura, el model matemàtic presentat en aquest treball no es fonamenta en cap desenvolupament analític, ni requereix tampoc l'estimació prèvia de complexos paràmetres estructurals, sinó tan sols la introducció d'algunes imatges de microscòpia electrònica de transmissió (TEM) obtingudes a partir de la secció transversal del nanocompòsit estudiat. Així, mitjançant el tractament gràfic d'aquestes micrografies, i la seva anàlisi subsegüent pel mètode dels elements finits (FEM), l'esmentat model es capaç d'estimar el valor aproximat de la difusivitat aparent del solut a través de la matriu nanocomposta i, en conseqüència, el valor corresponent de la difusivitat relativa, característica del citat material.

Així doncs, amb aquest nou model, esperava obtenir-se una estimació més acurada de l'abast de la millora assolida en la capacitat retenidora dels nanocompòsits polimèrics, en general, però més particularment d'aquells esmentats més amunt, de baixa fracció volumètrica i relació d'aspecte de les partícules, que constitueixen precisament l'objecte d'estudi del present treball. Per tal de comprovar aquest fet, es va dur a terme la validació de la seva capacitat descriptiva mitjançant la comparació de les seves prediccions teòriques amb dades obtingudes de mesuraments experimentals, així com d'altres resultats teòrics predits per 18 models anteriors seleccionats de la literatura. Amb aquest objectiu, es desenvoluparen en aquest treball diversos nanocompòsits d'EVOH i zeïna amb un 1 o 2 % $^{v}/_{v}$ de bentonita sòdica, els quals, en forma de pel·lícules o de recobriments sobre altres materials, foren sotmesos a assajos isostàtics de permeabilitat a l'oxigen, mentre les corresponents seccions transversals foren observades i capturades gràficament a través de microscòpia electrònica de transmissió (TEM).

Com a resultat d'aquestes anàlisis, es pogué confirmar l'assoliment d'una estructura nanocomposta intercalada, i pràcticament exfoliada, a la matriu dels materials, generada per les nombroses nanopartícules de bentonita que s'hi trobaven individualitzades i fermament encastades entre les seves cadenes polimèriques. Sota l'objectiu del microscopi, aquestes partícules presentaven, en general, una baixa relació d'aspecte, d'entre 2.7 i 4.4 de mitjana, en funció del material, una distribució aleatòria a la seva matriu, i una orientació aproximadament paral·lela a la direcció de la seva fabricació.

Pel que fa al model proposat, la seva resolució matemàtica donà lloc a un conjunt d'imatges computades que detallaven gràficament, i permetien confirmar, els diversos camins tortuosos que seguien les molècules de solut al voltant de les partícules argiloses, així com els diferents mecanismes de retenció que aquestes experimentaven amb la seva presència i que, per tant, conduïen a l'esperada reducció en la seva difusivitat aparent.

Respecte a aquest darrer paràmetre, el model estimà unes reduccions mitjanes en el seu valor d'entre el 3.8 i el 12.2 %, en funció del nanocompòsit estudiat, que es corresponien aproximadament amb els valors experimentals obtinguts en els assajos de permeació, amb uns errors d'estimació inferiors en tot cas al 2 %. Tanmateix, en comparar aquests errors amb els generats pels 18 models anteriors seleccionats de la literatura es constatà que la nova metodologia proposada proporcionava els millors resultats de forma simultània per als tres materials investigats, tan sols comparables als resultats produïts pels models més moderns i complexos, validant així definitivament la seva capacitat.

Un cop confirmada la major capacitat de retenció dels nanocompòsits d'EVOH i bentonita, i desenvolupada l'eina necessària per a estimar-la amb precisió, es va emprendre als **Treballs IV** i **V** d'aquesta tesi doctoral la caracterització de les seves propietats actives i funcionals en tant que materials d'envasat alimentari. Amb aquest objectiu, les pel·lícules nanocompostes d'EVOH i bentonita sòdica estudiades adés es prepararen de nou al **Treball IV** contenint un 2 % $^{m}/_{m}$ de càrrega inorgànica, per tal d'avaluar-los tot seguit l'aparença macroscòpica i la morfologia microestructural a través de microscòpia electrònica de rastreig (SEM) i de transmissió (TEM), determinar-los les temperatures de fusió i de transició vítria, i mesurar-los els coeficients de difusivitat, permeabilitat, i solubilitat de l'oxigen, diòxid de carboni, i vapor d'aigua, en funció de la humitat relativa. En paral·lel a aquestes anàlisis, es prepararen també les seves anàlogues actives, amb la incorporació d'un 5 % de carvacrol com a agent antimicrobià, i es sotmeteren a assajos cinètics i termodinàmics encaminats a determinar-los els coeficients de solubilitat i difusivitat del compost actiu en funció de la concentració d'aigua a la matriu polimèrica.

Així doncs, macroscòpicament, les pel·lícules nanocompostes presentaren un aspecte homogeni, incolor, i brillant, molt comparable al del polímer pur, malgrat resultar lleugerament més opaques i d'aparença més boirosa, degut òbviament a la presència de les partícules argiloses al seu interior. Tanmateix, aquestes nanopartícules resultaven invisibles a ull nu, i només podien apreciar-se amb claredat a les micrografies de transmissió, on apareixien generalment exfoliades i ben encastades a la matriu del material, al temps que orientades aproximadament en paral·lel a la direcció de la seva fabricació. Des del punt de vista tèrmic, s'observà que llur presència a la matriu polimèrica endarreria

la transició vítria del nanocompòsit entre 0.2 i 2.4 °C, mentre n'avançava la fusió entre 1.5 i 1.8 °C, depenent de la humitat relativa. Aquests resultats, concordants amb els recollits a la literatura, podien explicar-se, respectivament, per les restriccions en la mobilitat segmental de les cadenes polimèriques imposades per les partícules durant l'escalfament del material, i per l'intens efecte nucleant induït per aquestes durant la seva cristal·lització, d'acord amb l'esmentat a l'apartat 1.1.2.2.2.

Pel que fa al transport de vapor d'aigua, les isotermes de sorció generades pels materials posaren de manifest l'accentuada naturalesa hidròfila de la bentonita sòdica, la qual, amb només un 2 % $^{m}/_{m}$ de càrrega a l'EVOH nanocompost, era capaç d'incrementar-li la capacitat d'absorció d'aigua en un 17 % de mitjana respecte al polímer original. D'altra banda, l'ajustament d'aquestes corbes a l'equació de D'Arcy i Watt revelà l'esdeveniment d'una adsorció més ràpida a baixos valors de la humitat relativa, estretament vinculada a la presència de les nanopartícules argiloses a l'interior del material, així com una major contribució de la formació de clústers a humitats superiors. Aquests clústers moleculars resultaven precisament els responsables del descens observat en la permeabilitat del polímer al vapor d'aigua fins al seu punt de transició vítria. Un decreixement quadràtic amb la concentració d'aigua, al que devia afegir-se, en el cas del material nanocompost, una reducció addicional de fins al 35 % originada pels diversos mecanismes de retenció introduïts per les partícules a la seva matriu.

Respecte al transport dels altres gasos, oxigen i diòxid de carboni, els mesuraments realitzats en aquest treball permeteren constatar l'important creixement dels coeficients de solubilitat, difusivitat, i permeabilitat d'ambdós migrants a la matriu d'EVOH amb l'augment del seu contingut en aigua, seguint, a més a més, aquest darrer coeficient, l'evolució sigmoïdal descrita pel model de Peleg esmentat a l'apartat anterior. No obstant això, aquests esperats increments en els tres paràmetres de transport, associats tots ells als fenòmens de relaxació polimèrica explicats adés, arribaven a variar molt considerablement en el cas del polímer nanocompost. En aquest sentit, per mitjà dels citats mecanismes de retenció, les nanopartícules argiloses aconseguien reduir la permeabilitat del material entre un 3 i un 75 %, en funció de la humitat relativa, i la seva difusivitat aparent entre un 10.5 i un 17.6 %, en valors mitjans. En canvi, la solubilitat d'ambdós gasos a la matriu nanocomposta experimentava un augment substancial, d'entre el 6 i el 50 %, probablement degut a la seva major capacitat d'absorció d'aigua, observada anteriorment.

Aquestes notables variacions en les propietats de transport dels gasos permanents amb la presència de nanopartícules a la matriu polimèrica tingueren també el seu reflex en els paràmetres de transferència de matèria corresponents a l'agent actiu. En efecte, dels resultats obtinguts en la seva determinació s'evidencià que les partícules argiloses presents al material aconseguien augmentar la

seva capacitat de retenció pel carvacrol al voltant d'un 36 %, així com alentir-hi la seva difusió una mitjana del 23 %. No obstant això, a partir del punt de transició vítria, aquestes partícules també demostraven ser capaces de mantenir-hi constant la magnitud de la difusivitat aparent, assolint així, a la humitat de saturació del polímer, una reducció propera al 75 % en el valor d'aquest coeficient.

La diferència evident entre aquestes importants reduccions en la difusivitat del carvacrol i les reportades anteriorment per al transport dels gasos permanents podria ésser deguda, en termes generals, als efectes derivats de la mida superior de la molècula activa i, més particularment, a la seva decreixent compatibilitat química amb el material portador en augmentar aquest el seu contingut en aigua. Un comportament, aquest darrer, que fou confirmat posteriorment per la pròpia evolució de la constant de Henry de l'agent actiu amb la concentració d'aigua a la matriu nanocomposta, especialment a partir de la seva transició vítria, la magnitud de la qual arribà a triplicar els valors assolits pel polímer pur en condicions de saturació d'humitat.

Aquesta caracterització activa i funcional del nou material va ser finalment completada al **Treball V** de la present tesi doctoral amb la fabricació, a escala industrial, de pel·lícules bicapa per rotogravat, compostes per un substrat funcional de PP finament recobert amb una capa activa i nanocomposta d'EVOH que contenia un 2 % $^{m}/_{m}$ de bentonita sòdica com a càrrega inorgànica i un 7.5 % de carvacrol com a agent antimicrobià d'origen natural. A l'igual que els materials actius estudiats al capítol anterior, les pel·lícules fabricades en aquest treball foren sotmeses a diverses anàlisis fisicoquímiques encaminades a determinar la seva capacitat de retenció pel citat compost, així com altres característiques funcionals d'interès per al seu emprament en l'envasat alimentari, ço és, mecàniques, òptiques, superficials, i barrera.

Com a resultat d'aquestes anàlisis, es comprovà que la incorporació de nanopartícules a la matriu del recobriment actiu augmentava la seva capacitat de retenció pel carvacrol en un 22 % de mitjana respecte al seu anàleg pur, un valor molt proper a l'atès anteriorment a escala de laboratori. Pel que fa a les propietats funcionals, les pel·lícules nanocompostes resultaren al voltant d'un 37 % més mullables que les seves equivalents sense càrrega inorgànica, i entre un 5 i un 76 % més impermeables al pas de l'oxigen i el diòxid de carboni, en funció de la humitat relativa. En canvi, no mostraren diferències significatives amb aquestes últimes en termes de coloració o lluminositat, així com en la seva resistència a la tracció, deformació al trencament, o mòdul de Young, pel que podien considerar-se, en última instància, perfectament aptes per a les principals aplicacions d'envasat alimentari.

Per últim, aquestes noves pel·lícules de fabricació industrial s'empraren en la construcció d'envasos antimicrobians en forma de bosses per a la conservació de productes de IV gamma, amb l'objectiu de sotmetre-les als mateixos assajos d'alliberament de carvacrol que les seves anàlogues originals, i poder avaluar així la millora assolida en el seu rendiment actiu per la presència de nanopartícules argiloses a la seva estructura. Així doncs, i a l'igual que en el treball anterior, les noves bosses d'amanida es farciren amb aigua gelificada, es tancaren de forma hermètica, i s'emmagatzemaren en cambres climàtiques durant una setmana per tal de monitoritzar regularment la concentració d'agent actiu assolida a l'espai de cap durant tot el període de conservació de l'aliment. Com a resultat, s'observà que el valor màxim d'aquesta concentració, atès a l'inici de l'experiment, esdevenia un 21 % major als envasos confeccionats amb les pel·lícules nanocompostes, respecte dels originals sense farciment, i que el seu decreixement amb temps de conservació resultava, a més a més, un 24 % més lent. En conseqüència, la combinació efectiva d'ambdós fenòmens retentius sobre la concentració de carvacrol atesa finalment als envasos acabava produint-ne un increment del 38 % al terme d'una setmana del seu emmagatzemament, fet que suposava una millora considerable respecte de l'eficiència original del seu funcionament.

3.3. Materials actius basats en matrius de copolímers d'etilè de diversa polaritat

Una possible alternativa a la incorporació de nanopartícules argiloses a la matriu polimèrica a fi d'augmentar la seva capacitat de retenció per l'agent actiu, controlar en major mesura el seu alliberament, i millorar així, en darrer terme, el rendiment antimicrobià dels envasos finals, consisteix en la variació de la seva compatibilitat química amb el citat compost mitjançant l'emprament d'altres polímers de diferent polaritat en la seva composició. En efecte, i segons s'ha constatat adés, a l'apartat 3.1, la polaritat del polímer portador constitueix un factor determinant de l'estabilitat de l'agent actiu a la seva matriu, en promoure la seva retenció quan ambdós materials resulten químicament afins, o, per contra, el seu alliberament quan presenten unes polaritats més distanciades. Per aquesta raó, una modificació química de l'anterior matriu estudiada, de copolímer d'etilè i alcohol vinílic (EVOH), basada en la substitució d'aquest polímer hidròfil per altres copolímers d'etilè de diferent polaritat, constitueix també, en si mateixa, un nou mecanisme de control de la seva activitat, que pot contribuir, a més a més, al millorament de la seva capacitat retenidora pel compost actiu si s'atenyen les característiques de compatibilitat adequades entre ambdós materials.

Per tal d'avaluar l'abast d'aquesta potencial millora als nous materials polimèrics amb l'esmentada modificació química de la seva matriu, al darrer treball constituent d'aquesta tesi doctoral (**Treball VI**) es desenvoluparen algunes pel·lícules i recobriments actius de diversa polaritat, compostes de poli(etilè – co – octè) (LLDPE), poli(etilè – co – acetat vinílic) (EVA), poli(etilè – co – àcid metacrílic) (EMA), i poli(etilè – co – metacrilat alcalí) (ION), amb un 5 % de carvacrol com a agent antimicrobià, i es caracteritzaren, tot seguit, les seves propietats actives, amb el mesurament dels paràmetres de solubilitat, difusivitat, i retenibilitat de l'esmentat compost al seu interior, la seva morfologia microestructural, així com altres propietats funcionals de rellevància per al seu emprament en l'envasat alimentari, ço és, mecàniques, tèrmiques, òptiques, superficials, i barrera. A l'igual que els materials actius estudiats als capítols anteriors, totes aquestes pel·lícules i recobriments es fabricaren per via humida o càsting, si bé, degut a la baixa solubilitat dels seus polímers precursors en mescles hidroalcohòliques, aquests hagueren d'aplicar-se en forma de dispersions aquoses (làtex) en lloc de dissolucions convencionals, per tal d'evitar així la utilització de compostos orgànics volàtils (VOCs) en la seva formulació en tant que dissolvents portadors.

Així doncs, macroscòpicament, totes les pel·lícules desenvolupades presentaren un aspecte incolor i homogeni, sense partícules, agregats, o altres defectes observables a ull nu. No obstant això, tan sols les obtingudes amb les dispersions d'EMA i ION resultaren completament transparents i brillants, mentre que les d'EVA i LLDPE donaren lloc a materials més boirosos o opacs, amb una superfície mat i una coloració més blanquinosa, que podria ser indicadora d'una estructura interna més heterogènia. En efecte, sota l'objectiu del microscopi, els quatre materials resultaren molt diferents, amb un aspecte variant entre la completa homogeneïtat o uniformitat estructural de l'EMA i la gran heterogeneïtat del LLDPE, on les petites partícules esfèriques que formaven part de la seva dispersió apareixien unides solament per alguns punts de contacte, formant així una extensa xarxa tridimensional d'esferes i porus d'aparença semblant a una esponja. Entre aquests dos extrems es trobaven l'ION i l'EVA, amb unes estructures intermèdies de major homogeneïtat i menor porositat. Aquesta important variació microestructural entre els quatre materials estudiats evidenciava un diferent grau d'avanç del procés de coalescència o sinterització de les seves partícules per efecte d'una aportació tèrmica insuficient durant el seu procés d'assecament, la qual, en el cas concret del LLDPE i l'EVA, acabava traduint-se en una manca de polímer fos que impossibilitava l'adequat soldament de les seves partícules elementals, així com el correcte farciment dels nombrosos porus o buits existents entre elles.

En conseqüència, i segons l'esmentat, alguns dels materials desenvolupats en aquest treball arribaven a generar una porositat molt elevada, que, unida a la seva diferent polaritat, podia infligir importants

variacions en els paràmetres de retenció i transport de l'agent actiu al seu si, conduint així, al capdavall, a una substancial modificació, i potencial millora, de les seves propietats actives. En aquest sentit, respecte a la difusivitat del carvacrol, es constatà que la magnitud d'aquest coeficient es mantenia, en general, més baixa que a l'EVOH, tot i que es trobava directament relacionada amb les característiques d'heterogeneïtat i porositat observades anteriorment a la matriu portadora, resultant així la difusió del compost deu voltes més ràpida a través del LLDPE que de l'EMA o l'ION. En canvi, la seva solubilitat en aquests materials depenia més bé de la polaritat de la matriu polimèrica que de la seva estructura interna, assolint així a l'ION un valor 3 voltes superior que al LLDPE. Aquest fenomen podria explicar-se per la naturalesa amfifílica de la molècula activa, deguda a la hidrofòbia del seu cos monoterpènic i a la hidrofília del seu grup hidroxil, que la faria més compatible químicament amb matrius de polaritat dual, com les dels copolímers iònics d'etilè (EMA i ION), que amb matrius monopolars característiques d'homopolímers simples o de copolímers constituïts per monòmers similars, com el LLDPE o l'EVA. Pel que fa l'eficiència de la seva incorporació en aquests materials, al treball s'observà que totes les pel·lícules preparades foren capaces de retenir una quantitat prou elevada i similar de l'agent actiu, d'entre el 74 % per al LLDPE i el 81 % per a l'EMA, malgrat les notables diferències existents entre elles en termes de solubilitat i difusivitat aparent. A més a més, aquestes concentracions resultaven equiparables a les obtingudes per a l'EVOH als treballs anteriors, i molt superiors a les recollides a la literatura per a compostos semblants en matrius extruïdes, el que confirmava la seva excel·lent retenibilitat per aquesta molècula, fins i tot en els casos més adversos de major porositat.

Finalment, totes aquestes pel·lícules foren sotmeses de nou a diverses anàlisis fisicoquímiques, dirigides en aquest punt a la caracterització de les seves propietats funcionals en tant que materials d'envasat alimentari. En aquest respecte, les anàlisis tèrmiques realitzades revelaren una bona correspondència general entre les temperatures i rangs de fusió dels materials estudiats i la seva morfologia microestructural, tal com s'especulava inicialment, malgrat constituir-ne l'EVA una notable excepció, fet que suggeria una contribució no menyspreable de la cinètica del procés a l'abast final de la seva sinterització. Des del punt de vista mecànic, s'assajaren pel·lícules de PP recobertes amb aquests quatre materials sense trobar-se diferències significatives entre ells en termes de resistència a la tracció o mòdul de Young. Tanmateix, s'observà un augment important de la seva deformació al trencament degut als efectes d'una possible plastificació del substrat, causada probablement per l'absorció de residus de dissolvents, o d'altres additius, procedents de les dispersions aquoses. Aquests recobriments també mostraren diferències significatives en les seves propietats superficials, les quals, a més a més, es corresponien en gran mesura amb les polaritats característiques dels propis polímers purs. Aquest particular comportament podria deure's a què la major aportació tèrmica rebuda durant

el seu procés d'assecament els havia permès d'assolir un major grau de sinterització, atorgant-los així una estructura més homogènia, llisa, i compacta, que, a diferència de les pel·lícules anteriors, no podia influir de forma apreciable en les mesures de l'angle de contacte de l'aigua sobre la seva superfície. Per últim, respecte a les qualitats barrera, es constatà que la permeabilitat als gasos permanents de les quatre pel·lícules es correlacionava directament amb les característiques d'heterogeneïtat i porositat observades adés en la seva estructura, mentre que la seva permeabilitat al vapor d'aigua necessitava ésser explicada tant en termes d'estructura com de polaritat de la matriu polimèrica.

4. CONCLUSIONS

I. El copolímer d'etilè i alcohol vinílic (EVOH) resulta un polímer adequat per a l'envasat actiu d'aliments amb elevada activitat d'aigua, atès que la seva alta solubilitat i reduïda difusivitat pels agents antimicrobians volàtils, com el carvacrol, en condicions de sequedat, permet l'adequada preservació d'aquests compostos a la seva matriu fins que la humitat generada per l'aliment en el moment de l'envasat desferma el seu alliberament vers l'espai de cap del sistema.

II. La incorporació d'una capa activa d'EVOH amb carvacrol a pel·lícules comercials de PP destinades a la construcció d'envasos per a la conservació de peix fresc i de productes vegetals mínimament processats permet l'assoliment d'una concentració suficient de l'agent actiu al seu espai de cap com per a inhibir el creixement de microorganismes patògens o alterants dels aliments sobre la seva superfície. Aquest efecte té lloc als envasos fins al tercer dia del seu emmagatzemament, en cas d'ésser aplicada en forma de recobriment, o, a partir del quart, en cas de trobar-se inserida entre capes funcionals d'altres polímers aïllants o protectors, com ara el propi PP.

III. El desenvolupament de models matemàtics que descriguen adequadament tots els processos de transferència de matèria que intervenen en el funcionament dels envasos permet esbrinar, a través de simulacions computacionals, els diferents paràmetres estructurals i/o condicions ambientals que regeixen en major mesura el seu comportament, i trobar així, en darrer terme, els camins existents vers la seva optimització. En aquest respecte, els models desenvolupats en aquesta tesi predigueren l'assoliment d'un màxim en el rendiment antimicrobià dels envasos en triplicar la grossària de la capa activa d'EVOH, reduir a una setzena part la capa interna de PP, i evitar la seva exposició prolongada a humitats relatives superiors al 60 %.

IV. La incorporació d'un recobriment actiu d'EVOH amb agents antimicrobians d'origen natural, com ara carvacrol, citral, o altres olis essencials, a pel·lícules comercials de PP i PET, a través del seu tractament superficial previ amb descàrrega d'efecte corona i l'aplicació d'una imprimació basada en polietilenimina (PEI), permet obtenir pel·lícules bicapa amb capacitat antimicrobiana que presenten una excel·lent estabilitat estructural i unes característiques superficials millorades, sense deteriorar de forma important o apreciable les seves restants propietats funcionals, ço és, mecàniques, òptiques, i barrera.

V. La incorporació de nanopartícules de bentonita a la matriu d'EVOH com a càrrega inorgànica incrementa la seva capacitat de retenció pel carvacrol entre un 22 i un 36 %, reduint-hi la difusivitat en un 23 %. Les pel·lícules fabricades amb aquest nanocompòsit resulten, a més a més, un 37 % més mullables que les d'EVOH pur, i fins a un 76 % més impermeables al pas de l'oxigen, el diòxid de carboni, i el vapor d'aigua, en funció de la humitat relativa, sense comportar cap altra alteració significativa en les seves característiques òptiques o mecàniques.

VI. El desenvolupament d'un model matemàtic que descriga adequadament els principals processos de difusió de matèria que esdevenen a l'interior dels nanocompòsits polimèrics de menor fracció volumètrica i relació d'aspecte de les partícules, basat en el tractament gràfic de les seves micrografies de transmissió (TEM) i en la seva subsegüent anàlisi pel mètode dels elements finits (FEM), permet predir, a través de simulacions computacionals, la reducció en la difusivitat dels soluts induïda per les partícules amb una senzillesa superior i una exactitud similar a la oferida pels models teòrics més recents i complexos recollits a la literatura.

VII. La modificació química i estructural dels anteriors recobriments actius, d'EVOH amb carvacrol, basada en la substitució d'aquest polímer hidròfil per altres copolímers d'etilè de diferent polaritat, i en la seva aplicació en forma de dispersions aquoses, porta a l'obtenció d'un nou conjunt de materials polimèrics de diversa estructura i afinitat química. Aquests exhibeixen unes característiques variables de solubilitat i difusivitat per l'agent actiu que poden ésser fàcilment controlades o ajustades durant el seu procés de fabricació per tal d'adaptar-se acuradament als requeriments imposats pel sistema objectiu d'envasat alimentari, tot mantenint, al mateix temps, les seves propietats funcionals sense altres canvis rellevants o significatius.

REFERÈNCIES

Ahvenainen, R., Hurme, E. (1997). Active and smart packaging for meeting consumer demands for quality and safety. *Food Additives and Contaminants*, 14 (6 – 7), 753 – 763.

Amorós, J. L., Barba, A., Beltrán, V. (1994). *Estructuras cristalinas de los silicatos y óxidos de las materias primas cerámicas.* Instituto de Tecnología Cerámica – Asociación de Investigación de las Industrias Cerámicas, Castelló de la Plana.

Appendini, P., Hotchkiss, J. H. (2002). Review of antimicrobial food packaging. *Innovative Food Science & Emerging Technologies*, 3 (2), 113 – 126.

Arora, A., Padua, G. W. (2010). Review: Nanocomposites in food packaging. *Journal of Food Science*, 75 (1), R43 – R49.

Aucejo, S., Marco, C., Gavara, R. (1999). Water effect on the morphology of EVOH copolymers. *Journal of Applied Polymer Science*, 74 (5), 1201 – 1206.

Aucejo, S. (2000). *Estudi i caracterització de l'efecte de la humitat en les propietats barrera d'estructures polimèriques hidròfiles.* Tesi doctoral, Universitat de València, València.

Aucejo, S., Català, R., Gavara, R. (2000). Interactions between water and EVOH food packaging films. *Food Science and Technology International*, 6 (2), 159 – 164.

Bakkali, F., Averbeck, S., Averbeck, D., Idaomar, M. (2008). Biological effects of essential oils – a review. *Food and Chemical Toxicology*, 46 (2), 446 – 475.

Barba, A., Beltrán, V., Feliu, C., García, J., Ginés, F., Sánchez, E., Sanz, V. (2002). *Materias primas para la fabricación de soportes de baldosas cerámicas. 2ª ed.* Instituto de Tecnología Cerámica, Castelló de la Plana.

Barbosa – Cánovas, G. V., Juliano, P. (2005). *Introduction: Food engineering*. Barbosa – Cánovas, G. V. (ed.) *Food engineering. Encyclopedia of Life Support Systems (EOLSS).* EOLSS Publishers / United Nations Educational, Scientific and Cultural Organization (UNESCO), Paris, França.

Beers, K. (2007). *Numerical methods for chemical engineering.* Cambrigde University Press, Cambrigde, Regne Unit.

Brody, A. L., Strupinsky, E. R., Kline, L. R. (2001). *Active packaging for food applications.* CRC Press LLC, Boca Raton, FL, EEUU.

Bruneton, J. (2001). *Farmacognosia. Fotoquímica. Plantas medicinales.* 2ª ed. Acribia S. A., Saragossa, Espanya.

Burt, S. (2004). Essential oils: their antibacterial properties and potential applications in foods. A review. *International Journal of Food Microbiology*, 94 (3), 223 – 253.

Català, R., Gavara, R. (2001a). Materiales y estructuras poliméricas de alta barrera para el envasado de alimentos perecederos. *Plásticos modernos*, 81 (536), 221 – 228.

Català, R., Gavara, R. (2001b). Nuevos envases. De la protección pasiva a la defensa activa de los alimentos envasados. *Arbor*, CLXVIII, 661, 109 – 127.

Català, R., Gavara, R. (2005). *4.16 – Food packaging.* Barbosa – Cánovas, G. V. (ed.) *Food engineering. Encyclopedia of Life Support Systems (EOLSS).* EOLSS Publishers / United Nations Educational, Scientific and Cultural Organization (UNESCO), Paris, França.

Cha, D. S., Chinnan, M. S. (2004). Biopolymer – based antimicrobial packaging. A review. *Food Science and Nutrition*, 44 (4), 223 – 237.

Chalier, P., Arfa, A. B., Preziosi – Belloy, L., Gontard, N. (2007). Carvacrol losses from soy protein coated papers as a function of drying conditions. *Journal of Applied Polymer Science*, 106 (1), 611 – 620.

ChemSpider. Royal Society of Chemistry (RSC), Londres, Regne Unit. *http://www.chemspider.com/Chemical-Structure.21105867.html*

Choudalakis, G., Gotsis, A. D. (2009). Permeability of polymer / clay nanocomposites: A review. *European Polymer Journal*, 45 (4), 967 – 984.

Collins – Thompson, D., Hwang, C. – A. (2000). *Packaging with antimicrobial properties.* Robinson, R. K. (ed.) *Encyclopedia of food microbiology*, Academic Press, Londres, Regne Unit.

Cooksey, K. (2001). Antimicrobial food packaging materials. *Additives for Polymers*, 2001 (8), 6 – 10.

Crank, J. (1975). *The mathematics of diffusion*, Clarendon Press, Londres, Regne Unit.

Cuq, B., Gontard, N., Guilbert, S. (1995). *Edible films and coatings as active layers. Active food packaging.* Blackie Academic & Professional, Glasgow, Regne Unit.

Cushen, M., Kerry, J., Morris, M., Cruz – Romero, M., Cummins, E. (2012). Nanotechnologies in the food industry – Recent developments, risks and regulation. *Trends in Food Science and Technology*, 24 (1), 30 – 46.

Davidson, P. M., Naidu, A. S. (2000). *Phyto – phenols.* Naidu, A. S. (ed.) *Natural food antimicrobial systems*. CRC Press LLC, Boca Raton, FL, EEUU.

De Vincenzi, M., Stammati, A., De Vincenzi, A., Silano, M. (2004). Constituents of aromatic plants: carvacrol. *Fitoterapia*, 75 (7 – 8), 801 – 804.

Dorman, H. J. D., Deans, S. G. (2000). Antimicrobial agents from plants: antibacterial activity of plant volatile oils. *Journal of Applied Microbiology*, 88 (2), 308 – 316.

Du, M., Guo, B., Jia, D. (2010). Newly emerging applications of halloysite nanotubes: A review. *Polymer International*, 59 (5), 574 – 582.

Falla, W. R., Mulski, M., Cussler, E. L. (1996). Estimating diffusion through flake – filled membranes. *Journal of Membrane Science*, 119 (1), 129 – 138.

Feldman, D. (2013). Polymer nanocomposite barriers. *Journal of Macromolecular Science, Part A: Pure and Applied Chemistry*, 50 (4), 441 – 448.

Fernández, M. (2000). Review: Active food packaging. *Food Science and Technology International*, 6 (2), 97 – 108.

Floros, J. D., Dock, L. L., Han, J. H. (1997). Active packaging technologies and applications. *Food, Cosmetics and Drug Packaging*, 20 (1), 10 – 17.

Gavara, R., Català, R., Hernández – Muñoz, P. (2009). Extending the shelf – life of fresh – cut produce through active packaging. *Stewart Postharvest Review*, 5 (4), 1 – 5.

Gavara, R., Hernández, R. J. (1994). Sorption and transport of water in Nylon – 6 films. *Journal of Polymers Science. Part B: Polymer Physics*, 32 (14), 2367 – 2374.

Gerding, T. K., Rijk, M. A. H., Jetten, J., van den Berg, F., de Kruijf, N. (1996). Trends in food packaging: arising opportunities and shifting demands. *Packaging Technology and Science*, 9 (3), 153 – 165.

Gontard, N. (2000). *Panorama des emballages alimentaires actifs.* Gontard, N. (ed.) *Les emballages actifs*, Tech & Doc Lavoisier, França.

Han, J. H. (2000). Antimicrobial food packaging. *Food Technology*, 54 (3), 56 – 65.

Han, J. H. (2013). *10 – Antimicrobial packaging systems.* Ebnesajjad, S. (ed.) *Plastic films in food packaging*, Elsevier William Andrew, EEUU.

Hanle, J. E., Merz, E. H., Mesrobian, R. B. (1966). Polymers in packaging. *Journal of Polymer Science: Part C. Polymer Symposia*, 12 (1), 185 – 195.

Hernández, R. J., Gavara, R. (1999). *Plastics packaging: methods to evaluate food packaging interactions.* Pira International, Surrey, Regne Unit.

Hernández, R. J., Selke, S. E. M., Culter, J. D. (2000). *Plastics packaging: properties, processing, applications, and regulations.* Hanser Gardner Publications Inc., Munic, Alemanya.

Holley, R. A., Patel, D. (2005). Improvement in shelf – life and safety of perishable foods by plant essential oils and smoke antimicrobials. *Food Microbiology*, 22 (4), 273 – 292.

Joerger, R. D. (2007). Antimicrobial films for food applications: a quantitative analysis of their effectiveness. *Packaging Technology and Science*, 20 (4), 231 – 273.

Kiliaris, P., Papaspyrides, C. D. (2010). Polymer / layered silicate (clay) nanocomposites: An overview of flame retardancy. *Progress in Polymer Science (Oxford)*, 35 (7), 902 – 958.

Kumar, P., Sandeep, K. P., Alavi, S., Truong, V. D. (2011). A review of experimental and modeling techniques to determine properties of biopolymer – based nanocomposites. *Journal of Food Science*, 76 (1), 2 – 14.

Kuorwel, K. K., Cran, M. J., Sonneveld, K., Miltz, J., Bigger, S. W. (2011). Essential oils and their principal constituents as antimicrobial agents for synthetic packaging films. *Journal of Food Science*, 76 (9), R164 – R177.

Lagaron, J. M., Català, R., Gavara, R. (2004). Structural characteristics defining high barrier polymeric materials. *Materials Science and Technology*, 20 (1), 1 – 7.

Lee, D. S., Yam, K. L., Piergiovanni, L. (2008). *Food packaging science and technology.* CRC Press Taylor & Francis Group LLC, FL, EEUU.

López – Rubio, A., Almenar, E., Hernández – Muñoz, P., Lagarón, J. M., Catalá, R., Gavara, R. (2004). Overview of active polymer – based packaging technologies for food applications. *Food Reviews*

International, 20 (4), 357 – 386.

Manias, E., Polizos, G., Nakajima, H., Heidecker, M. J. (2007). *Fundamentals of polymer nanocomposite technology*. Wilkie, C., Morgan, A. (eds.) *Flame retardant polymer nanocomposites*, Wiley – Interscience, Hoboken, NJ, EEUU.

Naffakh, M., Díez – Pascual, A. M., Marco, C., Ellis, G. J., Gómez – Fatou, M. A. (2013). Opportunities and challenges in the use of inorganic fullerene – like nanoparticles to produce advanced polymer nanocomposites. *Progress in Polymer Science*, 38 (8), 1163 – 1231.

Nicolosi, V., Chhowalla, M., Kanatzidis, M. G., Strano, M. S., Coleman, J. N. (2013). Liquid exfoliation of layered materials. *Science*, 340 (6139), 1226419.

Nostro, A., Papalia, T. (2012). Antimicrobial activity of carvacrol: current progress and future prospectives. *Recent Patents on Anti – Infective Drug Discovery*, 7 (1), 28 – 35.

Osborn, K. R., Jenkins, W. A. (1992). *Plastic films. Technology and packaging applications.* Technomic Publishing Company Inc., Lancaster, PA, EEUU.

Oyane, A., Uchida, M., Onuma, K., Ito, A. (2006). Spontaneous growth of a laminin – apatite nano – composite in a metastable calcium phosphate solution. *Journal of Biomedical Materials Research*, 27 (2), 167 – 174.

Ozdemir, M., Floros, J. D. (2004). Active food packaging technologies. Critical Reviews in Food Science and Nutrition, 44 (3), 185 – 193.

Paul, D. R., Robeson, L. M. (2008). Polymer nanotechnology: Nanocomposites. *Polymer*, 49 (15), 3187 – 3204.

Pavlidou, S., Papaspyrides, C. D. (2008). A review on polymer – layered silicate nanocomposites. *Progress in Polymer Science (Oxford)*, 33 (12), 1119 – 1198.

Peltzer, M., Wagner, J., Jiménez, A. (2009). Migration study of carvacrol as a natural antioxidant in high – density polyethylene for active packaging. *Food Additives & Contaminants: Part A: Chemistry, Analysis, Control Exposure and Risk Assessment*, 26 (6), 938 – 946.

PubChem. National Center for Biotechnology Information (NCBI), Bethesda, MD, EEUU. *http://pubchem.ncbi.nlm.nih.gov/summary/summary.cgi?cid=10364*

Reglament (CE) 450/2009 de la Comissió de les Comunitats Europees de 29 de Maig de 2009 sobre materials i objectes actius i intel·ligents destinats a entrar en contacte amb aliments. Diari Oficial de la Unió Europea de 30 de Maig de 2009, L 135, 3 – 11.

Restuccia, D., Spizzirri, U. G., Parisi, O. I., Cirillo, G., Curcio, M., Iemma, F., Puoci, F., Vinci, G., Picci, N. (2010). New EU regulation aspects and global market of active and intelligent packaging for food industry applications. *Food Control*, 21 (11), 1425 – 1435.

Rhim, J. – W., Ng, P. K. W. (2007). Natural biopolymer – based nanocomposite films for packaging applications. *Critical Reviews in Food Science and Nutrition*, 47 (4), 411 – 433.

Rhim, J. – W., Park, H. – M., Ha, C. – S. (2013). Bio – nanocomposites for food packaging applications. *Progress in Polymer Science*, 38 (10 – 11), 1629 – 1652.

Ríos, J. L., Recio, M. C., Villar, A. (1987). Antimicrobial activity of selected plants employed in the Spanish Mediterranean area. *Journal of Ethnopharmacology*, 21 (2), 139 – 152.

Robertson, G L. (1993). *Food packaging: principles and practice.* Marcel Dekker, Inc., New York, NY, EEUU.

Rooney, M. L. (1995). *Active packaging in polymer films. Active food packaging.* Blackie Academic & Professional, Londres, Regne Unit.

Rooney, M. L. (1997). *Active packaging.* Brody, A. L., Marsh, K. S. (eds.) *The Wiley encyclopedia of packaging technology.* 2nd edition. John Wiley & Sons, New York, NY, EEUU.

Sadaka, F., Nguimjeu, C., Brachais, C., Vroman, I., Tighzert, L., Couvercelle, J. (2014). Review on antimicrobial packaging containing essential oils and their active biomolecules. *Innovative Food Science and Emerging Technologies*, (in press).

Silvestre, C., Duraccio, D., Cimmino, S. (2011). Food packaging based on polymer nanomaterials. *Progress in Polymer Science (Oxford)*, 36 (12), 1766 – 1782.

Singh, P., Wani, A. A., Saengerlaub, S. (2011). Active packaging of food products: recent trends. *Nutrition & Food Science*, 41 (4), 249 – 260.

Sinha Ray, S., Okamoto, M. (2003). Polymer / layered silicate nanocomposites: A review from preparation to processing. *Progress in Polymer Science (Oxford)*, 28 (11), 1539 – 1641.

Smid, E. J., Gorris, L. G. M. (2007). *Natural antimicrobials for food preservation.* Rahman, M. S. (ed.) *Handbook of food preservation.* 2nd edition. CRC Press Taylor & Francis Group LLC, Boca Raton, FL, EEUU.

Sorrentino, A., Gorrasi, G., Vittoria, V. (2007). Potential perspectives of bio – nanocomposites for food packaging applications. *Trends in Food Science and Technology*, 18 (2), 84 – 95.

Suppakul, P., Miltz, J., Sonneveld, K., Bigger, S. W. (2003). Active packaging technologies with an emphasis on antimicrobial packaging and its applications. *Journal of Food Science*, 68 (2), 408 – 420.

Tjong, S. C. (2006). Structural and mechanical properties of polymer nanocomposites. *Materials Science and Engineering R: Reports*, 53 (3 – 4), 73 – 197.

Tuley de Silva, K. (1996). *A manual on the essential oil industry.* United Nations Industrial Development Organization, Viena, Austria.

Tyagi, A. K., Malik, A., Gottardi, D., Guerzoni, M. E. (2012). Essential oil vapour and negative air ions: A novel tool for food preservation. *Trends in Food Science and Technology*, 26 (2), 99 – 113.

Van de Braak, S. A. A. J., Leijten, G. C. J. J. (1999). *Essential oils and oleoresins: a survey in the Netherlands and other major markets in the European Union.* CBI – Centre for the Promotion of Imports from Developing Countries, Rotterdam, Països Baixos.

Vermeiren, L., Devlieghere, F., Van Beest, M., de Kruijf, N., De – bevere, J. (1999). Developments in the active packaging of foods. *Trends in Food Science & Technology*, 10 (3), 77 – 86.

Vermeiren, L., Devlieghere, F., Debevere, J. (2002). Effectiveness of some recent antimicrobial packaging concepts. *Food Additives and Contaminants*, 19 (suppl. 1), 163 – 171.

Wagner, M. K.; Moberg, L. J. (1989). Present and future use of traditional antimicrobials. *Food Technology*, 43 (1), 143 – 147.

WPO – World Packaging Organisation. (1998). *Market statistics and future trends in global packaging*. WPO – World Packaging Organisation / Pira International Ltd., Brasil.

Yuan, Q., Jiang, W., An, L., Christiansen, J. D., Li, R. K. Y. (2005). Competing effect between filled glass bead and induced β crystal on the tensile properties of polypropylene / glass bead blends. *Journal of Applied Polymer Science*, 96 (5), 1729 – 1733.

I MATHEMATICAL MODEL TO DESCRIBE THE RELEASE OF AN ANTIMICROBIAL AGENT FROM AN ACTIVE PACKAGE CONSTITUTED BY CARVACROL IN A HYDROPHILIC EVOH COATING ON A PP FILM

Josep Pasqual Cerisuelo [a], Virginia Muriel – Galet [a], José María Bermúdez [b], Susana Aucejo [b], Ramon Català [a], Rafael Gavara [a, *], Pilar Hernández – Muñoz [a]

[a] Laboratori d'envasos, Institut d'Agroquímica i Tecnologia d'Aliments, IATA – CSIC.
Av. Agustí Escardino, 7. 46980 Paterna, València.

[b] Institut Tecnològic de l'Embalatge, Transport i Logística, ITENE.
Parc Tecnològic de Paterna.
C/ Albert Einstein, 1. 46980 Paterna, València.

* Autor de contacte. Tel.: +34 963900022, e-mail: rgavara@iata.csic.es

ABSTRACT

Antimicrobial active packaging is a novel technology in which a chemical compound (or mixture) is purposely incorporated into a packaging material to be released into the food to protect it from deterioration. The effectiveness of an antimicrobial package is strongly related to the balance between the controlled release of the active compound and microbial growth kinetics. This work characterizes and models the release of carvacrol from an EVOH coating on a PP film which can be employed as an active packaging system. The kinetics and extent of carvacrol mass transport within the packaging components were fully characterized as a function of relative humidity. As expected, water uptake by the EVOH coating acts as a triggering mechanism for activity. The partition equilibrium for carvacrol in the complex film largely favors (10000 fold) the EVOH layer in dry conditions, although in humid conditions the solubility in both polymers is very close (4 fold). Kinetically, the presence of humidity increases the value of D for carvacrol in EVOH from $3 \cdot 10^{-19}$ m^2/s in dry conditions to $3 \cdot 10^{-15}$ m^2/s in a wet environment.

After the experimental characterization of carvacrol transport, the efficiency of the release of carvacrol was estimated with a novel mathematical model based on the finite element method and successfully compared with the evolution of carvacrol concentration in a real packaging system. The model developed can be employed in the optimization of package design in order to ensure the maintenance of a specific concentration of the active agent in the headspace, high enough to prevent potential growth of a particular foodborne spoiling or pathogenic microorganism on the preserved foodstuffs. This model could easily be extended to similar packaging systems as long as an inventory of experimental data for all the parameters and coefficients involved is available, sufficiently complete to fulfill all the mathematical requirements demanded by the model.

***Journal of Food Engineering*, 2012, 110 (1), 26 – 37.**

1. INTRODUCTION

The growing demand for fresh and minimally processed food has recently increased the interest of manufacturers in prolonging the shelf-life of food products while ensuring that quality and safety are maintained (Gavara et al., 2009). Since the main factor limiting the shelf-life of these products is the potential growth of foodborne spoiling and pathogenic microorganisms (Han, 2005), various new processing technologies are being developed to avoid or delay their potential adverse effects. Antimicrobial active packaging is a novel technology in which a chemical compound (or mixture) is purposely incorporated into a packaging material to be released into the food and protect it from deterioration (Català & Gavara, 2001; Han, 2005). In these innovative materials, an antimicrobial compound is gradually delivered at the appropriate rate during commercialization and it is concentrated on the product surface where it is needed (Marcos et al., 2007).

Among the most common substances with proven antimicrobial effects, natural compounds obtained from vegetable extracts have attracted increasing interest because of their natural origin, better consumer acceptance, additional antioxidant activity, and biodegradable or edible capabilities (Han, 2005). One of these antimicrobial agents is carvacrol, a well-known phenolic monoterpene constituent of essential oils produced by various aromatic plants such as oregano, thyme, marjoram, and savory (De Vicenzi et al., 2004). Carvacrol is also a sweet-smelling aromatic compound that can take advantage of its volatile nature to treat “rough” products without direct contact with the package, and to protect them from a wide spectrum of bacteria and fungi by inhibiting their growth on the food surface (Mascheroni et al., 2010). Indeed, like other volatile antimicrobial agents, carvacrol can be particularly useful to preserve highly porous foods, and powdered, shredded, irregularly shaped, and particulate foods, such as ground beef, shredded cheese, small fruits, mixed vegetables, or ready-to-eat salad products (Han, 2005). It is also legally recognized as a food additive (under the flavorings category) by the EU and as a “Generally Recognized as Safe” (GRAS) substance by the US FDA (López et al., 2007).

The effectiveness of an antimicrobial package is strongly related to the balance between the controlled release of the active compound and microbial growth kinetics. Thus, microbial inhibition cannot be achieved if the release rate of the active agent is not sufficient to reach the minimum inhibition concentration (MIC) of the target microorganism or cannot be sustained throughout food shelf-life because it is too fast (Han, 2005). Moreover, the rate of release depends on the carrier material and its interactions with the active substance, as well as the film preparation method and environmental conditions (Tunç & Duman, 2010). It is also very advisable to introduce some activity triggering

mechanism into the packaging material to ensure its stability during storage, prevent losses of the active agent during package construction, transport, or manipulation, and thus ensure the maximum microbial inhibition efficiency for the preserved foodstuffs.

In this work, the triggering mechanism consists of a thin coating layer of a hydrophilic polymer on the functional layer of the package which acts as a carrier polymer matrix for the volatile antimicrobial compound. In this way, material stability can be guaranteed in dry conditions and antimicrobial activity can be triggered by the absorption of food moisture by the packaging materials. One of the best hydrophilic food-contact polymers that fits these goals well is ethylene-vinyl alcohol copolymer (EVOH), a well-known semicrystalline random copolymer widely used in the food packaging industry because of its outstanding, although moisture-sensitive, gas barrier properties with regard to oxygen and organic compounds (solvents and food aromas), as well as its considerable chemical and thermal resistance, and its great mechanical and optical properties (Aucejo et al., 1999, Aucejo et al., 2000, and López-Rubio et al., 2003). Furthermore, despite its petrochemical origin, it is also biodegradable, biocompatible, and recyclable (Oyane et al., 2006).

To accurately assess the performance and effectiveness of an antimicrobial package, several mass-transfer tests should be carried out using food simulants under controlled environmental conditions. However, the mass-transfer processes involved in the performance of an antimicrobial package might be so slow that their experimental determination could become very expensive and time-consuming, and even impossible in many cases owing to technical/analytical problems or non-availability of corresponding analytical methods (Begley et al., 2005). In all these situations, mathematical models that describe physicochemical processes occurring in the antimicrobial packages could become a valuable tool to assist, or at least partially replace, experimental study of the actual phenomena. The advantages of mathematical modeling and simulation have long been recognized by researchers, who in recent decades have concentrated their efforts on the development of deterministic migration models based on Crank's solutions to Fick's laws (Crank, 1975). These models have recently been adopted by the US Food and Drug Administration and by the European Union in Commission Regulation No 10/2011 as additional tools to estimate consumer exposure to potential packaging migrants, and thus to assist in making regulatory decisions (Poças et al., 2008).

Unfortunately, all the available models are inadequate to simulate mass-transfer processes in active packages because they are only intended to be used for assessing compliance with specific regulatory migration limits in food-contact polymeric materials. Hence, they can be regarded as "reasonable worst-case" models, since they calculate overestimated migration rates by using partitioning

coefficients with wide safety margins and “upper limit” equations for the diffusion coefficients (Begley et al., 2005). Consequently, the aim of this work was to develop, and experimentally validate, a mathematical model that adequately describes the mass-transfer phenomena that take place in a commercial active antimicrobial package for ready-to-eat salad products, consisting of a PP functional layer with a thin coating of EVOH-29 with 5 % carvacrol as antimicrobial active agent. This work also includes experimental determination of the mass transport parameters required in the calculations of this model.

2. MATERIALS AND METHODS

2.1. Materials

Ethylene-vinyl alcohol copolymer with a 29 % ethylene molar content (EVOH-29) was kindly supplied by The Nippon Synthetic Chemical Company (Osaka, Japan). Extrusion-grade Alcudia 45W1E (Repsol, Madrid, Spain) polypropylene (PP) was blended with 5 % carvacrol and extruded at 185 °C in films 100 µm thick using a twin screw extruder (DSE 20-40D, Brabender, Germany) equipped with a lateral liquid port. Commercial food-contact grade polypropylene (PP) films 30 µm thick were kindly supplied by Verdifresh (València, Spain).

Carvacrol of at least 98 % purity was purchased from Sigma-Aldrich (Barcelona, Spain), as well as reagent-grade potassium carbonate, magnesium nitrate, sodium nitrite, sodium chloride, potassium chloride, barium chloride, and phosphorus pentoxide. Reagent-grade 1-propanol and high-vacuum silicone were supplied by Panreac (Barcelona, Spain), and deionized water was obtained from a MilliPore Milli-Q Plus purification system (Molsheim, France).

2.2. Preparation of the EVOH-29 active films and coatings Construction of the packages

EVOH-29 films and coatings used in the construction of the packages were prepared from a hydroalcoholic solution of the polymer with the antimicrobial agent incorporated. The required amount of EVOH-29 pellets was placed in a glass flask with a 1:1 (w/w) mixture of deionized water and

1-propanol. The flask was then placed on a magnetic stirrer with heater plate (RCT basic model, IKA, Germany), coupled to a constant reflux vapor system, until the polymer was fully dissolved. Then the antimicrobial agent was added to the solution at a concentration of 5 g carvacrol / 100 g EVOH-29 and the solution was homogenized for 10 more minutes.

The formulated solution was used in the preparation of the active films by casting over several previously cleaned glass plates with the aid of a steel stud with a 100 µm deep thread (Lin-Lab Rioja, Logroño, Spain). Immediately afterwards, all the glass plates were placed under the heat radiation source of a home-made drying hood for 15 minutes. Homogeneous transparent active films were stored until utilization in drying chambers at ambient temperature in the presence of phosphorous pentoxide. The thickness of each film sample was measured individually, prior to testing, with a digital micrometer (Mitutoyo, Osaka, Japan), giving an average value of 15 ± 2 µm.

In order to prepare the active coatings on commercial PP films, PP sheets were irradiated under an indium amalgam UV lamp (NIQ 80/36 U model, Heraeus, Hanau, Germany) for 10 minutes in an air atmosphere to slightly modify their surface tension and to ensure adequate anchorage for the new polymer layer. Afterwards, the pretreated films were placed on an automatic coating applicator (4340 model, Elcometer, Hermalle-sous-Argenteau, Belgium), equipped with a steel stud with a 20 µm deep thread, and programmed to carry out a gradual deposition of the polymer solution at a temperature of 60 °C and an application velocity of 8 cm/s. The resulting 3 µm thick coatings were found to be highly homogeneous and transparent. The PP sheets coated with EVOH-29 and carvacrol were stored at ambient temperature in drying chambers.

Coated PP sheets were cut into pieces measuring 25 x 30 cm and used to make bags resembling those used in the commercialization of fresh salad, with the aid of a thermosealing machine (Audion Elektro, Weesp, Holland). Bags were filled with 1 L of air at atmospheric pressure by injecting this volume with a syringe through a septum adhered to the outer surface. In order to generate and maintain the inner relative humidity constant and close to 100 % (similar to that measured in the headspace of a real salad package), several small Petri dishes with 15 mL of gelified water were placed in the inner space of the packages before closing them with the sealing instrument.

2.3. Determination of carvacrol equilibrium parameters

To determine the extent of carvacrol release as a function of the relative humidity, and to measure the corresponding equilibrium parameters, equilibrium cells were prepared following the scheme represented in **Figure I.1**. Each cell consisted of a glass vial closed by a Mininert valve (Supelco, Teknokroma, Barcelona, Spain) for headspace sampling, a 5 cm^2 film sample (EVOH-29 or PP with carvacrol) inserted in a stainless steel holder in the headspace zone, and a saturated saline solution. Saturated salt solutions with excess salt were placed in the headspace zone 48 hours before the film samples in order to ensure that the critical relative humidities of the salts involved were reached and maintained during the tests. The salts and corresponding humidities employed were: KCO_3, 43.2 % RH; $MgNO_3$, 54.4 % RH; $NaNO_3$, 64.2 % RH; NaCl, 75.5 % RH; KCl, 85.1 % RH; and deionized water, 100 % RH. Samples were prepared in quadruplicate and stored in a dark room at 23 ± 2 °C for a period of at least two weeks in order to let them reach their state of equilibrium. Then the carvacrol concentration in the headspace was monitored until no differences were observed between three measurements taken on consecutive days.

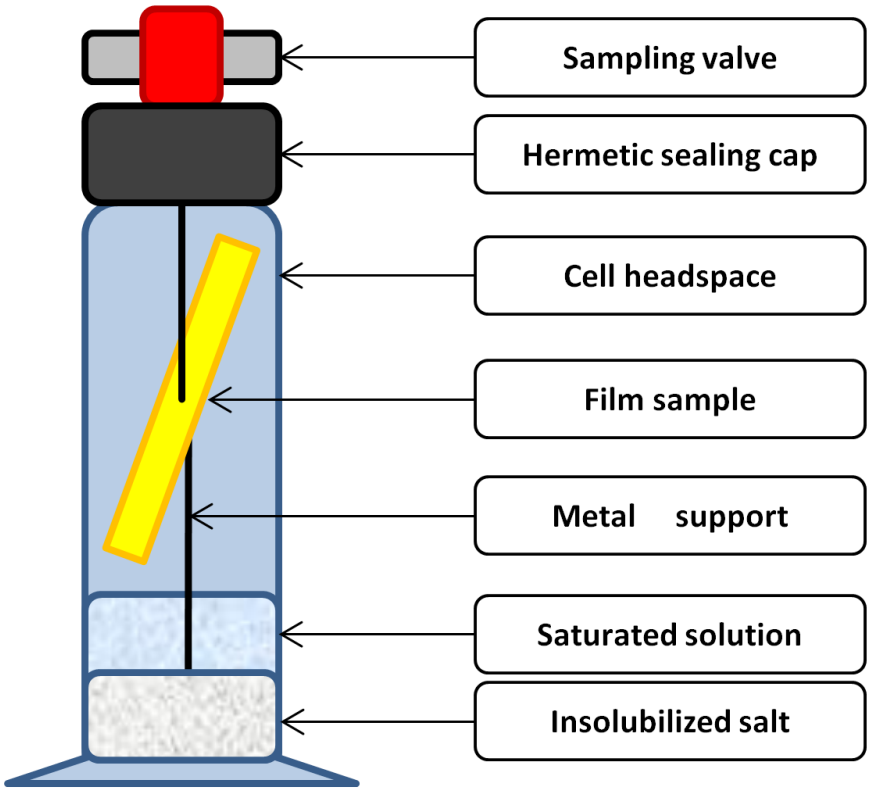

Figure I.1. Scheme of the equilibrium cell used for evaluation of Henry's constants for carvacrol in the air/polymer systems.

To measure the carvacrol concentrations in the headspace, 500 µL aliquots were taken with the aid of a precision gas syringe (1750 Gastight model, Hamilton, Bonaduz, Switzerland), and they were placed in the injection port of an HP 5890 Series II Plus gas chromatograph (Agilent Technologies, Wilmington, DE, USA) equipped with a flame ionization detector (FID) and a 30 m, 0.32 mm, 0.25 µm HP-5 capillary column. Chromatographic conditions were as follows: He as the carrier gas, splitless injection, 210 °C and 260 °C injector and detector temperatures, 1 min at 120 °C, heating ramp to 220 °C at 20 °C/min, and 1 min more at 220 °C. The sample volume withdrawn was restored with air to keep constant pressure. The GC response was previously calibrated by injecting known amounts of carvacrol.

Once the samples were at equilibrium and the headspace concentration measured, the equilibrium concentration of carvacrol in the polymer samples was determined by thermal desorption and GC analysis using a thermal desorber (890/891 model, Dynatherm Analytical Inst., Supelco, Bellafonte, PA, USA) connected in series to the gas chromatograph described previously. A portion of the tested film (about 20 mg) was placed in the desorption cell and heated at 210 °C for 7 minutes. A He gas stream carried the desorbed gaseous compounds to the GC through a transfer line heated at 230 °C. The GC was equipped with a 30 m, 0.53 mm, 2.65 µm Agilent HP-1 semicapillary column. The chromatographic conditions were: He as the carrier gas, 210 °C and 260 °C injector and detector temperatures, 7 min at 45 °C, heating ramp to 220 °C at 18 °C/min, and 12 min more at 220 °C. At the end of the desorption process the sample was weighed with a 0.1 mg precision balance (Voyager V11140 model, Ohaus, Switzerland). The response of the GC was calibrated by measuring polyethylene and polypropylene samples with known amounts of carvacrol.

The values of carvacrol Henry's constant for each film analyzed, H_c^P (P = E stands for EVOH-29 and P = PP stands for polypropylene), and for each relative humidity assayed, could easily be calculated from the concentrations in the headspace, C_c^{HS} , and in the PP and EVOH films, C_c^{PP} and C_c^E , by means of the following expressions:

$$H_c^{PP} = \frac{C_c^{HS}}{C_c^{PP}} \text{ and } H_c^E = \frac{C_c^{HS}}{C_c^E} \tag{I.1}$$

Once these constants had been quantified in both active films, carvacrol partition coefficients between the two materials, $K_c^{PP/E}$, were also estimated from the ratio between Henry's constants:

$$K_c^{PP/E} = \frac{C_c^{PP}}{C_c^E} = \frac{H_c^E}{H_c^{PP}} \tag{I.2}$$

2.4. Carvacrol evolution in package headspace

Bags made with the active coated films were placed in a thermostated room, at 23 ± 1 °C and 70 % RH, and the concentration of carvacrol in the package headspace was periodically checked for one week. A self-adhesive septum was fixed to the packages and 500 µL gas samples were withdrawn with the aid of a precision gas syringe (1750 Gastight model, Hamilton, Bonaduz, Switzerland) with no replacement of the volume removed. Gas aliquots collected were analyzed following the procedure described in the previous section.

2.5. Determination of carvacrol release kinetic parameters

To study the rate of carvacrol release from the active films as a function of the relative humidity, and to quantify the corresponding kinetics parameters, several samples of the active films were prepared, and analyzed in the experimental apparatus schematically represented in **Figure I.2**.

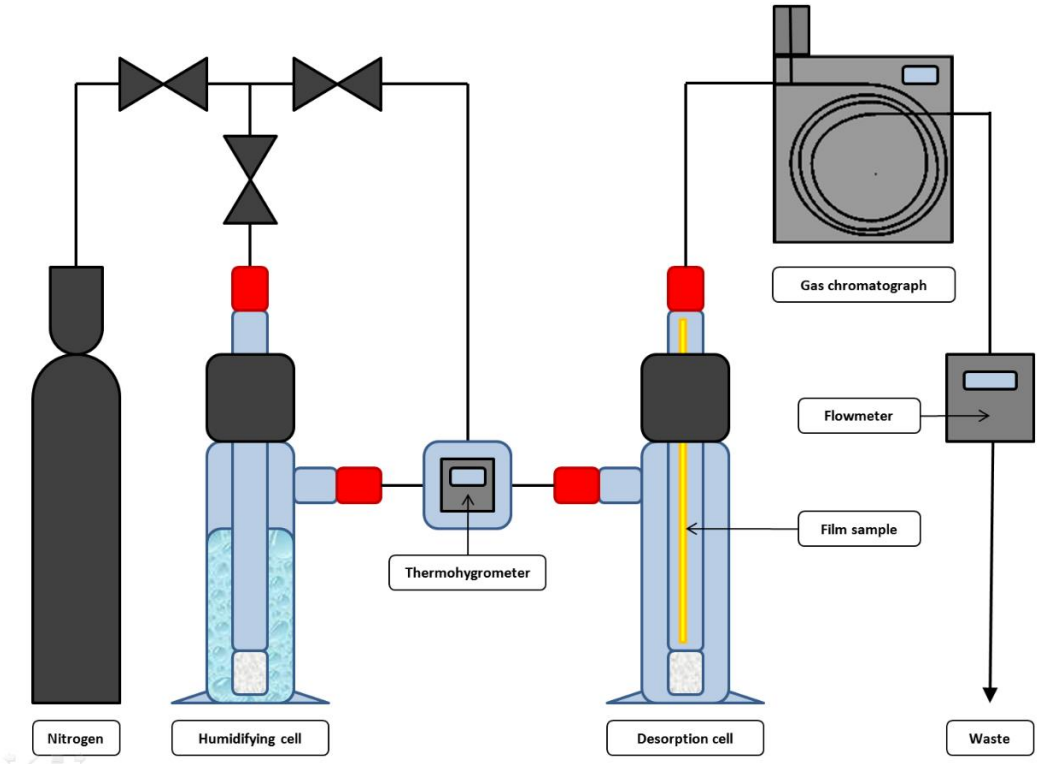

Figure I.2. Scheme of the apparatus used for characterization of the kinetics of carvacrol release from the polymer films.

Each polymer sample was inserted individually in a desorption tube. A humidified nitrogen stream was blown through the tube at a constant flow rate, high enough to avoid accumulation of the carvacrol molecules released in the inner space of the cell, and thus to remove any external resistance to their natural diffusion through the film. The carrier gas was partially humidified with the aid of a gas bubbler filled with deionized water and a needle valve system which allowed precise control of the relative humidity and flow rate so as to reach and maintain the required values for these parameters.

The gas mixture (carvacrol released and carrier gas) was injected in the inlet port of a gas chromatograph by means of an automatic 250 µL injection valve previously programmed to execute a sampling sequence. The GC conditions were those previously described in the analysis of carvacrol equilibrium parameters. At the end of the desorption process the sample was weighed, and its average thickness was measured, to properly evaluate the results obtained.

The evolution with time of the carvacrol mass flow released from the sample was converted to carvacrol concentration values, averaged for the whole film thickness, and they were introduced in the solution of Fick's law for a process of desorption from an infinite sheet (Crank, 1975):

$$C_c^P = \frac{2 \cdot C_{c0}^P}{\pi^2} \sum_{\nu=1}^{\infty} \frac{1}{\left(\nu - \frac{1}{2}\right)^2} \cdot e^{\frac{-\pi^2 \cdot \left(\nu - \frac{1}{2}\right)^2 \cdot D_c^P \cdot t}{l_p^2}} \qquad \text{(I.3)}$$

so that the value of D_c^P for each sample and RH condition could be evaluated. Each experiment was performed five times.

This experimental assay showed notable limitations when studying the performance of EVOH-29 films at low humidities owing to an extremely slow release rate. As an alternative, desorption tests at high temperature were conducted at 40, 55, 70, and 80 °C. Large EVOH-29 film samples containing carvacrol were hung on a metal grid and placed in a laboratory drying oven (Digitheat model, J. P. Selecta, Barcelona, Spain), previously filled with silica gel, to keep the relative humidity below 5 %. Periodically, a piece of film was cut and the average concentration of carvacrol was analyzed using the thermal desorption instrument coupled to the gas chromatograph previously described.

The evolution with time of the carvacrol concentration was then introduced in the solution of Fick's law for the desorption process (equation (I.3)) and solved for the determination of D_c at each

temperature. The value of D_c at 23 °C in dry conditions was estimated by thorough extrapolation of the Arrhenius plot:

$$D_c = D_c^0 \cdot e^{\frac{-E_D}{R \cdot T}} \quad \text{(I.4)}$$

where E_D is the activation energy of the carvacrol diffusion process, and D_c^0 the value of the D_c coefficient at 0 K.

2.6. Mathematical modeling

With regard to the simulation of the mass-transfer processes occurring in the environment / package / headspace system, the central objective of this research, a more complex mathematical model based on the finite elements method was developed with the aid of the Chemical Transport of Diluted Species physics interface included in the Chemical Reaction Engineering module of the COMSOL Multiphysics 4.2 modeling suite. The system to be modeled consisted of a real pillow-type bag of three-dimensional structure and finite volume (≈ 1000 cm^3) made up of four different material layers: environment, PP (30 µm), EVOH-29 (3 µm), and package headspace (HS). Owing to the limited calculation power of the available computing system it was decided to reduce the complexity of the model, and calculation time, by considering the environment to be independent of the package, and therefore the concentrations of all compounds in this layer could be taken as constant and defined in the boundary conditions of the system. Furthermore, even though mass-transfer phenomena in the modeled system were multidirectional, its particular shape also allowed the approximation of its geometry to a multilayer infinite sheet with only three spatial domains: PP, EVOH-29, and headspace (**Figure I.3**). In this way, the number of actual system dimensions could be reduced, and at the same time the modeling of the mass transport phenomena could be substantially simplified as they became processes of unidirectional progression.

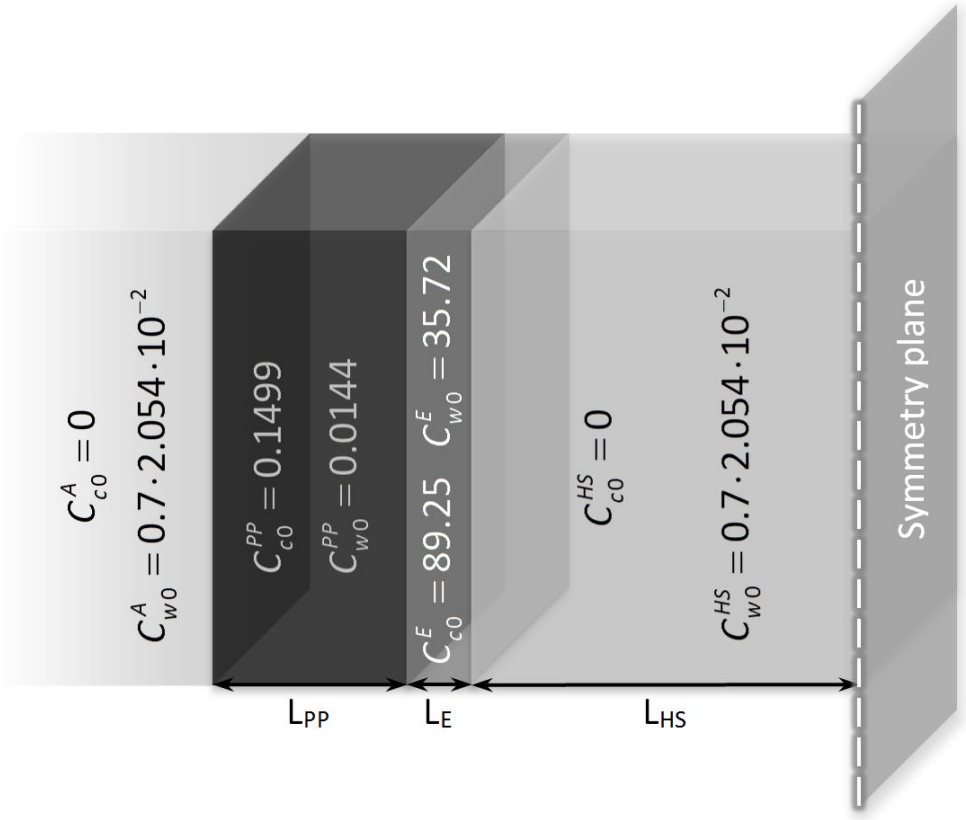

Figure I.3. Scheme of the simplified 1D system used to model the mass transport processes occurring in a pillow-type bag for fresh produce, and the corresponding initial concentrations for water and carvacrol in each material layer (kg/m^3).

However, to be sure that this new geometry could represent a good approximation to the original structure of the packages it was essential to accurately estimate the thickness of the gaseous layer, the main constituent of the package headspace, which was covering its polymer wall. In order to do so, the volume taken up by the inner atmosphere was mathematically distributed all over the inner surface of the package, thus leading to the following detailed calculation:

$$L_{HS} = \frac{V}{S} = \frac{1000\ \text{cm}^3}{36 \cdot 24\ \text{cm}^3} = \frac{1000\ \text{cm}^3}{864\ \text{cm}^3} = 1.16\ \text{cm} = 1.16 \cdot 10^{-2}\ \text{m} \qquad \text{(I.5)}$$

In addition, in view of the hydrophilic nature of the EVOH-29 coatings, and thus the great impact of material moisture on their physicochemical properties, it was essential to consider a multicomponent theoretical model in which all the water vapor transfer processes of the system could be included, as well as all the transport phenomena associated with carvacrol.

With this objective, the mathematical model was developed with the aid of the multiphysics analysis mode of the COMSOL Multiphysics 4.2 suite, where two dependent, interconnected variables, $C_c^{\alpha}(z,t)$ and $C_w^{\alpha}(z,t)$, were used in each material domain α (α = PP, E, or HS) to describe the carvacrol (subscript c) and water (subscript w) concentration profiles, respectively, at every position (z) within the film structures and at every instant of elapsed time (t). Furthermore, in order to properly model the water vapor mass-transfer processes in the system studied a thorough search in the literature was carried out, and the values of various kinetic and thermodynamic parameters for water transport phenomena in EVOH-29 (Aucejo, 2000), PP (Marais et al., 2000), and air (EPA On-line tools, 2011) were compiled and prepared as model inputs.

Finally, in order to solve the model accurately, it was necessary to set all the fundamental hypothesis and integration conditions of the system being modeled, and enter them in the software database. With respect to the hypotheses formulated, compliance with the following set of general assumptions was considered:

- Solid phases (films) and confined fluid phases (headspace) were static (absence of net mass flux in any direction) and initially homogeneous (isotropic properties at any point).
- Free fluid phases (surrounding atmosphere) were dynamic but perfectly agitated, hence homogeneous too.
- Interfaces were in thermodynamic equilibrium (thus, chemical potentials were identical in both phase thresholds).
- No interfacial volume (thus, mass flux densities were identical in both phase thresholds).
- Pressure and temperature were uniform and constant in the whole system.
- The overall concentration of every chemical species was constant in the whole system (absence of mass generation or degradation).
- Transient state lacking a period of induction.
- Unidirectional molecular mass transfer, which was well described at all times by Fick's law, with negligible mixing effects or competitive sorption effects.

Integration conditions were chosen as follows:

$C_c^{PP}(0,t)=\frac{C_c^A}{H_c^{PP}}=\frac{0}{H_c^{PP}}=0$ kg/m^3, since the environment was considered to be independent of the package and there was no carvacrol concentration in this material layer.

$C_w^{PP}(0,t)=\frac{C_w^A}{H_w^{PP}}=\frac{RH/100\cdot C_w^0(23\ ^\circ\text{C})}{H_w^{PP}}=\frac{0.7\cdot 2.054\cdot 10^{-2}}{1.426\cdot 10^{-1}}=0.1008$ kg/m^3, since the atmosphere of the thermostatic room was constantly maintained at a temperature of 23 °C and RH of 70 %.

$\nabla C_c^{HS}(L_{PP+E+HS},t)=0$ kg/m^4, since a symmetry plane was defined at the center of the package (**Figure I.3**).

$C_w^{HS}(L_{PP+E+HS},t)=RH/100\cdot C_w^0(23\ ^\circ\text{C})=2.054\cdot 10^{-2}$ kg/m^3, since some gelified water was placed in the headspace of the package.

Because there were discontinuities in the concentration profile at the boundary between the EVOH-29 and PP layers, two different dependent variables were used and were interrelated with the aid of a partition coefficient, $K_i^{PP/E}(C_w^E)$. Nevertheless, in order to get a continuous flux over the phase boundaries a special type of boundary condition using the stiff-spring method was applied (COMSOL Model Examples: Separation through dialysis, 2011): $J_i^{PP/E}=M_i\cdot\left(C_i^E\cdot K_i^{PP/E}\left(C_w^E\right)-C_i^{PP}\right)$, where M_i is the stiff-spring velocity (m/s) for i species.

Finally, initial conditions for every physical domain were defined so as to approximately meet the physicochemical state of the active packages at the first stage of the experiment, as **Figure I.3** shows, taking into account the fact that all the packaging materials had been stored at a maximum of 10 % relative humidity (silica gel containing desiccators). Then, once the system had been graphically designed, a complete database of experimental and bibliographical values for physicochemical properties was created, and all hypothesis and integration conditions were set out, the spatial and temporal discretization of the model was carried out, and it was solved numerically by applying the finite element method according to the terms previously described in the mathematical modeling section. In this last modeling stage, the final solution of the function $C_c^\alpha(z,t)$ was obtained by first calculating the approximate solution of the function $C_w^\alpha(z,t)$. In this way, the model was first solved only for the water vapor mass-transfer processes (since they were independent of carvacrol presence),

and the results obtained were stored, to be used later in the solving of the carvacrol mass-transfer phenomena as initial values for the variables already solved in the previous step.

In view of the one-dimensional structure of the model, the spatial discretization of its three physical domains was carried out with a freely distributed mesh of 1000 edge elements per domain and 4 additional vertex elements, involving 6006 degrees of freedom in all. The numerical solving of the model was constrained by 6 dependent variables, that were solved with the aid of a direct transient solver algorithm called PARDISO, using the BDF time-stepping method with 100 strict logarithmic time steps, and scaled tolerances of very low relative ($<10^{-5}$) and absolute ($<10^{-6}$) magnitudes.

3. RESULTS AND DISCUSSION

3.1. Assessment of carvacrol equilibrium as a function of water concentration

The effect of moisture sorption by EVOH-29 and PP active films on the extent of carvacrol release was studied with the aid of the equilibrium cells described in the experimental sections. From the carvacrol concentration values obtained in the gas phase and the polymer phase, the values of the equilibrium parameters (Henry's constants, H_c^P) were quantified as a function of the water concentration in the polymer. The values of the water concentration in both films were calculated by means of a D'Arcy and Watt water sorption isotherm reported for EVOH-29 (Aucejo, 2000), and from literature values of water vapor Henry's constant in an air/polymer system for PP (Marais et al., 2000).

The evolution of carvacrol Henry's constant with water concentration presented a different profile for EVOH-29 and PP active films. As **Figure I.4** shows, the values of carvacrol Henry's constant for the air / EVOH-29 system, H_c^E, increase sigmoidally with water concentration in the film samples, C_w^E, up to two orders of magnitude when relative humidity rises from 40 to 100 %. This progression can be described with Peleg's model, a 3-parameter sigmoidal equation based on the mathematical form of Fermi's distribution function (Peleg, 1993):

$$H_c^E = \frac{H_{c0}^E}{1 + e^{\frac{C_{wc}^E - C_w^E}{a}}} \qquad \text{(I.6)}$$

where H_{c0}^{E} is the carvacrol Henry's constant at the maximum value of water concentration in films, C_{wc}^{E} is the critical concentration of water that decreases H_{c}^{E} to 50 % below H_{c0}^{E} and a is a dimensionless constant that accounts for the steepness of the drop in the magnitude of H_{c}^{E}. By adjusting the plotted points to Peleg's model with the aid of a nonlinear regression analysis, the following expression was obtained for the evolution of H_{c}^{E} with the water concentration in the polymer, C_{w}^{E} (kg/m^3):

$$H_{c}^{E} = \frac{(2.51 \pm 0.09) \cdot 10^{-6}}{1 + e^{\frac{(98 \pm 4) - C_{w}^{E}}{(12.5 \pm 1.6)}}} \qquad \text{(I.7)}$$

The curve predicted by Peleg's model presented good agreement with the experimental results as **Figure I.4** shows.

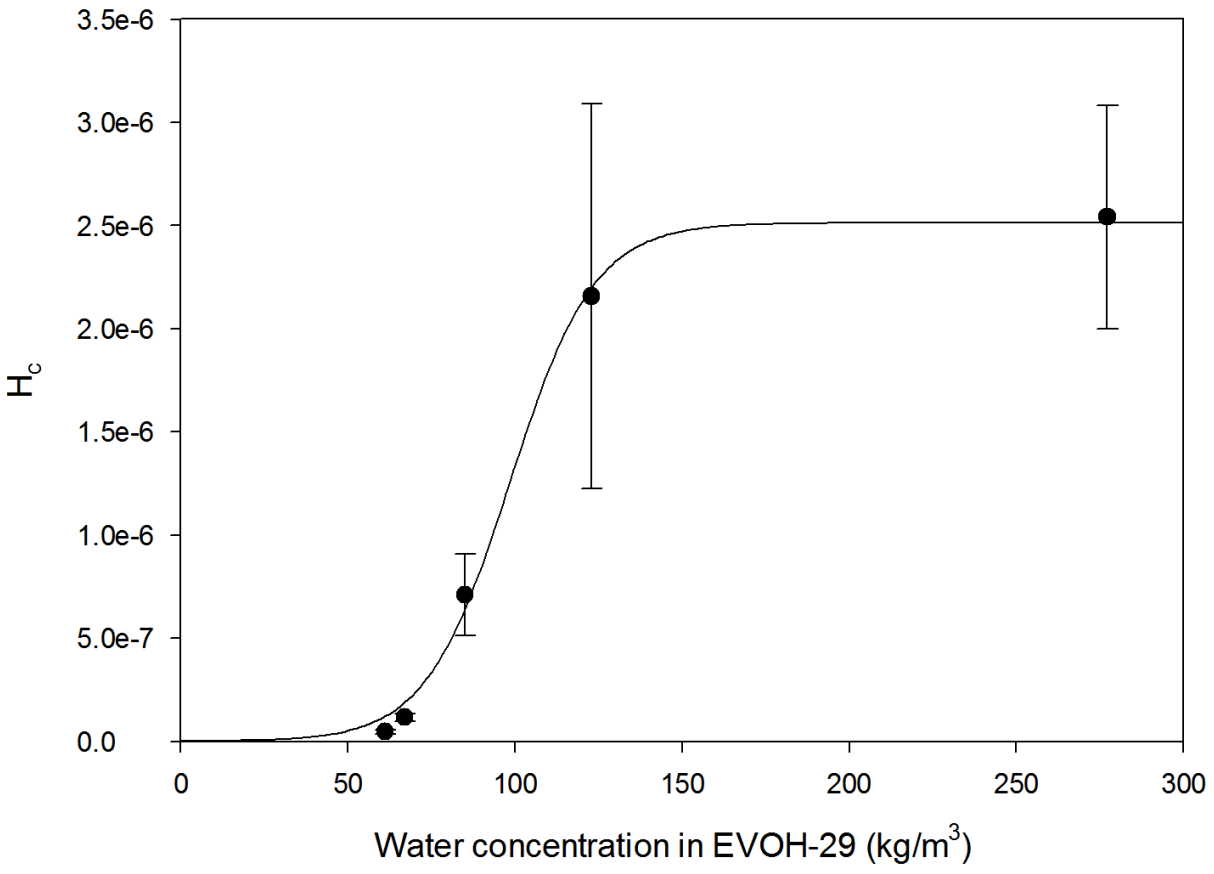

Figure I.4. Effect of water concentration in the EVOH-29 films on the values of Henry's constant for carvacrol in the air/polymer system. Symbols are experimental values and the curve is the representation of Peleg's model (equation (I.7)) for EVOH-29 films.

The observed behavior of EVOH-29 with moisture absorption could be explained in terms of the hydrophobicity of the solute and the hydrophilicity of the polymer matrix. On the one hand, the hydrophobic nature of carvacrol could cause its transfer to the cell atmosphere when the increase in water concentration in the polymer matrix could increase the polarity of the solid media and create a thermodynamic disequilibrium great enough to reduce the solubility of the antimicrobial agent in the polymer phase. Moreover, the markedly hydrophilic nature of EVOH-29 could be responsible for the weakening of its intermolecular hydrogen bonds, and thus for the relaxation of its polymer structure, leading to a substantial reduction in its glass-transition temperature, ultimately allowing a greater release of carvacrol in the headspace of the system (Long & Richman, 1960).

The critical concentration of plasticizer (water in this study, C_{wc}^{E}) has been related to the point at which glass transition takes place (Hernández-Muñoz et al., 2004). According to the values in **Figure I.4** and the result of the application of Peleg's model, the glass transition for EVOH-29 takes place at about 80 % RH and 23 °C, in agreement with previous studies (Cabedo et al., 2006). The value of Henry's coefficient in very dry conditions could not be obtained experimentally because there were large deviations at low humidities owing to difficulties in keeping the sample dry with this analytical procedure. Therefore an extrapolated value of $1.0 \cdot 10^{-9}$ was calculated using Peleg's model.

Unlike the air / EVOH-29 system, in the case of PP films the carvacrol Henry's constant for the air / PP system, H_c^{PP}, barely changes with the water concentration in their polymer matrix, with an average value:

$$H_c^{PP} = (1.0 \pm 0.2) \cdot 10^{-5} \qquad \text{(I.8)}$$

In this case, the hydrophobicity/hydrophilicity relationship continues to play a fundamental role in the assessment of the system. Specifically, as the olefinic nature of PP gives greater hydrophobicity to its structure, its properties are predictably unaltered under the influence of environmental humidity. PP should also enjoy good compatibility (i.e. solubility) with other hydrophobic molecules such as carvacrol, but the values of the Henry's parameter are higher than those of EVOH-29 at any RH. A possible explanation for these low values of Henry's constant for the air / EVOH-29 system might be interactions between the OH groups of the alcohol segments of the polymer and the phenol structure of carvacrol. In fact, carvacrol is slightly soluble in water.

By substitution of the two Henry's parameters in equation (I.2), the carvacrol partition coefficient between the two polymeric materials can be expressed as a function of the water concentration in EVOH-29, C_w^E:

$$K_c^{PP/E} = \frac{H_c^E}{H_c^{PP}} = \frac{H_{c0}^E}{H_c^{PP}} \cdot \frac{1}{1+e^{\frac{C_{wc}^E - C_w^E}{a}}} = \frac{K_{c0}^{PP/E}}{1+e^{\frac{C_{wc}^E - C_w^E}{a}}} = \frac{(2.5 \pm 0.7) \cdot 10^{-1}}{1+e^{\frac{(98 \pm 4) - C_w^E}{(12.5 \pm 1.6)}}} \quad \text{(I.9)}$$

On the basis of the values provided by this equation it can be stated that when EVOH-29 remains in dry conditions this polymer shows an affinity for carvacrol up to 10^4 times more than PP does, whereas in saturated humidity conditions the affinity decreases to about 4 times higher than in PP. Naturally, this considerable difference also comes from the evolution of the carvacrol balance between the two polymers, EVOH-29 and PP, when the water concentration rises in the former, since the solubility of the hydrophobic molecules diminishes in the EVOH-29 matrix, and also its internal structure relaxes, thus substantially reducing its overall capacity to retain the compound.

3.2. Assessment of carvacrol kinetics as a function of water concentration

The influence of moisture absorption by EVOH-29 and PP active films on the rate of carvacrol release was studied with the aid of the experimental apparatus described in **Figure I.2**. As an example, **Figure I.5** shows the evolution of carvacrol release from EVOH-29 at 99 % RH. For the determination of the diffusion coefficient values, D_c, equation (I.3) was used, assuming that during the desorption process the water concentration in the film remained constant and uniform throughout the thickness, and also the diffusion coefficient value. This approach was successfully applied elsewhere (López-Carballo et al., 2005). As can also be seen in **Figure I.5**, the curve obtained by the fitting of equation (I.3) agreed very well with the experimental values.

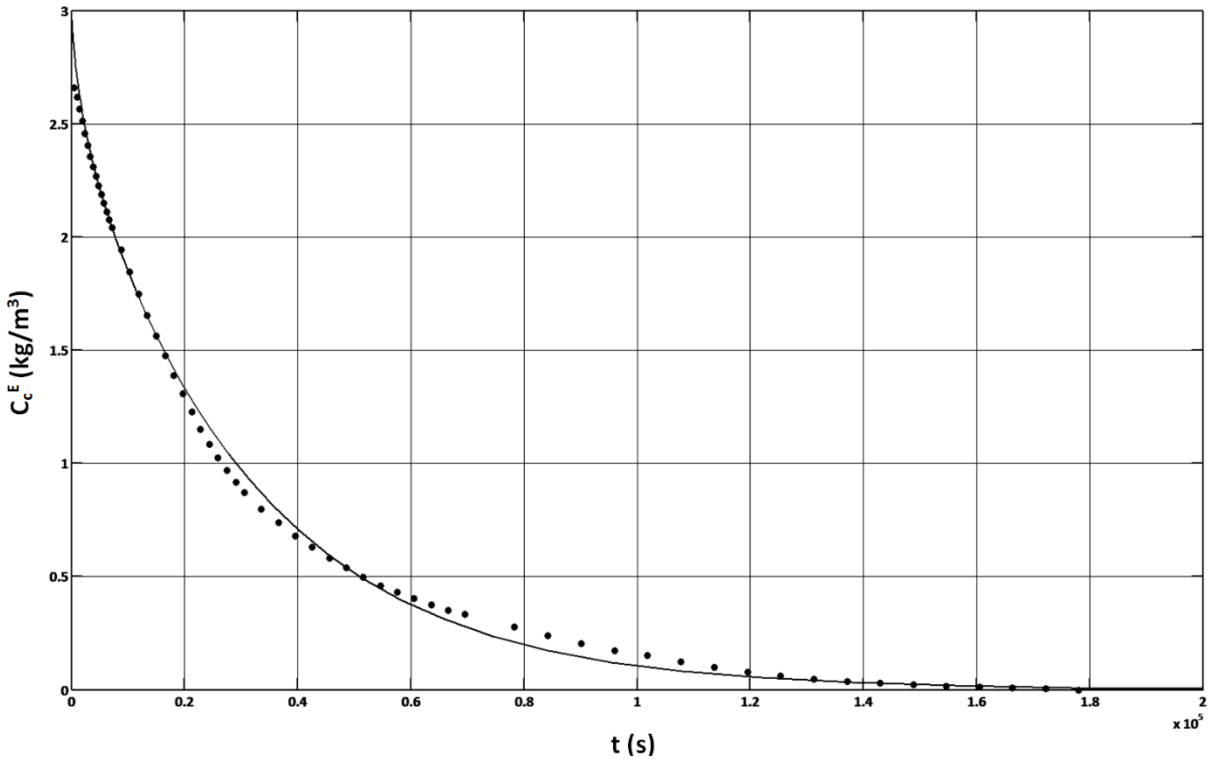

Figure I.5. Experimental evolution of carvacrol release from an EVOH-29 film at ambient temperature and 99% RH, and the descriptive curve obtained by using the appropriate solution of Fick's law (equation (I.3)).

Figure I.6 is the plot of the values of the carvacrol diffusion coefficients in the EVOH-29 active films, D_c^E, for every water concentration assayed in the polymer matrix, C_w^E. Unfortunately, no values could be obtained in medium to low water humidities with the apparatus described in **Figure I.2**. At low relative humidities, EVOH copolymers present strong interchain interactions through H-bonds, which increases the cohesive energy and decreases the chain mobility and consequently, the diffusivity of penetrants. Thus, the high barrier nature of dry EVOH-29 prevented the determination of the carvacrol release kinetics in low humidity conditions using the experimental apparatus described in **Figure I.2**, and a new experimental methodology had to be designed to overcome this limitation. In this new approach, carvacrol desorptions from dry EVOH-29 films at four temperatures above ambient were monitored. As an example, **Figure I.7** shows the results obtained experimentally together with the best fit of the analytical solution of Fick's law to the desorption process (equation (I.3)).

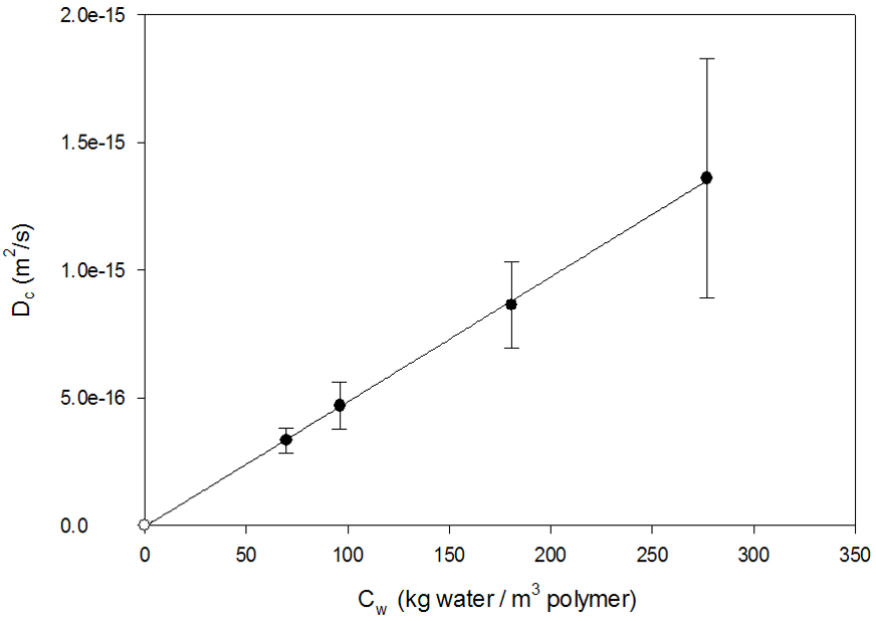

Figure I.6. **Effect of water concentration in the EVOH-29 films on the values of the diffusion coefficient for carvacrol. Symbols are experimental results and the curve is the representation of a linear regression.**

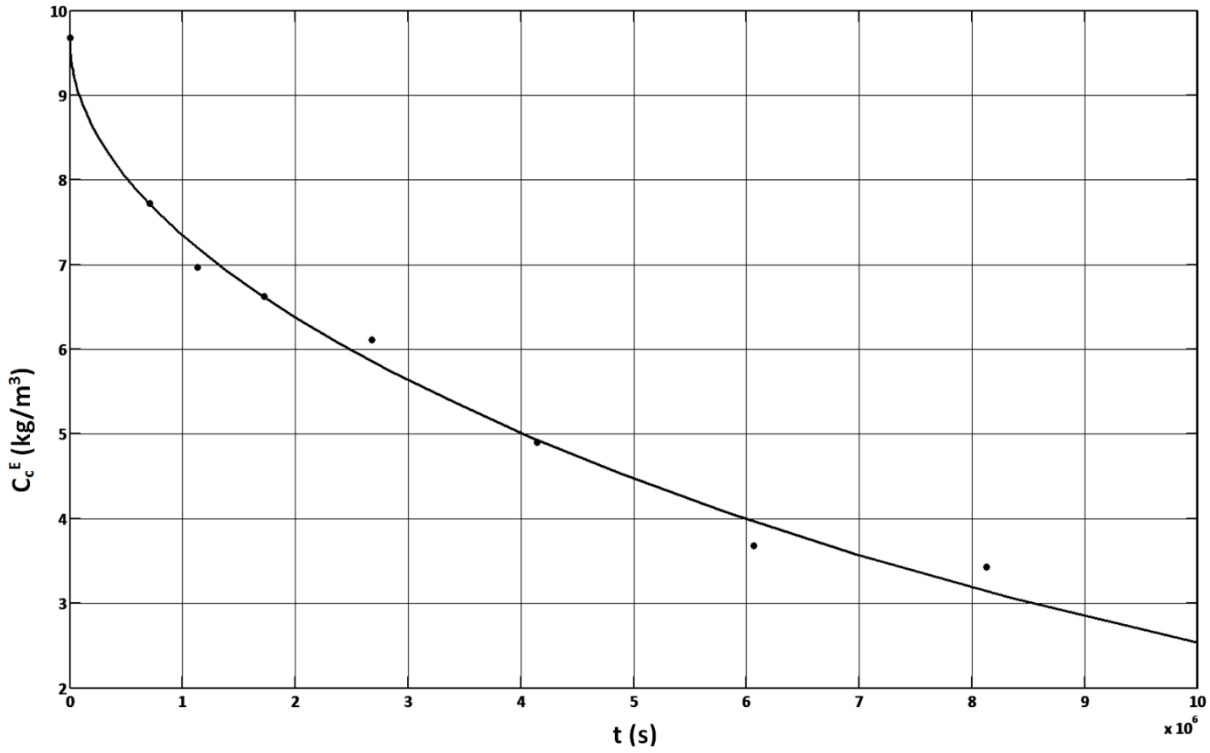

Figure I.7. **Experimental evolution of carvacrol release from an EVOH-29 film at 70 °C in dry conditions and the descriptive curve obtained by using the appropriate solution of Fick's law (equation (I.3)).**

The values of the diffusion coefficient obtained at various temperatures were plotted against the inverse of the absolute temperature in **Figure I.8**. Although the glass-transition temperature of EVOH-29 in dry conditions was found at 52 °C (Aucejo et al., 1999), the points plotted do not show any deviation or change of slope at that temperature. As can be seen in this semi-log plot, a linear correlation was observed, confirming the validity of the Arrhenius law to describe the evolution of D_c^E with temperature in the desorption process. This goodness of fit can be explained, in general terms, by the fact that the thermal motion of carvacrol molecules is probably more sensitive to changes in environmental temperature than the thermal motion of EVOH-29 polymer chains. Therefore, the temperature dependence of carvacrol diffusion processes would be more associated with the temperature dependence of carvacrol molecular mobility than with EVOH-29 structural changes.

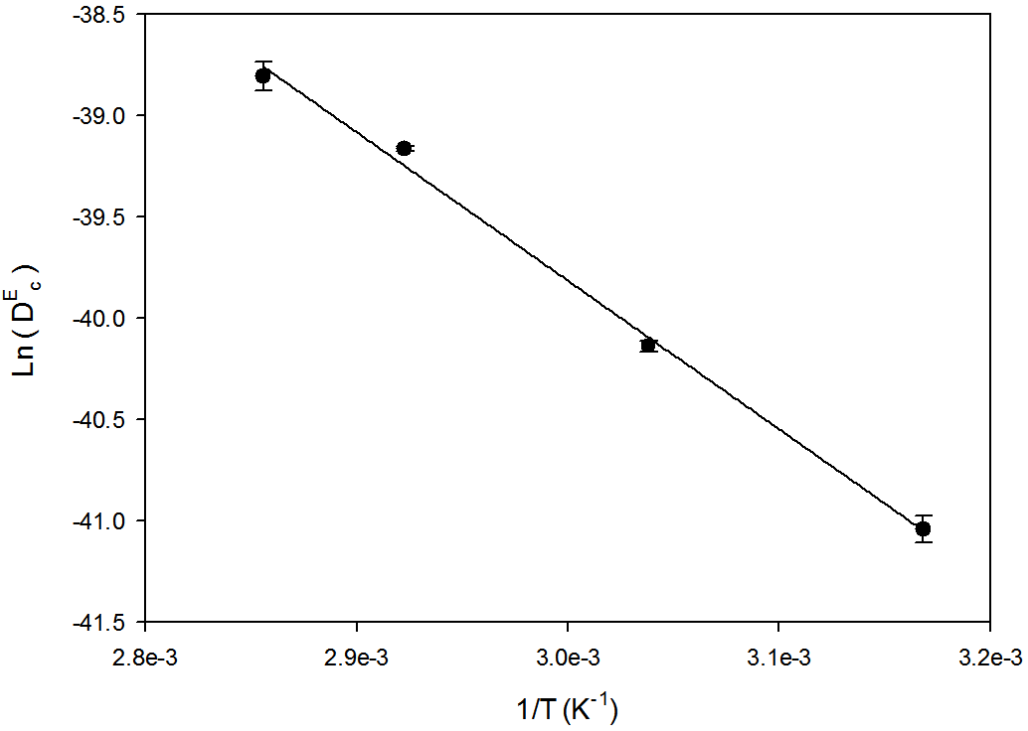

Figure I.8. Arrhenius plot of the diffusion coefficient values for carvacrol release from EVOH-29 films in dry conditions.

By introducing the ambient temperature, 23 °C, in the Arrhenius equation, an extrapolated value for the carvacrol diffusion coefficient in the EVOH-29 matrix at 0 % RH can be estimated:

$$D_{c0}^E = D_c^{E0} \cdot e^{\frac{-E_D}{R \cdot T}} = 2 \cdot 10^{-8} \cdot e^{\frac{-73 \cdot 10^2}{T}} = 2 \cdot 10^{-8} \cdot e^{\frac{-73 \cdot 10^2}{273.15+23}} \approx 3 \cdot 10^{-19} \ \mathrm{m^2/s} \qquad \text{(I.10)}$$

When this value is plotted in **Figure I.6** as a function of the water concentration, together with the values measured at the various RH conditions tested, they all form a straight line that fits well with the classical slope-intercept equation of a linear trend line:

$$D_c^E = D_{c0}^E + \gamma \cdot C_w^E = (3 \pm 7) \cdot 10^{-19} + (4.94 \pm 0.08) \cdot 10^{-18} \cdot C_w^E \qquad \text{(I.11)}$$

where D_{c0}^E is the extrapolated carvacrol diffusion coefficient in EVOH-29 in the absence of sorbed water and γ the water plasticization coefficient for EVOH-29.

As **Figure I.6** shows, the carvacrol diffusion coefficient in EVOH-29 exhibits a strong linear dependence on water concentration that increases D_c^E values up to four orders of magnitude when the relative humidity rises from 0 to 100 %. This variation can be attributed to the combined effects of the polymer relaxation phenomena mentioned earlier and the reduction of carvacrol solubility in the material as its moisture content increases with environmental relative humidity. Polypropylene active films, in turn, displayed a great independence of their kinetic and thermodynamic properties on water concentration, as previously stated in the equilibrium study. For this reason, an average value was assumed for the carvacrol diffusion coefficient in PP:

$$D_c^{PP} = (3 \pm 1) \cdot 10^{-15} \qquad \text{(I.12)}$$

3.3. Simulation of active package performance

In order to validate the model, its descriptive capabilities must be properly evaluated by comparing the simulation results with experimental observations of the behavior of the active packages in actual working conditions. For this purpose, the evolution with time of the average carvacrol concentration in the headspace of the packages, manufactured and stored as described in the experimental section, was plotted (**Figure I.9**), together with the theoretical curve of the same function, $C_c^{HS}(t)$, obtained as a result of the mathematical solving of the model developed to simulate the system. In light of the data plotted in the figure it could be said that the theoretical model applied to the system studied satisfactorily describes the evolution of the experimental results, although it shows slight deviations that are probably a consequence of random errors made during the course of the experiments.

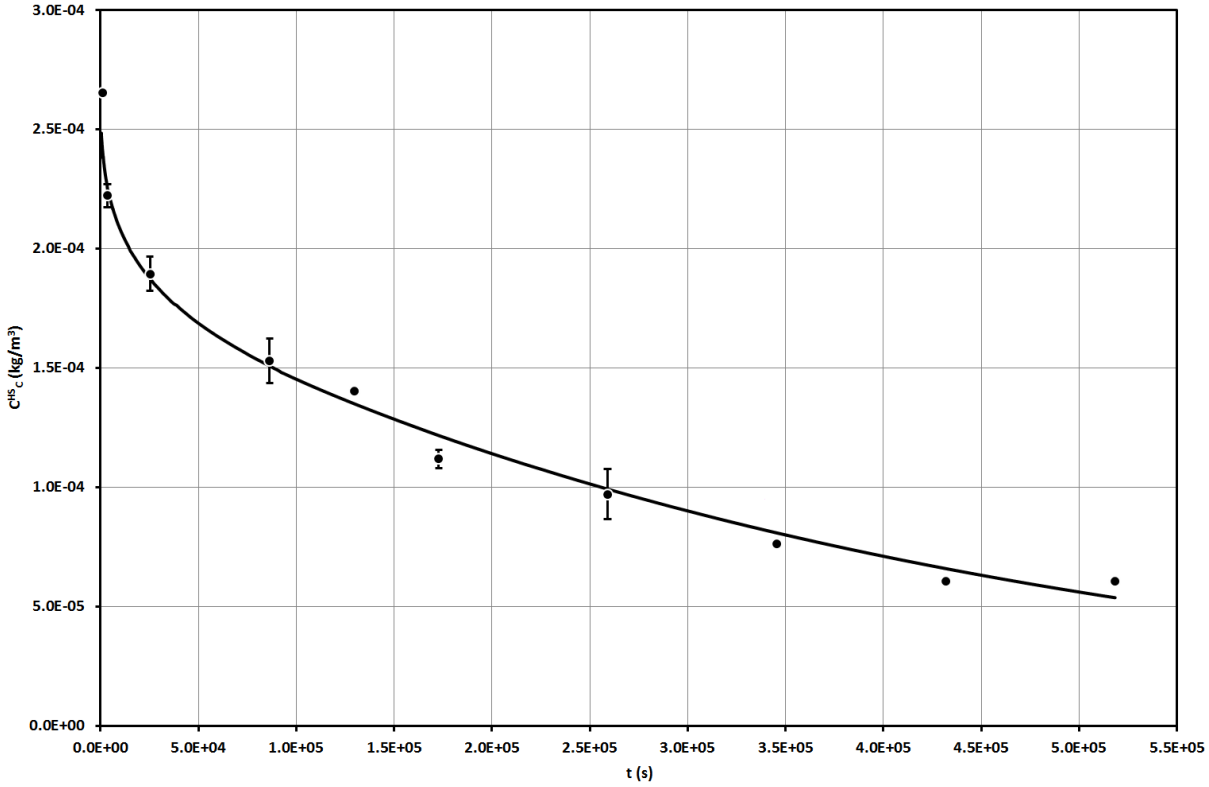

Figure I.9. Evolution in time of average carvacrol concentration released in the headspace of a bag for fresh produce at 23 °C. Symbols correspond to experimental values and the curve presents the behavior predicted with the finite elements model.

3.4. Optimization of active packages by model simulations

Once all the theoretical results given by the mathematical model have been experimentally contrasted, it can be used to describe all mass transport phenomena occurring simultaneously in the environment/package/headspace system, to detect the most relevant variables that affect the effectiveness of the package, and, of course, to optimize the package design. Thus, the model can be systematically applied to the simulation and prediction of behavior of the system in working conditions (environment or system design) that differ from the ones considered in this paper. Consequently, this theoretical model could be a very useful tool for optimizing the design of active packages, since it is able to predict their long-term evolution when the value of any of their fundamental parameters has been modified. As examples, the theoretical results estimated by the model for the mathematical simulation of the performance of the active packages when certain geometric characteristics or

environmental conditions are modified, namely, the thickness of the PP layer or EVOH-29 coating, and the environmental relative humidity, are presented below.

Figures I.10 and **I.11** show the evolution of the average carvacrol concentration in the headspace of the packages when the thickness of the PP substrate is varied from 1 to 100 µm, or when the thickness of the EVOH-29 coating is varied from 0.1 to 10 µm.

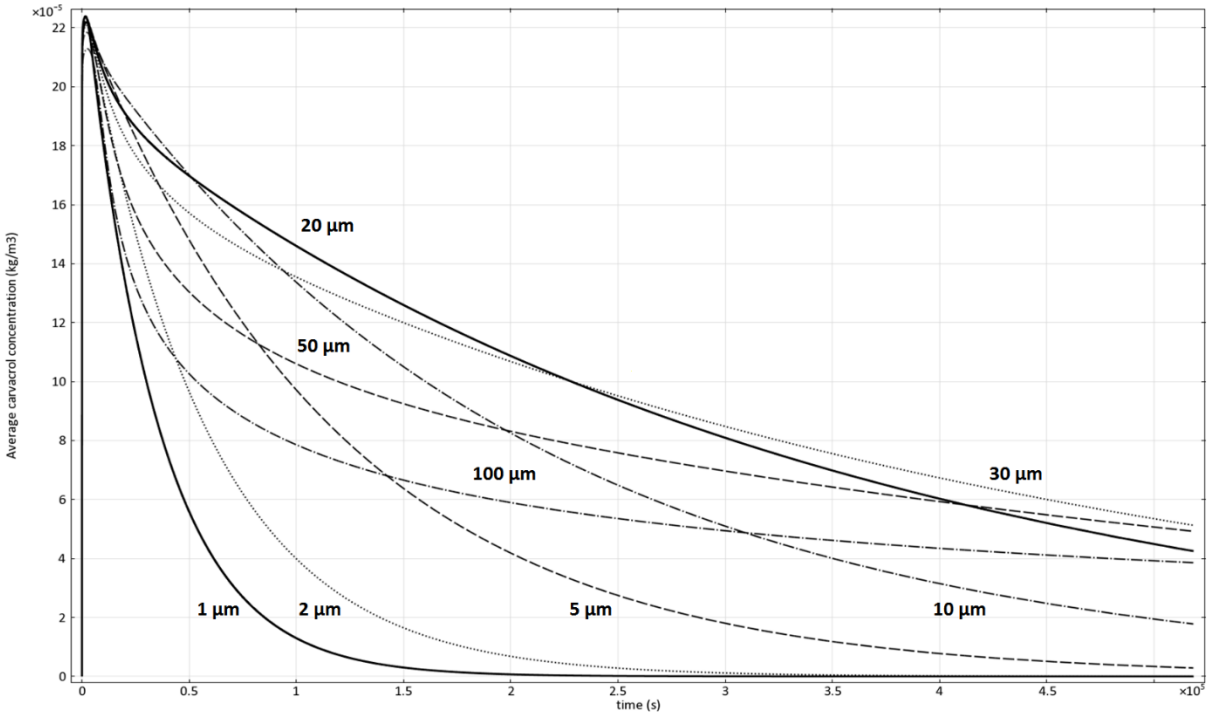

Figure I.10. Evolution in time of carvacrol concentration released in the package headspace as a function of PP layer thickness.

As **Figure I.10** shows, the thickness of the PP wall has two different effects on the average carvacrol concentration in the atmosphere inside the package. On the one hand, the "barrier" effect of the package wall increases with the increase in thickness, thus making outflow of the antimicrobial agent through the system more difficult and consequently contributing to its accumulation in the headspace of the package. On the other hand, the increase in thickness of the PP layer also causes greater absorption (scalping) of the active agent within its polymer matrix, which leads to a rapid and dramatic fall in its concentration in the atmosphere inside the system, which can be clearly noticed at the beginning of the storage time in the curves of greatest thickness. As a consequence of both effects, the evolution of the average concentration of antimicrobial agent in the package headspace reaches maximum values at a thickness of 30 µm. Hence, it can be stated that the current package design is optimized for maximum performance with respect to PP layer thickness.

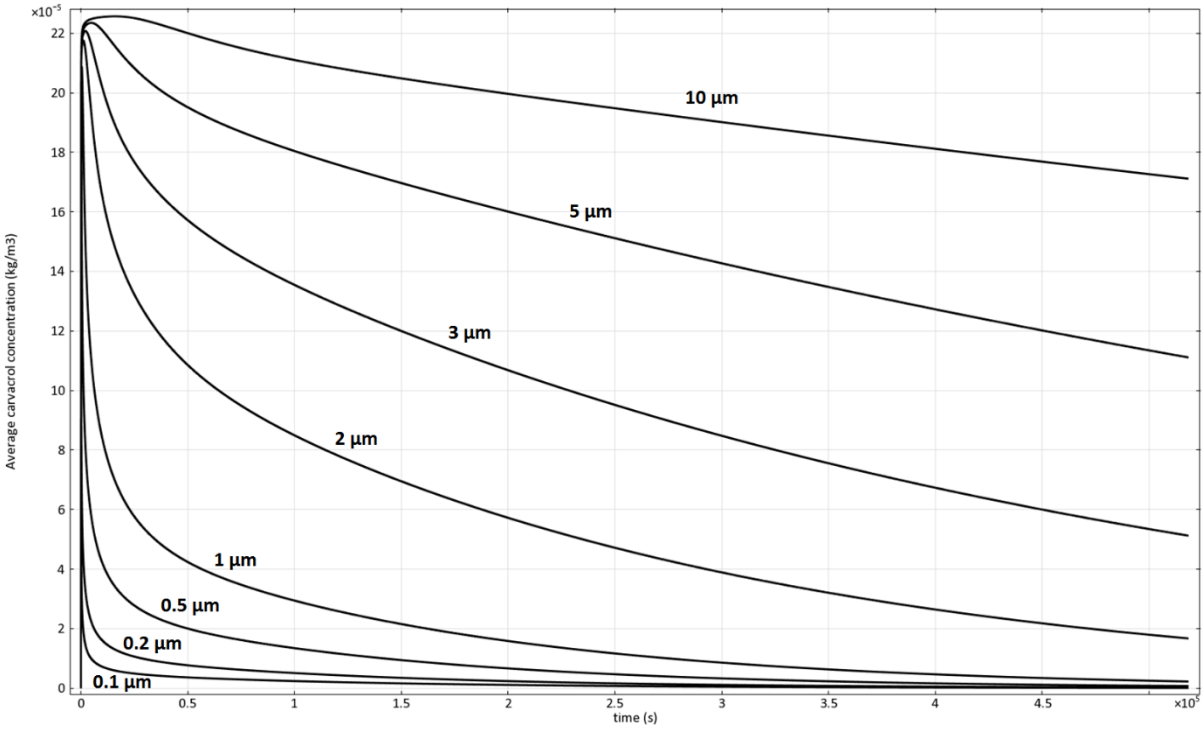

Figure I.11. Evolution in time of carvacrol concentration released in the package headspace as a function of EVOH-29 layer thickness.

With respect to the coating, an increase in EVOH-29 thickness contributes to the insulation of the inner atmosphere (a highly humid ambience) from the outer environment (intermediate humidity). After a few hours of exposure, a stationary humidity gradient is established in the EVOH-29 layer. Near the interface with the headspace the polymer matrix is highly humidified and plasticized, so that there is a fast diffusion of carvacrol in its vicinity, while near the boundary with the PP layer the lower moisture content reduces matrix plasticization and compound diffusivity. As the thickness of EVOH-29 increases, the stationary water content in the part adjacent to the PP layer decreases, thus reducing the diffusion coefficient of the antimicrobial agent and consequently slowing down compound losses through the polymer wall. Obviously, the effects observed in this material prove to be much stronger than the ones found for PP owing to its better barrier properties.

The other very important variable is the environmental relative humidity, because the water uptake in the EVOH-29 layer is decisive for the mass transport of carvacrol in the whole system and also very important for the storability (aging) of the active coated structure. **Figure I.12** shows the evolution in time of the average carvacrol concentration in the package headspace when the environmental relative humidity ranges from 10 to 100 %. As can be seen, the effects that this variable has on carvacrol concentration are very similar to the ones previously observed for the variation in EVOH-29 thickness.

Indeed, the drier the outer atmosphere, the higher the concentration during storage time. In this case, a lower external humidity results in a higher moisture gradient in the film thickness, and subsequently a lower stationary water content at the EVOH-29 interface with PP decreases outward carvacrol diffusivity, thus contributing to the concentration of the active agent in the package headspace, and consequently increasing the effectiveness of the package.

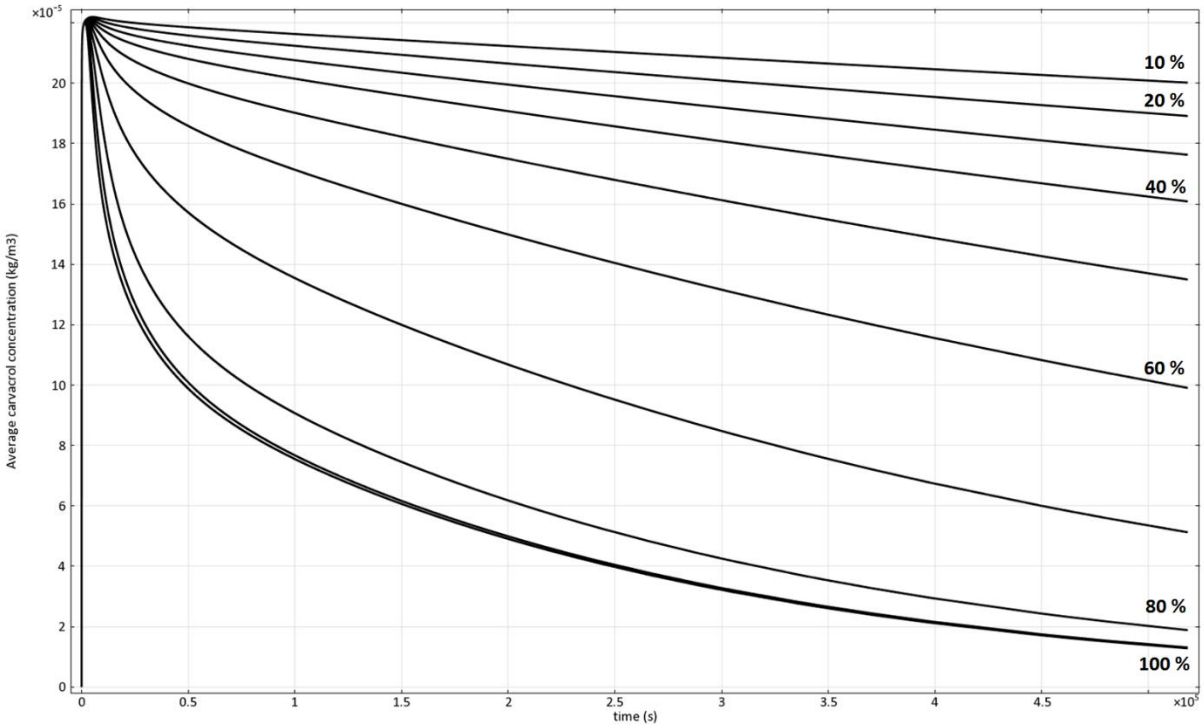

Figure I.12. Evolution in time of carvacrol concentration released in the package headspace as a function of environmental relative humidity.

As mentioned in the introduction, a key issue in the design of an active package is the availability of a triggering mechanism to avoid total or partial exhaustion of activity during storage. In this work, the triggering mechanism is the environmental humidity. The proposed model was also used to estimate the carvacrol mass transport that should take place in a reel of the coated film during storage at various RH values, **Figure I.13** shows the average concentration in EVOH-29 and in PP when equilibrium is achieved in various RH conditions. As expected, there is an improvement in the storability of the films in dry conditions.

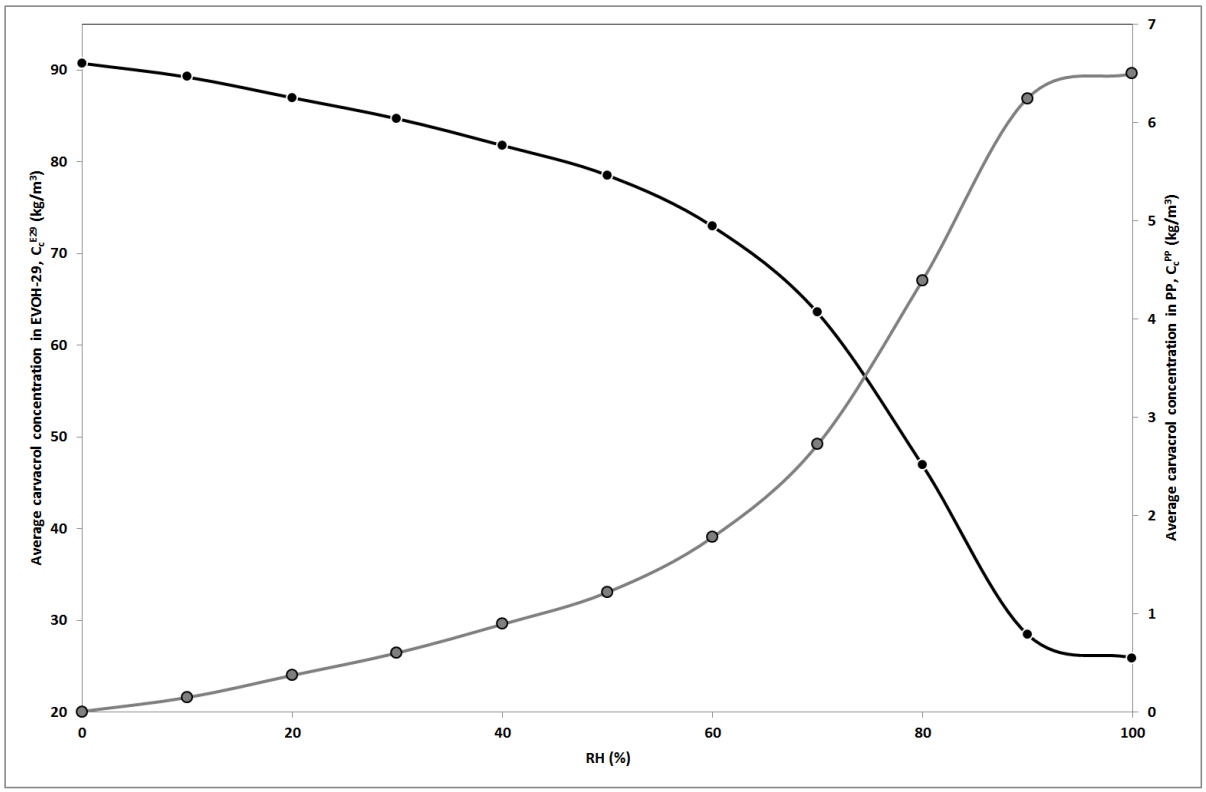

Figure I.13. Average carvacrol concentration at equilibrium when a reel of the EVOH-29 coated PP film is stored at different relative humidities. (●), concentration in the EVOH-29 layer, (●), concentration in the PP layer.

3.5. Data analysis

The values for all the measured parameters and coefficients presented in this research work are expressed as: "$(\bar{x} \pm \varepsilon)$ units", where $\bar{x}$ stands for the sample mean of parameter x, and ε stands for the absolute error of parameter x. This absolute error equals to sample standard deviation for measured parameters, and was determined by means of propagation of uncertainty (partial derivatives method) for calculated parameters.

Data fitting to Peleg's equation was fulfilled through a non-linear regression analysis of a 3-parameter sigmoidal function. Data fitting to water-dependent diffusion equation and to linearized Arrhenius equation were fulfilled by means of a linear regression analysis of the classical slope-intercept equation. Both linear and non-linear regression analysis were carried out with the aid of SigmaPlot 12.1 regression wizard.

4. CONCLUSIONS

In this work a novel mathematical model was developed to successfully describe all the mass-transfer processes that occur in a commercial active package for ready-to-eat salad products, consisting of a PP functional layer thinly coated with a hydrophilic copolymer of ethylene-vinyl alcohol that carries a controlled amount of carvacrol as antimicrobial active agent.

This model can be employed in the optimization of package design in order to ensure the maintenance of a specific concentration of the active agent in the headspace, high enough to prevent potential growth of a particular foodborne spoiling or pathogenic microorganism on the preserved foodstuffs, but not so high that at some point it may exceed the thresholds set by current legislation. At the same time, this model could also be helpful when trying to achieve maximum efficiency of the preservation system because it gives the key factors to minimize potential losses of the active compound through the polymer wall.

The model could also lead to the mathematical simulation and prediction of other preservation systems similar to the one studied in this paper, where other polymer matrices or active agents might be involved, or where different geometric characteristics or physicochemical properties might be present, as long as an inventory of experimental data for all the parameters and coefficients involved is available, sufficiently complete to fulfill all the mathematical requirements demanded by the model.

ACKNOWLEDGMENTS

Authors thank the financial support of the Spanish Ministry of Science and Innovation (projects AGL2006-02176 and AGL2009-08776), EU (Nafispack project 212544), Generalitat Valenciana (J.P.C. fellowship) and Mr. Karel Clapshaw (English edition services).

REFERENCES

Aucejo, S., Marco, C., Gavara, R. (1999). Water effect on the morphology of EVOH copolymers. *Journal of Applied Polymer Science*, 74 (5), 1201 – 1206.

Aucejo, S. (2000). *Estudi i caracterització de l'efecte de la humitat en les propietats barrera d'estructures polimèriques hidròfiles.* Tesi doctoral, Universitat de València, València.

Aucejo, S., Català, R., Gavara, R. (2000). Interactions between water and EVOH food packaging films. *Food Science and Technology International*, 6 (2), 159 – 164.

Begley, T., Castle, L., Feigenbaum, A., Franz, R., Hinrichs, K., Lickly, T., Mercea, P., Milana, M., O'Brien, A., Rebre, S., Rijk, R., Piringer, O. (2005). Evaluation of migration models that might be used in support of regulations for food – contact plastics. *Food Additives and Contaminants*, 22 (1), 73 – 90.

Cabedo, L., Lagarón, J. M., Cava, D., Saura, J., Giménez, E. (2006). The effect of ethylene content on the interaction between ethylene – vinyl alcohol copolymers and water – II: influence of water sorption on the mechanical properties of EVOH copolymers. *Polymer Testing*, 25 (7), 860 – 867.

Català, R., Gavara, R. (2001). Nuevos envases. De la protección pasiva a la defensa activa de los alimentos envasados. *Arbor*, CLXVIII, 661, 109 – 127.

COMSOL Model Examples: Separation through dialysis. COMSOL Multiphysics Modeling Guide, version 4.2. (2011). COMSOL AB.

Crank, J. (1975). *The mathematics of diffusion*. Clarendon Press, London, UK.

De Vincenzi, M., Stammati, A., De Vincenzi, A., Silano, M. (2004). Constituents of aromatic plants: carvacrol. *Fitoterapia*, 75 (7 – 8), 801 – 804.

EPA on – line tools for site assessment calculation: estimated diffusion coefficients in air and water – extended version. United States Environmental Protection Agency, USA. *http://www.epa.gov/athens/learn2model/part–two/onsite/estdiffusion–ext.html*

Gavara, R., Català, R., Hernández – Muñoz, P. (2009). Extending the shelf – life of fresh – cut produce through active packaging. *Stewart Postharvest Review*, 5 (4), 1 – 5.

Han, J. H. (2005). *Antimicrobial packaging systems.* Han, J. H. (ed.) *Innovations in food packaging*. Elsevier Academic Press, USA.

Hernández – Muñoz, P., López – Rubio, A., Lagarón, J. M., Gavara, R. (2004). Formaldehyde cross – linking of gliadin films: effects on mechanical and water barrier properties. *Biomacromolecules*, 5 (2), 415 – 421.

Long, F. A., Richman, D. (1960). Concentration gradients for diffusion of vapors in glassy polymers and their relation to time dependent diffusion phenomena. *Journal of American Chemical Society*, 82 (3), 513 – 519.

López, P., Sánchez, C., Battle, R., Nerín, C. (2007). Development of flexible antimicrobial films using essential oils as active agents. *Journal of Agricultural and Food Chemistry*, 55 (21), 8814 – 8824.

López – Carballo, G., Cava, D., Lagarón, J. M., Català, R., Gavara, R. (2005). Characterization of the interaction between two food aroma components, α – pinene and ethyl butyrate, and ethylene – vinyl alcohol copolymer (EVOH) packaging films as a function of environmental humidity. *Journal of Agricultural and Food Chemistry*, 53 (18), 7212 – 7216.

López – Rubio, A., Lagarón, J. M., Giménez, E., Cava, D., Hernández – Muñoz, P., Yamamoto, T., Gavara, R. (2003). Morphological alterations induced by temperature and humidity in ethylene – vinyl alcohol copolymers. *Macromolecules*, 36 (25), 9467 – 9476.

Marais, S., Nguyen, Q. T., Devallencourt, C., Metayer, M., Nguyen, T. U., Schaetzel, P. (2000). Permeation of water through polar and nonpolar polymers and copolymers: determination of the concentration – dependent diffusion coefficient. *Journal of Polymer Science. Part B: Polymer Physics*, 38 (15), 1998 – 2008.

Marcos, B., Aymerich, T., Monfort, J. M., Garriga, M. (2007). Use of antimicrobial biodegradable packaging to control *Listeria monocytogenes* during storage of cooked ham. *International Journal of Food Microbiology*, 120 (1 – 2), 152 – 158.

Mascheroni, E., Chalier, P., Gontard, N., Gastaldi, E. (2010). Designing of a wheat gluten / montmorillonite based system as carvacrol carrier: Rheological and structural properties. *Food Hydrocolloids*, 24 (4), 406 – 413.

Official Journal of the European Union (OJEU) L12/1 (15/01/2011). COMMISSION REGULATION (UE) No 10/2011 of 14 January 2011 on plastic materials and articles intended to come into contact with food. Annex V: Compliance testing. Article 2.2.3.: Migration modelling.

Oyane, A., Uchida, M., Onuma, K., Ito, A. (2006). Spontaneous growth of a laminin – apatite nano – composite in a metastable calcium phosphate solution. *Journal of Biomedical Materials Research*, 27 (2), 167 – 174.

Peleg, M. (1993). Mapping the stiffness – temperature – moisture relationship of solid biomaterials at and around their glass transition. *Rheologica Acta*, 32 (6), 575 – 580.

Poças, M., Oliveira, J., Oliveira, F., Hogg, T. (2008). A critical survey of predictive mathematical models for migration from packaging. *Critical Reviews in Food Science and Nutrition*, 48 (10), 913 – 928.

Tunç, S., Duman, O. (2011). Preparation of active antimicrobial methyl cellulose / carvacrol / montmorillonite nanocomposite films and investigation of carvacrol release. *LWT – Food Science and Technology*, 44 (2), 465 – 472.

Zagory, D., Kader, A. A. (1988). Modified atmosphere packaging of fresh produce. *Food Technology*, 42 (4), 70 – 77.

II DESCRIBING AND MODELING THE RELEASE OF AN ANTIMICROBIAL AGENT FROM AN ACTIVE PP / EVOH / PP PACKAGE FOR SALMON

Josep Pasqual Cerisuelo [a], José María Bermúdez [b], Susana Aucejo [b], Ramon Català [a], Rafael Gavara [a,*], Pilar Hernández – Muñoz [a]

[a] Laboratori d'envasos, Institut d'Agroquímica i Tecnologia d'Aliments, IATA – CSIC.
Av. Agustí Escardino, 7. 46980 Paterna, València.

[b] Institut Tecnològic de l'Embalatge, Transport i Logística, ITENE.
Parc Tecnològic de Paterna.
C/ Albert Einstein, 1. 46980 Paterna, València.

* Autor de contacte. Tel.: +34 963900022, e-mail: rgavara@iata.csic.es

ABSTRACT

Natural antimicrobial active packaging is an emerging technology for fresh fish preservation in which a chemical compound of natural origin is purposely incorporated into a packaging material to be released into the food surface in order to protect it from spoilage by foodborne microorganisms. The maximum efficiency of an antimicrobial package can only be obtained when an adequate activity is achieved immediately after the packaging operation and is maintained constant throughout the product's shelf life. This work develops an active package designed for the preservation of fresh farmed salmon in cubes or slices, made up of a rigid polypropylene / ethylene – vinyl alcohol / polypropylene tray heat – sealed with an active polypropylene / ethylene – vinyl alcohol / polypropylene film lid in which 6.5 % carvacrol is incorporated in the EVOH kernel as an antimicrobial active agent. The work also includes the measurement of the carvacrol kinetics and equilibrium parameters in the preserved salmon fillets, and proposes a mathematical model based on the finite element method to describe and simulate the common performance of the developed package / food system, and to predict its behavior under different working conditions or system configurations with the objective of finding the optimum combination of variables that ensure the best packaging performance. The results obtained from the determination of parameters showed a rapid migration of the active compound through the fish muscle, and a low affinity of the agent molecules for the food matrix. The active package was successfully developed, and the proposed model was satisfactorily used to detect the key factors that govern the package performance, and also to improve the package design by modifying the thickness distribution of the multilayer active film.

***Journal of Food Engineering*, 2013, 116 (2), 352 – 361.**

1. INTRODUCTION

Whereas fresh packed meat has been very common in supermarket refrigerators since the past century, fresh packed fish is currently being introduced in the food market at a slow pace. The reason is that fresh fish products are usually more perishable than most other foodstuffs, mainly owing to their high water activity, neutral pH, and presence of autolytic enzymes, making preservation of them much more difficult (Sivertsvik, 2003). Nevertheless, just as occurred for packed meat, fresh packed fish is experiencing growing demand by consumers due to its greater advantages with respect to the raw fish market, and because of being perceived as better in quality terms with respect to the traditional frozen fish (Trondsen, 1997). This has encouraged the food industry to improve the preservation of these food products, and its efforts are currently concentrating on research into new packaging technologies such as modified atmosphere packaging (MAP) or active packaging.

Among the several packaging technologies developed for fresh or minimally processed food products, antimicrobial active packaging is one of the most innovative. In this technique an antimicrobial compound is deliberately integrated into a packaging material to be released into the food where necessary to prevent its natural spoilage (Catalá and Gavara, 2001; Han, 2005). Recent developments have been characterized by the use of active agents of natural origin embedded in the walls of polymeric packages, in the carrier layer of multilayer packaging films, or in the divider sheets of sliced food packages (Marcos et al., 2007; Rodríguez et al., 2007; Siripatrawan and Noipha, 2011; Ahmad et al., 2012; Barbiroli et al., 2012; Lara-Lledó et al., 2012). In addition, these prototypes often include a triggering mechanism and / or a retaining system in the active layer in order to control the initiation, kinetics, and final extension of the release of the agent, with the aim of ensuring an antimicrobial activity that is as constant as possible throughout the product's shelf life (Mascheroni et al., 2011; Tunç and Duman, 2011; Muriel-Galet et al., 2012a and 2012b).

In a previous work, a commercial active antimicrobial package for ready-to-eat salad products was successfully developed by coating a conventional polypropylene film with a thin layer of a hydrophilic ethylene-vinyl alcohol copolymer with 5 % carvacrol as a natural antimicrobial agent. In order to fully understand the underlying mechanisms governing all the mass transfer phenomena occurring in the package a mathematical model was developed and the necessary mass transport parameters were experimentally determined and introduced. As a result of the mathematical simulations carried out, the model showed the way toward optimization of the package through minimization of losses of the volatile active agent (Cerisuelo et al., 2012).

In the case of fresh packed fish, little has been investigated regarding the natural antimicrobial active packaging technology (Gómez-Estaca et al., 2009; Galotto et al., 2011). Instead, most researchers have preferred the incorporation of the active agent through an edible coating or wrapping (Ahmad et al., 2012; Chamanara et al., 2012), or the direct addition on the fish surface (Corbo et al., 2008 and 2009; Mexis et al., 2009; Mastromatteo et al., 2010), and none have proposed a mathematical model to understand and improve the performance of their preservation systems.

The aim of this work, therefore, was to develop a mathematical model that adequately describes the mass-transfer phenomena taking place in a commercial active antimicrobial package for fresh farmed salmon (*Salmo salar*), consisting of a rigid PP / EVOH-32 / PP tray heat-sealed with a coextruded multilayer film lid made up of two functional layers of PP, two tie layers, and a kernel layer of EVOH-29 with 6.5 % carvacrol as a natural antimicrobial active agent. This work also includes experimental determination of all the mass transport parameters required in the model calculations, and also validation of the model by comparing its predicted results with experimental values obtained from the analysis of real fish packages.

2. MATERIALS AND METHODS

2.1. Materials

Coextruded multilayer films 73 µm thick, made up of two external layers of polypropylene, two tie layers, and an internal layer of ethylene-vinyl alcohol copolymer with a 29 % ethylene molar content (EVOH-29) blended with 6.5 % carvacrol, were prepared by ITENE (Paterna, Spain). The compound of EVOH-29 and carvacrol was obtained by extrusion processes, using a twin screw extruder model ZSK26MC (Coperion GmbH, Germany) with a screw diameter of 26 mm and L (screw length) to D (screw diameter) ratio of 42. Temperature profile from the hooper to the die was 90-120-150-180-200-210-210 °C, working at a screw speed of 450 rpm. EVOH-29 and carvacrol were fed into the extruder by means of a loss in weight feeder and of a liquid gravimetric feeder, respectively (Brabender GmbH & Co. KG, Germany). Multilayer films were obtained by extrusion processes using a flat sheet die 500 mm wide and three single screw extruders (Dr. Collin GmbH, Germany) with 30 mm of screw diameter and L/D ratio of 30. Temperature profiles were 45-180-200-240-250 °C for PP layers, 45-190-200-220-260 °C for tie layers, and 45-180-210-220-250 °C for the EVOH-29 kernel. Screw speeds were 110, 40, and 30 rpm, and screw compression ratios were 1:3, 1:3, and 1:4, respectively. Die, feeding block, and

transfer lines were maintained at 250 °C. Temperature of chill roll was set at 45 °C and an additional air-knife was used. Line speed was 9.5 m/min.

Commercial rigid PP / EVOH-32 / PP trays, 20 cm long x 15 cm wide x 2 cm high x 0.5 – 1 mm thick, with a total filling capacity of 500 cm^3, were supplied by VIDUCA S.L.U. (Alcoy, Spain).

Carvacrol of at least 98 % purity was purchased from Sigma-Aldrich Co. LLC. (St. Louis, MO, USA), high-vacuum silicone was supplied by Panreac Química S.L.U. (Barcelona, Spain), and deionized water was obtained from a Millipore Milli-Q Plus purification system (Molsheim, France).

2.2. Determination of film structure

The multilayer structure of the manufactured film was studied by optical microscopy, by blocking film samples in a cured epoxy resin and cutting them with a microtome. Layer detection and measurements were carried out with the aid of image processing software.

2.3. Salmon processing, sampling, packaging, and analysis

Five small, fresh farmed salmon (*Salmo salar*), weighing approximately 1 kg each and caught during the month of December, were purchased at a local market in València (Spain). All the fish were headed, tailed, and gutted, backbones were removed, the skin was preserved, and the pieces obtained were cut in half in order to obtain ten identical fillets of fish muscle. Immediately afterward, the fillets were washed in cold tap water and suitably dried with absorbent paper.

Fish sampling was randomly performed in one salmon fillet by means of a kitchen knife and a copper hole puncher 8 mm in diameter. As a result, several thin muscle fillets about 1 mm thick and muscle cylinders about 8 mm in diameter and 2.4 cm in height were obtained. All the prepared fish samples were stored at 4 ± 0.5 °C until experimental utilization.

Fish packing was carried out by randomly placing the remaining salmon fillets in nine commercial plastic trays and heat-sealing them with nine active film lids in a nitrogen atmosphere with the aid of a SMART 300 semiautomatic tray sealing machine (ULMA Packaging S.Coop., Spain). All the prepared fish packages were kept at 4 ± 0.5 °C in dark conditions for 7 days. At days 2, 4, and 7 of storage three

trays were opened, the fillet surfaces were carefully scraped with a scalpel, and the collected samples of salmon muscle were subsequently analyzed for carvacrol quantification.

The antimicrobial concentration in the fish muscle samples was determined by thermal desorption and GC analysis using a thermal desorber (model 890/891, Dynatherm Analytical Inst., Supelco Inc., Bellafonte, PA, USA) connected in series to an HP 5890 Series II Plus gas chromatograph (Agilent Technologies, Wilmington, DE, USA) equipped with a flame ionization detector (FID) and a 30 m, 0.53 mm, 2.65 µm Agilent HP-1 semi-capillary column (Teknokroma S.C.L., Barcelona, Spain). The chromatographic conditions were as follow: He as the carrier gas, splitless injection mode, 220 °C and 250 °C injector and detector temperatures, 7 min at 45 °C, first heating ramp to 150 °C at 4 °C/min, second heating ramp to 220 °C at 40 °C/min, and 25 min more at 220 °C. A portion of the tested muscle (about 20 mg) was placed in the desorption cell and heated at 210 °C for 7 min. A He gas stream carried the desorbed gaseous compounds to the GC through a transfer line heated at 230 °C. At the end of the desorption process the sample was weighed with a 0.1 mg precision balance (Voyager model V11140, Ohaus Corp., Pine Brook, NJ, USA). The response of the GC was calibrated by measuring polyethylene and polypropylene samples with known amounts of carvacrol.

2.4. Determination of carvacrol equilibrium parameters

To determine the extent of carvacrol release, and to measure the corresponding equilibrium parameters, equilibrium cells were prepared following the scheme represented in **Figure II.1**. Each cell consisted of a glass vial closed by a hermetic sealing cap, a 1-mm-thick thin muscle fillet of salmon resting on a stainless steel tripod in the headspace zone, and about 10 g of carvacrol below the fish sample. Cells were filled with the active compound 48 hours before the salmon fillets in order to ensure that the carvacrol vapor pressure was reached and maintained in the headspace zone during the tests. Samples were prepared in quadruplicate and stored at 4 ± 0.5 °C in dark conditions for a period of at least two weeks in order to let them reach their state of equilibrium. Then the carvacrol concentration in the fish muscle was monitored until no differences were observed between three measurements taken on consecutive days.

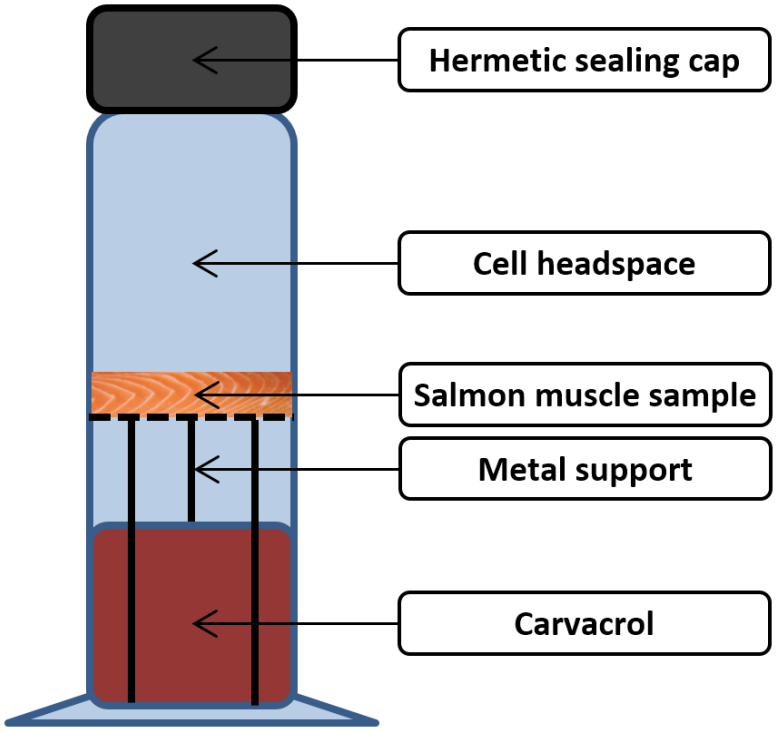

Figure II.1. Scheme of the equilibrium cell used for evaluation of the carvacrol Henry's constant in the air / salmon muscle system.

The equilibrium concentration of carvacrol in the salmon fillets was determined by thermal desorption and GC analysis according to the methodology previously described. The values of carvacrol Henry's constant for salmon muscle, H_c^S, could easily be calculated from the carvacrol concentration in the fish sample, C_c^S, and in the headspace at equilibrium, C_c^{HS} (determined from the carvacrol vapor pressure), by means of the following expression:

$$H_c^S = \frac{C_c^{HS}}{C_c^S} \qquad \text{(II.1)}$$

2.5. Determination of carvacrol migration kinetic parameters

To study the rate of carvacrol migration through the salmon muscle, and to quantify the corresponding kinetic parameters, several cylindrical fish samples were analyzed in the diffusion cells schematically represented in **Figure II.2**. Each cell consisted of a 0.5 L hermetically closed glass container half filled with deionized water, and an open glass vial 8 mm in diameter placed at the center of its headspace

zone. The vial, in turn, contained a cylinder of salmon muscle, 8 mm in diameter and 2.4 cm in height, resting on a stainless steel tripod and perfectly fitting in its headspace zone up to rim level, and about 10 g of carvacrol below the fish sample. The vials were filled with the active compound 48 hours before the salmon cylinders in order to ensure that the carvacrol vapor pressure was reached and maintained in the vial headspace zone during the tests. At the beginning of the tests salmon muscle samples were placed on the metal supports and the containers were immediately filled with deionized water and hermetically closed with high-vacuum silicone in order to avoid fish dehydration by generating and maintaining a constant inner relative humidity close to 100 %. Diffusion cells were prepared in sextuplet and stored in a dark room at 4 ± 0.5 °C until sample examination in pairs, after 3, 6, and 12 days. At these times, the carvacrol concentration profiles in the salmon muscle were determined by axially cutting the fish cylinders into several slices between 1 and 3 mm thick and analyzing them following the procedure described in previous sections. The average concentration values obtained from each pair of slices were then assigned to their corresponding central points.

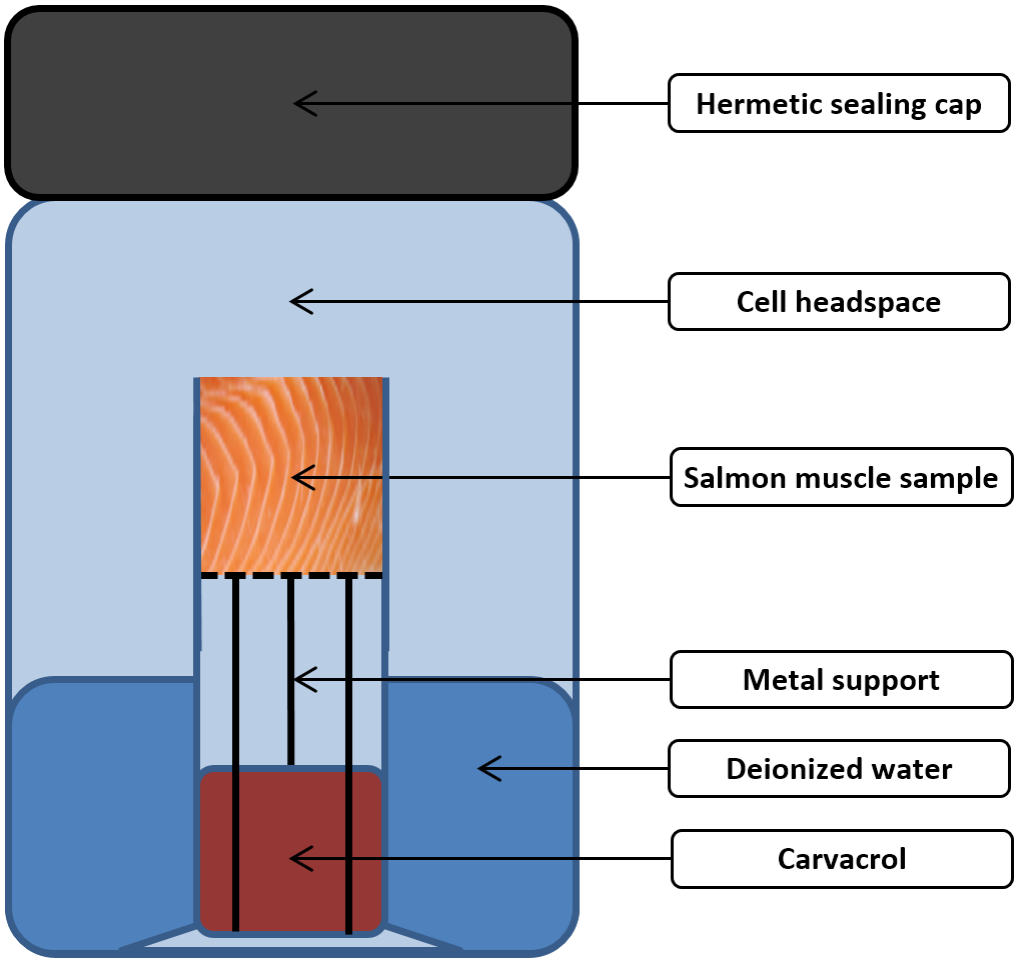

Figure II.2. Scheme of the diffusion cell used for evaluation of carvacrol diffusivity in salmon muscle.

The carvacrol concentration distributions throughout the fish sample, $C_c^S(z)$, obtained for each assayed time, t, together with the carvacrol concentration at the interface with the headspace zone, C_{ci}^S, were introduced in the solution of Fick's law for a process of permeation through an infinite sheet of thickness L_S (Crank, 1975):

$$\frac{C_c^S}{C_{ci}^S} = 1 - \frac{z}{L_S} - \frac{2}{\pi}\sum_{\nu=1}^{\infty}\frac{1}{\nu}\cdot e^{\frac{-\pi^2\cdot\nu^2\cdot D_c^S\cdot t}{L_S^2}}\cdot\sin\left(\frac{\pi\cdot\nu\cdot z}{L_S}\right) \qquad \text{(II.2)}$$

so that the value of D_c^S for each sample and time could be evaluated.

2.6. Mathematical modeling and simulation

In order to thoroughly study all the mass-transfer phenomena taking place in the developed fish packages, the entire environment / package / headspace / food system was mathematically modeled and simulated using the finite element method in the Transport of Diluted Species physics interface of the Chemical Reaction Engineering module included in the COMSOL Multiphysics 4.2a modeling suite. This system involved a real active package for fresh salmon cubes or slices 2 cm thick, made up of eight different material layers: environment (EA), external PP (EPP) (25 µm), tie layer (8 µm), EVOH-29 kernel (E29) (7 µm), tie layer (8 µm), internal PP (IPP) (25 µm), package headspace (HS) (2 cm), and salmon slice (S) (2 cm), which was intended to be preserved in a refrigerator at 4 °C and 50 % RH on average. However, it was presumed that the calculations demanded by such a complex model might exceed the capabilities of a common computing system. In view of this, some simplifications were made in order to reduce the complexity, and thus the calculation time. In particular, the external atmosphere was considered to be independent of the package, and therefore the concentrations of all compounds in this layer could be taken as constant and defined in the boundary conditions of the system. Furthermore, the tie layers were not considered and their contribution to the model was ascribed to the corresponding adjacent PP layers because of the difficulties inherent in the determination of carvacrol kinetics and equilibrium parameters in that material. Finally, all multidirectional mass-transfer phenomena occurring in the modeled system were approximated to only one process of unidirectional progression through the package layers. In this way, the number of actual system dimensions could be reduced, given that the system's geometry could be assimilated to an infinite multilayer sheet with only five spatial domains: external PP, EVOH-29 kernel, internal PP, package

headspace, and salmon slice (**Figure II.3**).

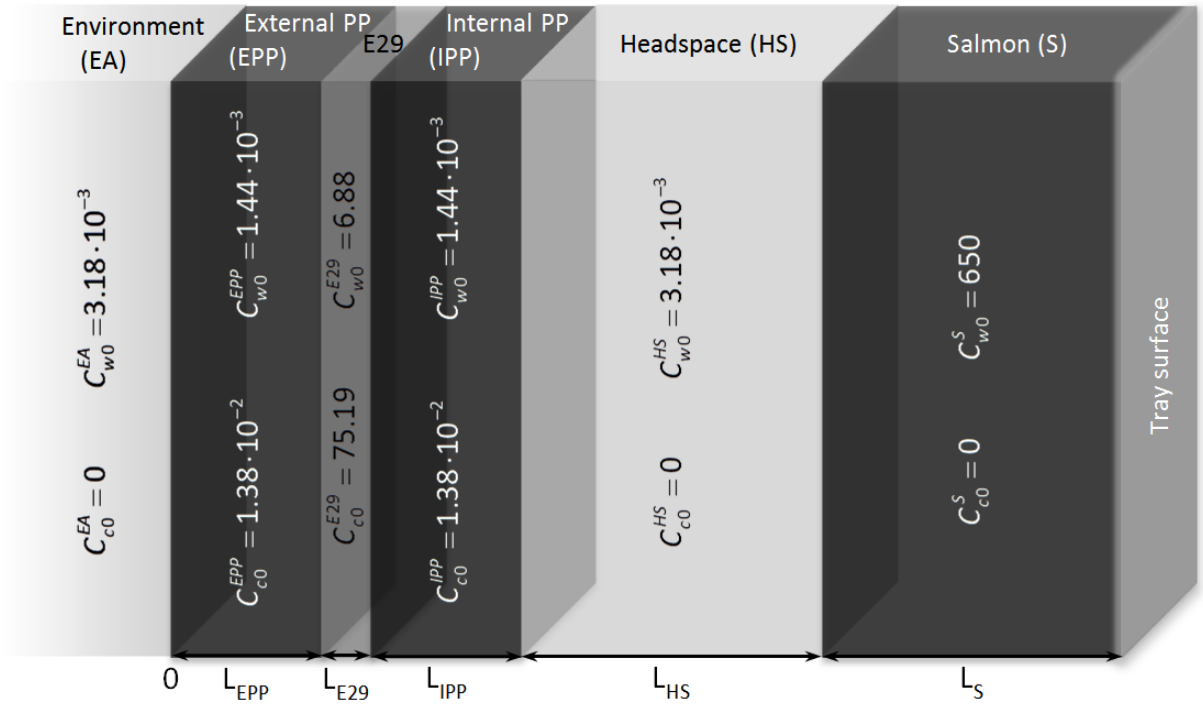

Figure II.3. Scheme of the simplified 1D system used to model the mass transport phenomena occurring in the salmon package, and the corresponding initial values for the water and carvacrol concentrations in each material layer (kg / m^3).

In accordance with the methodology described in a previous work (Cerisuelo et al., 2012), it was critical to consider a multicomponent theoretical model that included not only the carvacrol transport phenomena but also the water vapor transfer processes, on account of the highly hydrophilic nature of the EVOH-29 kernel, which is responsible for the severe changes observed in its physicochemical properties when exposed to highly humid conditions. In addition, some researchers have observed a substantial water swelling in several EVOH copolymers studied under these conditions, and in the literature matrix expansion values of up to 35 % have been reported for EVOH-29 when subjected to relative humidities close to 100 % (Cava et al., 2006 and 2007). Hence, in order to faithfully represent the real modeled system, the possible increase in kernel thickness as a result of EVOH-29 moisture sorption was also included in the final developed model with the aid of the Moving Mesh physics interface of the Mathematics module included in the modeling suite.

Taking all these premises into consideration, the mathematical model was finally developed by using the multiphysics analysis mode of COMSOL Multiphysics 4.2a, where two dependent, interconnected

variables, $C_w^{\alpha}(z,t)$ and $C_c^{\alpha}(z,t)$, were used in each material domain α (EPP, E29, IPP, HS, or S) to describe the water (w) and carvacrol (c) concentration profiles, respectively, at every position (z) within the layer structures and at every instant (t) of elapsed time. The values of all the kinetic and thermodynamic parameters required by the model were collected from the literature for water and carvacrol transport phenomena in EVOH-29 (Aucejo, 2000, and Cerisuelo et al., 2012), PP (Marais et al., 2000, and Cerisuelo et al., 2012), and air (EPA On-line Tools, 2011), and prepared as model inputs. Additionally, all the fundamental hypotheses and integration conditions of the modeled system had to be set out and entered in the software database. Regarding the hypotheses formulated, full compliance with the postulations posed in the previous work was assumed (Cerisuelo et al., 2012), whereas the boundary conditions, in this case, were chosen as follows:

The carvacrol concentration in the external PP layer at its interface with the external atmosphere: $C_c^{EPP}(0,t)=\frac{C_c^{EA}}{H_c^{EPP}}=\frac{0}{H_c^{EPP}}=0$ kg/m^3, since the environment was considered to be independent of the package and there was no carvacrol concentration in this layer.

The water concentration in the external PP layer at its interface with the external atmosphere: $C_w^{EPP}(0,t)=\frac{C_w^{EA}}{H_w^{EPP}}=\frac{RH/100\cdot C_w^0(4\ ^{\circ}\text{C})}{H_w^{EPP}}=\frac{0.5\cdot 6.354\cdot 10^{-3}}{4.413\cdot 10^{-2}}=7.2\cdot 10^{-2}$ kg/m^3, since the atmosphere of the refrigerator was constantly maintained at 4 ± 0.5 °C temperature and 50 ± 5 % RH.

The carvacrol concentration gradient in the salmon slice at its interface with the tray surface: $\nabla C_c^S(L_{EPP+E29+IPP+HS+S},t)=0$ kg/m^4, since the preserved salmon slice was resting on the bottom surface of the rigid tray, which was considered to be completely impermeable (**Figure II.3**).

The water concentration in the headspace layer at its interface with the salmon slice: $C_w^{HS}(L_{EPP+E29+IPP+HS},t)=H_w^S\cdot C_w^S=9.775\cdot 10^{-3}\cdot 650=6.354$ kg/m^3, since salmon muscle is considered to have a constant and uniform water content of about 185.7 % on a dry basis (USDA National Nutrient Database for Standard Reference, Release 24, 2012).

Since the concentration profiles in the system domains were known to be discontinuous at the boundaries between the PP and EVOH-29 layers, and between the headspace and PP or salmon layers, five different dependent variables were used (in accordance with the five domains α) for each component i, and were interrelated by means of a partition coefficient, $K_i^{PP/E29}(C_w^{E29})$, and two Henry's constants, H_i^{PP} and H_i^S. Nevertheless, in order to get a continuous flux over the phase boundaries a

special type of boundary condition using the stiff-spring method was applied (COMSOL Model Examples: Separation through dialysis, 2011): $J_i^{\alpha/\beta} = M_i \cdot \left(C_i^{\beta} \cdot K_i^{\alpha/\beta} \left(C_w^{\beta} \right) - C_i^{\alpha} \right)$, where M_i is the stiff-spring velocity (m/s) for *i* species.

Finally, initial integration conditions for each system domain were defined so as to represent as well as possible the physicochemical state of the active packages at the beginning of the food preservation, as **Figure II.3** shows, taking into consideration that all the antimicrobial film lids had previously been stored at a temperature of 23 °C and at a maximum of 1 % RH in order to avoid potential activity losses.

Once the model was properly set out and all its physicochemical properties were consistently defined, its spatial and temporal discretization could be carried out, and its mathematical solution could be numerically approximated by applying the finite element method. In this final modeling phase the solution of function $C_w^{\alpha}(z,t)$ was calculated in the first place by solving the model solely for the water vapor mass-transfer processes, taking into account the expected deformation of the material frame occurring in the EVOH-29 kernel as a result of water swelling effects. The results thus obtained were then stored to be used subsequently in the calculations of the carvacrol mass-transport phenomena as initial values for the variables already solved in the previous step, thus leading to the final solution of function $C_c^{\alpha}(z,t)$. Given the one-dimensional structure of the model, the spatial discretization of its five physical domains was carried out with a freely distributed mesh of 100 edge elements per domain and 6 additional vertex elements, involving 505 degrees of freedom in all. The numerical solving of the model was constrained by 9 dependent variables, which were solved with the aid of a direct transient solver algorithm (PARDISO), using the BDF time-stepping method with 100 free logarithmic time steps, and very low relative and absolute scaled tolerances ($<10^{-6}$) for all them.

2.7. Data analysis

The values for all the parameters measured and coefficients presented in this research work are expressed as "$(\bar{x} \pm \varepsilon)$ units," where $\bar{x}$ stands for the sample mean of parameter x, and ε stands for the absolute error of parameter x. This absolute error is equal to the sample standard deviation for the parameters measured, and was determined by propagation of uncertainty (partial derivatives method) for the parameters calculated.

3. RESULTS AND DISCUSSION

3.1. Assessment of film structure

The multilayer structure of the coextruded film was confirmed by the images obtained by optical microscopy. With the aid of image processing software five layers were detected and measured. The total thickness was found to be about 73 µm with a quasi-symmetrical structure, containing an EVOH-29 kernel of approximately 7 µm between two tie layers 8 µm thick well adhered to two more external layers of polypropylene about 25 µm thick. Since the mathematical model developed in this work could not account for tie layers in its calculations, the film structure had to be simplified to a three-layer system where the contribution of the tie layers was attributed to the corresponding adjacent PP layers by increasing their thickness by 8 µm, from 25 to 33 µm.

3.2. Assessment of carvacrol equilibrium in salmon muscle

Carvacrol solubility in the salmon muscle was studied with the aid of the equilibrium cells described in the experimental section. From the carvacrol concentration values estimated in the gas phase and measured in the fish fillets, the values of the equilibrium parameters (Henry's constant, H_c^S) were quantified for all samples by introducing both figures in equation (II.1), yielding an average value of $(1.24 \pm 0.04) \cdot 10^{-3}$.

On the basis of the values obtained in a previous work for the polypropylene Henry's constant, $(1.0 \pm 0.2) \cdot 10^{-5}$ (Cerisuelo et al., 2012), it can be stated that this material shows 124 times higher affinity for carvacrol than salmon muscle. This result could be explained by the hydrophobic nature of carvacrol, which is responsible for its high solubility in hydrophobic polymeric matrixes, such as polypropylene or other polyolefins, and its low compatibility with hydrophilic food matrices, such as salmon muscle or other high water content foodstuffs. Equally, this phenomenon was also observed in the previous work when studying the carvacrol partition coefficient between PP and EVOH-29 films.

3.3. Assessment of carvacrol kinetics in salmon muscle

The carvacrol migration rate within salmon muscle was studied with the aid of the diffusion cells

detailed in **Figure II.2**. As an example, **Figure II.4** shows the evolution of the carvacrol concentration profiles throughout the fish cylinders after 3, 6, and 12 days. For the determination of the diffusion coefficient values, D_c^S, equation (II.2) was used, assuming that during the migration process the water concentration in the salmon samples remained constant and uniform throughout the thickness, and also the diffusion coefficient value. This approach was successfully applied elsewhere (López-Carballo et al., 2005). As can be seen in **Figure II.4**, the curves obtained by the fitting of equation (II.2) agreed satisfactorily with the experimental values, and yielded an average value of $(3.92 \pm 0.12) \cdot 10^{-12}$ m^2/s for the carvacrol diffusivity through the salmon muscle. This figure, much smaller than those for carvacrol through PP or EVOH, is in good agreement with the values found in the literature for the diffusion coefficients of carbon dioxide, sodium chloride, and lysozyme in salmon fillets, estimated at $1.62 - 1.84 \cdot 10^{-9}$ m^2/s (Sivertsvik, 2004), $2.27 \cdot 10^{-11} - 2.03 \cdot 10^{-9}$ m^2/s (Wang et al., 1998 and 2000, Gallart-Jornet et al., 2007a and 2007b, and Alizadeh et al., 2009), and $2.57 - 4.79 \cdot 10^{-11}$ m^2/s (Min et al., 2008), respectively.

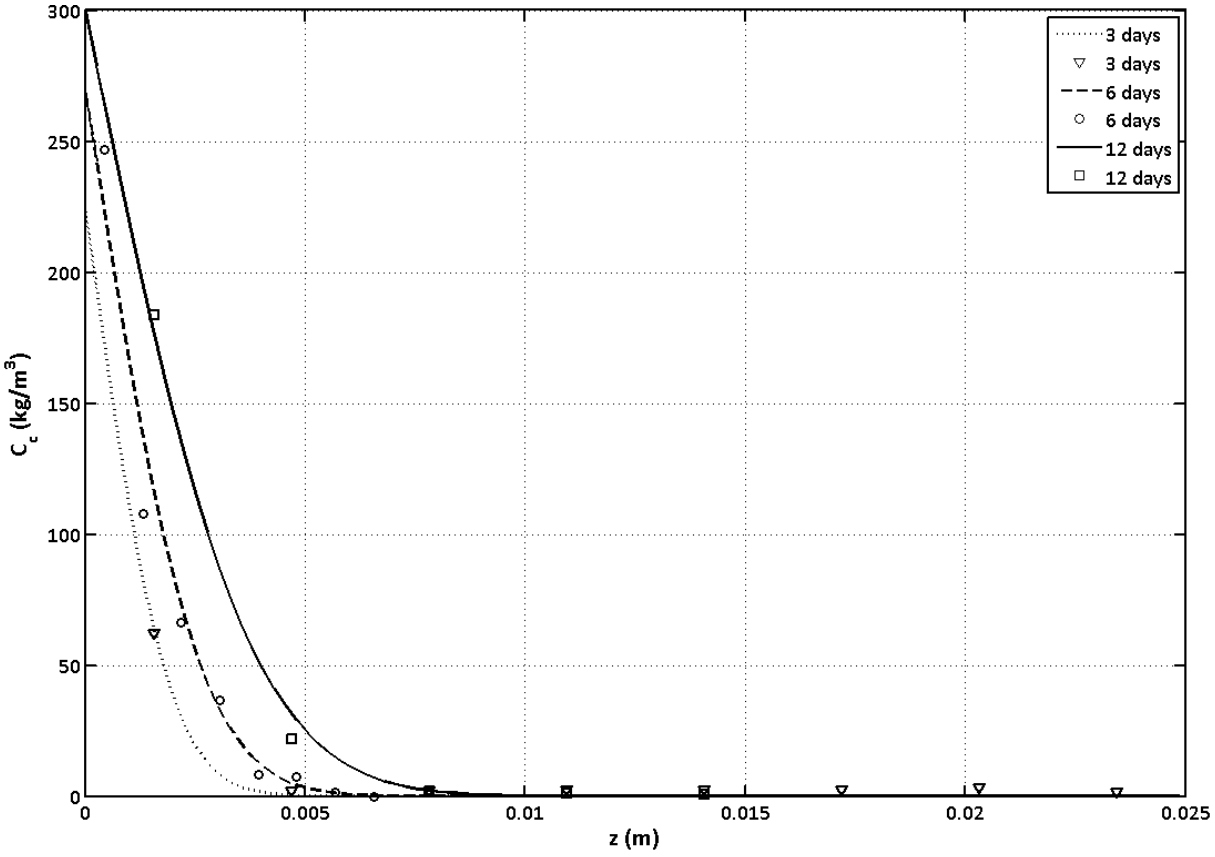

Figure II.4. Experimental data (symbols) for the carvacrol concentration measured throughout the salmon cylindrical samples after 3, 6, and 12 days of agent migration, and theoretical curves (lines) fitted with equation (II.2).

3.4. Simulation of active package performance

With the numerical solving of the model, the performance of the active package made up of a rigid PP / EVOH-32 / PP tray heat-sealed with an active PP / EVOH-29 / PP film lid, designed for fresh salmon preservation, could finally be simulated under all the working conditions, fundamental hypotheses, simplifications, considerations, and constraints detailed above in the experimental section. Results for the evolution in time of the water concentration profiles in the external PP layer, EVOH-29 kernel, and internal PP layer from 0 to 7 days of package simulation are displayed in **Figures II.5a**, **II.5b,** and **II.5c**, and results for the carvacrol transport are shown in **Figures II.6a**, **II.6b,** and **II.6c**, respectively.

As **Figures II.5** show, during the first moments of the package activity water molecules coming from both the food and the external atmosphere rapidly penetrate through the two PP layers and begin to humidify the EVOH-29 active kernel from its two boundaries. The water uptake occurring in these zones causes a gradual swelling of the polymer matrix that leads to a substantial increase in the layer thickness, as we will see later. Moreover, since the salmon moisture is higher than the environmental humidity the EVOH-29 humidification is faster and more severe around its inner boundary, leading to the generation of a water gradient from the inner to the outer side of the package after some time, and thus to a sudden change in the direction of the water diffusion around its outer boundary at that moment. Finally, after 7 days of food preservation, the stationary state is nearly achieved, the water concentration profiles become almost straight lines, and water molecules are permanently diffusing from the preserved fish to the external atmosphere.

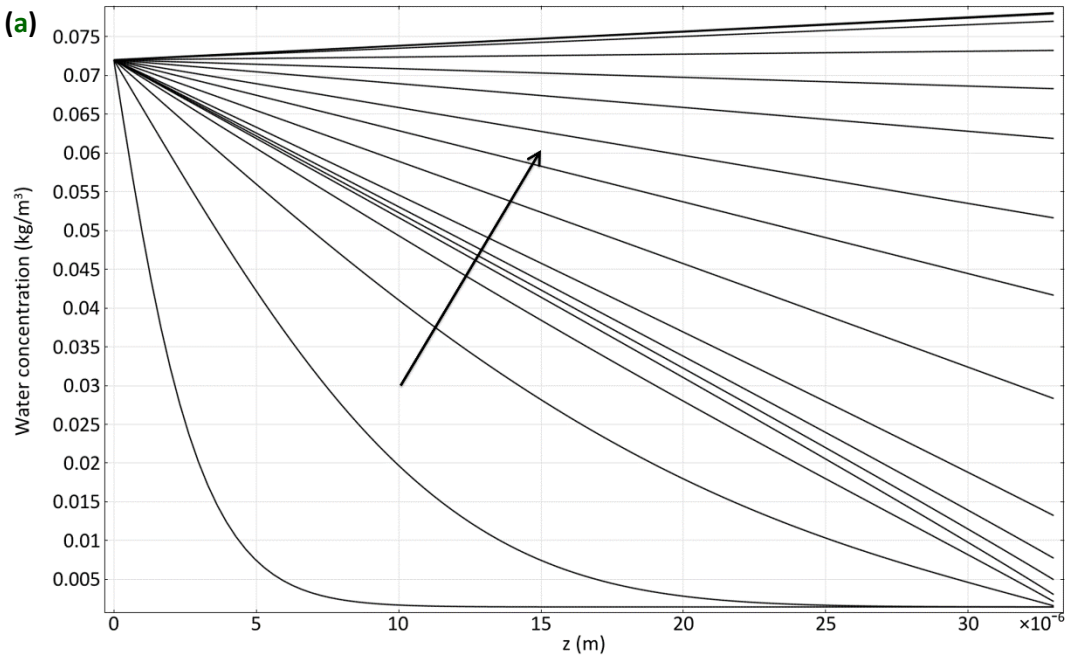

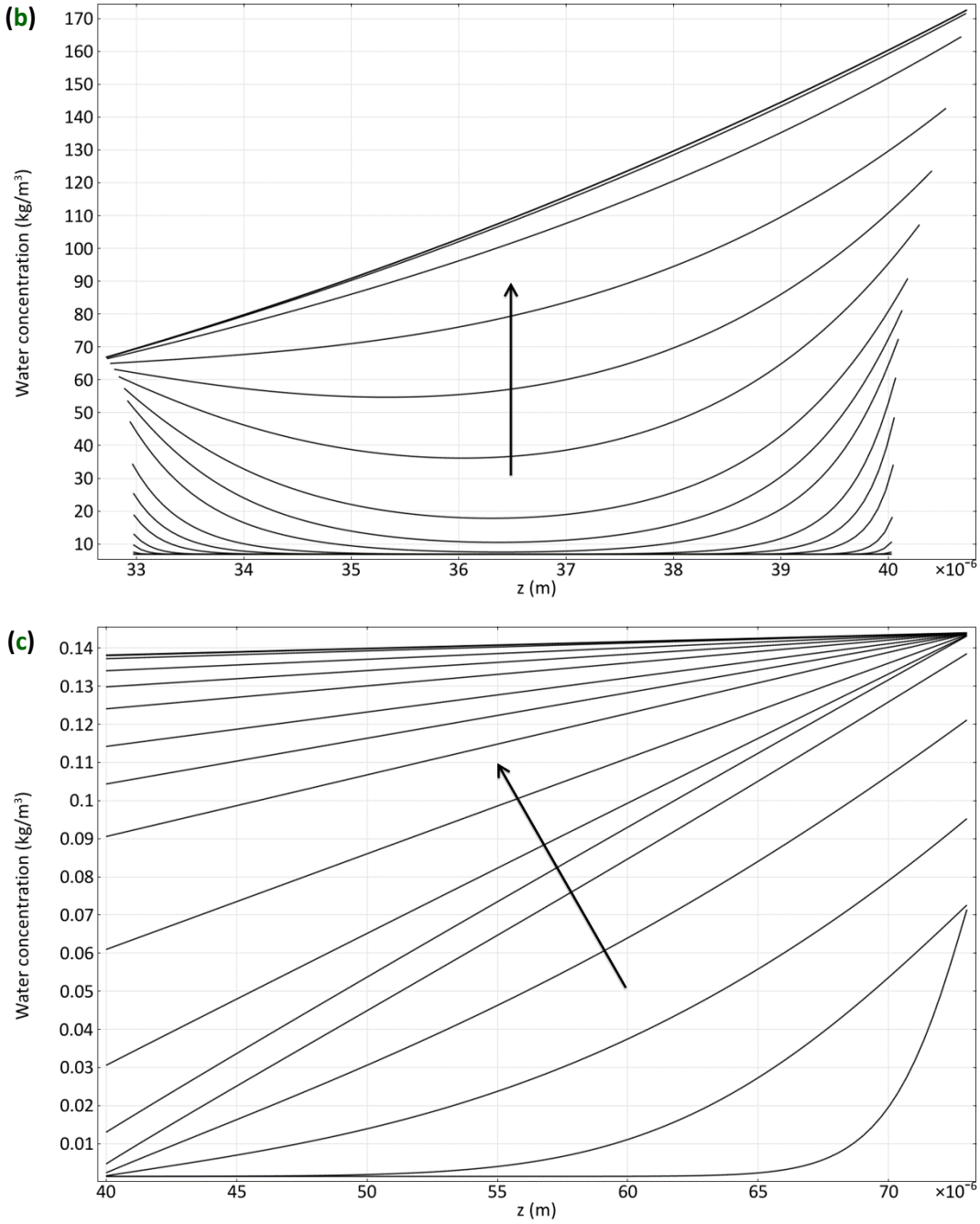

Figures II.5. Theoretical profiles for the water concentration predicted by the model throughout the external PP layer (a), EVOH-29 kernel (b), and internal PP layer (c), at 16 logarithmically spaced times.

With respect to the active compound, according to **Figures II.6** the carvacrol concentrations in the active film are constant in each layer for a brief moment before the beginning of the package activity. Once water molecules begin to diffuse in direction to the EVOH-29 kernel a large amount of carvacrol molecules is released from both sides of this layer, leading to a sudden raise in the carvacrol concentration in both adjacent PP layers. This increase is particularly high in the internal PP layer,

because of the faster and greater humidification undergone by the EVOH-29 kernel in the surroundings of its boundary, driving to the generation of a considerable carvacrol gradient toward the package headspace and thus toward the preserved food. However, as the EVOH-29 kernel approaches its maximum humidification, after some days of food preservation, and the water molecules begin to change their diffusion direction, the carvacrol gradient in the EVOH-29 vanishes and the carvacrol concentration in both PP layers reaches its maximum value. From this point a slow decline in the antimicrobial concentration begins throughout the multilayer film, until almost all available active agent has been consumed by either food absorption or atmosphere dilution after 7 days have passed.

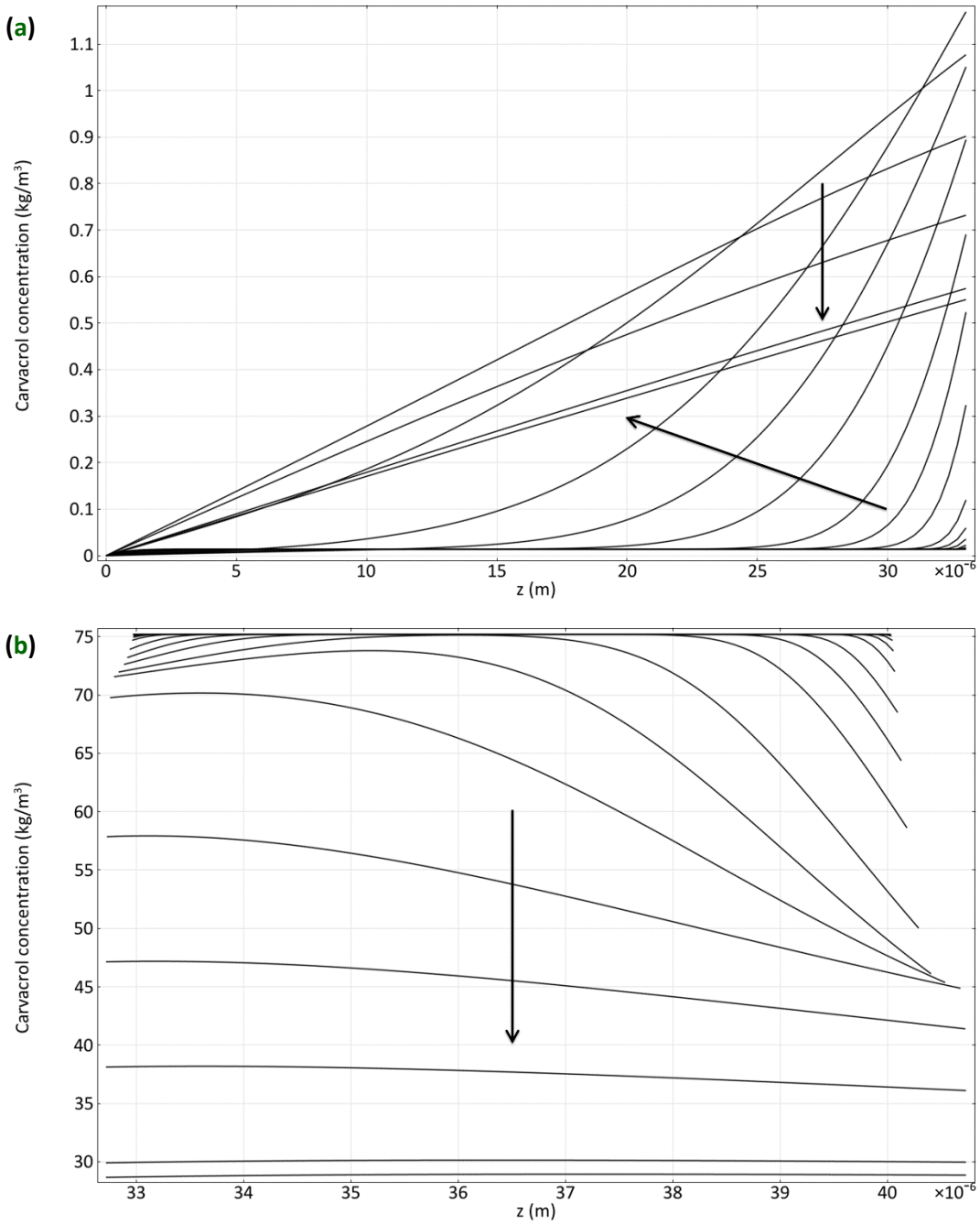

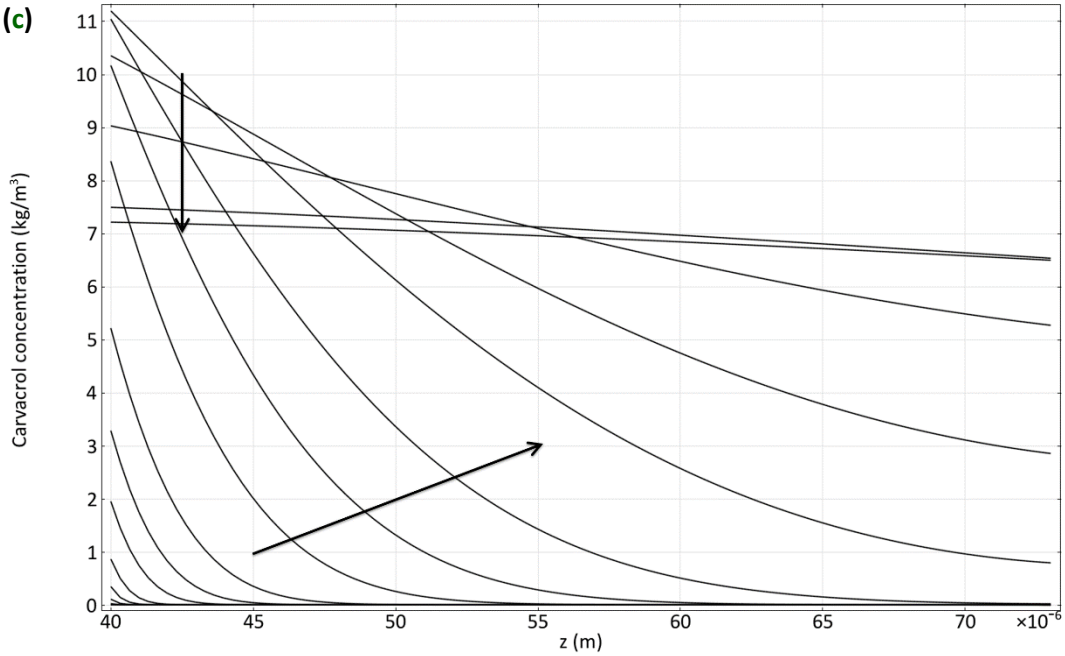

Figures II.6. Theoretical profiles for the carvacrol concentration predicted by the model throughout the external PP layer (a), EVOH-29 kernel (b), and internal PP layer (c), at 16 logarithmically spaced times.

Additionally, a closer examination of **Figures II.5b** and **II.6b** also reveals the dimensional changes undergone by the EVOH-29 kernel as a result of the water swelling effects. As the figures show, the deformation experienced by the material frame is equally visible in both the water and the carvacrol concentration profiles, though its connection with the water uptake is more obvious in **Figure II.5b**. In particular, this figure reveals a slight increase in thickness of about 4 % in the material region proximate to the external PP layer, in contrast with a greater increase of about 10 % in the vicinity of the internal PP layer. Hence, it can be stated that, by the end of the experiment, the global expansion estimated for the EVOH-29 matrix reaches a total value of 14 % with respect to its original dimensions, and that this dimensional change takes place at a rate and to an extent in accordance with the moisture sorption process.

3.5. Validation of mathematical model

In order to assess the reliability of the results yielded by the model simulations it was necessary to compare the predicted values with experimental ones obtained from the analysis of the salmon packages after operating in real working conditions. With this objective, the concentration of carvacrol in the surface of the salmon slices, quantified after 2, 4, and 7 days of package activity, was plotted in

Figure II.7 together with the corresponding theoretical curve predicted by the model. In light of these data it can be said that the developed model satisfactorily describes the behavior of the package studied and can be reliably used to predict its performance in time. Aside from that, on observing the evolution in time of the carvacrol concentration in the salmon muscle throughout the slice thickness as predicted by the model, **Figure II.8**, the resulting curves proved to be analogous to the experimental curves plotted above in **Figure II.4** for the concentration profiles measured in the salmon cylindrical samples for the determination of diffusivity, and this also contributed to the validation of the consistency of the model results.

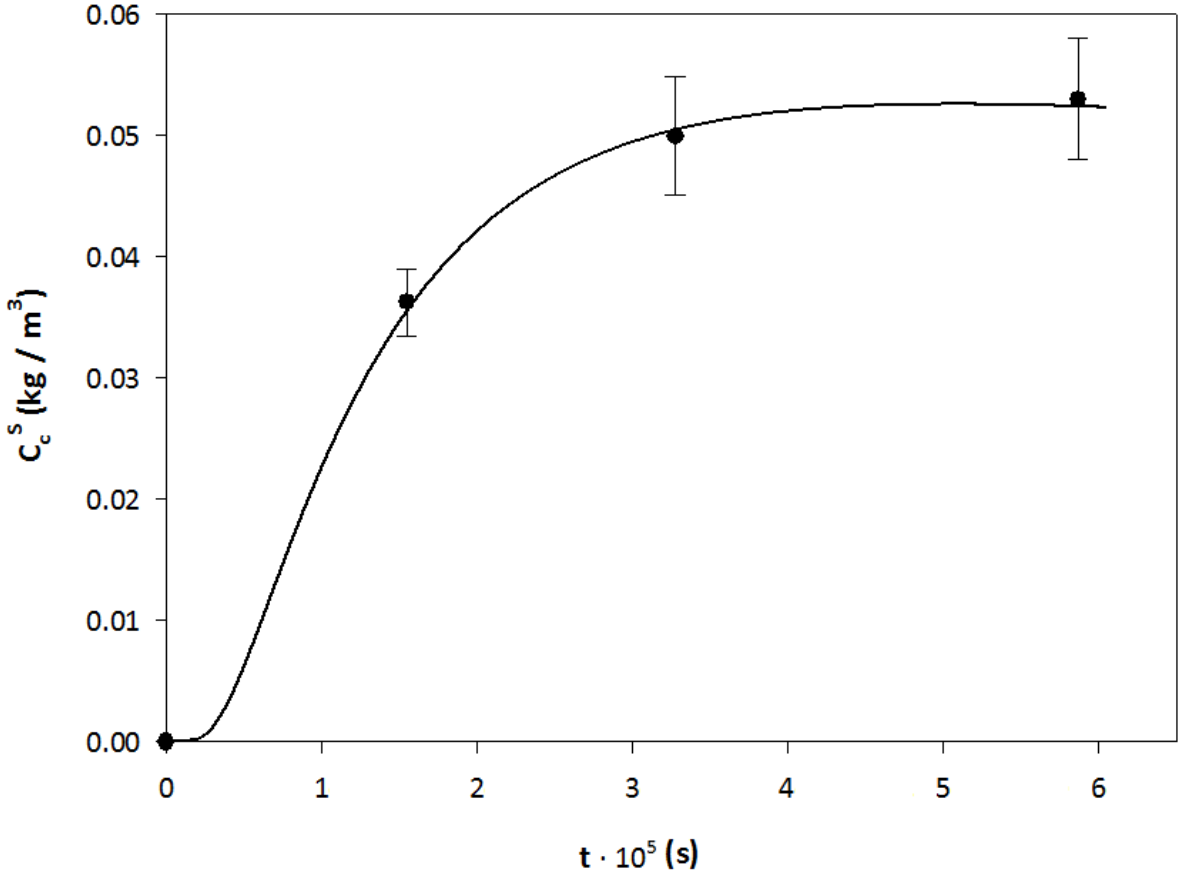

Figure II.7. Evolution in time of the carvacrol concentration in the surface of the salmon slice. Symbols correspond to the experimental values measured at 2, 4, and 7 days of food preservation, and curves correspond to the performance predicted by the mathematical model.

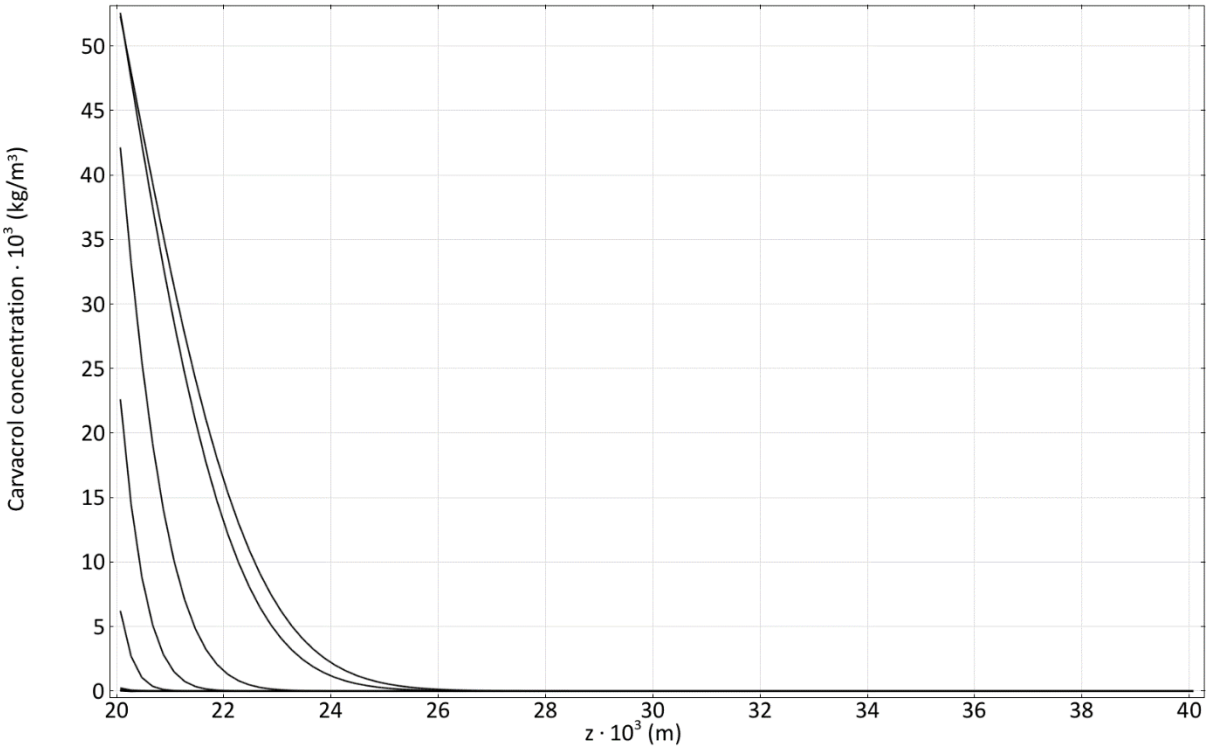

Figure II.8. Theoretical profiles for the carvacrol concentration predicted by the model throughout the salmon slice at 16 logarithmically spaced times.

3.6. Optimization of active packages by model simulations

Once the outputs yielded by the model simulations have been carefully assessed and experimentally validated, they can be used to describe all the mass transport phenomena taking place concurrently in the environment / package / headspace / food system, to identify the most significant variables that affect the efficiency of the active package, and, as a result, to improve and optimize the package design. Therefore the model can be used to simulate and predict system performance in operational contexts different from the one considered in this work, namely environmental conditions or structural design, and, as a result, it can be a useful tool to discern the way toward the optimization of an active package. As examples, the results predicted by the mathematical model when some of the conditions are modified, such as the thickness of the active film layers and the environmental or storage relative humidity, are presented and discussed below.

Figure II.9 shows the evolution of the carvacrol concentration in the surface of the preserved salmon slice when the storage relative humidity of the active multilayer film reel is varied from 0 to 100 %. As

can be seen, the environmental humidity of the reel storing chamber mainly affects the initial equilibrium carvacrol concentration distribution among all the film layers, by modifying the partition coefficient values between EVOH-29 and PP, as reported in the literature (Cerisuelo et al., 2012), while the final predicted values seem to vary significantly only when the storage relative humidity exceeds a value of 60 %. In consequence, and according to the plotted curves, as the RH rises the EVOH-29 loses affinity for the carvacrol molecules and the PP layers increase their initial carvacrol concentration, thus promoting its release to the preserved food, and also to the external atmosphere, during the first moments of the package activity.

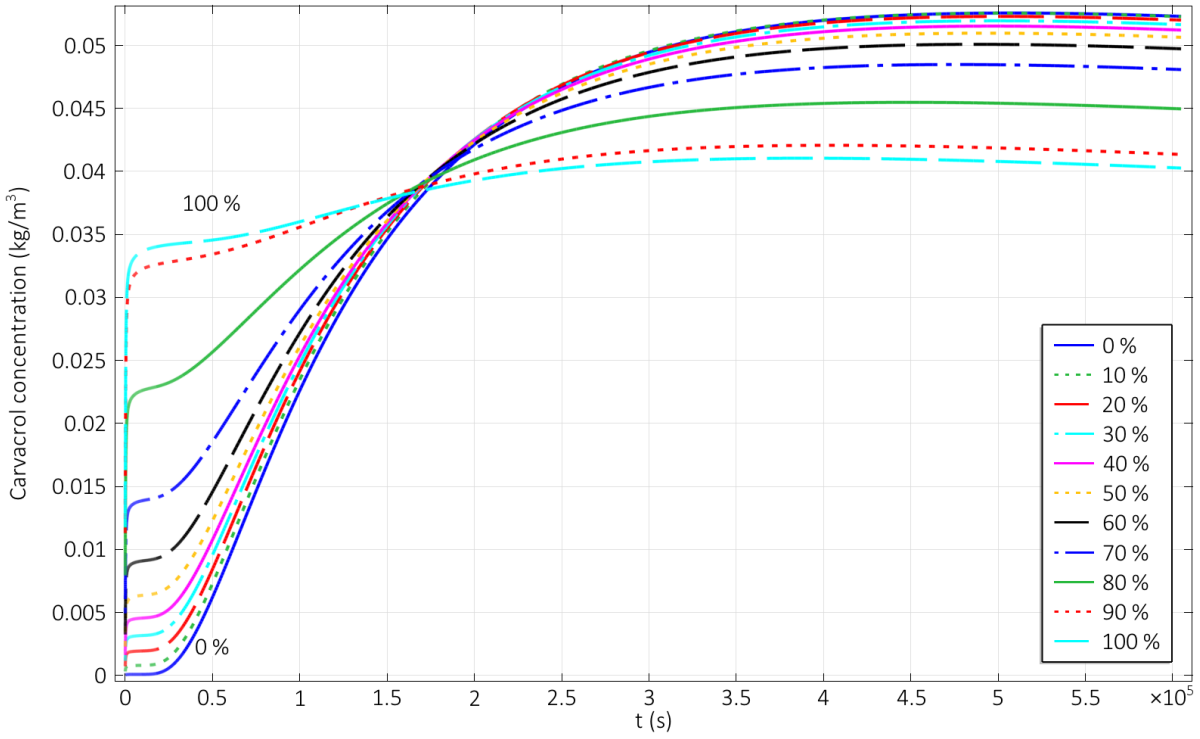

Figure II.9. Evolution in time of the carvacrol concentration in the surface of the salmon slice, as predicted by the model, as a function of the storage relative humidity.

In turn, the environmental humidity also plays an important role in the package performance, because the water uptake in the EVOH-29 kernel strongly affects the release rate of the antimicrobial agent to the whole system. This influence from 0 to 100 % RH can be evaluated in **Figure II.10**, which shows that the average carvacrol concentration in the fish muscle hardly changes its evolution with the growth of atmospheric relative humidity from dry to 60 % RH, whereas in highly humid conditions carvacrol molecules are more easily released to the external atmosphere and this loss of package activity turns into a lesser carvacrol concentration in the food matrix.

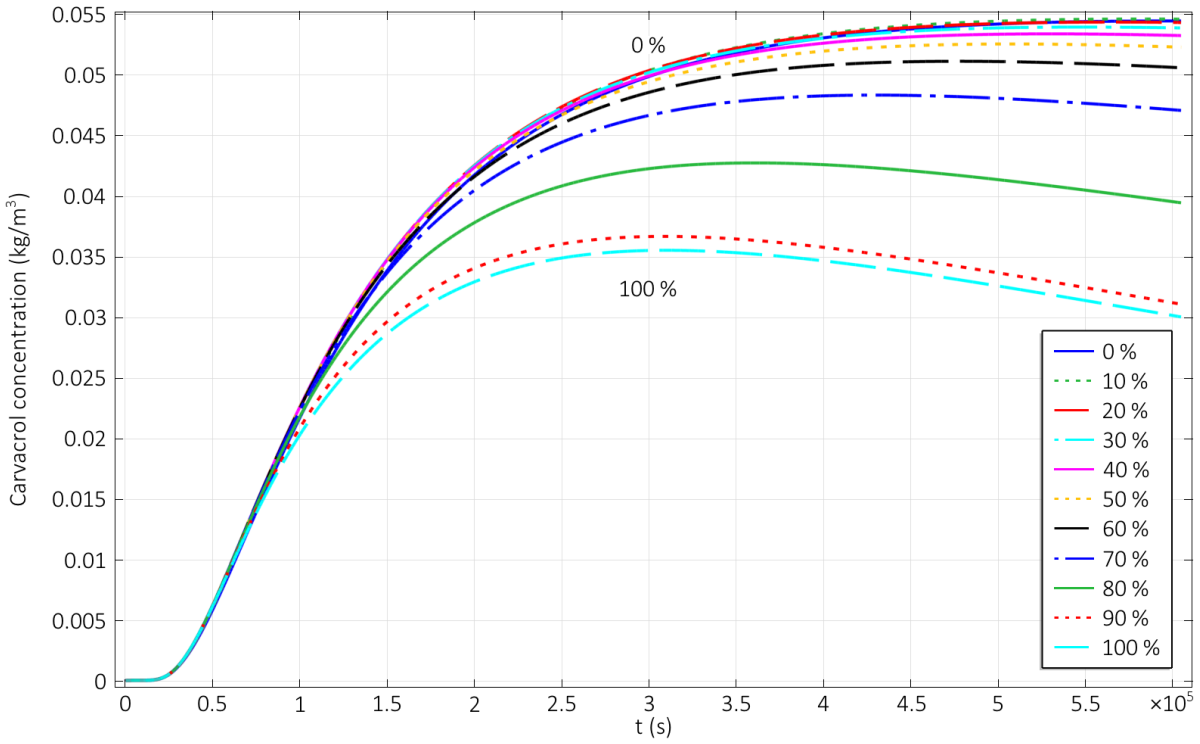

Figure II.10. Evolution in time of the carvacrol concentration in the surface of the salmon slice, as predicted by the model, as a function of the environmental relative humidity.

Turning to a different aspect, when the system design is modified by varying the layer thickness distribution of the active film the results obtained are very similar to those explained above when changing the relative humidity of the surrounding package atmosphere. **Figures II.11**, **II.12**, and **II.13** show the evolution of the carvacrol concentration in the surface of the preserved salmon slice when the thickness of the external PP layer (EPP), the EVOH-29 kernel (E29), and the internal PP layer (IPP) are varied from 1 to 100 µm.

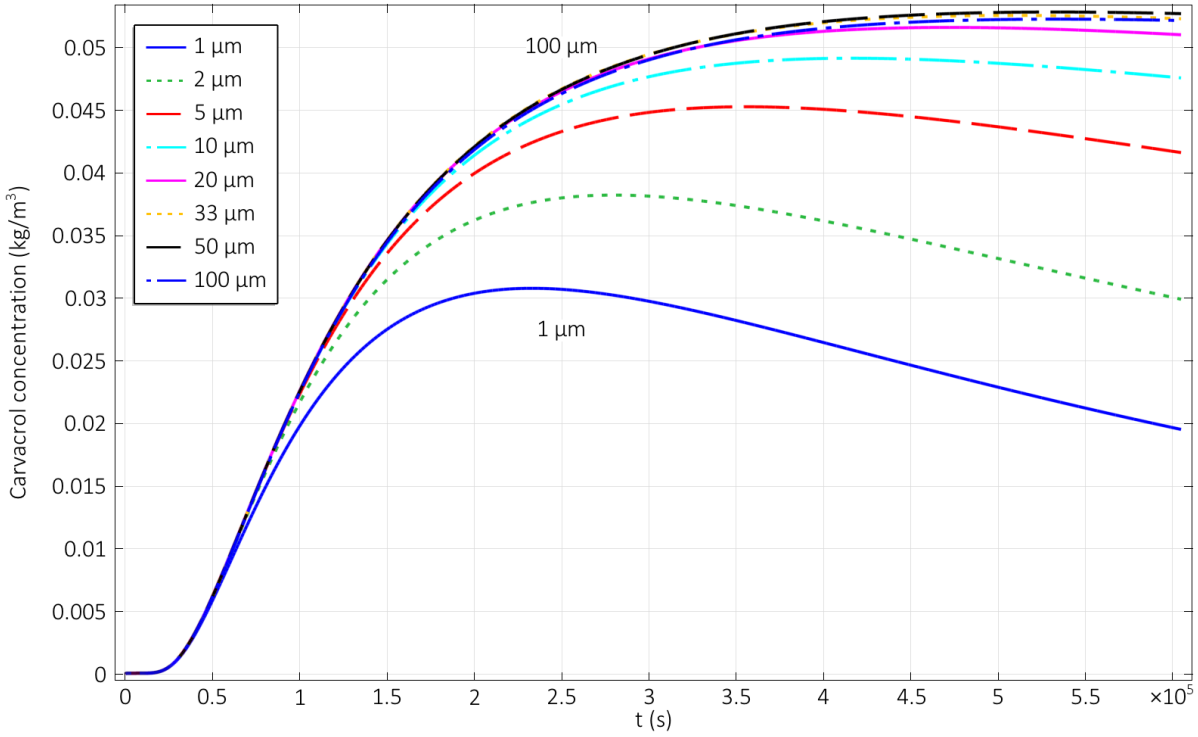

Figure II.11. Evolution in time of the carvacrol concentration in the surface of the salmon slice, as predicted by the model, as a function of the external PP layer thickness.

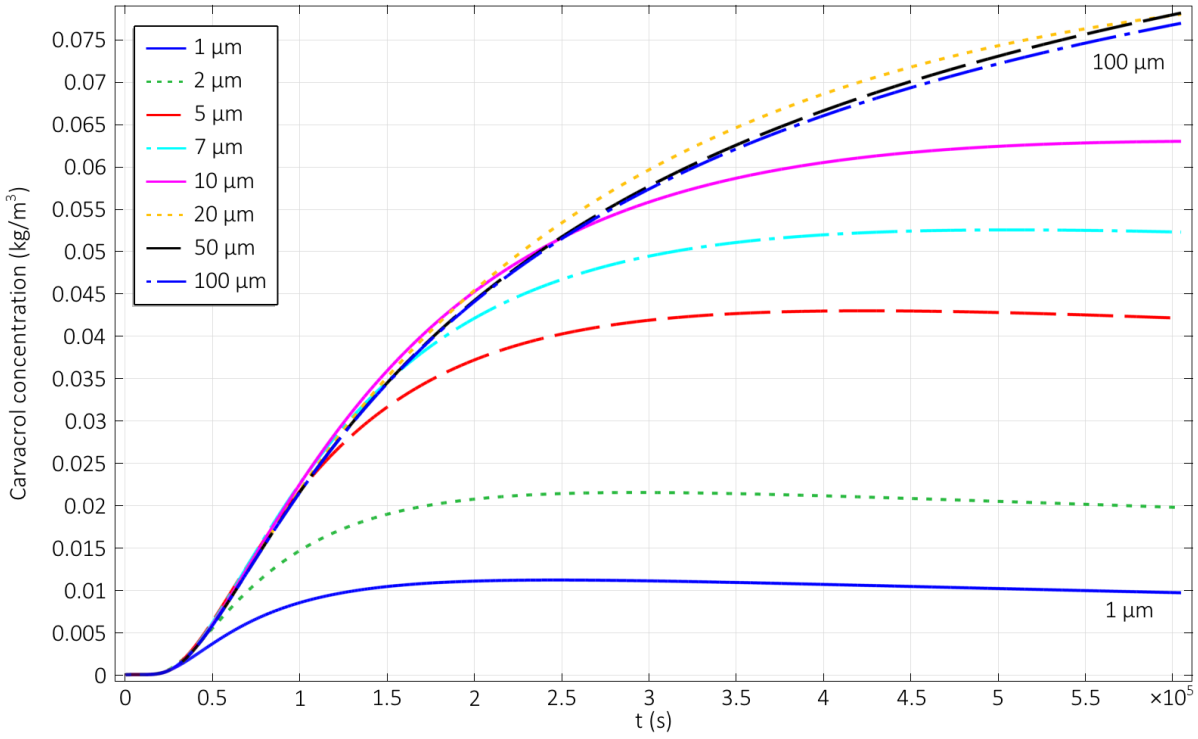

Figure II.12. Evolution in time of the carvacrol concentration in the surface of the salmon slice, as predicted by the model, as a function of the EVOH-29 kernel layer thickness.

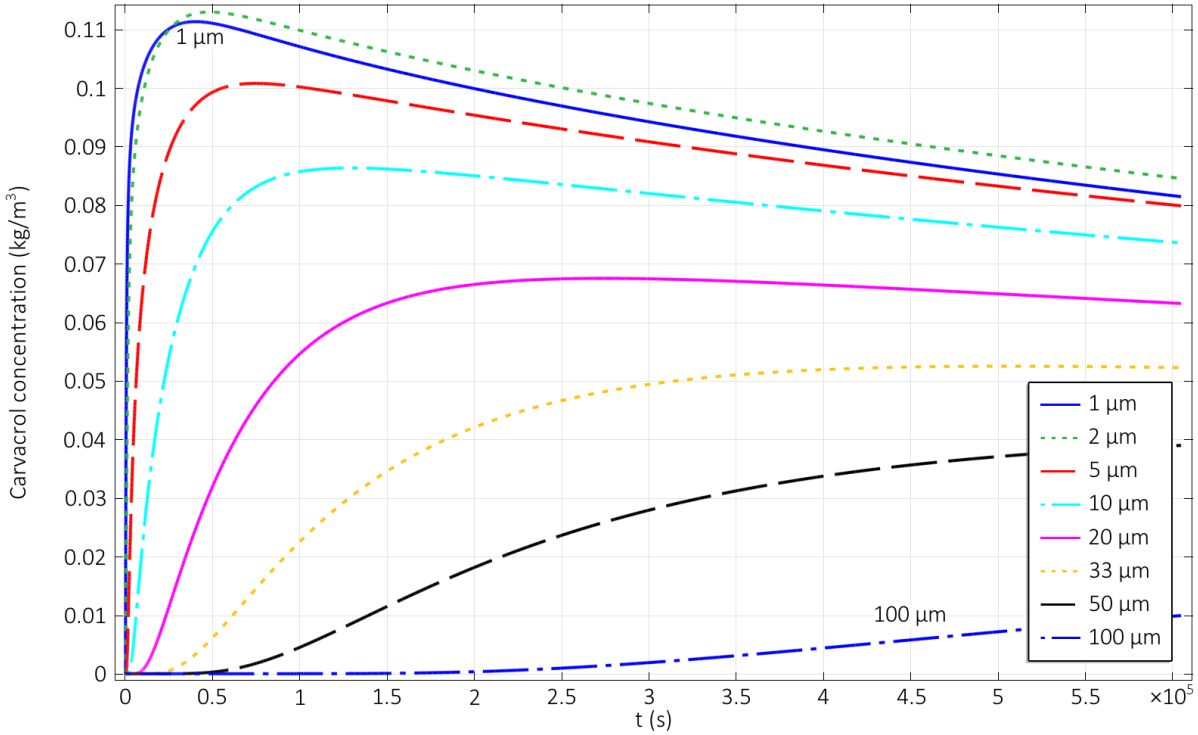

Figure II.13. Evolution in time of the carvacrol concentration in the surface of the salmon slice, as predicted by the model, as a function of the internal PP layer thickness.

As the figures show, the effects of reducing the thickness of the external PP layer are almost identical to the effects of increasing the environmental relative humidity, because this film layer is responsible for the insulation of the active EVOH-29 kernel, and thus for maintaining the package's antimicrobial activity. The EVOH-29 kernel, in turn, shows similar although more pronounced effects when its thickness is increased, because of a) the higher carvacrol content in the active layer, and b) the improvement in the layer insulation from external humidity, even though these effects seem to vanish or be delayed from 20 µm on. Finally, regarding the effects of the thickness of the internal PP layer, the curves displayed in **Figure II.13** unveil the existence of a significant time lag in the rise of the superficial carvacrol concentration of the salmon slice, which strongly depends on the thickness of the film. As the figure shows, this time lag is inversely proportional to the IPP thickness, so that the maximum carvacrol concentration attained in the preserved salmon is reached after a time ranging from as little as a few seconds with a thickness of 2 µm to as much as several weeks with a thickness of 100 µm.

In conclusion, it can be stated that in order to maximize package effectiveness and ensure immediate and constant activity after the beginning of the food preservation the original package design should be modified to increase as much as possible the thickness of the EVOH-29 kernel and to reduce as

much as possible the thickness of the internal PP layer. Regarding the external PP layer, the current configuration seems to be adequate although, according to **Figure II.11**, the same package activity could be achieved with a thinner layer only 20 µm thick. In light of this evidence, and considering exclusively the release of carvacrol into the food, a new active film design consisting of EPP (20 µm) / E29 (20 µm) / IPP (2 µm) could be proposed, and it could be recommended that exposure of the multilayer film reel and the final packages to environmental relative humidities higher than 60 % should be avoided. Cost issues and mechanical requirements of the package should also be considered in the final structure design, as well as antimicrobial and sensory characteristics of the food product, although all these are outside the scope of the present work.

4. CONCLUSIONS

In this paper a commercial active antimicrobial package designed to preserve fresh salmon cubes or slices, consisting of a rigid PP / EVOH-32 / PP tray heat-sealed with an active PP / EVOH-29 + 6.5 % carvacrol / PP film lid, was successfully developed and a mathematical model based on the finite element method was proposed to satisfactorily describe all the mass transport phenomena occurring in the environment / package / headspace / food system.

This model was employed in the optimization of the package design and in the identification of the best environmental conditions that would lead to the achievement of maximum package efficiency. As a result, it was concluded that immediate and constant activity after the beginning of the food preservation could be achieved by modifying the original package design to EPP (20 µm) / E29 (20 µm) / IPP (2 µm) and by avoiding exposure of the package and the packaging material to environmental relative humidities higher than 60 %.

The developed model could also be modified to undertake mathematical simulation and prediction of other preservation systems analogous to the one presented in this work, where other polymers or active compounds might be involved, or where different structural compositions, physicochemical properties, or working conditions might be present, as long as an inventory of experimental data for all the parameters and coefficients involved is available, sufficiently complete to fulfill all the mathematical requirements demanded by the model.

ACKNOWLEDGMENTS

The authors are grateful to the Spanish Ministry of Science and Innovation (project AGL2009-08776), EU (Nafispack project 212544), and Generalitat Valenciana (J.P.C. fellowship) for financial support, and to Mr. Karel Clapshaw (translation services).

REFERENCES

Ahmad, M., Benjakul, S., Sumpavapol, P., Prakash, N. (2012). Quality changes of sea bass slices wrapped with gelatin film incorporated with lemongrass essential oil. *International Journal of Food Microbiology*, 155 (3), 171 – 178.

Alizadeh, E., Chapleau, N., de – Lamballerie, M., Le – Bail, A. (2009). Impact of freezing process on salt diffusivity of seafood: Application to salmon (*Salmo salar*) using conventional and pressure shift freezing. *Food and Bioprocess Technology*, 2 (3), 257 – 262.

Aucejo, S. (2000). *Estudi i caracterització de l'efecte de la humitat en les propietats barrera d'estructures polimèriques hidròfiles.* Tesi doctoral, Universitat de València, València.

Barbiroli, A., Bonomi, F., Capretti, G., Iametti, S., Manzoni, M., Piergiovanni, L., Rollini, M. (2012). Antimicrobial activity of lysozyme and lactoferrin incorporated in cellulose – based food packaging. *Food Control*, 26 (2), 387 – 392.

Català, R., Gavara, R. (2001). Nuevos envases. De la protección pasiva a la defensa activa de los alimentos envasados. *Arbor*, CLXVIII, 661, 109 – 127.

Cava, D., Sammon, C., Lagaron, J. M. (2006). Water diffusion and sorption – induced swelling as a function of temperature and ethylene content in ethylene – vinyl alcohol copolymers as determined by attenuated total reflection Fourier transform infrared spectroscopy. *Applied Spectroscopy*, 60 (12), 1392 – 1398.

Cava, D., Sammon, C., Lagaron, J. M. (2007). Sorption – induced release of antimicrobial isopropanol in EVOH copolymers as determined by ATR – FTIR spectroscopy. *Journal of Applied Polymer Science*, 103 (5), 3431 – 3437.

Cerisuelo, J. P., Muriel – Galet, V., Bermúdez, J. M., Aucejo, S., Català, R., Gavara, R., Hernández – Muñoz, P. (2012). Mathematical model to describe the release of an antimicrobial agent from an active package constituted by carvacrol in a hydrophilic EVOH coating on a PP film. *Journal of Food Engineering*, 110 (1), 26 – 37.

Chamanara, V., Shabanpour, B., Gorgin, S., Khomeiri, M. (2012). An investigation on characteristics of rainbow trout coated using chitosan assisted with thyme essential oil. *International Journal of Biological Macromolecules*, 50 (3), 540 – 544.

COMSOL Model Examples: Separation through dialysis. COMSOL Multiphysics Modeling Guide, version 4.2. (2011). COMSOL AB.

Corbo, M. R., Speranza, B., Filippone, A., Granatiero, S., Conte, A., Sinigaglia, M., Del Nobile, M. A. (2008). Study on the synergic effect of natural compounds on the microbial quality decay of packed fish hamburger. *International Journal of Food Microbiology*, 127 (3), 261 – 267.

Corbo, M. R., Speranza, B., Filippone, A., Conte, A., Sinigaglia, M., Del Nobile, M. A. (2009). Natural compounds to preserve fresh fish burgers. *Food Science & Technology*, 44 (10), 2021 – 2027.

Crank, J. (1975). *The mathematics of diffusion*. Clarendon Press, London, UK.

EPA on – line tools for site assessment calculation: estimated diffusion coefficients in air and water – extended version. United States Environmental Protection Agency, USA. *http://www.epa.gov/athens/learn2model/part-two/onsite/estdiffusion-ext.html*

Galotto, M. J., Valenzuela, X., Rodriguez, F., Bruna, J., Guarda, A. (2012). Evaluation of the effectiveness of a new antimicrobial active packaging for fresh atlantic salmon (*Salmo salar* L.) shelf life. *Packaging Technology and Science*, 25 (6), 363 – 372.

Gallart – Jornet, L., Barat, J. M., Rustad, T., Erikson, U., Escriche, I., Fito, P. (2007). A comparative study of brine salting of Atlantic cod (*Gadus morhua*) and Atlantic salmon (*Salmo salar*). *Journal of Food Engineering*, 79 (1), 261 – 270.

Gallart – Jornet, L., Barat, J. M., Rustad, T., Erikson, U., Escriche, I., Fito, P. (2007). Influence of brine concentration on Atlantic salmon fillet salting. *Journal of Food Engineering*, 80 (1), 267 – 275.

Gómez – Estaca, J., López De Lacey, A., Gómez – Guillén, M. C., López – Caballero, M. E., Montero, P. (2009). Antimicrobial activity of composite edible films based on fish gelatin and chitosan incorporated with clove essential oil. *Journal of Aquatic Food Product Technology*, 18 (1 – 2), 46 – 52.

Han, J. H. (2005). *Antimicrobial packaging systems.* Han, J. H. (ed.) *Innovations in food packaging*. Elsevier Academic Press, USA.

Lara – Lledó, M., Olaimat, A., Holley, R. (2012). Inhibition of *Listeria monocytogenes* on bologna sausages by an antimicrobial film containing mustard extract or sinigrin. *International Journal of Food Microbiology*, 156 (1), 25 – 31.

López – Carballo, G., Cava, D., Lagarón, J. M., Català, R., Gavara, R. (2005). Characterization of the interaction between two food aroma components, α – pinene and ethyl butyrate, and ethylene – vinyl alcohol copolymer (EVOH) packaging films as a function of environmental humidity. *Journal of Agricultural and Food Chemistry*, 53 (18), 7212 – 7216.

Marais, S., Nguyen, Q. T., Devallencourt, C., Metayer, M., Nguyen, T. U., Schaetzel, P. (2000). Permeation of water through polar and nonpolar polymers and copolymers: determination of the concentration – dependent diffusion coefficient. *Journal of Polymer Science. Part B: Polymer Physics*, 38 (15), 1998 – 2008.

Marcos, B., Aymerich, T., Monfort, J. M., Garriga, M. (2007). Use of antimicrobial biodegradable packaging to control *Listeria monocytogenes* during storage of cooked ham. *International Journal of Food Microbiology*, 120 (1 – 2), 152 – 158.

Mascheroni, E., Guillard, V., Gastaldi, E., Gontard, N., Chalier, P. (2011). Anti – microbial effectiveness of relative humidity – controlled carvacrol release from wheat gluten / montmorillonite coated papers. *Food Control*, 22 (10), 1582 –1591.

Mastromatteo, M., Danza, A., Conte, A., Muratore, G., Del Nobile, M. A. (2010). Shelf life of ready to use peeled shrimps as affected by thymol essential oil and modified atmosphere packaging. *International Journal of Food Microbiology*, 144 (2), 250 – 256.

Mexis, S. F., Chouliara, E., Kontominas, M. G. (2009). Combined effect of an oxygen absorber and oregano essential oil on shelf life extension of rainbow trout fillets stored at 4 °C. *Food Microbiology*, 26 (6), 598 – 605.

Min, S., Rumsey, T. R., Krochta, J. M. (2008). Diffusion of the antimicrobial lysozyme from a whey protein coating on smoked salmon. *Journal of Food Engineering*, 84 (1), 34 – 47.

Muriel – Galet, V., Cerisuelo, J. P., López – Carballo, G., Lara, M., Gavara, R., Hernández – Muñoz, P. (2012). Development of antimicrobial films for microbiological control of packaged salad. *International Journal of Food Microbiology*, 157 (2), 195 – 201.

Muriel – Galet, V., Cerisuelo, J. P., López – Carballo, G., Aucejo, S., Gavara, R., Hernández – Muñoz, P. (2013). Evaluation of EVOH – coated PP films with oregano essential oil and citral to improve the shelf – life of packaged salad. *Food Control*, 30 (1), 137 – 143.

Rodríguez, A., Batlle, R., Nerín, C. (2007). The use of natural essential oils as antimicrobial solutions in paper packaging. Part II. *Progress in Organic Coatings*, 60 (1), 33 – 38.

Siripatrawan, U., Noipha, S. (2011). Active films from chitosan incorporating green tea extract for shelf life extension of pork sausages. *Food Hydrocolloids*, 27 (1), 102 – 108.

Sivertsvik, M. (2003). *Active packaging in practice: fish. Novel food packaging techniques*. Woodhead Publishing Limited and CRC Press LLC, Cambridge, UK.

Sivertsvik, M., Rosnes, J. T., Jeksrud, W. K. (2004). Solubility and absorption rate of carbon dioxide into non – respiring foods. Part 2: Raw fish fillets. *Journal of Food Engineering*, 63 (4), 451 – 458.

Trondsen, T. (1997). Marketing potential and barriers for fresh packed fish. A survey of buyer perception in UK and French seafood distribution. *Journal of Food Products Marketing*, 4 (2), 79 – 99.

Tunç, S., Duman, O. (2011). Preparation of active antimicrobial methyl cellulose / carvacrol / montmorillonite nanocomposite films and investigation of carvacrol release. *LWT – Food Science and Technology*, 44 (2), 465 – 472.

USDA National Nutrient Database for Standard Reference – Release 24. United States Department of Agriculture, USA.
http://ndb.nal.usda.gov

Wang, D., Correia, L. R., Tang, J. (1998). Modeling of salt diffusion in Atlantic salmon muscle. *Canadian Agricultural Engineering*, 40 (1), 29 – 34.

Wang, D., Tang, J., Correia, L. (2000). Salt diffusivities and salt diffusion in farmed Atlantic salmon muscle as influenced by rigor mortis. *Journal of Food Engineering*, 43 (2), 115 – 123.

III DIFFUSION MODELING IN POLYMER – CLAY NANOCOMPOSITES FOR FOOD PACKAGING APPLICATIONS THROUGH FINITE ELEMENT ANALYSIS OF TEM IMAGES

Josep Pasqual Cerisuelo [a], Rafael Gavara [a, *], Pilar Hernández – Muñoz [a]

[a] Laboratori d'envasos, Institut d'Agroquímica i Tecnologia d'Aliments, IATA – CSIC.
Av. Agustí Escardino, 7. 46980 Paterna, València.

* Autor de contacte. Tel.: +34 963900022, e-mail: rgavara@iata.csic.es

ABSTRACT

Nanocomposites are novel materials which are being increasingly used in the food packaging industry because of their enhanced properties with respect to the original unfilled polymers, more specifically in the active packaging area because of their great potential to retain the active molecules and to control their release into the preserved food. The estimation of the improvement achieved in the barrier or retention properties of those materials is usually performed through the calculation of their relative diffusivity, which can be obtained through the application of any of the theoretical models available in literature. However, their results are disparate and quite inaccurate when working with nanocomposites with low values of volume fraction and aspect ratio of particles.

This motivates the development of new and alternative methods to undertake this estimation in a more reliable way. The method presented in this work is based on the mathematical modeling and simulation of the diffusion processes taking place, and, unlike the previous models, it only requires as input some TEM micrographs of actual polymer nanocomposites. By subjecting such micrographs to image and finite element analysis the model can yield accurate values of their relative diffusivity. The materials studied in this work, and afterwards employed to validate the model, consist of EVOH – 29 or zein matrices with approximately 1 or 2 % $^{v}/_{v}$ of bentonite nanoparticles as inorganic filler.

Results showed that all the materials reached a quite satisfactory nanocomposite structure, and, after being analyzed with the new method, average reductions of between 3.8 and 12.2 % in their solute diffusivities could be expected. In spite of the possible size effects of the diffusing molecules, not considered in the developed model, the values found accorded with experimental values obtained from permeability measurements and from other data reported in a previous work for the diffusion of permanent gases in analogous materials, thus validating the new propounded method.

***Journal of Membrane Science*, 2015, 482, 92 – 102.**

1. INTRODUCTION

Nanocomposites are two-phase systems typically consisting of a polymeric matrix and dispersed inorganic particles of nanometric size, usually belonging to the family of 2:1 phyllosilicates [1]. These novel materials are increasingly being used in numerous applications mostly due to their enhanced properties with respect to the original unfilled polymers. Reinforcement of mechanical [2] and thermal [3, 4] properties has been demonstrated widely in literature, as well as improvements in barrier properties to water vapor, permanent gases (nitrogen, oxygen, and carbon dioxide), and aromatic compounds [1, 5], flammability resistance [6], chemical compatibility [3], and biodegradability [4, 7]. All these features make nanocomposites of great interest for the food packaging industry, but more particularly in the active and intelligent packaging fields, since they also allow the control of active molecules release rate and extent to the preserved foodstuffs [7 – 12]. In fact, in recent works several polymer-clay nanocomposites have successfully been developed and tested as carrier materials for natural volatile antimicrobial agents in active packages [13 – 18].

Both enhancement in barrier properties and control of release rates are a result of the reduction in solubility and diffusivity, and thus permeability, of the gas molecules when migrating within the nanocomposite matrix. Observed decreases of these parameters are attributed to the incorporation of impermeable fillers to the original polymer, since they are expected to affect the path tortuosity directly, when penetrants are forced to travel around them, and indirectly, when they induce polymer chain alignment, or alignment and modification of polymer crystallites [19]. In the first case, in addition to the resistance to diffusion caused by the increased distance of the tortuous path around the filler particles, and by the reduced cross-sectional area between them, some authors also consider to be significant the resistance caused by the displacement of the solute through the slits between adjacent particles in the same horizontal plane, and by its constriction or “necking” when passing into and out of the narrower ones [20].

Given all those retention mechanisms, platelet-like nanoparticles are especially effective in the enhancement of the barrier properties of polymer nanocomposites, due to their two-dimensional nature, and their performance is also further improved as their degree of exfoliation and alignment increases, as well as their aspect ratio [5]. In fact, under those ideal conditions, platelet-like nanoparticles are reported to reduce the gas permeability by 50 – 500 times, even at low loading levels [1]. However, the degree of improvement finally reached in such materials is highly variable and dependent on their geometrical characteristics (particle size, shape, distribution, orientation, etc.). For

this reason, several attempts to theoretically model and mathematically estimate this improvement have been carried out since the 19th century, although with different degrees of success [21 – 46].

That is because most theoretical approaches assume no permeability changes in the polymer matrix and consider fillers as impermeable pseudo-two-dimensional non-overlapping particles of regular and uniform shape (rectangular, hexagonal or circular), regularly or randomly distributed in the polymer, and parallel or perpendicularly orientated with respect to the direction of diffusion [1, 19]. Although some of these models have been repeatedly validated over the years by contrasting their outputs with experimental data [47 – 50], almost none of them has demonstrated to be capable of providing fully satisfactory results for a majority of cases. This is due, unfortunately, to the fact that the microstructure of actual nanocomposites is far away from those idealized characteristics, which is leading new models to become increasingly complex in their attempt to improve its simulation and to achieve results closer to experimental data, thus requiring every time more parameters of more arduous estimation.

In view of this, the purpose of this work is to present a new and alternative way to estimate the improvement achieved in the barrier properties of diverse actual nanocomposite materials through the mathematical modeling and simulation of the diffusion processes taking place. Unlike the previous models reviewed from literature, the basis for the new model will not be any analytical development, but the image and finite element analysis of various TEM micrographs acquired from actual polymer nanocomposites, consisting of EVOH and zein matrices containing small amounts of bentonite nanoclay as inorganic filler. Furthermore, this new model will be also validated by comparing its results with measured data of oxygen permeability, as well as with other theoretical results yielded by a selection of previous literature models.

2. REVIEW OF PREVIOUS MODELS

Almost all theoretical models developed in previous papers start from simple 2D systems where particles of rectangular shape resembling ribbons, with finite width (w), and thickness (t), and infinite length, are regularly distributed in the polymer matrix and parallel or perpendicularly oriented with respect to the direction of diffusion. In these approaches, several geometrical parameters are defined in order to fully characterize the structure of the modeled system, namely: the volume fraction of particles (ϕ), the aspect ratio of particles (α), and the aspect ratio of slits or pores between adjacent

particles in the same horizontal plane (σ). The volume fraction is considered the main descriptive parameter of composite systems and, accordingly, it has been present in all propounded equations since the first developed models. If particles are considered to be surrounded by a repeating unit cell of polymer with finite width (W), and thickness (T), and infinite length, the volume fraction of particles in a 2D system can be unequivocally defined as:

$$\phi_{2D} = \frac{w \cdot t}{W \cdot T} \tag{III.1}$$

As for particle and slit aspect ratio, both parameters were absent in the first models or were given little importance in the equations, while currently they are increasingly being incorporated in the new models as they become more complex and require a better characterization of the actual nanocomposite systems. Definitions of both variables differ among authors, yet some agreement has been reached in recent years around the following equations [51]:

$$\alpha = \frac{w}{t} \tag{III.2}$$

$$\sigma = \frac{W - w}{t} \tag{III.3}$$

Apart from geometrical parameters, theoretical models also introduce a transport coefficient intended to evaluate the improvements in the barrier properties achieved by the nanocomposite with respect to the original polymer: the relative diffusivity (D_n/D_0). This parameter is defined as the ratio between the diffusion coefficients of any solute in both materials, although it can also be expressed as the inverse of the tortuosity factor (or geometric-hindered factor) (τ), another structural parameter accounting for the global resistance to diffusion offered by nanoparticles. This variable, in turn, is dependent upon the geometrical characteristics of the nanocomposite, which are usually described by the volume fraction, and the particle and slit aspect ratio, as defined above:

$$\frac{D_n}{D_0} = \frac{1}{\tau} = \frac{1}{f(\phi, \alpha, \sigma)} \tag{III.4}$$

By expressing the enhancement attained in the barrier properties through this mathematical equation, theoretical models can focus their efforts only on the determination of the function of the tortuosity factor, and thus on finally find an analytical solution for the model equations set out. Aside from this, it must be mentioned that some recently developed models for simple 2D systems do not follow these principles, and thus do not yield a mathematical expression for the relative diffusivity, they are solved numerically instead, obtaining equally good results [40, 43 – 46].

In subsequent refinements of the early nanocomposite models, random distribution [38, 39, 44, 52] and variable orientation [33, 34, 36, 41, 46, 52] were also considered, although, according to most authors, only a simple modification of the first expressions obtained for the function of the tortuosity factor was needed to account for these new features. In contrast, some recent models, in their search for a more realistic representation of the nanocomposite structures, have undertaken the simulation of complex 3D systems where particles are no longer considered infinite ribbons, but symmetrical discs or flakes of rectangular or hexagonal shape instead, with finite width (w), thickness (t), and length (l) [35, 37, 38, 42, 44].

These new models are usually too complex to yield a simple expression for the relative diffusivity in the form of equation (III.4). Hence, most of them must be solved numerically, often with the aid of the finite difference [40], volume [44, 45], or element [37, 43, 46] methods. Nevertheless, in some cases, the analytical equations derived for 2D systems have proven to be fully applicable to their 3D counterparts by introducing only slight modifications in the definitions of the model's geometrical parameters [44], or at least to be a good base to develop new valid expressions [35, 38]. In any case, it must be noticed that the definition of the volume fraction of particles in 3D systems differs significantly from that which was given in equation (III.1) for 2D systems. Indeed, if particles are considered to be surrounded by a repeating unit cell of polymer with finite width (W), thickness (T), and length (L), as outlined in **Figure III.1**, the volume fraction of particles in a 3D system can be univocally defined as:

$$\phi_{3D} = \frac{w \cdot t \cdot l}{W \cdot T \cdot L} \qquad \text{(III.5)}$$

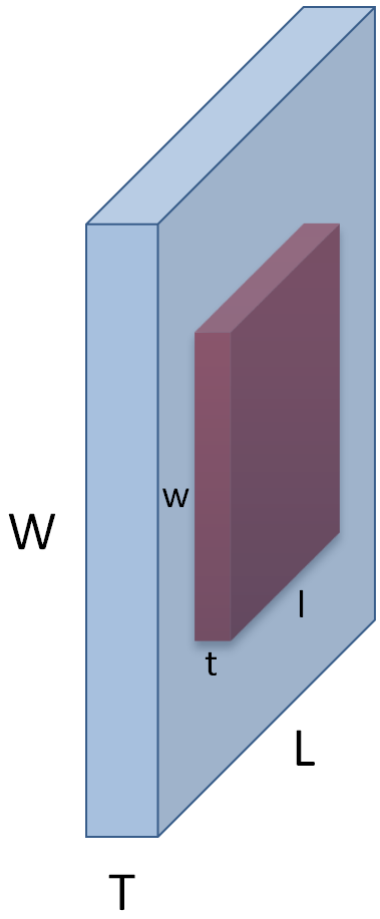

Figure III.1. Repeating unit cell of polymer of dimensions proportional to the particle in a regularly distributed nanocomposite structure.

However, if particles are considered to be regularly distributed in the polymer matrix, that is, equally separated with distances proportional to their length in every direction, the dimensions of this repeating unit cell must be fully proportional to the dimensions of the particle, with a unique factor of proportionality (f). In this case, the equation (III.5) can be properly rewritten to:

$$\phi_{3D} = \frac{w \cdot t \cdot l}{(w \cdot f) \cdot (t \cdot f) \cdot (l \cdot f)} = \frac{1}{f^3} \qquad \text{(III.6)}$$

Likewise, by applying the same premise to the definition of the volume fraction of particles in a 2D system, the equation (III.1) can equally be expressed as:

$$\phi_{2D} = \frac{w \cdot t}{(w \cdot f) \cdot (t \cdot f)} = \frac{1}{f^2} \qquad \text{(III.7)}$$

Hence, by isolating the factor of proportionality in both equations (III.6) and (III.7), and by comparing the expressions thus obtained, the relation between the actual volume fraction in a 3D system (ϕ_{3D}) and the apparent volume fraction according to its cross-sectional 2D image (ϕ_{2D}), as obtained from its cut in the direction of the length, can be finally determined as:

$$\phi_{3D}^2 = \phi_{2D}^3 \qquad \text{(III.8)}$$

In consequence, equations developed for 2D systems should be applied to their 3D counterparts carefully because, as equation (III.8) shows, volume fraction of particles in a cross-sectional image of an actual nanocomposite will always be apparently higher than its actual known value. A visual demonstration of equation (III.8) has been included in the supporting information provided.

As mentioned above, some of these theoretical models have been validated experimentally on numerous occasions after being successfully applied to the estimation of the relative diffusivity in diverse nanocomposite materials [47 – 50]. Such estimation should be ever possible by just introducing known values of the volume fraction and measured values of the particle and slit aspect ratios in their general equations. However, values of particle aspect ratio actually measured in polymer nanocomposites are usually substituted by literature values estimated from neat filler crystals, because of their complex determination through the image analysis of TEM or SEM micrographs, whereas values of slit aspect ratio are almost impossible to measure in a reliable way, even when good images of regularly distributed and oriented particles are available. These two difficulties, together with the fact that almost all theoretical models are based on highly idealized structures, which are far from reality, prevent them from being valid in a wide range of situations.

This problem can be easily visualized when graphically comparing the outputs of diverse theoretical models available in the literature for low values of particles' volume fraction and aspect ratio. For this purpose, **Table III.1** gathers a selection of theoretical models which are only dependent upon these two parameters, and **Figure III.2** shows the corresponding plots of their estimated relative diffusivities for a particle aspect ratio value of 5 and for particles' volume fraction values ranging from 0 to 0.1. As can be seen, curves plotted in **Figure III.2** evidence a great disparity in results for the estimated parameter even when only the simplest models are considered, after having ruled out those including the slit aspect ratio in their general equations. Furthermore, in many cases these discrepancies seem to worsen at lower values of the volume fraction and of the particles' aspect ratio. As an example, for a volume fraction of about 2 % (typical filler loading of numerous polymer nanocomposites studied in

the literature) model equations produce disparate values of the relative diffusivity, ranging from 0.8 to the unity. This suggests that most theoretical models will only be able to yield consistent results at high values of both parameters, and therefore motivates the development of alternative methods to undertake this estimation in a more reliable way.

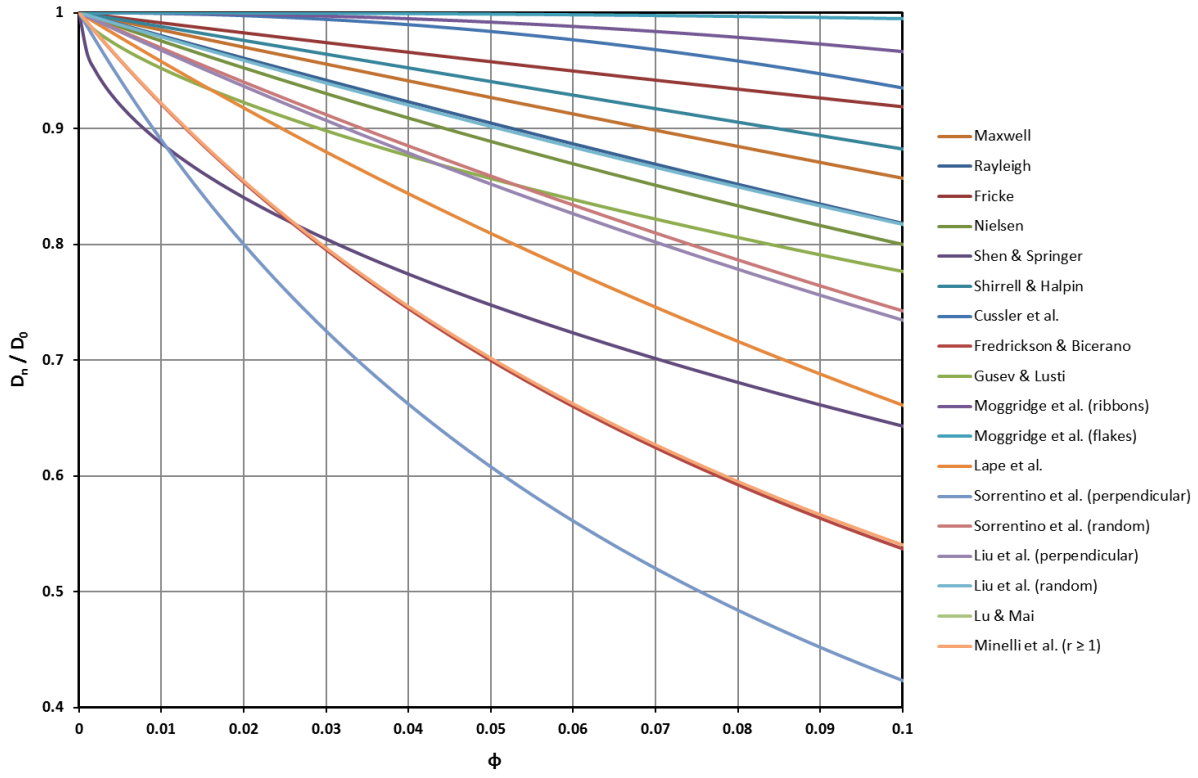

Figure III.2. Relative diffusivity as a function of the volume fraction of particles, for α = 5, as yielded by the theoretical models reviewed from the literature.

Table III.1. **Theoretical models dependent only upon the volume fraction and the aspect ratio of particles, as reviewed from the literature.***

Model	Maxwell [21]	Rayleigh [22]	Fricke [23]	Nielsen [24]	Shen & Springer [28]	Shirrell & Halpin [29]	Cussler et al. [32]
Particle type	Spheres	Fibers	Oblate spheroids	Ribbons	Fibers	Fibers	Ribbons
Distribution	Regular	Regular	Regular	Regular	Regular	Regular	Regular
Orientation	-	Perpendicular	-	Perpendicular	Perpendicular	Perpendicular	Perpendicular
Dimension	-	2D	-	2D	2D	2D	2D
Tortuosity factor, τ	$\frac{1+\phi/2}{1-\phi}$	$\frac{1+\phi}{1-\phi}$	$1+\frac{\phi}{3}\left(\frac{\alpha^2}{1.57\alpha-1}-1\right)$	$1+\frac{\alpha\phi}{2}$	$\left(1-2\sqrt{\frac{\phi}{\pi}}\right)^{-1}$	$\frac{1+\phi/\alpha}{1-\phi}$	$1+\frac{\alpha^2\phi^2}{4(1-\phi)}$

Model	Fredrickson & Bicerano [35]	Gusev & Lusti [37]	Moggridge et al. [38]		Lape et al. [39]	Sorrentino et al. [41]	
Particle type	Disks	Disks	Ribbons	Hexagonal flakes	Ribbons	Ribbons	
Distribution	Random	Random	Random		Random	Regular	
Orientation	Perpendicular	Perpendicular	Perpendicular		Perpendicular	Perpendicular	Random
Dimension	3D	3D	2D	3D	2D	2D	
Tortuosity factor, τ	$\left(\frac{1}{2+\frac{\left(2-\sqrt{2}\right)\pi\alpha\phi}{4\ln(\alpha/2)}}+\frac{1}{2+\frac{\left(2+\sqrt{2}\right)\pi\alpha\phi}{4\ln(\alpha/2)}}\right)^{-2}$	$e^{\left(\frac{\alpha\phi}{3.47}\right)^{0.71}}$	$1+\frac{\alpha^2\phi^2}{8(1-\phi)}$	$1+\frac{\alpha^2\phi^2}{54(1-\phi)}$	$\frac{1}{1-\phi}\left(1+\frac{\alpha\phi}{3}\right)^2$	$1+\frac{\phi}{1-\phi}\left(1+\frac{\alpha}{2}\right)^2$	$1+\frac{4\phi}{\pi(1-\phi)}\left(1+\frac{1}{\alpha}+\frac{\alpha}{4}\right)$

Model	Liu et al. [42]		Lu & Mai [52]	Minelli et al. [44]
Particle type	Rectangular flakes		Ribbons	Disks and rectangular, hexagonal or octagonal flakes
Distribution	Regular		Random	Random
Orientation	Perpendicular	Random	Random	Perpendicular
Dimension	3D		2D	3D
Tortuosity factor, τ	$\left(1+\frac{\alpha\phi}{3}\right)^2$	$\left(1+\frac{2\alpha\phi}{3\pi}\right)^2$	$\frac{1}{1.65}\left(1+\frac{\alpha\phi}{2}\right)^{5/3}$	$\begin{cases} r\le 1 & \frac{(\alpha+2)^2\phi}{2\alpha}+\frac{(\alpha+2)^4\phi^2}{4\left(\alpha^2-\alpha\phi(\alpha+2)\right)}+\frac{2(\alpha+2)^2\phi}{\pi\alpha}\ln\left(\frac{2}{\pi}\left(\frac{\alpha}{(\alpha+2)\phi}-1\right)\right) \\ r\ge 1 & 1+\frac{(\alpha+2)\phi}{2}+\frac{2(\alpha+2)^2\phi}{\pi\alpha}\ln\left(\frac{\alpha+2}{\pi}\right) \end{cases}$ $\quad r=\frac{2\left(\alpha-\phi(\alpha+2)\right)}{\phi(\alpha+2)^2}$

* Equations presented in the table have been checked, correcting the errata found in the literature, and rewritten in accordance with the definition of α given in the present work.

3. MATERIALS AND METHODS

3.1. Materials

Ethylene-vinyl alcohol copolymer with a 29 % ethylene molar content (EVOH-29) was kindly supplied by The Nippon Synthetic Chemical Industry Co., Ltd. (Osaka, Japan), deodorized maize zein was provided by Kobayashi Perfumery Co., Ltd. (Chuo-ku, Tokyo, Japan), sodium bentonite nanoclay was purchased from Sigma-Aldrich Co. LLC (St. Louis, MO, USA), reagent-grade 1-propanol and high-vacuum silicone were acquired from Panreac Química S.L.U. (Castellar del Vallès, Barcelona, Spain), extra pure ethanol absolute was supplied by Scharlab S. L. (Sentmenat, Barcelona, Spain), and deionized water was obtained from a Milli-Q Plus purification system of EMD Millipore Corp. (Billerica, MA, USA).

3.2. Preparation of nanocomposite films

Nanocomposite films were prepared from hydroalcoholic solutions of the polymers with the inorganic filler incorporated. Concretely, the required amount of sodium bentonite was thoroughly mixed with deionized water in an Ultra-Turrax T25 basic disperser (IKA-Werke GmbH & Co. KG, Staufen, Germany) for 30 seconds at 24000 rpm, in order to wet all clay agglomerates and break them down into primary particles. The mixture obtained was then placed in an Ultrasons ultrasonic bath (J.P. Selecta S.A., Barcelona, Spain) for at least 1 hour to allow optimal splitting (delamination) of the agglomerates. When a stable suspension was formed, it was left to rest overnight to allow intensive swelling and hydration of the remaining agglomerates, and to achieve the optimal suspension characteristics.

The next day, the clay suspension was divided into three aliquots to prepare the necessary solutions of both polymers. In particular, for EVOH solutions, a precise amount of 1-propanol was incorporated to one of the abovementioned aliquots in order to form a 1:1 (w/w) mixture with the water contained in the suspension. This solution obtained was further homogenized in the ultrasonic bath for at least 15 minutes more, and was then used to dissolve EVOH-29 pellets following the procedure described elsewhere [54], finally yielding a total content of 15 g of polymer per 100 g of solution, and of 4 g of bentonite per 100 g of EVOH-29 ($\phi \approx 0.02$). The second aliquot, in turn, was firstly diluted to half, and afterwards used to prepare a hydroalcoholic solution of EVOH-29 containing 2 g of bentonite per 100

g of polymer ($\phi \approx 0.01$), by following the same procedure described above. Finally, the third aliquot of the clay suspension was mixed with absolute ethanol at a 1:4 (w/w) proportion, and subsequently homogenized in the ultrasonic bath for a minimum of 15 minutes. Immediately afterwards, the solution was heated to 80 °C, mixed with the required amount of zein powder to reach a final concentration of 15 g of polymer per 100 g of solution, and of 2 g of bentonite per 100 g of polymer ($\phi \approx 0.01$), and thoroughly stirred for at least one hour more to allow complete dispersion and dissolution of the zein particles.

The three formulated solutions were used in the preparation of nanocomposite films by casting them over glass plates with the aid of various Mayer rods of different deep thread (Lin Lab Rioja S.L., Logroño, Spain), one of 50 µm for EVOH-29 with ≈2 % $^{v}/_{v}$ bentonite, another of 100 µm for EVOH-29 with ≈1 % $^{v}/_{v}$ bentonite, and another of 200 µm for zein with ≈1 % $^{v}/_{v}$ bentonite. Immediately afterwards, all the glass plates were placed under the heat radiation source of a 2500 W home-made drying hood, to be dried for 15 min at a minimum temperature of 80 °C, and the dry films obtained were stored at room temperature until utilization. The thickness of each film was measured, prior to analysis, with an ABSOLUTE Digimatic Indicator ID-C Series 543 digital micrometer (Mitutoyo America Corp., Aurora, IL, USA), giving an average value of 6 ± 1 µm for EVOH-29 with ≈2 % $^{v}/_{v}$ bentonite, 12 ± 1 µm for EVOH-29 with ≈1 % $^{v}/_{v}$ bentonite, and 25 ± 1 µm for zein with ≈1 % $^{v}/_{v}$ bentonite.

3.3. Determination of microstructural morphology

The microstructural morphology of the prepared films was studied by transmission electron microscopy (TEM), with the purpose of verifying the achievement of a nanocomposite structure and of characterizing it through the determination of its fundamental parameters. TEM analysis was carried out in a JEM-1010 unit (JEOL Ltd., Tokyo, Japan), equipped with an AMT XR-80 digital camera (Advanced Microscopy Techniques Corp., Woburn, MA, USA) and its proprietary image acquisition software, using 60 kV of accelerating voltage, thus yielding 8-megapixel transmission micrographs in 8-bit TIFF image format. Samples for TEM were embedded in cured epoxy resin, and ultra-thin sections of between 60 and 90 nm were extracted with a Leica EM UC6 ultramicrotome (Leica Microsystems GmbH, Wetzlar, Germany) and mounted on a 100 mesh cupper micro-grid covered by a Formvar supporting film. Image analysis of the obtained micrographs, aimed at the measurement of the filler

particles' aspect ratio, was carried out with the aid of ImageJ image processing software (National Institutes of Health, USA).

3.4. Measurement of relative diffusivity

Improvements in the barrier properties achieved by the nanocomposite materials with respect to their neat polymers were initially determined through permeability measurements $\left(P_n/P_0\right)$, and afterwards converted into relative diffusivities $\left(D_n/D_0\right)$ by means of the following equation:

$$\frac{D_n}{D_0}=\frac{P_n/S_n}{P_0/S_0}=\frac{S_0}{S_n}\cdot\frac{P_n}{P_0}=\frac{S_0}{S_0\cdot\left(1-\phi\right)}\cdot\frac{P_n}{P_0}=\frac{1}{\left(1-\phi\right)}\cdot\frac{P_n}{P_0} \qquad \text{(III.9)}$$

Permeability to oxygen of both neat and nanocomposite films was measured in controlled conditions of temperature and relative humidity by following the procedures described in a previous work [17], based on the ASTM D1434 – 82(2009)e1 standard method [53]. In brief, the transport of oxygen through the studied materials was analyzed with an OX-TRAN model 2/21 ML permeation system (Paul Lippke Handels – GmbH, Neuwied, Germany), programmed to measure oxygen transmission rates at 23 ± 1 °C and at 0 ± 0.01 % RH, and to subsequently convert them into permeability data. Prior to the permeation tests, four film samples of each tested material were placed in the instrument cells, held in place with high-vacuum silicone, and conditioned for at least 8 h. Immediately afterwards, the gas transmission rates were measured every 45 min until constant, and, from that moment, at least five more points were acquired in order to obtain good average values for the gas permeabilities.

3.5. Estimation of relative diffusivity

The relative diffusivity of any solute through the prepared nanocomposite films was estimated by means of a new and alternative method, consisting on the image processing of the obtained micrographs, their introduction in a mathematical model based on the finite element method, and the subsequent simulation of the diffusion processes taking place.

Firstly, a total number of 24 micrographs (between 3 and 12 of each studied material) were carefully selected from the images captured in the TEM unit as fully representative of the materials' structure,

and were then introduced in ImageJ image processing software in order to prepare them as inputs for the mathematical model. In this stage, images were rotated, cropped and enlarged, with the intention of orientating the film captures parallel to the pictures, and of removing their edges and their background. Then, images were digitally enhanced by equalizing them and by filtering them, and finally converted from 8-bit TIFF to 8-bit PNG format. Equalization allowed correcting their brightness and contrast, thus ensuring pure black and white tonalities were reached in the images' grayscales. Digital filters were in turn applied with several purposes, such as improving the sharpness and definition of the images, or removing their artifacts and background noise.

Once the selected micrographs were properly deblurred and cleaned they could be introduced as image variables in a mathematical model developed by using the Transport of Diluted Species physics interface of the Chemical Reaction Engineering module included in the COMSOL Multiphysics 4.2a modeling suite (COMSOL AB, Stockholm, Sweden). With the aid of this simulation software each image could be easily digitalized by assigning to every pixel a fractional value ranging from 0 (black) to 1 (white) as a function of its gray intensity, also known as relative luminance (Y). In this point, by selecting a particular cut-off value for this parameter, the software was able to yield binary images of the original micrographs, after assigning zero to the pixels located below the threshold, according to their Y value, and unity to the pixels located above. In this way, the inorganic filler became completely distinguishable from the embedding polymer and, as a result, its particles could be definitely separated from the polymer matrix for the subsequent analyses.

In turn, the model developed consisted of a rectangular domain of dimensions equal to those of the image being analyzed. To properly study the transport phenomena taking place in the system, some material properties must be defined and all the fundamental hypotheses and integration conditions had to be set out and introduced into the software database. If diffusion is considered to be responsible for all the mass transfer processes occurring in the studied material then the solute diffusivity is the only physical property that must be taken into account. Since the nanocomposite material is of a heterogeneous nature, binary images of its internal structure can be used to define the solute diffusivity therethrough as a discontinuous function, which takes a zero value in the regions occupied by particles and a unity value in the regions corresponding to the polymer matrix. This way, the behavior of a discontinuous material with continuous properties can be successfully, and more easily, represented through that of a continuous material with discontinuous properties [55]. With respect to the fundamental hypotheses, full compliance with the postulations posed in previous works was assumed [54], whereas initial and boundary conditions, in this case, were chosen as follows:

- The solute concentration in every point of the system domain was considered to be nil at the beginning of the diffusion processes.
- The solute concentration at the upper boundary was fixed as unity, whereas at the lower boundary it was fixed as zero, thus generating a solute gradient and flux from the top to the bottom of the system domain.
- Lateral boundaries were considered to be isolated, that is, fully impermeable, since the diffusion of the solute was considered to be a unidirectional process of vertical direction and, consequently, no flux was allowed to cross such boundaries in a horizontal way.

Once the bases of the model were properly set out and its properties were consistently defined, its spatial discretization had to be carried out prior to its mathematical solving by the application of the finite element method. In effect, this methodology requires generating a mesh in the material domain by dividing it into numerous finite elements where solute fluxes and concentrations can be evaluated. In this case, an extremely fine mapped mesh was first created and subsequently triangulated by splitting its rectangular elements from its central point. In addition, the simulation software was instructed to perform an adaptive mesh refinement, with a maximum of 5 element refinements, depending upon the changes observed in the solute fluxes and concentrations, as calculated during the solving progression. This way, the final adapted mesh consisted of about 1500000 free triangular elements on average, mostly distributed around the filler particles, and more particularly around their sharpest corners and most irregular areas.

Then, taking all these premises into consideration, the mathematical model could be finally solved for each studied image, yielding the estimated values of the solute flux and concentration at the stationary state in every finite element of the system domain. In general, the model's solving process required less than one minute of computing time in a 3.40 Ghz 4-core CPU, given that, in this study, the model solution was constrained by only one dependent variable, the solute flux (J), which was numerically approached with the aid of a direct stationary solver algorithm (PARDISO) using a very low relative tolerance (10^{-6}). The solution thus obtained allowed to compute the average value of such parameter over the global system domain after the stationary state was fully reached. Finally, if the first Fick's law is considered to be applicable to the studied system, then:

$$J = -D \cdot \nabla C \quad \rightarrow \quad D = \frac{-J}{\nabla C} \tag{III.10}$$

Therefore, since ∇C was preset and thus had a known magnitude, and J was estimated from the model solution, the value of the solute diffusivity through the nanocomposite material and, consequently, of its relative diffusivity, could be easily estimated for each studied film image.

4. RESULTS AND DISCUSSION

4.1. Assessment of microstructural morphology

The microstructure of the three prepared nanocomposite materials was studied by means of the visual analysis and computer processing of their TEM images. For this purpose, some example micrographs of their corresponding film samples are displayed in **Figures III.3a**, **III.3b** and **III.3c**. The twelve selected micrographs from the films of EVOH-29 with ≈1 % $^{v}/_{v}$ bentonite are included in the supporting information (**Figure SI-1**). As pictures show, bentonite particles were reasonably well exfoliated and thus randomly distributed in the polymer in most areas, whereas particle agglomerates were still present and thus the polymer matrix remained almost unfilled in a few zones. In light of this, it can be stated that all the manufactured films reached an intercalated, nearly exfoliated, nanocomposite structure, where the majority of clay flakes were almost individualized and properly embedded in between the polymer chains. Aside from that, pictures also display that most of the clay particles were not randomly oriented, but oriented parallel to the films instead, especially in the case of EVOH-29 with ≈2 % $^{v}/_{v}$ bentonite, particularly characterized by its higher values of the particles' volume fraction and aspect ratio. This can be explained by the fact that during the casting process flakes tend to orientate in the direction of the extension of the clay suspensions. Hence, when they are dried and give rise to nanocomposite films, clay particles remain mostly oriented to them, being parallel to their surface and thus perpendicular to the diffusion processes taking place. Consequently, the solute diffusivity is further reduced in comparison with a randomly oriented structure, which leads to a greater enhancement of the barrier properties than it should be expected from a random orientation.

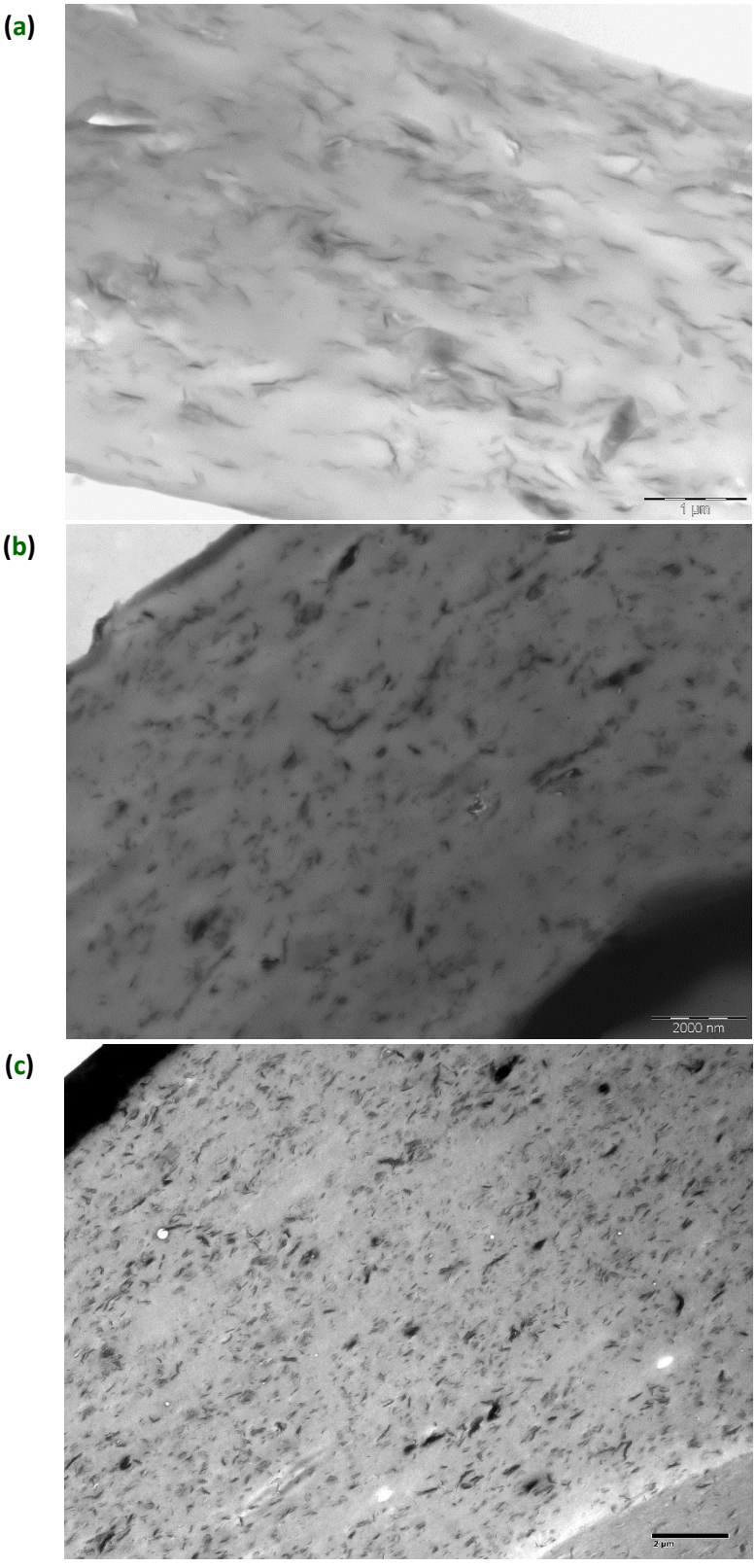

Figure III.3. Example micrographs of film samples corresponding to the three prepared nanocomposite materials: EVOH-29 with 2 % $^{v}/_{v}$ bentonite (a), EVOH-29 with 1 % $^{v}/_{v}$ bentonite (b), and zein with 1 % $^{v}/_{v}$ bentonite (c), as obtained from TEM analysis.

When film micrographs were introduced in ImageJ image processing software for image analysis the aspect ratio of the filler particles could be graphically estimated. In detail, particles present in each TEM image were firstly identified by the software, and their equivalent ellipse, that is, the ellipse with the same area, first and second moments of inertia as the particle, was subsequently calculated. In this way, the values of the particles' aspect ratio could be found by just computing the ratio between the major and the minor axis of their corresponding equivalent ellipses, and the results thus obtained were subsequently averaged to yield the mean aspect ratio of each analyzed film micrograph. Hence, by averaging such values among all the film micrographs acquired from each nanocomposite material, the corresponding mean values of the particles' aspect ratio could be finally found, and afterwards gathered in **Table III.2**. The individual results obtained from each micrograph for the EVOH-29 with ≈1 % $^{v}/_{v}$ bentonite are included in the supporting information (**Table SI-1**).

Table III.2. Calculated volume fractions and measured aspect ratios of the filler particles, estimated and measured relative diffusivities, and model estimation error for the diverse studied nanocomposite materials.

Nanocomposite material	$\phi \cdot 10^2$	α	$\left[D_n/D_0\right]_e$	$\left[D_n/D_0\right]_m$	Error (%)
EVOH-29 + ≈2 % $^{v}/_{v}$ bentonite	1.862	4.4 ± 0.4	0.878 ± 0.012	0.895 ± 0.002	-1.9 ± 1.3
EVOH-29 + ≈1 % $^{v}/_{v}$ bentonite	0.931	2.7 ± 0.3	0.962 ± 0.007	0.971 ± 0.006	-0.9 ± 0.7
Zein + ≈1 % $^{v}/_{v}$ bentonite	0.946	3.3 ± 0.3	0.954 ± 0.006	0.962 ± 0.008	-0.8 ± 0.6

Albeit the figures collected in the table, of between 2.7 and 4.4, could seem to be fairly low it must be noticed that, in view of the images displayed, most particles were not straightly placed in the polymer matrix, but bended instead, and also that both particle agglomerates and particle fragments were included in the software computations. In consequence, the final estimated values of the particles' aspect ratio could have been reduced due to their rounder shape. In addition, as both **Figure III.3** and **Table III.2** show, the mean aspect ratio of the filler particles in the most loaded polymer nanocomposite, EVOH-29 with ≈2 % $^{v}/_{v}$ bentonite, was about 48 % higher in average than in the other two studied materials. This can be explained by the higher viscosity of its precursor solution, which could have contributed to prevent the breakage of the filler particles (understood as exfoliated individual sheets) by excessive shear forces during their dispersion, sonication, and stirring processes. In any case, the numbers obtained confirmed the achievement of an intercalated to exfoliated structure, which was considered to be satisfactory when dealing with a natural non-organically modified clay.

4.2. Assessment of relative diffusivity

As mentioned above, a new method has been proposed in this work to estimate the relative diffusivity of any solute in a nanocomposite material through a finite element analysis of its TEM images, based on the mathematical modeling and simulation of the diffusion processes taking place.

In order to properly assess the results yielded by this new method the film micrograph displayed in **Figure III.3a** will be used as an example to illustrate in detail the procedure explained. This way, **Figure III.4a** shows the enhanced image of the nanocomposite material, as resulting from the graphical treatment performed by the image processing software upon the original picture. **Figure SI-2** of the supporting information includes the digital image processing of the twelve micrographs selected from the films of EVOH-29 with ≈1 % $^{v}/_{v}$ bentonite. The treatment operation included rotation, cropping, enlargement, equalization and filtration of the picture, and yielded an improved image of the material microstructure in which filler particles were much more defined, and therefore distinguishable from the embedding polymer, than in the raw picture. Then, the enhanced image was introduced as an image variable in COMSOL Multiphysics, in order to get their pixels digitalized as a function of their relative luminance (Y). The output resulting from this process is displayed in **Figure III.4b**, where the relative luminance is plotted in a surface graph versus the position coordinates of every image pixel. As the graph shows, the largest part of the image area is occupied by the background, evidenced by the high relative luminance of its pixels, with values mainly ranging from 0.8 to 1. However, the graph also exhibits some narrow and deep depressions which, starting from the background, reach very low Y values, ranging from 0 to 0.2 approximately. Obviously, these depressions correspond to the filler particles, and the values of the relative luminance around their limits change so sharply owing to the increased definition and sharpness of the processed picture.

As explained before, by converting pixels to numbers, and thus images to numerical matrices, based on their relative luminance, the digitalization procedure allows to set up a threshold value for this parameter which is able to unequivocally discriminate particle pixels from polymer pixels and, in consequence, to convert grayscale images into binary ones. Although no guidelines are yet available to help in the selection of this cut-off point, a value of 0.5 is generally recommended if the processed image is properly equalized [55]. Nevertheless, in this work lower values were generally selected in order to generate binary images with estimated volume fractions of particles approaching 0.01 or 0.02, in agreement with the actual filler loadings of the diverse studied nanocomposite materials. Hence, the final binary image resulting from all these considerations is displayed in **Figure III.4c**. The results

obtained from the twelve micrographs selected for the films of EVOH-29 with ≈1 % $^{v}/_{v}$ bentonite are included in **Figure SI-3** of the supporting information. As can be seen, filler particles and polymer matrix can be clearly distinguished from each other in the picture by simply identifying their binary colors, black and white respectively.

Finally, after the mathematical model was properly set up, according to the procedure described in the experimental section, a spatial discretization of the system domain was carried out, yielding an adapted mesh of free triangular elements which **Figure III.4d** details. As the image shows, the adaptive mesh refinement programmed in the software let the unfilled polymer zones with the original split mapped mesh, and performed several consecutive refinements in the most irregular areas, that is, around the filler particles, and more particularly around their sharpest corners.

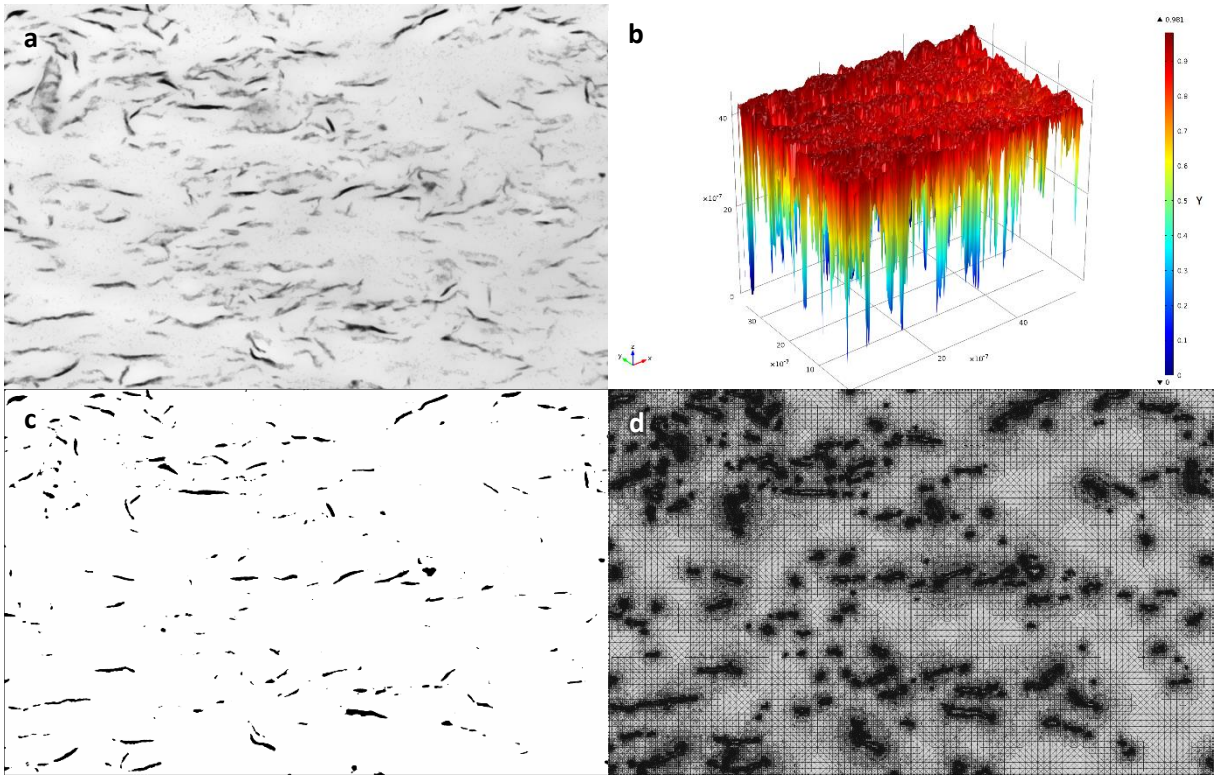

Figure III.4. Images of the nanocomposite structure as obtained from the first micrograph after undergoing enhancement by graphical processing (a), digitalization (b), binarization (c), and adaptive meshing (d).

Once the model was completed with the spatial discretization the simulation software was instructed to solve the system set out by computing the value of the solute flux in every finite element of the system domain after reaching the stationary state. In response, the software yielded the image exposed in **Figure III.5a**, where values of solute flux are represented by means of a rainbow color scale,

and by the size of the arrows drawn in the inset picture. As figures show, the simulation results predict a continuous flux of solute molecules going through the nanocomposite material, but, as the arrows point out, they do not follow a straight path but a marked tortuous path instead when bypassing the filler particles. In effect, as the insert shows, whereas molecules move following a straight line in the unfilled polymer zones, when they approach clay flakes, mainly oriented in perpendicular to the diffusion way, the molecules are forced to detour around particles and pass through the slits between them. Hence, in agreement with the simulation results and with the experimental observations, filler particles are responsible for the reduction in the solute diffusivity, since they increase the distance of the diffusion path, reduce the crossing area, and, as a result, increase the resistance undergone by the solute when it is displaced through the slits between adjacent particles in the same horizontal plane, and when it is constrained or "necked" while passing into and out of the narrower ones. All these phenomena are clearly visible in the detailed figures, where it is possible to observe that the solute flux is slowed down in the front and back of each and every of the particles, with respect to the average value computed in the neat polymer, whereas it is accelerated in their lateral edges and in the narrower slits between them. Regarding the path tortuosity of the diffusing molecules, it can also be visualized in a streamline plot, where the *x* and *y* components of the solute flux in every point of the system domain determine the direction of 200 streamlines starting from its upper boundary, as **Figure III.5b** shows. In light of the displayed plot, it can finally be stated that the filler particles of a nanocomposite material effectively increase the path tortuosity of the solute molecules and, in consequence, must produce a significant reduction of its relative diffusivity.

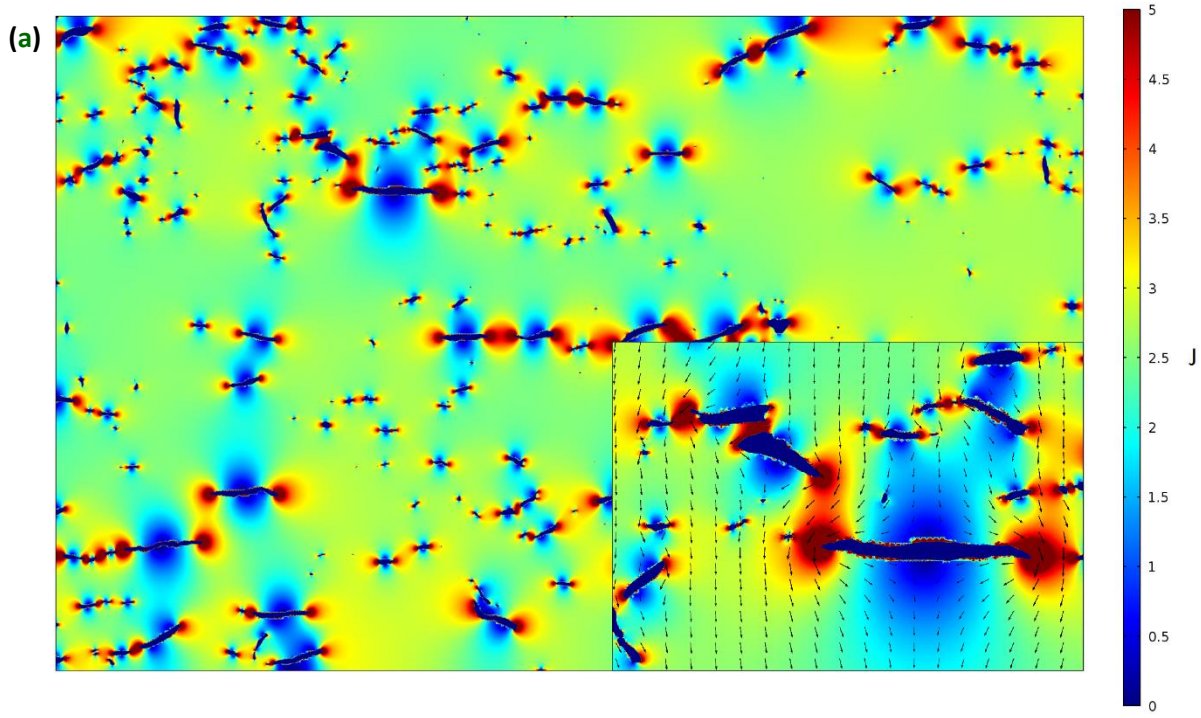

(b)

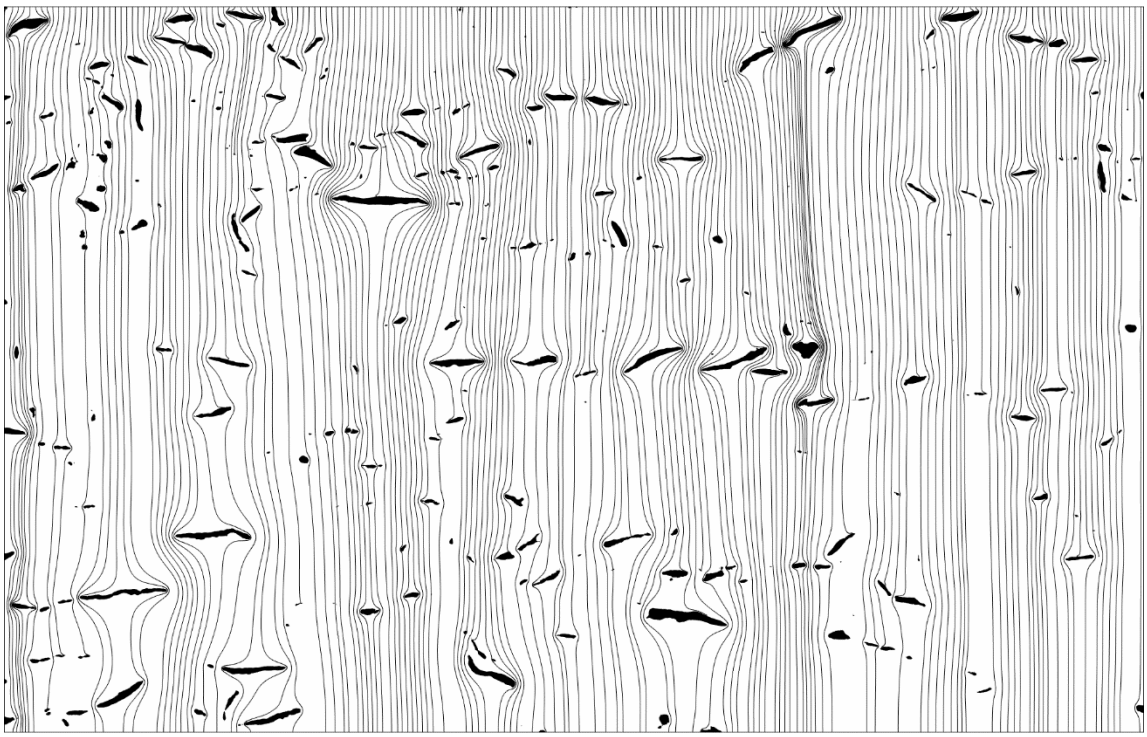

Figure III.5. Binary image of the nanocomposite structure as obtained from the first micrograph together with the representation of the solute flux magnitude and direction (a), and of 200 flux streamlines starting from its upper boundary (b).

Concerning this parameter, and following the procedure explained in the experimental section, its value can be calculated by averaging the solute flux over all the system domain, and by inserting the resultant number, together with the known preset value of the solute concentration gradient, in the previous equation (III.10). This way, the estimated values of the relative diffusivity of any solute molecule through the three studied nanocomposite materials could be finally obtained, and were collected in **Table III.2** together with their experimentally measured counterparts, and with the percentage relative error between both (model estimation error). As table shows, the diffusivity values predicted by the mathematical model were in good agreement with the measured values obtained from permeability data, as well as with other experimental values reported in a previous work [17], yielding model estimation errors located always under 2 %. However, and as can be seen in the table, those errors are negative in all cases, therefore suggesting that the model developed in this work tends to slightly overestimate the resistance to diffusion offered by the particles.

Nevertheless, when such estimation errors are compared with those yielded by the 18 previous theoretical models selected from the literature (**Figure III.6**), and collected above in **Table III.1**, it can be stated that the new propounded model and methodology produce the most accurate results

simultaneously for the three studied nanocomposite materials, only comparable to those of the newer and most complex theoretical approaches. **Tables SI-1** and **SI-2** of the supporting information include the results obtained for the relative diffusivities and estimation errors of the films of EVOH-29 with ≈ 1 % $^{v}/_{v}$ bentonite considering the particle parameters determined from their twelve micrographs. Indeed, as figures and tables show, for all the three cases treated in this paper model estimation errors typically range between 2 and 12 %, but these figures exhibit a decreasing trend in newer and more sophisticated theoretical developments, especially in those from the past decade, reaching values below 2 % in the two latest, including that of the present work. It must be noticed though that neither the model presented in this work nor the previous models reviewed from literature can take into account the size effects of the diffusing molecules, which, as suggested by the results experimentally found and those reported by other authors, could also become of great importance in certain cases.

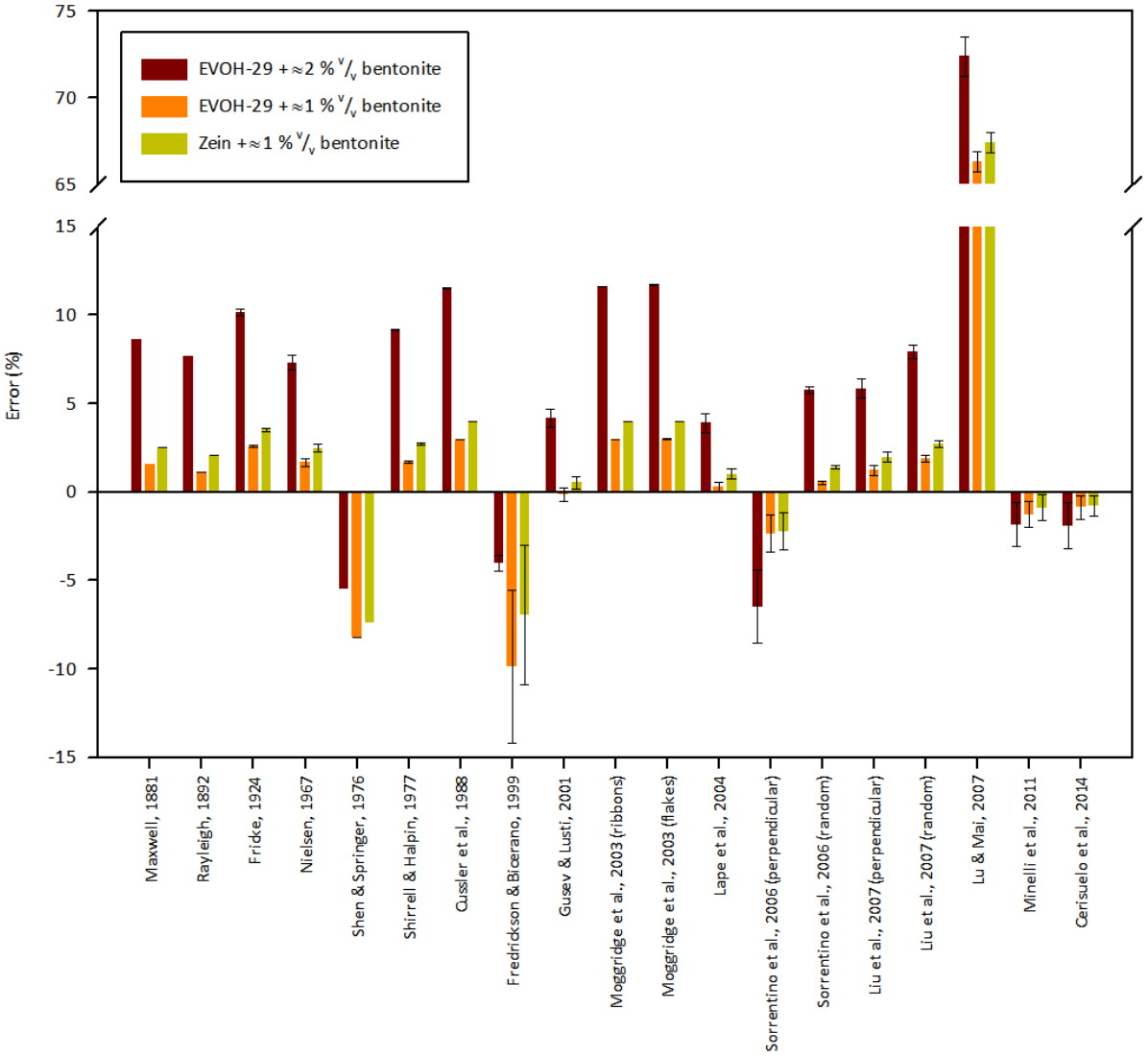

Figure III.6. Estimation errors of the new developed model and the 18 previous theoretical models selected from the literature for the diverse studied nanocomposite materials.

5. CONCLUSIONS

In this work, three nanocomposite materials intended for food packaging applications, consisting of EVOH-29 or zein matrices with approximately 1 or 2 % $^{v}/_{v}$ of bentonite nanoparticles as inorganic filler, were successfully developed in form of thin films, reaching an intercalated, nearly exfoliated, microstructure where most of the clay flakes remained oriented in parallel to the film surfaces.

These developed materials were considered to be very appropriate for active packaging applications, because of their great potential for slowing down the diffusion processes of solute or permeant compounds therethrough. However, their relative diffusivities could not be estimated in a reliable way through the application of most theoretical models reported in the literature, owing to their great disparity of results and low accuracy when working with low values of volume fraction and aspect ratio of particles.

With the aim of estimating the expected improvements in the barrier or retention properties of the developed nanocomposites a new and alternative method has been presented, which, based on the mathematical modeling and simulation of the diffusion processes taking place, can approach the value of their relative diffusivities by means of an analysis by the finite element method (FEM) of their micrographic film images, as observed by transmission electron microscopy (TEM).

The results yielded by this new method estimated average reductions of between 3.8 and 12.2 % in the value of their solute diffusivity, which, despite of the possible size effects of the diffusing molecules, was in considerable agreement with the measured values obtained from permeability data, as well as with other experimental values reported in a previous work for the diffusion of permanent gases in analogous materials, therefore validating the new propounded methodology.

Finally, this work also clearly visualized and modeled the tortuosity and necking effects of the filler nanoparticles on the mass transport processes occurring in nanocomposite materials, which has been the base for most theoretical developments from the 19th century to the present.

ACKNOWLEDGMENTS

The authors are grateful to the Spanish Ministry of Science and Innovation (project AGL2009-08776, AGL2012-39920-C03-01), EU (Nafispack project 212544), and Generalitat Valenciana (J.P.C. fellowship) for financial support, to ITENE (CSIC associate Unit) for technical collaboration, and to Mr. Tim Swillens (English edition services).

APPENDIX. SUPPORTING INFORMATION

Supplementary data associated with this article can be found in the online version at: *http://dx.doi.org/10.1016/j.memsci.2015.02.031*

REFERENCES

[1] Choudalakis, G., Gotsis, A. D. (2009). Permeability of polymer / clay nanocomposites: A review. *European Polymer Journal*, 45 (4), 967 – 984.

[2] Tjong, S. C. (2006). Structural and mechanical properties of polymer nanocomposites. *Materials Science and Engineering R: Reports*, 53 (3 – 4), 73 – 197.

[3] Paul, D. R., Robeson, L. M. (2008). Polymer nanotechnology: Nanocomposites. *Polymer*, 49 (15), 3187 – 3204.

[4] Pavlidou, S., Papaspyrides, C. D. (2008). A review on polymer – layered silicate nanocomposites. *Progress in Polymer Science (Oxford)*, 33 (12), 1119 – 1198.

[5] Feldman, D. (2013). Polymer nanocomposite barriers. *Journal of Macromolecular Science, Part A: Pure and Applied Chemistry*, 50 (4), 441 – 448.

[6] Kiliaris, P., Papaspyrides, C. D. (2010). Polymer / layered silicate (clay) nanocomposites: An overview of flame retardancy. *Progress in Polymer Science (Oxford)*, 35 (7), 902 – 958.

[7] Rhim, J. – W., Park, H. – M., Ha, C. – S. (2013). Bio – nanocomposites for food packaging applications. *Progress in Polymer Science*, 38 (10 – 11), 1629 – 1652.

[8] Rhim, J. – W., Ng, P. K. W. (2007). Natural biopolymer – based nanocomposite films for packaging applications. *Critical Reviews in Food Science and Nutrition*, 47 (4), 411 – 433.

[9] Sorrentino, A., Gorrasi, G., Vittoria, V. (2007). Potential perspectives of bio – nanocomposites for food packaging applications. *Trends in Food Science and Technology*, 18 (2), 84 – 95.

[10] Azeredo, H. M. C. (2009). Nanocomposites for food packaging applications. *Food Research International*, 42 (9), 1240 – 1253.

[11] Imran, M., Revol – Junelles, A. – M., Martyn, A., Tehrany, E. A., Jacquot, M., Linder, M., Desobry, S. (2010). Active food packaging evolution: Transformation from micro– to nanotechnology. *Critical Reviews in Food Science and Nutrition*, 50 (9), 799 – 821.

[12] Silvestre, C., Duraccio, D., Cimmino, S. (2011). Food packaging based on polymer nanomaterials. *Progress in Polymer Science (Oxford)*, 36 (12), 1766 – 1782.

[13] Persico, P., Ambrogi, V., Carfagna, C., Cerruti, P., Ferrocino, I., Mauriello, G. (2009). Nanocomposite polymer films containing carvacrol for antimicrobial active packaging. *Polymer Engineering and Science*, 49 (7), 1447 – 1455.

[14] Mascheroni, E., Chalier, P., Gontard, N., Gastaldi, E. (2010). Designing of a wheat gluten / montmorillonite based system as carvacrol carrier: Rheological and structural properties. *Food Hydrocolloids*, 24 (4), 406 – 413.

[15] Mascheroni, E., Guillard, V., Gastaldi, E., Gontard, N., Chalier, P. (2011). Anti – microbial effectiveness of relative humidity – controlled carvacrol release from wheat gluten / montmorillonite coated papers. *Food Control*, 22 (10), 1582 – 1591.

[16] Tunç, S., Duman, O. (2011). Preparation of active antimicrobial methyl cellulose / carvacrol / montmorillonite nanocomposite films and investigation of carvacrol release. *LWT – Food Science and Technology*, 44 (2), 465 – 472.

[17] Cerisuelo, J. P., Alonso, J., Aucejo, S., Gavara, R., Hernández – Muñoz, P. (2012). Modifications induced by the addition of a nanoclay in the functional and active properties of an EVOH film containing carvacrol for food packaging. *Journal of Membrane Science*, 423 – 424, 247 – 256.

[18] Cerisuelo, J. P., Gavara, R., Hernández – Muñoz, P. (2014). Natural antimicrobial – containing EVOH coatings on PP and PET films: Functional and active property characterization. *Packaging Technology and Science*, 27 (11), 901 – 920.

[19] Manias, E., Polizos, G., Nakajima, H., Heidecker, M. J. (2007). *Fundamentals of polymer nanocomposite technology*. Wilkie, C., Morgan, A. (eds.) *Flame retardant polymer nanocomposites.* Wiley – Interscience, Hoboken, NJ, USA.

[20] Falla, W. R., Mulski, M., Cussler, E. L. (1996). Estimating diffusion through flake – filled membranes. *Journal of Membrane Science*, 119 (1), 129 – 138.

[21] Maxwell, J. C. (1881). *Treatise on Electricity and Magnetism.* Clarendon Press, London, UK.

[22] Rayleigh, Lord. (1892). On the influence of obstacles arranged in rectangular order upon the properties of a medium. *Philosophical Magazine*, 34 (211), 481 – 502.

[23] Fricke, H. (1924). A mathematical treatment of the electrical conductivity and capacity of disperse systems. I. The electrical conductivity of a suspension of homogeneous spheroids. *Physical Review*, 24, 575 – 587.

[24] Nielsen, L. E. (1967). Models for the permeability of filled polymer systems. *Journal of Macromolecular Science (Chemistry)*, A1 (5), 929 – 942.

[25] Barrer, R. M. (1968). *Diffusion and permeation in heterogeneous media.* Crank, J., Park, G. S. (eds.) *Diffusion in polymers.* Academic Press, New York, NY, USA.

[26] Michaels, A. S., Chandrasekaran, S. K., Shaw, J. E. (1975). Drug permeation through human skin: Theory and in vitro experimental measurement. *AIChE Journal*, 21 (5), 985 – 996.

[27] Brydges, W. T., Gulati, S. T., Baum, G. (1975). Permeability of glass ribbon – reinforced composites. *Journal of Materials Science*, 10 (12), 2044 – 2049.

[28] Shen, C. H., Springer, G. S. (1976). Moisture absorption and desorption of composite materials. *Journal of Composite Materials*, 10 (1), 2 – 20.

[29] Shirrell, C. D., Halpin, J. (1977). Composite materials: testing and design [fourth conference]. *American Society for Testing and Materials Special Technical Publications*, 617, 514 – 528.

[30] Wakeham, W. A., Mason, E. A. (1979). Diffusion through multiperforate laminae. *Industrial and Engineering Chemistry Fundamentals*, 18 (4), 301 – 305.

[31] Aris, R. (1986). On a problem in hindered diffusion. *Archive for Rational Mechanics and Analysis*, 95 (2), 83 – 91.

[32] Cussler, E. L., Hughes, S. E., Ward, W. J., Aris, R. (1988). Barrier membranes. *Journal of Membrane Science*, 38 (2), 161 – 174.

[33] Eitzman, D. M., Melkote, R. R., Cussler, E. L. (1996). Barrier membranes with tipped impermeable flakes. *Fluid Mechanics and Transport Phenomena*, 42 (1), 2 – 9.

[34] Ly, Y. P., Cheng, Y. (1997). Diffusion in heterogeneous media containing impermeable domains arranged in parallel arrays of variable orientation. *Journal of Membrane Science*, 133 (2), 207 – 215.

[35] Fredrickson, G. H., Bicerano, J. (1999). Barrier properties of oriented disk composites. *Journal of Chemical Physics*, 110 (4), 2181 – 2188.

[36] Bharadwaj, R. K. (2001). Modeling the barrier properties of polymer – layered silicate nanocomposites. *Macromolecules*, 34 (26), 9189 – 9192.

[37] Gusev, A. A., Lusti, H. R. (2001). Rational design of nanocomposites for barrier applications. *Advanced Materials*, 13 (21), 1641 – 1643.

[38] Moggridge, G. D., Lape, N. K., Yang, C., Cussler, E. L. (2003). Barrier films using flakes and reactive additives. *Progress in Organic Coatings*, 46 (4), 231 – 240.

[39] Lape, N. K., Nuxoll, E. E., Cussler, E. L. (2004). Polydisperse flakes in barrier films. *Journal of Membrane Science*, 236 (1 – 2), 29 – 37.

[40] Liu, Q., De Kee, D. (2005). Modeling of diffusion through nanocomposite membranes. *Journal of Non – Newtonian Fluid Mechanics*, 131 (1 – 3), 32 – 43.

[41] Sorrentino, A., Tortora, M., Vittoria, V. (2006). Diffusion behavior in polymer – clay nanocomposites. *Journal of Polymer Science*, 44 (2), 265 – 274.

[42] Liu, W., Hoa, S. V., Pugh, M. (2007). Water uptake of epoxy – clay nanocomposites: Model development. *Composites Science and Technology*, 67 (15 – 16), 3308 – 3315.

[43] Statler, D. L., Gupta, R. K. (2007). A finite element analysis of the influence of morphology on barrier properties of polymer – clay nanocomposites. *Proceedings of the COMSOL Conference, October 5, 2007, Boston.*

[44] Minelli, M., Giacinti Baschetti, M., Doghieri, F. (2011). A comprehensive model for mass transport properties in nanocomposites. *Journal of Membrane Science*, 381 (1 – 2), 10 – 20.

[45] Minelli, M., Giacinti Baschetti, M., Doghieri, F. (2009). Analysis of modeling results for barrier properties in ordered nanocomposite systems. *Journal of Membrane Science*, 327 (1 – 2), 208 – 215.

[46] Bhunia, K., Dhawan, S., Sablani, S. S. (2012). Modeling the oxygen diffusion of nanocomposite – based food packaging films. *Journal of Food Science*, 77 (7), 29 – 38.

[47] DeRocher, J. P., Gettelfinger, B. T., Wang, J., Nuxoll, E. E., Cussler, E. L. (2005). Barrier membranes with different sizes of aligned flakes. *Journal of Membrane Science*, 254 (1 – 2), 21 – 30.

[48] Swannack, C., Cox, C., Liakos, A., Hirt, D. (2005). A three – dimensional simulation of barrier properties of nanocomposite films. *Journal of Membrane Science*, 263 (1 – 2), 47 – 56.

[49] Takahashi, S., Goldberg, H. A., Feeney, C. A., Karim, D. P., Farrell, M., O'Leary, K., Paul, D. R. (2006). Gas barrier properties of butyl rubber / vermiculite nanocomposite coatings. *Polymer*, 47 (9), 3083 – 3093.

[50] Picard, E., Vermogen, A., Gérard, J. F., Espuche, E. (2007). Barrier properties of nylon 6 – montmorillonite nanocomposite membranes prepared by melt blending: Influence of the clay content and dispersion state. Consequences on modeling. *Journal of Membrane Science*, 292 (1 – 2), 133 – 144.

[51] Kumar, P., Sandeep, K. P., Alavi, S., Truong, V. D. (2011). A review of experimental and modeling techniques to determine properties of biopolymer – based nanocomposites. *Journal of Food Science*, 76 (1), 2 – 14.

[52] Lu, C., Mai, Y. (2007). Permeability modeling of polymer – layered silicate nanocomposites. *Composites Science and Technology*, 67 (14), 2895 – 2902.

[53] ASTM D1434 – 82(2009)e1. Standard test method for determining gas permeability characteristics of plastic film and sheeting. ASTM International, West Conshohocken, PA, USA.

[54] Cerisuelo, J. P., Muriel – Galet, V., Bermúdez, J. M., Aucejo, S., Català, R., Gavara, R., Hernández – Muñoz, P. (2012). Mathematical model to describe the release of an antimicrobial agent from an active

package constituted by carvacrol in a hydrophilic EVOH coating on a PP film. *Journal of Food Engineering*, 110 (1), 26 – 37.

[55] Image import: homogenized pore scale flow and thermal conduction. Model ID: 12211. COMSOL Multiphysics Model Gallery, version 4.2a. COMSOL AB, Stockholm, Sweden.
http://www.comsol.com/showroom/gallery/12211/

IV MODIFICATIONS INDUCED BY THE ADDITION OF A NANOCLAY IN THE FUNCTIONAL AND ACTIVE PROPERTIES OF AN EVOH FILM CONTAINING CARVACROL FOR FOOD PACKAGING

Josep Pasqual Cerisuelo [a], José Alonso [b], Susana Aucejo [b], Rafael Gavara [a, *], Pilar Hernández – Muñoz [a]

[a] Laboratori d'envasos, Institut d'Agroquímica i Tecnologia d'Aliments, IATA – CSIC.
Av. Agustí Escardino, 7. 46980 Paterna, València.

[b] Institut Tecnològic de l'Embalatge, Transport i Logística, ITENE.
Parc Tecnològic de Paterna.
C/ Albert Einstein, 1. 46980 Paterna, València.

* Autor de contacte. Tel.: +34 963900022, e-mail: rgavara@iata.csic.es

ABSTRACT

A nanoclay/EVOH composite has been developed to retard the release of a volatile antimicrobial from an EVOH film with application in active packaging. Concretely, 2 % of bentonite nanoclay was added to the EVOH – 29 matrix to modify its mass transport properties and consequently the activity of the antimicrobial film. The nanocomposite obtained, containing 5 % of carvacrol as antimicrobial compound, is characterized in terms of antimicrobial solubility and release, water vapor solubility and permeability, oxygen and carbon dioxide permeability, diffusivity and solubility, thermal properties, and microstructural morphology.

The clay – filled EVOH – 29 film had a similar macroscopic appearance to the unfilled film, thanks to the excellent dispersion of bentonite nanoparticles as revealed by TEM images. Glass transition temperature was higher in the modified material, whereas fusion temperature was slightly lower, although the differences found were not significant. Water vapor, oxygen, carbon dioxide, and carvacrol solubilities were found to be higher for the modified polymer, whereas water vapor permeability, carvacrol diffusivity, and oxygen and carbon dioxide permeabilities and diffusivities were found to be lower for the nanocomposite. All parameters, with the exception of water vapor permeability, increased with the water concentration in the polymeric matrix. Therefore, the incorporation of 2 % bentonite nanoclay in EVOH – 29 provides a significant improvement in the controlled released of the antimicrobial agent with no relevant drawbacks.

***Journal of Membrane Science*, 2012, 423 – 424, 247 – 256.**

1. INTRODUCTION

Controlled release of substances from polymeric matrices is being applied in several industrial sectors including drug delivery in medical and pharmaceutical devices, active membranes and active food packages. In the latter, antimicrobial packaging is the focus of attention of the food processing sector. An antimicrobial agent is incorporated into the packaging walls and released to the food surface where it is needed [1]. The effectiveness of the active packaging material is related to the existence of a triggering mechanism involved in the commencement of the agent release and to the control of the extent and kinetics of the release in such way that the minimum inhibitory concentration for the target microorganism is achieved and maintained as long as possible during product commercialization [2].

In a previous study [3], carvacrol, a well-known phenolic monoterpene constituent of essential oils produced by various aromatic plants such as oregano, thyme, marjoram, and savory [4], was incorporated in an EVOH matrix to protect a salad from deterioration by microbial growth. In that work, the triggering mechanism of carvacrol release was the absorption of food moisture by EVOH, a highly hydrophilic material which is plasticized by the sorption of humidity from the package headspace [5 – 7]. Unfortunately, the application of the active film to the preservation of high water content food products showed an unconstrained free diffusion from the packaging materials that induces an early peak of high antimicrobial concentration, followed by a rapid decay below the MIC in a few days [2, 3].

One of the well-known alternatives to modify mass transport in polymeric matrices is to incorporate an inorganic filling, preferably of nanometric dimensions, into the packaging material. The resulting nanocomposite may present a reduction in the diffusivity of all migrating compounds and enhancement of the thermal and mechanical properties and the barrier to atmospheric gases [8, 9]. Some of the most reported filling materials are montmorillonitic nanoclays, such as sodium bentonite, a hydrophilic aluminum phyllosilicate with high water sorption and swelling capacity that can be homogeneously dispersed in a polymeric matrix to form the new nanocomposite.

Consequently, the aim of this work was to study the modifications induced in an EVOH-29 film containing 5 % carvacrol as antimicrobial active agent, by the addition of 2 % of bentonite nanoclay. The modification has been characterized in terms of thermal properties and microstructural morphology, carvacrol solubility and release, water vapor solubility and permeability, oxygen and carbon dioxide permeability, diffusivity, and solubility.

2. MATERIALS AND METHODS

2.1. Materials

Ethylene-vinyl alcohol copolymer with a 29 % ethylene molar content (EVOH-29) was kindly supplied by The Nippon Synthetic Chemical Company (Osaka, Japan).

Carvacrol of at least 98 % purity was purchased from Sigma-Aldrich (Barcelona, Spain), as well as sodium bentonite nanoclay and reagent-grade lithium chloride, potassium acetate, magnesium chloride, potassium carbonate, magnesium nitrate, sodium nitrite, sodium chloride, potassium chloride, barium chloride, and phosphorus pentoxide. Reagent-grade 1-propanol and high-vacuum silicone were supplied by Panreac (Barcelona, Spain), and deionized water was obtained from a Millipore Milli-Q Plus purification system (Molsheim, France).

2.2. Preparation of the EVOH-29 and nanocomposite active films

EVOH-29 and nanocomposite active films were prepared from a hydroalcoholic solution of the polymer with the antimicrobial agent incorporated. For the simple EVOH-29 films, the required amount of EVOH-29 pellets was fully dissolved in a glass flask with a 1:1 (w/w) mixture of deionized water and 1-propanol. Then the antimicrobial agent was added to the solution at a concentration of 5 g carvacrol / 100 g EVOH-29 and the solution was homogenized for 10 more minutes, as described elsewhere [3].

As for the nanocomposite films, the required amount of bentonite nanoclay was thoroughly mixed with deionized water in a disperser (Ultra-Turrax T25 basic model, IKA, Germany) for 30 seconds at 24000 rpm in order to wet all clay agglomerates and break them down into primary particles. The mixture obtained was then placed in an ultrasonic bath (Ultrasons model, J. P. Selecta, Spain) for at least 1 hour to allow optimal splitting (delamination) of the agglomerates. When a stable suspension was formed, it was left to rest overnight to allow intensive swelling and hydration of the remaining agglomerates and to achieve the optimal suspension characteristics. A given amount of carvacrol was dissolved in 1-propanol, and the solution obtained was mixed in the ultrasonic bath for at least 15 minutes with the suspension prepared the day before. The resulting mixture was then used to dissolve EVOH-29 pellets following the procedure explained before for the simple EVOH-29 films. The final hydroalcoholic solution contained 5 g of carvacrol and 2 g of bentonite per 100 g of EVOH-29.

Both formulated solutions were used in the preparation of the active films by casting over previously cleaned glass plates with the aid of a steel stud with a 200 µm deep thread (Lin-Lab Rioja, Logroño, Spain). Dry films were stored in drying chambers with phosphorus pentoxide at room temperature until utilization. In these conditions, the volatiles remaining in the films (including alcohol and water is below 2 % as it was reported previously [3]. The thickness of each film sample was measured individually, prior to testing, with a digital micrometer (Mitutoyo, Osaka, Japan), giving an average value of 30 ± 2 µm.

2.3. Determination of microstructural morphology

The microstructural morphology of the prepared films was studied by transmission electron microscopy (TEM) and scanning electron microscopy (SEM) with the objective of confirming the achievement of a nanocomposite structure by comparison with the appearance of the unmodified polymer. TEM analysis was carried out in a JEM-1010 unit (JEOL, Germany) with 100 kV accelerating voltage and equipped with a Megaview III digital camera and analySIS image acquisition software. Samples for TEM were prepared by blocking both films in cured epoxy resin and cutting them by ultramicrotomy. SEM analysis was carried out in a Hitachi S-4100 unit (Hitachi, Spain) with 30 kV accelerating voltage and equipped with a BSE Autrata detector and an EMIP 3.0 image capture system. Film samples were prepared by cryofracture under liquid nitrogen and were adhered to the faces of a copper cube by fixing them with double-sided carbon tape and silver paint. Samples were also coated with gold–palladium under vacuum in a sputter coating unit prior to inserting them in the SEM unit.

2.4. Determination of water vapor solubility

Differences in water vapor solubility between EVOH-29 and EVOH-29 + 2 % bentonite were studied by evaluation of their corresponding moisture sorption isotherm. With this aim samples of both films were cut into small pieces weighing 400 – 500 mg in total, placed in aluminum dishes, and allowed to reach the corresponding moisture equilibrium when exposed to various relative humidities in 10 L sealed containers placed in an environmental chamber conditioned at 23 ± 2 °C. Silica gel and nine saturated salt solutions with excess salt were placed in the containers 48 hours before the film samples. The salts and corresponding humidities employed were: silica gel, 4.5 % RH; LiCl, 11.3 % RH;

CH_3COOK, 23.1 % RH; $MgCl_2$, 33.1 % RH; KCO_3, 43.2 % RH; $MgNO_3$, 54.4 % RH; $NaNO_3$, 64.2 % RH; NaCl, 75.5 % RH; KCl, 85.1 % RH; $BaCl_2$, 91.0 % RH; and deionized water, 100 % RH. The samples rested in the containers for approximately two weeks and their weight was monitored periodically until no differences were observed between three measurements taken on consecutive days. Once constant weights were obtained, the samples were removed and dried in a vacuum oven at 60 °C for 24 h to record their dry weight. The equilibrium moisture content was calculated on a dry basis and reported as the average of three replicates assayed at each RH condition. The experimental values were fitted by the D'Arcy & Watt equation [10, 11]:

$$\frac{m_w}{m_p} = \frac{\chi_1 \chi_2 a_w}{1+\chi_1 a_w} + \chi_3 a_w + \frac{\chi_4 \chi_5 a_w}{1-\chi_4 a_w} \qquad \text{(IV.1)}$$

where m_w / m_p is the water concentration in the polymer on a dry basis (kg water / kg dry polymer), a_w stands for the water activity, and χ_i are different parameters related with the bond energy (χ_1 and χ_4), the number of active sites involved in the Langmuir sorption isotherm (χ_2), the water solubility in the polymeric matrix (Henry's law) (χ_3), and the capacity of water molecules to form multilayers (χ_5). To evaluate the goodness of the fit the root mean squared error (RMSE) of each regression model was calculated for both fittings.

2.5. Determination of carvacrol equilibrium parameters

To determine the extent of carvacrol release as a function of the relative humidity, and to measure the corresponding equilibrium parameters, equilibrium cells were built as described in a previous work [3]. Each closed vial included a 5 cm^2 film sample (EVOH-29 or EVOH-29 + 2 % bentonite) and a saturated saline solution to ensure constant relative humidity during the test. The salts and corresponding humidities employed were: KCO_3, 43.2 % RH; $MgNO_3$, 54.4 % RH; NaCl, 75.5 % RH; $BaCl_2$, 91.0 % RH; and deionized water, 100 % RH. Samples were prepared in quadruplicate and stored in a dark room at 23 ± 2 °C for at least two weeks in order to let them reach their state of equilibrium. Then the carvacrol concentration in the headspace was monitored by headspace sampling and GC analysis until no differences were observed between three measurements taken on consecutive days [3]. To measure the carvacrol concentrations in the headspace, 500 µL aliquots were taken from the vial with a precision gas syringe (1750 Gastight model, Hamilton, Bonaduz, Switzerland), and they were placed in the injection port of an HP 5890 Series II Plus gas chromatograph (Agilent Technologies, Wilmington,

DE, USA) equipped with a flame ionization detector (FID) and a 30 m, 0.32 mm, 0.25 µm HP-5 capillary column. Chromatographic conditions were as follows: He as the carrier gas, splitless injection, 210 °C and 260 °C injector and detector temperatures, 1 min at 120 °C, heating ramp to 220 °C at 20 °C/min, and 1 min more at 220 °C. The sample volume withdrawn was restored with air to keep constant pressure. The GC response was previously calibrated by injecting known amounts of carvacrol. Difficulties to obtain reliable results with this technique impeded the equilibrium characterization at relative humidities below 43.2 %.

Once the samples were at equilibrium, the carvacrol concentration in the polymer samples was determined by thermal desorption and GC analysis using a thermal desorber (890/891 model, Dynatherm Analytical Inst., Supelco, Bellafonte, PA, USA) connected in series to the gas chromatograph described previously. A portion of the tested film (about 20 mg) was placed in the desorption cell and heated at 210 °C for 7 minutes. A He gas stream carried the desorbed gaseous compounds to the GC through a transfer line heated at 230 °C. The GC was equipped with a 30 m, 0.53 mm, 2.65 µm Agilent HP-1 semicapillary column. The chromatographic conditions were: He as the carrier gas, 210 °C and 260 °C injector and detector temperatures, 7 min at 45 °C, heating ramp to 220 °C at 18 °C/min, and 12 min more at 220 °C. At the end of the desorption process the sample was weighed with a 0.1 mg precision balance (Voyager V11140 model, Ohaus, Switzerland). The response of the GC was calibrated by measuring polyethylene and polypropylene samples with known amounts of carvacrol.

The values of carvacrol Henry's constant for each film analyzed, H_c^P (P = E stands for EVOH-29 and P = B stands for EVOH-29 + 2 % bentonite), and for each relative humidity assayed, could easily be calculated from the concentrations in the headspace, C_c^{HS}, and in both films, C_c^E and C_c^B, by means of the following expressions:

$$H_c^E = \frac{C_c^{HS}}{C_c^E} \text{ and } H_c^B = \frac{C_c^{HS}}{C_c^B} \qquad \text{(IV.2)}$$

Since the drying processes during film casting always entail some losses of the antimicrobial agent in the films obtained, carvacrol retention in both original and filled polymers was measured in order to assess the possible differences existing between their manufacturing efficiencies. These evaluations were carried out by analyzing film samples in the thermal desorber described above, immediately after they were produced in the drying hood.

2.6. Determination of carvacrol release kinetic parameters

To study the rate of carvacrol release from the active films as a function of the relative humidity, and to quantify the corresponding kinetics parameters, a polymer sample was inserted individually in a desorption tube where a humidified nitrogen stream blowing at a constant flow rate carried the carvacrol molecules released to a gas chromatograph for their analysis as described in a previous work [3]. The evolution with time of the carvacrol mass flow released from the sample was converted to carvacrol concentration values, averaged for the whole film thickness, and they were introduced in the solution of Fick's law for a process of desorption from an infinite sheet [12]:

$$C_c^P = \frac{2 \cdot C_{c0}^P}{\pi^2} \sum_{\nu=1}^{\infty} \frac{1}{\left(\nu - \frac{1}{2}\right)^2} \cdot e^{\frac{-\pi^2 \cdot \left(\nu - \frac{1}{2}\right)^2 \cdot D_c^P \cdot t}{L_P^2}} \qquad \text{(IV.3)}$$

so that the value of D_c^P for each sample and RH condition could be evaluated. Each experiment was performed five times.

2.7. Thermal characterization

Differences between the thermal behavior of the two materials were studied by means of differential scanning calorimetry (DSC) with a Q2000 unit (TA instruments, USA). Film samples, previously equilibrated at 23 ± 2 °C and at 4.5 % RH with silica gel and 91.0 % RH with a saturate saline solution of $BaCl_2$ were cut into small pieces weighing 10 – 20 mg in total, and were placed in T-zero aluminum hermetic pans. Thermal tests were conducted from –60 to 220 °C with 10 °C/min heating rate. Thermograms of first and second heating cycles were obtained, and glass transition and fusion temperatures were measured.

2.8. Determination of water vapor permeability

Water vapor permeability tests were carried out using Elcometer 5100 Payne permeability cups (Elcometer, England) in accordance with ASTM E96/E96M-10 [13]. The cups were filled with 10 g of deionized water, the rims were coated with silicone vacuum grease (Sigma, Spain), and the film to be tested was held in place with a flat Viton ring, an aluminum ring, and three press-screws. Then the cups were exposed to various relative humidities in 10 L sealed containers placed in an environmental chamber conditioned at 23 ± 2 °C. In this case, phosphorous pentoxide and three saturated salt solutions with excess salt were employed to achieve four different relative humidities in the headspace of the containers: P_4O_{10}, 0 % RH; $MgCl_2$, 33.1 % RH; $MgNO_3$, 54.4 % RH; and NaCl, 75.5 % RH. Samples were prepared in quadruplicate and were weighed daily. The initial slope of the weight loss versus time curve yielded the water vapor transmission rate values. These rates were then divided by the water vapor pressure gradient and multiplied by sample thickness to obtain the water vapor permeability coefficient.

2.9. Determination of oxygen permeability, diffusivity, and solubility

Improvements in the barrier properties to oxygen for the nanocomposite with respect to the unmodified polymer were evaluated with the aid of an OX-TRAN model 2/21 ML (Lippke, Germany) programed to measure the oxygen permeability at 23 ± 2 °C and at (0, 35, 50, 75, and 90 ± 0.01) % RH. Two film samples were placed in both instrument cells and conditioned for 8 hours. The transmission values were determined every 45 min until constant. After the permeation tests were completed, continuous permeation experiments were carried out on each sample to determine the oxygen diffusion coefficient at 23 ± 2 °C and at (0, and 90 ± 0.01) % RH. The value of this parameter was calculated from the solution to Fick's second law for the boundary conditions of an isostatic permeation experiment, by introducing in equation (IV.3) all the transmission rate values measured during the transient state. Both permeation and diffusion experiments were performed on four film samples per studied material. To determine the oxygen solubility coefficient the values of oxygen permeability and diffusivity obtained at 0 and 90 % RH were introduced in the following expression:

$$S = \frac{P}{D} \qquad \text{(IV.4)}$$

2.10. Determination of carbon dioxide permeability, diffusivity, and solubility

Enhancements in the barrier properties to carbon dioxide for the filled polymer were evaluated with the aid of an isostactic permeation apparatus at 23 ± 2 °C and at (0, 25, 50, 75, 85, and 100 ± 0.1) % RH for gas permeability, and at (0, and 90 ± 0.1) % RH for gas diffusivity. In brief: a stainless-steel cell with two chambers separated by the film to be tested was used. A constant gas stream was passed through each chamber at the required relative humidity. The permeant gas, carbon dioxide, flowed through the upper chamber while the carrier gas, nitrogen, flowed through the lower chamber and drove the permeated molecules to the detector system. To humidify the gases, each source gas stream was split into two separate flows. The first flow was bubbled through a gas washing bottle filled with deionized water and then mixed with the second flow of dry gas to achieve the appropriate humidity. Rotameters (Dakota Instruments, USA), needle valves (Swagelok, USA), and digital thermo-hygrometers (TFA, Germany) were used to adjust and control each split gas stream. The flow rate of the combined carrier gas was measured by a mass flowmeter (Dakota Instruments, USA) at the exit of the lower chamber. The concentration of CO_2 in this stream was analyzed by gas chromatography. An HP 5890 Series II Plus gas chromatograph (Agilent Technologies, USA) equipped with a thermal conductivity detector (TCD), a Chromosorb 102, 80/100 mesh, 12" × 1/8" column (Teknokroma, Spain), a manual injection valve, and a 250 µL injection loop was used. The instrument was calibrated by injecting known amounts of carbon dioxide. At the beginning of the test the carrier gas was passed through both chambers for at least 12 h to remove residuals of all gases present in the cell during film handling and cell assembling, and to equilibrate the assayed film to the relative humidity of the test. At time zero, the permeant gas started to flow into the upper chamber and to permeate through the film being tested. The concentration of carbon dioxide in the lower chamber was monitored until constant and converted to transmission rate values by accounting for the measured gas flow rate. Gas permeability was calculated from the average of the last three CO_2TR values, permeant diffusivity was assessed by introducing in equation (IV.3) all the transmission rate values measured during the transient state, and CO_2 solubility coefficients were calculated by introducing the permeability and diffusivity values measured at 0 and 90 % RH in equation (IV.4).

2.11. Data analysis

The values for all the measured parameters and coefficients presented in this research work are expressed as "$(\bar{x} \pm \varepsilon)$ units," where $\bar{x}$ stands for the sample mean of parameter x, and ε stands for the absolute error of parameter x. This absolute error is equal to sample standard deviation for measured parameters, and was determined by means of propagation of uncertainty (partial derivatives method) for calculated parameters.

Data fitting to Peleg's equation was performed using a nonlinear regression analysis of a 3-parameter sigmoidal function. Data fitting to water-dependent diffusion or permeability equations was performed using a linear regression analysis of the classical slope-intercept or quadratic equations respectively. Both linear and nonlinear regression analyses were carried out with the aid of the SigmaPlot 12.1 Dynamic Fit Wizard. Values obtained for regression parameters are also expressed as "$(\bar{x} \pm \varepsilon)$ units," where $\bar{x}$ stands for the sample mean of parameter x, and ε stands for the asymptotic standard error of parameter x calculated by the regression software.

Statistical analysis of the results obtained for gas diffusivities and solubilities was performed with the aid of IBM SPSS Statistics 20 commercial software (IBM Corp., Armonk, NY. USA). Differences found between pairs of mean values for both studied materials were assessed by means of an independent-samples T test at a $p \leq 0.10$ level of significance.

3. RESULTS AND DISCUSSION

3.1. Film appearance and microstructural morphology

EVOH films are known to have great optical properties, with high transparency, a high glossy surface, and little to no coloration. With the incorporation of 2 % bentonite in the polymeric matrix the material attains a slightly cloudy appearance, thus reducing its transparency but maintaining its original gloss and color properties. The presence of clay particles in the film is not visible to the naked eye.

SEM and TEM micrographs of both control and nanocomposite materials are displayed in **Figure IV.1**. In the SEM images the unfilled polymer (**A**) has a clean appearance with the exception of some debris formed in the cryofracture process, whereas the nanocomposite material (**B**) shows a grainier surface

suggesting the presence of clay nanoparticles well embedded in the polymeric matrix. In the TEM pictures the unmodified EVOH image (**C**) shows a clean and spotless appearance, whereas the one for the nanocomposite (**D**) displays a clear view of the embedded particles of bentonite nanoclay, oriented mostly in parallel to the direction of casting. As the picture shows, the exfoliation of clay agglomerates during the preparation of the suspension was reasonably acceptable.

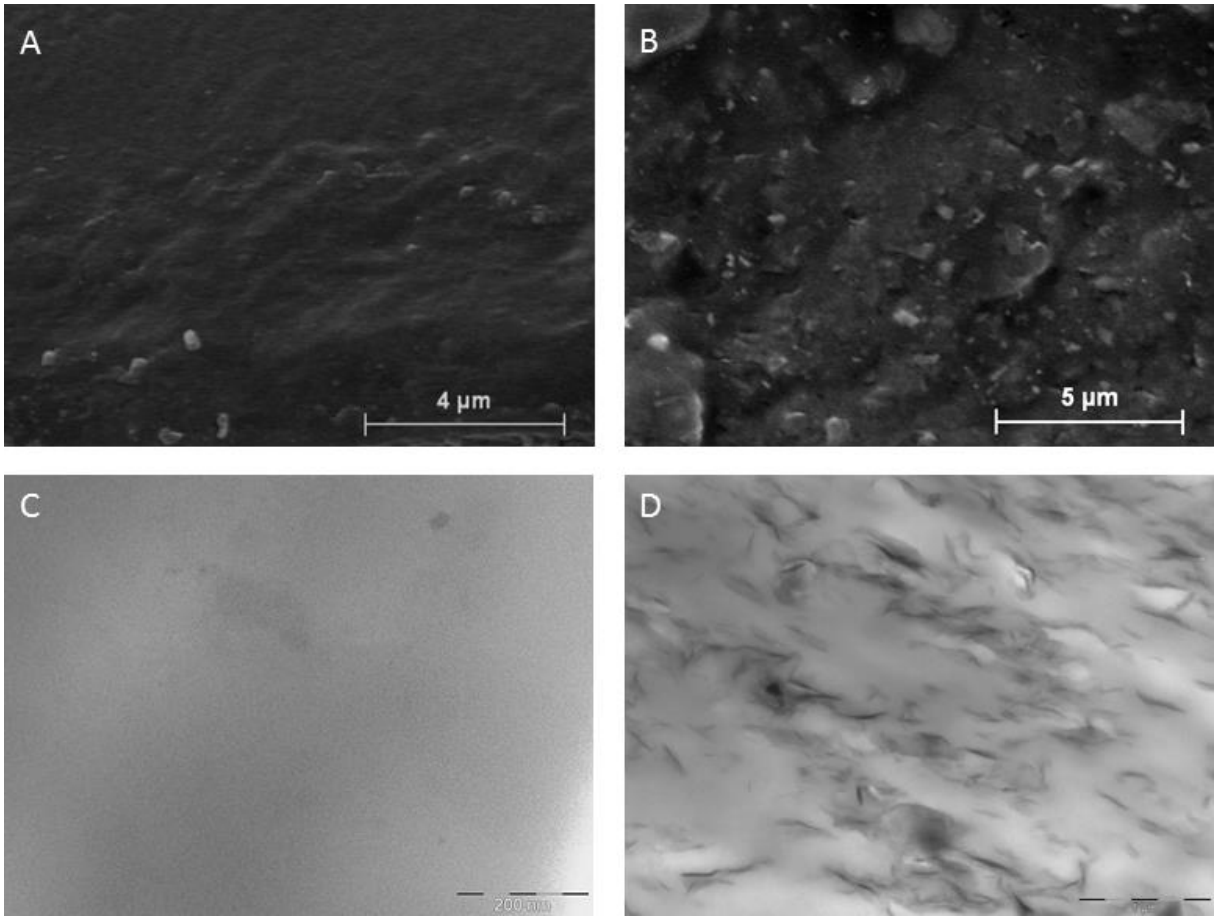

Figure IV.1. SEM images of the control EVOH-29 film (A) and the nanocomposite containing 2 % of bentonite (B). TEM images of the same samples (C: EVOH-29 and D: nanocomposite).

3.2. Assessment of water vapor solubility

Water sorption isotherms obtained for EVOH-29 and EVOH-29 + 2 % bentonite are displayed in **Figure IV.2**. As the graph shows, the two materials have similar behavior when exposed to water vapor since their moisture contents grow almost in parallel when the relative humidity increases, although the nanocomposite seems to absorb about 17 % more than the original polymer along the whole isotherm.

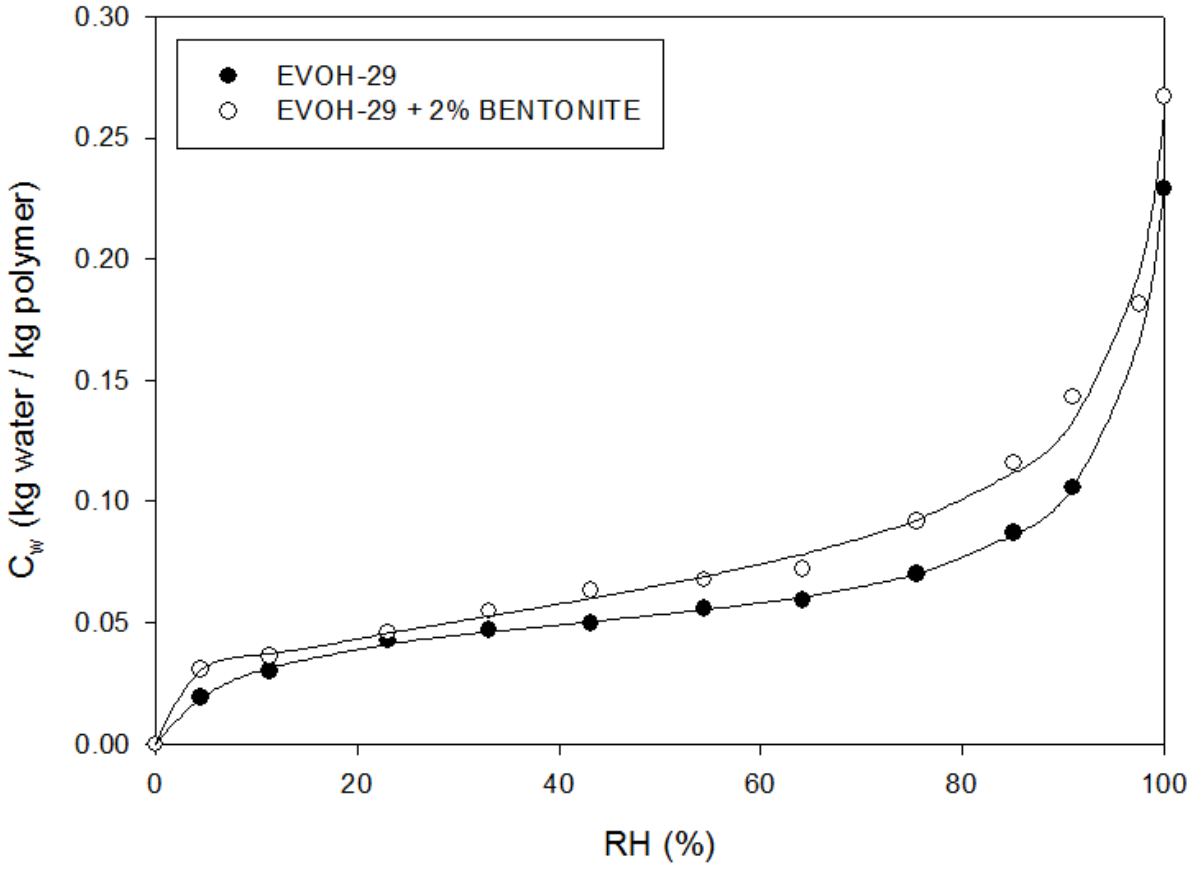

Figure IV.2. Water sorption isotherms of the control and bentonite-containing EVOH-29 films.

Plotted values for both polymers were fitted to the D'Arcy & Watt model, yielding the estimated values for all χ_j parameters, as detailed in **Table IV.1**.

Table IV.1. Estimated values for the D'Arcy & Watt equation parameters as obtained from the isotherm curves fitted to the EVOH-29 and EVOH-29 + 2 % bentonite experimental points.

D'Arcy & Watt model parameters	EVOH-29	EVOH-29 + 2 % bentonite
χ_1	11.8154	31.4963
χ_2	0.0530	0.0480
χ_3	0.0000	0.0000
χ_4	0.9536	0.9035
χ_5	0.0088	0.0210

The greater water solubility exhibited by the filled EVOH can be explained by the water sorption properties of bentonite nanoclay, since its high hydrophilic nature allows it to absorb several times its

weight in water when exposed to ambient humidity, by including numerous water molecules between its molecular sheets. The Langmuir contribution to the D'Arcy & Watt equation is indicative of faster water adsorption involving the clay platelets. No Henry's contribution was estimated, owing to the substantial Langmuir contribution at low humidities and the considerable contribution of the water cluster formation and at high humidities.

3.3. Assessment of carvacrol equilibrium as a function of water concentration

The effect of moisture sorption by EVOH-29 and EVOH-29 + 2 % bentonite active films on the extent of carvacrol release was studied with the aid of the equilibrium cells described in the experimental sections. The values of the water concentration in both materials, C_w^P, were calculated by means of the D'Arcy and Watt water sorption isotherms obtained before (**Table IV.1**). The values of the Henry's constants, H_c^P, obtained experimentally have been plotted in **Figure IV.3**. The evolution of carvacrol Henry's constant with water concentration presented a similar profile for the unfilled and filled active films. As **Figure IV.3** shows, the values of this parameter for both air / polymer systems increase sigmoidally with water concentration in the polymeric matrix, although nanocomposite active films seem to display less affinity for carvacrol, since their Henry's constant values are always approximately 3-fold higher on average than those attained by the unmodified polymer. Both progressions can be described with Peleg's model [14]:

$$H_c^P = \frac{H_{c0}^P}{1 + e^{\frac{C_{wc}^P - C_w^P}{a}}} \qquad \text{(IV.5)}$$

where H_{c0}^P is the carvacrol Henry's constant at the maximum value of water concentration in the films, C_{wc}^P is the critical concentration of water at the inflexion point of the curve, and a accounts for the steepness of the drop in the magnitude of H_c^P. By adjusting the plotted points to Peleg's model the values for all the equation parameters could be finally obtained (**Table IV.2**). The curves predicted by Peleg's model presented good agreement with the experimental results in both materials, as **Figure IV.3** shows.

Table IV.2. Estimated values for the Peleg's equation parameters as obtained from the carvacrol equilibrium curves fitted to the EVOH-29 and EVOH-29 + 2 % bentonite experimental points.

Peleg's model parameters	EVOH-29	EVOH-29 + 2 % bentonite
$H^{P}_{c0} \cdot 10^{6}$	2.51 ± 0.05	7.5 ± 0.1
$C^{P}_{wc}\ (kg/m^3)$	96.2 ± 1.6	118.9 ± 1.5
a	11.2 ± 1.0	27.5 ± 1.5

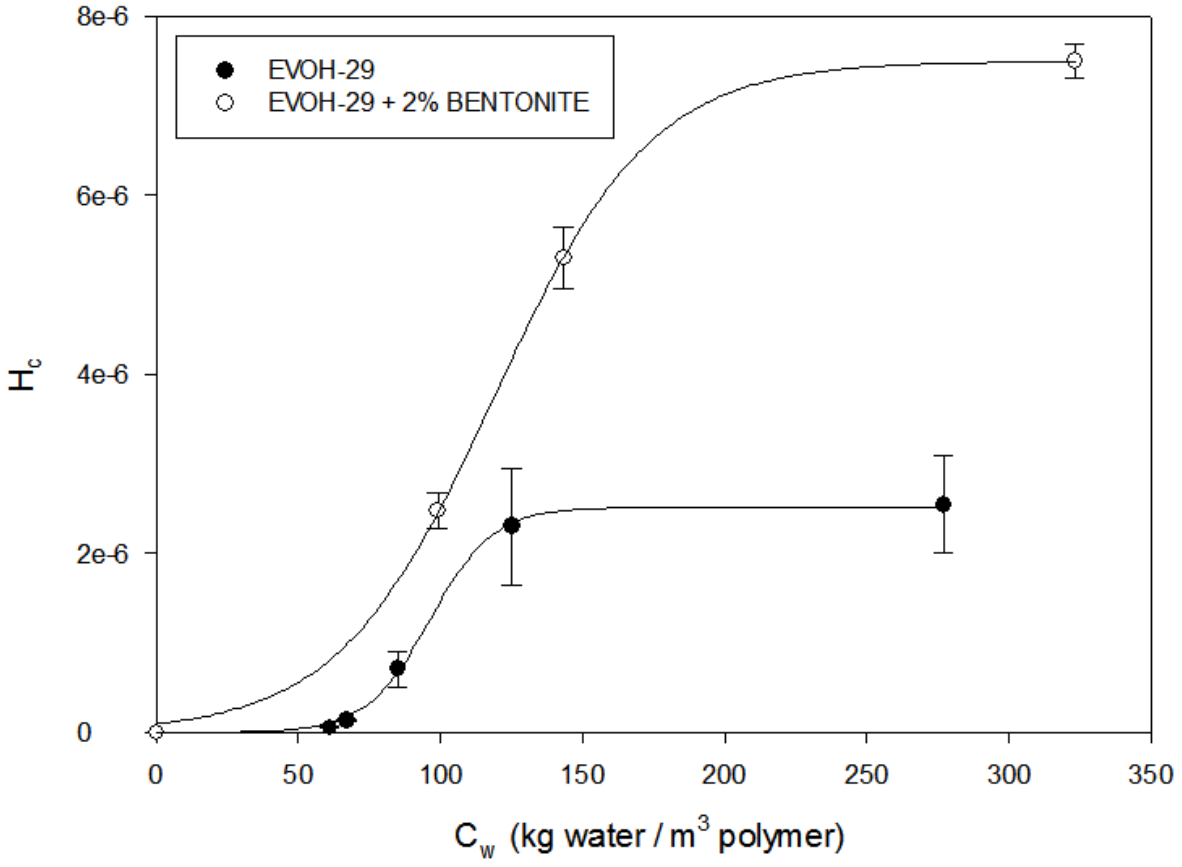

Figure IV.3. Values of Henry's constant for carvacrol in control and bentonite-containing EVOH-29 films as affected by the water content.

The low values of Henry's constant observed in both air / polymer systems could be explained by means of the interactions existing between the OH groups of the alcohol segments of the EVOH-29 and the phenol structure of carvacrol, and the low vapor pressure at saturation for this compound. At dry and very low relative humidity, the values of Henry's constant are very low because of the low concentration of carvacrol in air. In any case, the measured headspace concentration for both samples

was well below the concentration corresponding to saturation, 0.246 g/m^3 (measured in a closed vial with pure carvacrol) [15]. At humid conditions, the hydrophobic nature of carvacrol could cause its transfer to the cell atmosphere when the water concentration increase in the polymer matrix increases the polarity of the solid media and reduces the solubility of the antimicrobial agent in the polymer phase. The addition of the clay particles was expected to increase both the hydrophilicity of the nanocomposite matrix and the moisture uptake, both effects contributing to an increase in the Henry's constant values in the whole water concentration range. Nevertheless, the carvacrol concentration in the headspace was always far below saturation, even for the nanocomposite exposed at the highest humidity ($C_c^{HS} < 0.1$ g/m^3), indicating sufficient solubilization of the compound in the control polymer and in the composite.

The value of the critical water concentration increases by 22.7 kg/m^3 with the addition of the nanoclay, which might be related with an increase in rigidity of the sample. The higher value of *a* measured for the nanocomposite indicates the higher values of Henry's constant measured at high humidities. The critical concentration of plasticizer (water in this study, C_{wc}^P) has been related to the point at which glass transition takes place [16]. According to the values in **Figure IV.3** and the result of the application of Peleg's model, the glass transition takes place at about 23 °C and 82.0 % RH for the unfilled polymer and at 23 °C and 84.4 % RH for the filled material, in agreement with previous studies [17]. An explanation for the slightly higher value obtained for the nanocomposite might be a higher constraint on polymer chain motions induced by the presence of the clay platelets.

The value of Henry's coefficient in very dry conditions could not be obtained experimentally because there were large deviations at low humidities owing to difficulties in keeping the sample dry with this analytical procedure. Therefore extrapolated values of $1.0 \cdot 10^{-9}$ and $1.0 \cdot 10^{-7}$ for the original and filled EVOH-29, respectively, were calculated using Peleg's model.

With respect to the antimicrobial retention during the drying step of the film-forming processes, EVOH-29 showed a reasonable retention capacity of about 70 %, whereas the nanocomposite exhibited an excellent efficiency of approximately 95 %. The presence of clay platelets and aggregates with a high capacity to entrap numerous microdrops or clusters of carvacrol molecules, and restrictions during the diffusion of the carvacrol molecules from the film during the drying process, are the causes of this improvement. These results are in high agreement with others reported in the literature for similar polymer/clay systems [18, 19].

3.4. Assessment of carvacrol kinetics as a function of water concentration

For the determination of the carvacrol diffusivity values, D_c^P, equation (IV.3) was used, assuming that during the desorption process the water concentration in the films remained constant and uniform throughout the thickness, and subsequently also the diffusion coefficient value for carvacrol. This approach was successfully applied elsewhere [20]. **Figure IV.4** is the plot of the values of the carvacrol diffusion coefficient measured in both active films, D_c^P, for every water concentration assayed in each polymer, C_w^P. The value in dry conditions was estimated by extrapolation since the slow release impeded its determination with the experimental approach used. Nevertheless, when diffusivity values obtained for both materials are plotted versus water concentration in its polymeric matrix, they all form a straight line that fits well with the classical slope-intercept equation of a linear trend line:

$$D_c^P = D_{c0}^P + \gamma^P \cdot C_w^P \qquad \text{(IV.6)}$$

where D_{c0}^P is the carvacrol diffusion coefficient in the absence of absorbed water and γ^P is the water plasticization coefficient.

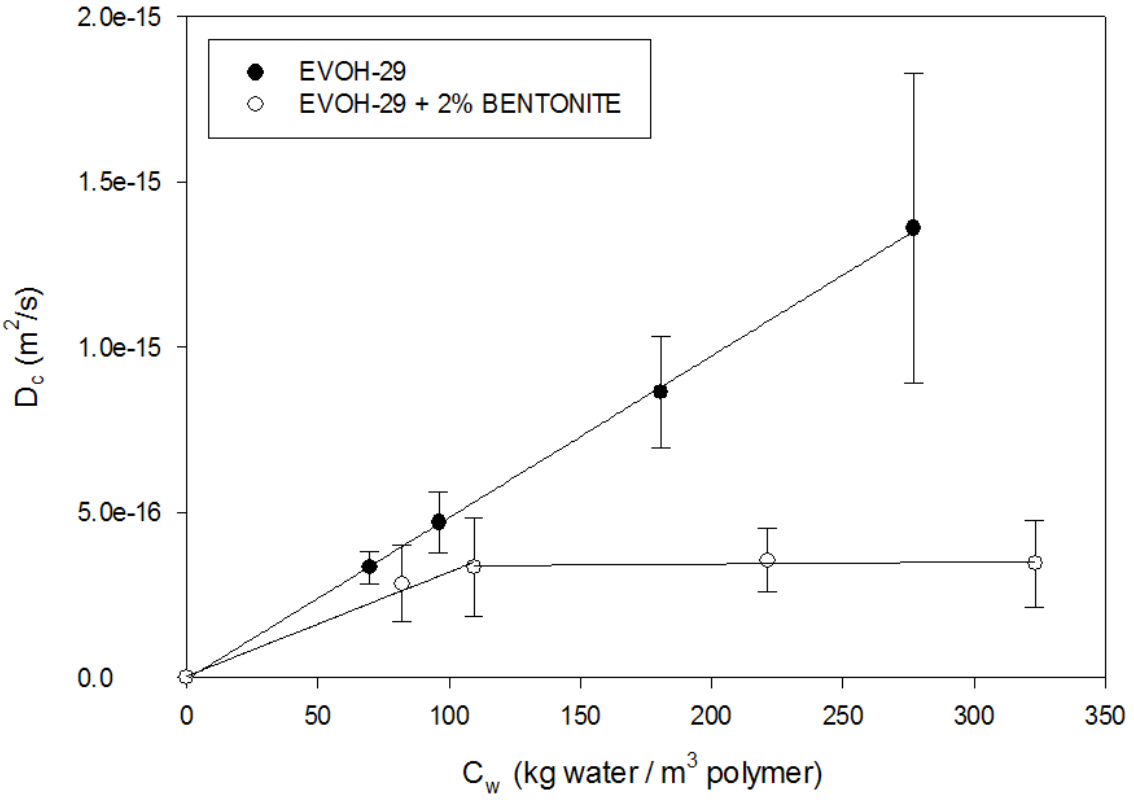

Figure IV.4. Values of the diffusion coefficient for the release of carvacrol from control and bentonite-containing EVOH-29 films into external atmosphere as affected by the water content.

The values of these parameters, as estimated for both materials by the corresponding fitting straight lines, are collected in **Table IV.3**.

Table IV.3. Estimated values for the slope-intercept equation parameters as obtained from the carvacrol diffusion curves fitted to the EVOH-29 and EVOH-29 + 2 % bentonite experimental points.

Slope-intercept equation parameters	EVOH-29	EVOH-29 + 2 % bentonite
$D_{c0}^{P} \cdot 10^{19}\ \left(m^2/s\right)$	3 ± 7	3 ± 7
$\gamma^{P} \cdot 10^{18}\ \left(m^5/kg \cdot s\right)$	4.87 ± 0.03	3.73 ± 0.17

As **Figure IV.4** shows, the carvacrol diffusivity in EVOH-29 exhibits a strong linear dependence on water concentration, increasing ca. four orders of magnitude from dry to wet conditions. The polymer relaxation phenomena caused by water plasticization could be responsible for this effect. In the case of the clay-filled polymer, the linear dependence is slightly weaker and is interrupted at about 80 % RH, giving a constant value of (3.45 ± 0.09) · 10^{-16} m^2/s for carvacrol diffusivity, D_c^B. The lower values of this parameter measured for the nanocomposite might be explained by the increase in the carvacrol diffusion path as a consequence of the presence of bentonite platelets homogeneously dispersed in the polymeric matrix [9]. The break in linearity observed in the evolution of carvacrol diffusivity with water concentration reveals the strong barrier effect exerted by clay nanoparticles on carvacrol diffusion when the barrier provided by EVOH-29 fails at the glass transition point (23 °C and 80 % RH) as a consequence of its moisture sorption.

3.5. Thermal assessment

Thermal characterization of EVOH-29 and EVOH-29 + 2 % bentonite was carried out at 4.5 and 91.0 % RH by means of difference scanning calorimetry (DSC). **Figure IV.5** displays thermograms obtained during the first heating cycle for both materials in both humidity conditions. As the figure shows, plain EVOH-29 at 4.5 % RH exhibits a slight decay in heat flow at about 48.5 °C that could easily be related with its glass transition point, whereas EVOH-29 equilibrated at 91 % RH lowers its transition temperature up to –2.1 °C, similar values to those reported in the literature [17]. Furthermore, the fusion temperature falls from 186.5 to 140.8 °C with the growth of the moisture content in the polymeric matrix. When bentonite nanoclay is incorporated in this material a rise in glass transition

temperatures is observed up to 50.9 and –1.9 °C in dry and humid conditions, respectively, which might be related with a slight increase in rigidity caused by the presence of the nanoparticles, in agreement with the water uptake observations. The fusion point, in contrast, attains slightly lower temperatures of 185 and 139 °C at the same humidity conditions, which could be related to a nucleating effect of the filling resulting in crystals of a smaller size.

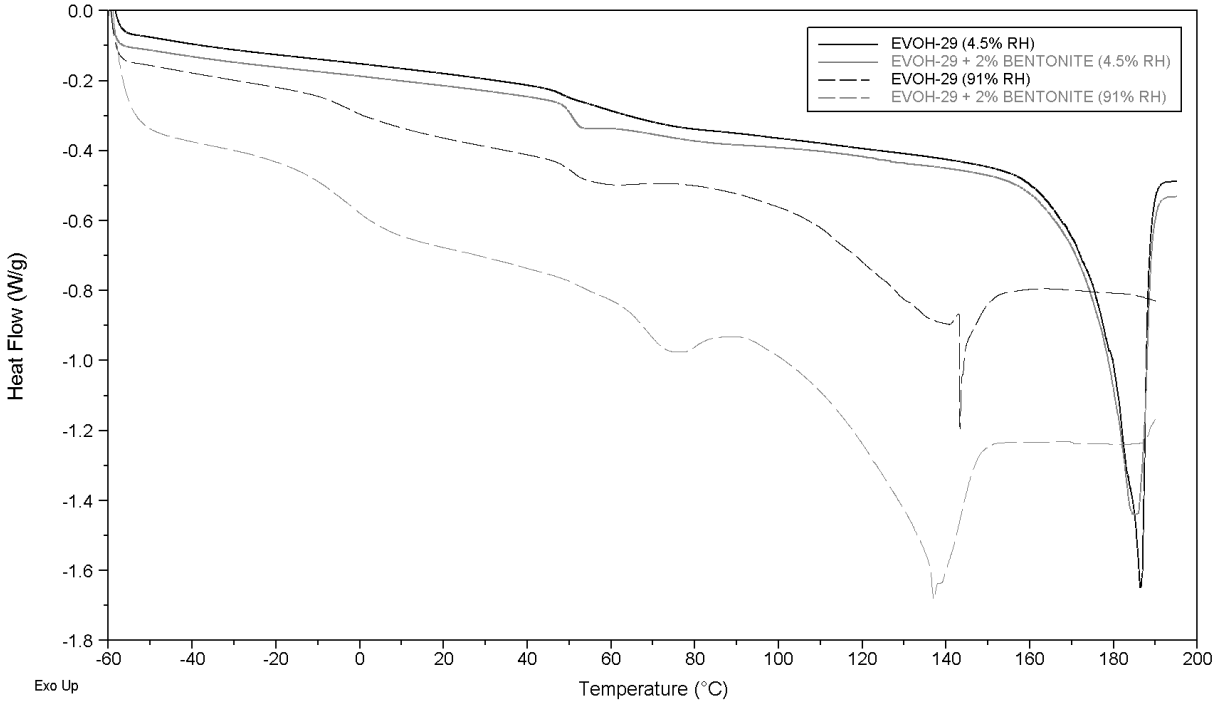

Figure IV.5. DSC thermograms obtained during the first heating for control and bentonite-containing EVOH-29 films conditioned at 4.5 % and 91 % RH.

3.6. Assessment of barrier properties to water vapor, oxygen, and carbon dioxide

Barrier properties of the original and clay-filled polymers in different humidity conditions were characterized for the transport of atmospheric gases, namely: water vapor, oxygen, and carbon dioxide, since they are the main constituents of package headspace.

3.6.1. Water vapor permeability

Figure IV.6 shows the evolution of water vapor permeability with the growth of water concentration in both materials. As evidenced in the graph, at low water contents in the polymer matrix (< 120 kg/m^3) both permeabilities decay with the increase in water concentration up to about a sixth of their initial value in dry conditions. In contrast, near the glass transition point (23 °C and 80 % RH) this decay tends to slow down and begin a slight recovery. This evolution was also observed in the literature for the water vapor permeability and diffusivity in several EVOH copolymers ranging from 29 to 44 % ethylene content at humidity conditions below their glass transition point (23 °C and 50 %), from which permeability values began to grow again exponentially. In addition, the measured values are in high agreement with the reported values for EVOH-29 [21].

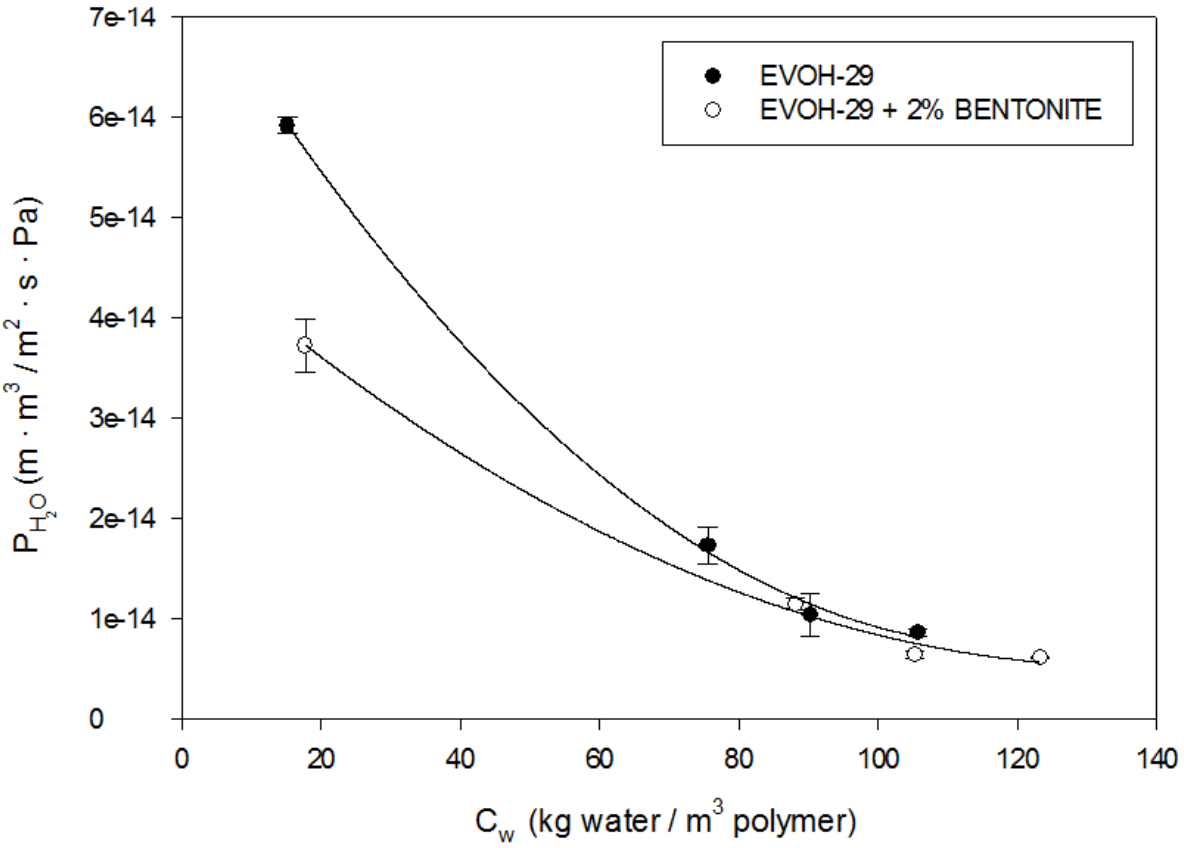

Figure IV.6. Values of the water vapor permeability for control and bentonite-containing EVOH-29 films as affected by the water content.

This behavior could be explained by the fact that up to the glass transition point the polymer structure is not modified, whereas the migrating water molecules form an increasing number of clusters with the growth of water concentration in the polymeric matrix that can hinder the diffusion of further molecules. Clustering in the water/EVOH interaction was studied in the literature to detect the possible existence of autoassociated water molecules in binary systems, and it was concluded that this phenomenon occurs at water contents above 50 kg/m^3 [21], as might be the case in the systems studied here.

In the case of the nanocomposite, the figure shows a clear reduction in the permeability coefficient of about 35 % on average with respect to the unmodified polymer. This behavior could be explained by the increase in the diffusion path of water molecules as a result of the presence of homogeneously dispersed clay nanoparticles, just as was observed in the carvacrol release.

The evolution of water vapor permeability with water concentration in both materials was fitted to the classical equation of a quadratic trend line with excellent results:

$$P^P_{H_2O} = P^P_{H_2O0} - \gamma'^P \cdot C^P_w + \gamma^P \cdot \left(C^P_w\right)^2 \qquad \text{(IV.7)}$$

where $P^P_{H_2O0}$ is the water vapor permeability coefficient in the absence of absorbed water, γ^P is the water plasticization coefficient, and γ'^P is the water antiplasticization coefficient. The values for the equation parameters, as estimated by the fitting curves, are presented in **Table IV.4**.

Table IV.4. Estimated values for the quadratic equation parameters as obtained from the water vapor permeability curves fitted to the EVOH-29 and EVOH-29 + 2% bentonite experimental points.

Quadratic equation parameters	EVOH-29	EVOH-29 + 2 % bentonite
$P^P_{H_2O0} \cdot 10^{14}$ $\left(\mathrm{m \cdot m^3 / m^2 \cdot s \cdot Pa}\right)$	7.5 ± 0.2	4.7 ± 0.2
$\gamma'^P \cdot 10^{16}$ $\left(\mathrm{m \cdot m^3 \cdot m^3 / m^2 \cdot s \cdot Pa \cdot kg}\right)$	11.3 ± 0.1	6 ± 1
$\gamma^P \cdot 10^{18}$ $\left(\mathrm{m \cdot m^3 \cdot m^6 / m^2 \cdot s \cdot Pa \cdot kg^2}\right)$	4.7 ± 0.9	2.2 ± 0.7

3.6.2. Oxygen and carbon dioxide permeability

Figure IV.7 and **Figure IV.8** display the evolution of oxygen and carbon dioxide permeability with the increase in water content in both polymers. As the figures show, both permeabilities increase up to about 480 and 40 times their original value in dry conditions, for oxygen and carbon dioxide respectively, with the growth of water concentration in each material. This increase may be a result of the polymer relaxation phenomena explained before, and it follows a sigmoidal progression that can again be described with Peleg's model as for the carvacrol solubilities studied above:

$$P_G^P = \frac{P_{G0}^P}{1 + e^{\frac{C_{wc}^P - C_w^P}{a}}} \qquad \text{(IV.8)}$$

where P_{G0}^P is the gas permeability coefficient at the maximum value of water concentration in the films, C_{wc}^P is the critical concentration of water that decreases P_G^P to 50 % below P_{G0}^P, and a is a dimensionless constant that accounts for the steepness of the drop in the magnitude of P_G^P.

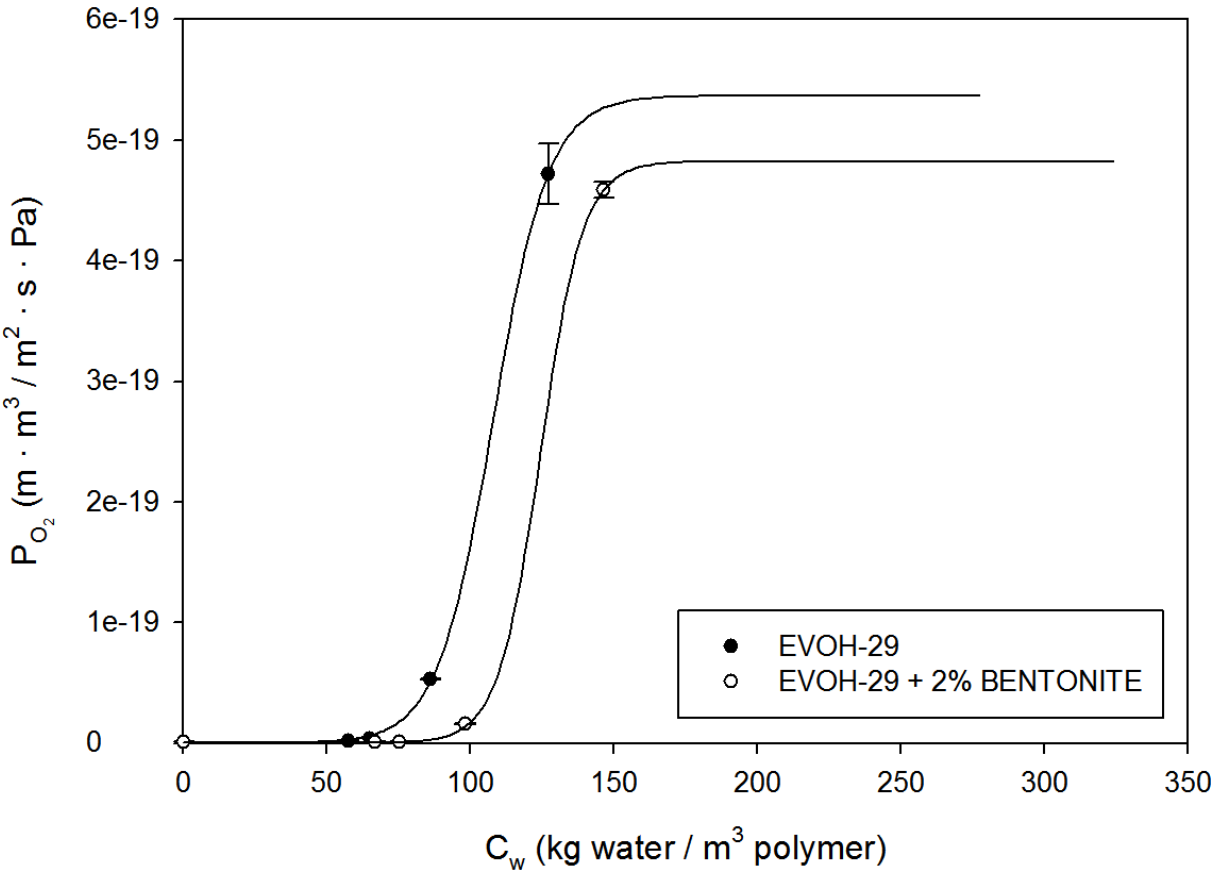

Figure IV.7. Values of the oxygen permeability for control and bentonite-containing EVOH-29 films as affected by the water content.

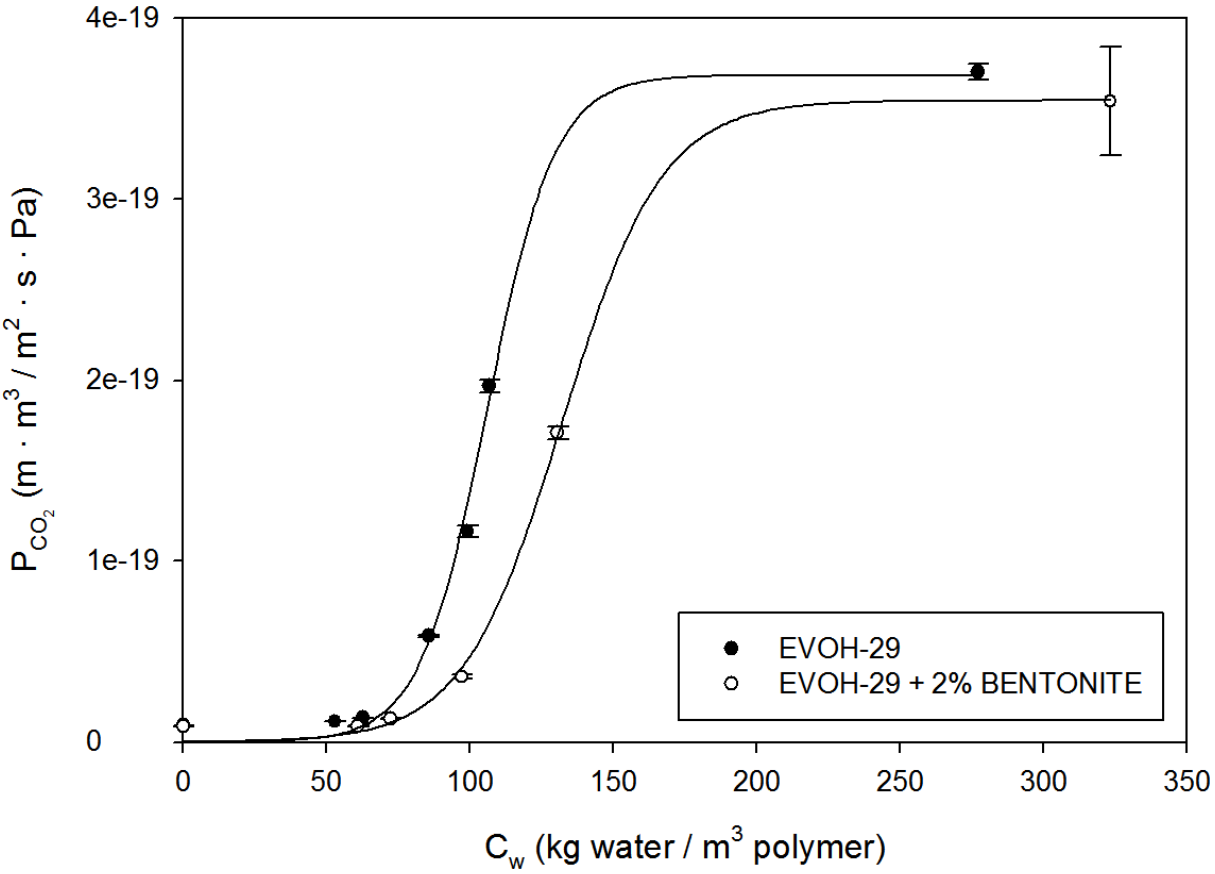

Figure IV.8. Values of the carbon dioxide permeability for control and bentonite-containing EVOH-29 films as affected by the water content.

Tables IV.5 and **IV.6** display the corresponding values of the model parameters for both gases and polymers.

Table IV.5. Estimated values for the Peleg's equation parameters as obtained from the oxygen permeability curves fitted to the EVOH-29 and EVOH-29 + 2 % bentonite experimental points.

Peleg's model parameters	EVOH-29	EVOH-29 + 2 % bentonite
$P^P_{O_2 0} \cdot 10^{19}$ $\left(m \cdot m^3 / m^2 \cdot s \cdot Pa\right)$	5.4 ± 0.6	4.8 ± 1.5
C^P_{wc} $\left(kg/m^3\right)$	108 ± 5	120 ± 30
a	9.7 ± 1.7	7 ± 7

Table IV.6. Estimated values for the Peleg's equation parameters as obtained from the carbon dioxide permeability curves fitted to the EVOH-29 and EVOH-29 + 2 % bentonite experimental points.

Peleg's model parameters	EVOH-29	EVOH-29 + 2 % bentonite
$P^{P}_{CO_2 0} \cdot 10^{19}$ $\left(m \cdot m^3/m^2 \cdot s \cdot Pa\right)$	3.69 ± 0.11	3.55 ± 0.06
C^{P}_{wc} $\left(kg/m^3\right)$	105.9 ± 1.3	132.2 ± 1.4
a	11.7 ± 1.5	17.3 ± 1.4

Since the critical concentration of water in the polymer can be related with the glass transition point, as explained before, according to the values expressed in the above equations it can be confirmed that glass transition for EVOH-29 occurs at 23 °C and 86.1 ± 0.3 % RH on average for both gases, whereas for EVOH-29 + 2 % bentonite it occurs at a slightly higher value of 23 °C and 86.3 ± 1.6 % RH, although the differences found are not significant.

Regarding the nanocomposite material, both figures reveal that the incorporation of 2 % bentonite in the original polymer reduces its permeability to oxygen and carbon dioxide between 3 to 75 % in average, depending on the material water content.

Another relevant aspect reflected in **Figures IV.7** and **IV.8**, and in **Tables IV.5** and **IV.6**, is that the values of oxygen permeability are of the same order as or slightly higher than the carbon dioxide permeability. Although a P_{CO_2}/P_{O_2} ratio of ca. 3 can be found in the literature for EVOH, it is also worth mentioning that none of the values reported for CO_2 permeability has been measured on EVOH cast films.

3.6.3. Oxygen and carbon dioxide diffusivity

Oxygen and carbon dioxide diffusion coefficients in extreme humidity conditions at 0 and 90 % RH were measured in order to assess potential improvements in barrier properties for the filled polymer with respect to the original material. The results found are displayed in **Figure IV.9**.

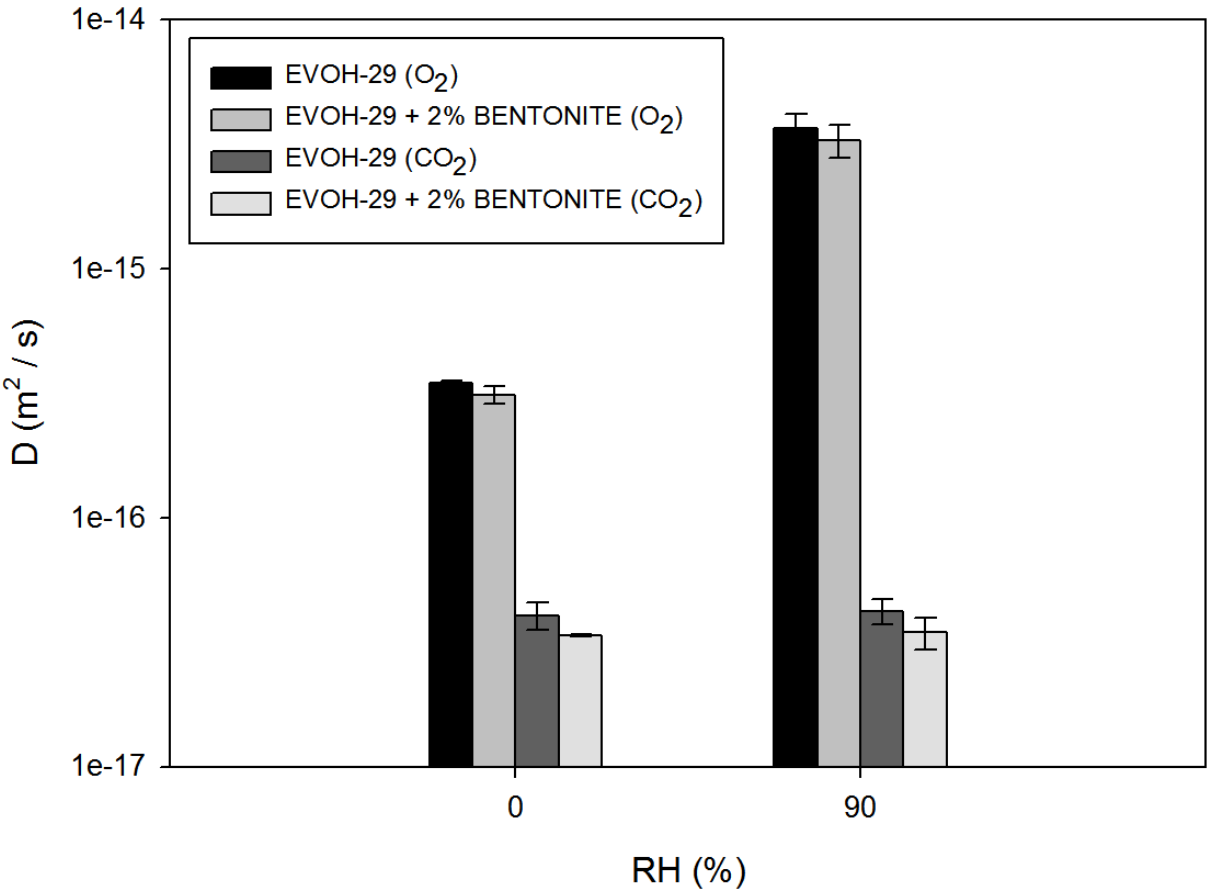

Figure IV.9. Values of the oxygen and carbon dioxide diffusivity for control and bentonite-containing EVOH-29 films at 0 and 90 % RH.

As the figure shows, oxygen diffusivity in dry conditions is approximately 9 times greater on average than carbon dioxide diffusivity, whereas in highly humid conditions this ratio increases to about 90 times greater on average for both materials. These results can be explained by two factors: the greater size of the carbon dioxide molecule, which could slow down its diffusion into the polymer in comparison with oxygen; and the water content effects, which a) relax the polymer matrix allowing low molecular mass molecules to diffuse quicker in wet (11 times on average at 90 % RH for oxygen) than in dry conditions, but b) increase the interaction between CO_2 and water molecules and reduce the increase in D value resulting from the matrix plasticization. When the nanocomposite is compared with plain EVOH a considerable improvement in barrier properties is observed, with reductions of 10.5 and 17.6 % on average in oxygen and carbon dioxide diffusion coefficients, respectively, albeit only the differences found in dry conditions resulted statistically significant.

3.6.4. Oxygen and carbon dioxide solubility

The solubility coefficient of oxygen and carbon dioxide at limit relative humidities of 0 and 90 % was calculated for EVOH-29 and EVOH-29 + 2 % bentonite by introducing the measured values at these conditions of permeability and diffusivity in equation (IV.4), and the resulting values are displayed in **Figure IV.10**. According to the graph, oxygen and carbon dioxide solubilities increase 39 and 20 times on average for both materials, respectively, with the growth of the polymer water content. This behavior could be explained by the additional gas solubility occurring in the water retained by the polymers. In addition, as the figure shows, the incorporation of bentonite nanoclay in the original polymer entails a further increase of between 6 and 50 % in the gas solubility coefficients, which resulted statistically significant except for carbon dioxide in wet conditions, and which might corroborate this statement, given the greater water solubility observed in this material, as discussed before. Finally, the graph reveals that the carbon dioxide solubility is approximately 83 times greater on average than the oxygen solubility in dry conditions, whereas at 90 % RH this ratio reduces to about 43 times more on average for both materials. From these values it can be stated that dry polymer allows a higher solubilization of carbon dioxide with regard to oxygen, but the presence of water in the material structure reduces this advantage by favoring oxygen molecules.

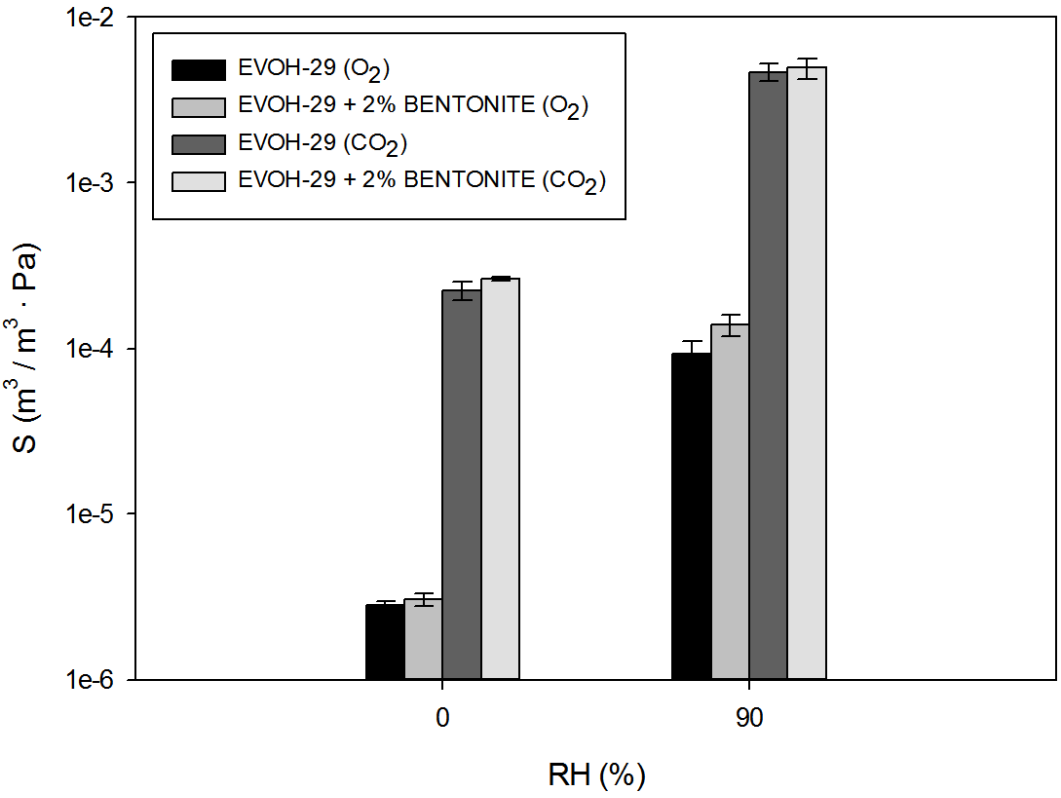

Figure IV.10. Values of the oxygen and carbon dioxide solubility for control and bentonite-containing EVOH-29 films at 0 and 90 % RH.

4. CONCLUSIONS

In this work, modifications induced in terms of carvacrol solubility and diffusivity, water vapor solubility and permeability, oxygen and carbon dioxide permeability, diffusivity and solubility, glass transition and fusion temperatures, and microstructural morphology of an EVOH-29 film with 5 % carvacrol as antimicrobial active agent and 2 % of bentonite nanoclay as inorganic filler were studied with respect to the original unmodified polymer.

Clay-filled EVOH-29 film showed a similar macroscopic appearance to the unfilled film, even though on a microscopic point of view it showed a good dispersion of bentonite nanoparticles. Water vapor, oxygen, carbon dioxide, and carvacrol solubilities were found to be higher for the modified polymer, whereas water vapor permeability, carvacrol diffusivity, and oxygen and carbon dioxide permeabilities and diffusivities were found to be lower for the nanocomposite. All the parameters, with the exception of water vapor permeability, increased with the growth of the water concentration in the polymeric matrix, and they could all be fitted with good agreement to different regression models. Glass transition temperature was higher in the modified material, whereas fusion temperature was slightly lower, although the differences found were not significant.

The incorporation of 2 % bentonite nanoclay in EVOH-29 provides a significant improvement in several properties of manufactured films with few or no drawbacks. Films obtained with the newly developed material can be used in active food packaging with better results than the original films.

ACKNOWLEDGMENTS

The authors thank the Spanish Ministry of Science and Innovation (project AGL2009-08776), EU (Nafispack project 212544), and Generalitat Valenciana (J.P.C. fellowship) for financial support and Mr. Karel Clapshaw (English edition services).

REFERENCES

[1] Marcos, B., Aymerich, T., Monfort, J. M., Garriga, M. (2007). Use of antimicrobial biodegradable packaging to control *Listeria monocytogenes* during storage of cooked ham. *International Journal of Food Microbiology*, 120 (1 – 2), 152 – 158.

[2] Han, J. H. (2005). *Antimicrobial packaging systems.* Han, J. H. (ed.) *Innovations in food packaging.* Elsevier Academic Press, USA.

[3] Cerisuelo, J. P., Muriel – Galet, V., Bermúdez, J. M., Aucejo, S., Català, R., Gavara, R., Hernández – Muñoz, P. (2012). Mathematical model to describe the release of an antimicrobial agent from an active package constituted by carvacrol in a hydrophilic EVOH coating on a PP film. *Journal of Food Engineering*, 110 (1), 26 – 37.

[4] De Vincenzi, M., Stammati, A., De Vincenzi, A., Silano, M. (2004). Constituents of aromatic plants: carvacrol. *Fitoterapia*, 75 (7 – 8), 801 – 804.

[5] Aucejo, S., Català, R., Gavara, R. (2000). Interactions between water and EVOH food packaging films. *Food Science and Technology International*, 6 (2), 159 – 164.

[6] Aucejo, S., Marco, C., Gavara, R. (1999). Water effect on the morphology of EVOH copolymers. *Journal of Applied Polymer Science*, 74 (5), 1201 – 1206.

[7] López – Rubio, A., Lagarón, J. M., Giménez, E., Cava, D., Hernández – Muñoz, P., Yamamoto, T., Gavara, R. (2003). Morphological alterations induced by temperature and humidity in ethylene – vinyl alcohol copolymers. *Macromolecules*, 36 (25), 9467 – 9476.

[8] Persico, P., Ambrogi, V., Carfagna, C., Cerruti, P., Ferrocino, I., Mauriello, G. (2009). Nanocomposite polymer films containing carvacrol for antimicrobial active packaging. *Polymer Engineering and Science*, 49 (7), 1447 – 1455.

[9] Tunç, S., Duman, O. (2011). Preparation of active antimicrobial methyl cellulose / carvacrol / montmorillonite nanocomposite films and investigation of carvacrol release. *LWT – Food Science and Technology*, 44 (2), 465 – 472.

[10] D'Arcy, R. L., Watt, I. C. (1970). Analysis of sorption isotherms of non – homogeneous sorbents. *Transactions of the Faraday Society*, 66, 1236 – 1245.

[11] Vertucci, C. W., Leopold, A. C. (1987). Water binding in legume seeds. *Plant Physiology*, 85, 224 – 231.

[12] Crank, J. (1975). *The mathematics of diffusion*. Clarendon Press, London, UK.

[13] ASTM E96 / E96M – 10. Standard test methods for water vapor transmission of materials. ASTM International, West Conshohocken, PA, USA.

[14] Peleg, M. (1993). Mapping the stiffness – temperature – moisture relationship of solid biomaterials at and around their glass transition. *Rheologica Acta*, 32 (6), 575 – 580.

[15] Van Roon, A., Parsons, J. R., Govers, H. A. J. (2002). Gas chromatographic determination of vapour pressure and related thermodynamic properties of monoterpenes and biogenically related compounds. *Journal of Chromatography A*, 955, 105 – 115.

[16] Hernández – Muñoz, P., López – Rubio, A., Lagarón, J. M., Gavara, R. (2004). Formaldehyde cross – linking of gliadin films: effects on mechanical and water barrier properties. *Biomacromolecules*, 5 (2), 415 – 421.

[17] Cabedo, L., Lagarón, J. M., Cava, D., Saura, J., Giménez, E. (2006). The effect of ethylene content on the interaction between ethylene – vinyl alcohol copolymers and water – II: influence of water sorption on the mechanical properties of EVOH copolymers. *Polymer Testing*, 25 (7), 860 – 867.

[18] Mascheroni, E., Guillard, V., Gastaldi, E., Gontard, N., Chalier, P. (2011). Anti – microbial effectiveness of relative humidity – controlled carvacrol release from wheat gluten / montmorillonite coated papers. *Food Control*, 22 (10), 1582 – 1591.

[19] Mascheroni, E., Chalier, P., Gontard, N., Gastaldi, E. (2010). Designing of a wheat gluten / montmorillonite based system as carvacrol carrier: Rheological and structural properties. *Food Hydrocolloids*, 24 (4), 406 – 413.

[20] López – Carballo, G., Cava, D., Lagarón, J. M., Català, R., Gavara, R. (2005). Characterization of the interaction between two food aroma components, α – pinene and ethyl butyrate, and ethylene – vinyl alcohol copolymer (EVOH) packaging films as a function of environmental humidity. *Journal of Agricultural and Food Chemistry*, 53 (18), 7212 – 7216.

[21] Aucejo, S. (2000). *Estudi i caracterització de l'efecte de la humitat en les propietats barrera d'estructures polimèriques hidròfiles.* Tesi doctoral, Universitat de València, València.

V NATURAL ANTIMICROBIAL – CONTAINING EVOH COATINGS ON PP AND PET FILMS: FUNCTIONAL AND ACTIVE PROPERTY CHARACTERIZATION

Josep Pasqual Cerisuelo [a], Rafael Gavara [a, *], Pilar Hernández – Muñoz [a]

[a] Laboratori d'envasos, Institut d'Agroquímica i Tecnologia d'Aliments, IATA – CSIC.
Av. Agustí Escardino, 7. 46980 Paterna, València.

* Autor de contacte. Tel.: +34 963900022, e-mail: rgavara@iata.csic.es

ABSTRACT

Natural antimicrobials are currently being tested by many researchers for active packaging applications as a response to consumer demands for safer food products. In previous work, several packaging materials consisting of ethylene – vinyl alcohol copolymer (EVOH) – coated polypropylene (PP) films containing essential oils or their constituents as active agents were successfully developed and tested for antimicrobial activity. In this work, selected films from those materials, namely EVOH coatings with carvacrol, citral, marjoram essential oil, or cinnamon bark essential oil, on PP and polyethylene terephthalate (PET) substrates, were subjected to diverse physicochemical analysis in order to assess their suitability for food packaging applications. Concretely, the investigated properties were: the stability of EVOH coatings on PP and PET substrates, the retainability of EVOH matrices for active compounds, the mechanical, optical, surface, and barrier properties of the final active films, and the effects of a matrix modification based on the addition of bentonite nanoclay on the performance of PP / EVOH active packages studied in actual working conditions.

Results showed that the application of corona discharge followed by a polyethyleneimine (PEI) – based primer was the best anchorage treatment available to stabilize EVOH coatings on PP and PET substrates. Furthermore, they demonstrated that the retention of active agents into EVOH matrices ranged from low to moderate, depending on the embedded substance, and that their presence into an EVOH coating in the final multilayer films did not noticeably affect their mechanical, optical, or barrier properties, although it considerably improved their wettability. They also indicated that the inclusion of bentonite nanoparticles into their carrier layers substantially enhanced the performance of the final packages, while maintaining or slightly improving their other physical properties. Hence, as a conclusion, all the assayed multilayer films were considered perfectly valid for food packaging applications, and the incorporation of bentonite nanoclay to their carrier layers was also highly recommended.

***Packaging Technology and Science*, 2014, 27 (11), 901 – 920.**

1. INTRODUCTION

Consumption habits in our society have recently been changing towards healthier, fresher, and more natural, additive free, food products, preserved in safer, more convenient, and eco-friendly food packages which could extend their shelf life while maintaining quality and sensory characteristics. These present demands are leading manufacturers to introducing novel food products in the market, such as fresh-cut vegetables and ready-to-eat meals, and researchers to developing novel technologies, such as modified-atmosphere packaging or active packaging, in order to preserve them while satisfying both consumer and manufacturer expectations [1 – 9].

The main hazard to face in the preservation of these kinds of foodstuffs is the potential contamination and growth of pathogenic or spoiling microorganisms, and antimicrobial active packaging has proven to be a quite effective technique in preventing their deterioration. In some applications of this technology, a volatile antimicrobial agent embedded in the packaging materials is progressively released into the package headspace to be concentrated on the food surfaces and thus inhibit bacterial proliferation [10 – 17]. However, current consumer concerns about the use of chemical preservatives in food products are making researchers direct their efforts towards alternative compounds of natural origin, such as vegetal extracts or essential oils of herbs and spices. These latter substances, in particular, are already recognized as food additives by the EFSA and as GRAS (Generally Recognized As Safe) substances by the US FDA, and have been the object of numerous studies demonstrating their effectiveness against a wide spectrum of microorganisms, as well as their advantages in matters of consumer acceptance, antioxidant activity, and biodegradable or edible capabilities in recent years [18 – 22].

In previous works [23 – 26] some essential oils and their constituents were successfully incorporated into polymeric matrices and tested for antimicrobial activity. The packaging material carrying the active agents was EVOH, an ethylene-vinyl alcohol copolymer whose hydrophilic nature can strongly modify its barrier characteristics with the absorption of water vapor [27 – 29] thus allowing for a high retention or protection of the embedded compounds in dry conditions while triggering their activity when exposed to the humid environment generated by a packaged food product [25, 30]. The composite materials obtained were used as active layers in multilayer packaging films, which were employed in the construction of active packages for fresh products and studied by means of mathematical models. Results showed good chemical compatibility between the active agents and the packaging materials, a gradual release of the embedded compounds into the package headspace as a function of the water

activity, and a significant inhibition of numerous spoiling bacteria and microflora at the beginning of the storage period. In addition, some EVOH matrix modifications with β-cyclodextrin [31, 32] or bentonite nanoclay [33, 34] were evaluated in order to increase the retention capacity or to reduce the active agents' release rate.

In this work, some selected films from the active materials developed in previous studies [23, 25, 26, 33] were subjected to several analyses with the aim of assessing their suitability for food packaging applications. Firstly, the stability of EVOH coatings on pretreated polypropylene (PP) and polyethylene terephthalate (PET) substrates was investigated by evaluating the results yielded by four different anchorage technologies, namely UV radiation, corona treatment, and corona treatment followed by the application of primers based on polyurethane (PU) and polyethyleneimine (PEI), in essays of adhesion and thermosealability. Secondly, active multilayer films consisting of EVOH coatings containing natural antimicrobials on PP and PET substrates were manufactured and subsequently analyzed, together with their passive counterparts, for the determination of several physical properties of relevance for food packaging applications, as well as for the retention of the active agents in the coating matrices. In particular, films were assayed for mechanical, optical, surface, and barrier properties, as well as for the partition coefficients of the active agents between the material layers, and for the efficiency of their incorporation. The embedded compounds were carvacrol (main component of *Origanum vulgare* essential oil, b.p.: 236 °C), citral (main component of *Litsea cubeba* essential oil, b.p.: 229 °C), and marjoram essential oil (extracted from *Thymus mastichina*, b.p.: 168 °C) in PP films, and citral and cinnamon bark essential oil (extracted from *Cinnamonum zeylanicum*, b.p.: 249 °C) in PET films. The improvements expected from an EVOH matrix modification on the retention capacity and on the rate of release of the active agents were assessed by manufacturing two different active multilayer films consisting of PP substrates coated by either neat EVOH or EVOH and bentonite nanocomposites, both containing carvacrol as antimicrobial agent, and employing them in the construction of active packages intended to preserve fresh-cut salad products, and by comparing their performance in actual working conditions.

2. MATERIALS AND METHODS

2.1. Materials

Ethylene-vinyl alcohol copolymer with a 29 % ethylene molar content (EVOH-29) was kindly supplied by The Nippon Synthetic Chemical Industry Co., Ltd. (Osaka, Japan). Food-contact grade bi-oriented polypropylene (PP) and polyethylene terephthalate (PET) films 30 µm thick were kindly supplied by Envaflex S.A. (Utebo, Spain).

H-760-A primer, consisting of an aqueous solution of 12 % polyethyleneimine (PEI), was purchased from MICA Corp. (Shelton, CT, USA), and NAF-1 primer, consisting of an ethyl acetate solution of 43 % polyurethane (PU), was kindly provided by Artibal S.A. (Sabiñánigo, Spain).

Reagent-grade phosphorus pentoxide and sodium bentonite nanoclay were purchased from Sigma-Aldrich Co. LLC. (St. Louis, MO, USA), as well as several food-grade essential oils and their constituents, concretely, carvacrol of at least 98 % purity, citral of at least 96 % purity, marjoram essential oil, and cinnamon bark essential oil. Reagent-grade 1-propanol and high-vacuum silicone were supplied by Panreac Química S.L.U. (Barcelona, Spain), and deionized water was obtained from a Milli-Q Plus purification system of EMD Millipore Corp. (Billerica, MA, USA).

2.2. Preparation of the active multilayer films. Construction of the packages

All the multilayer films assayed in this work, active as well as passive, were manufactured by coating PP or PET substrates, previously treated with an anchorage technology, with hydroalcoholic solutions of EVOH-29. These solutions contained, depending on the case, an essential oil, such as marjoram or cinnamon bark oil, or one of its constituents, such as carvacrol or citral, as active antimicrobial agent, and / or an inorganic filling material, namely sodium bentonite nanoclay, as polymer matrix modifier. The preparation of EVOH-29 solutions with one or both incorporated additives is described in detail in previous works: [23, 33], respectively. In brief, active solutions with the neat polymer were prepared by dissolving a given amount of EVOH-29 pellets in a 1:1 (w/w) mixture of deionized water and 1-propanol, at a concentration of 15 % (w/w), into a glass flask placed on a RTC basic magnetic stirrer with heater plate (IKA-Werke GmbH & Co. KG, Staufen, Germany), coupled to a constant reflux vapor system. Once the polymer was fully dissolved the antimicrobial compound was added to the mixture

at a concentration of either 7.5 or 10 g / 100 g EVOH-29, depending on the substance incorporated, and was let then homogenizing for at least 10 minutes more. Regarding the active solutions with EVOH-29 nanocomposite, their preparation was analogous to the previous ones with just substituting deionized water by a hydrocolloidal dispersion of bentonite nanoparticles. Such dispersion was obtained by thoroughly mixing sodium bentonite in deionized water, at a concentration of 0.6 % (w/w), with the aid of an Ultra-Turrax T25 basic disperser (IKA-Werke GmbH & Co. KG, Staufen, Germany) and of an Ultrasons ultrasonic bath (J. P. Selecta S. A., Barcelona, Spain). Specifically, the initial mixture was firstly stirred for 30 s at 24000 rpm, afterwards sonicated for 1h, left then resting overnight, and finally sonicated again for at least 15 minutes more to obtain a stable colloidal suspension.

In the case of the films tested for coating stability, several sheets of PP and PET were subjected to four different anchorage treatments, namely UV irradiation, corona discharge, and corona discharge followed by the application of PU and PEI-based primers, prior to being coated by a solution of neat EVOH-29. Sheets subjected to UV irradiation were placed under a VUV Xe excimer lamp with 6 W at 172 nm (UV-Consulting Peschl España S.L., València, Spain) for 1 min in an air atmosphere, whereas sheets subjected to corona discharge were passed through the plasma region generated by the electrode of a BD-20AC high frequency corona surface treater three times (Electro-Technic Products, Inc., Chicago, IL, USA). Both technologies were able to create ozone molecules from air ionization, which could react with surface polymeric chains and break some of their covalent bonds. Hence, they were aimed at reducing the surface tension of the polymers, and thus at improving their wettability with the primers or their adhesiveness with the coatings. Primers, in turn, were casted on the polymer sheets with the aid of an Elcometer 4340 automatic coating applicator (Elcometer Ltd., Manchester, UK), equipped with a Mayer rod of 10 µm deep thread, and programmed to carry out a gradual deposition of the solutions at a temperature of 60 °C and an application velocity of 8 cm/s. The same instrument and conditions were also used to apply the neat EVOH-29 solution on the four pretreated PP and PET sheets to yield the final multilayer films. After manufacturing, the deposited layers of primer and EVOH-29 were found to be homogeneous and transparent, and their thickness could be estimated by measuring both coated and uncoated areas of the substrate sheets with an ABSOLUTE Digimatic Indicator ID-C Series 543 digital micrometer (Mitutoyo America Corp., Aurora, IL, USA) and subtracting the results obtained, yielding values of about 1 and 1.5 µm, respectively.

With respect to the active films tested for various physicochemical properties, a coating technology based on gravure printing was used at the facilities of Envaflex S.A. (Utebo, Spain). In this case, the coating system was fed with reels of PP and PET films, which were pretreated with corona discharge

and subsequently coated with a PEI-based primer, followed by a layer of the corresponding polymer solution. Production speed was about 60 m/min, and solvent evaporation was rapidly performed in drying tunnels, fed by hot air at 40 °C, after the deposition of each layer. The diverse active multilayer films finally produced were: PP / PEI / EVOH + 10 % (w/w) citral (PP / E + CI), PP / PEI / EVOH + 7.5 % (w/w) marjoram essential oil (PP / E + MO), PET / PEI / EVOH + 10 % (w/w) citral (PET / E + CI), and PET / PEI / EVOH + 7.5 % (w/w) cinnamon bark essential oil (PET / E + CO). In addition, two passive multilayer films were also obtained to be used as controls in the tests carried out: PP / PEI / EVOH (PP / E), and PET / PEI / EVOH (PET / E). In this case, the coated areas of the manufactured films presented a homogeneous, translucent, and matte appearance, similar to the materials previously produced at laboratory scale, and the thickness of PEI and EVOH layers was estimated at about 0.8 and 1.15 µm, respectively. In order to avoid potential activity losses all the films were rolled in reels, packaged in hermetic aluminum-coated polyethylene bags, and stored until utilization in thermostatic chambers at 4 ± 1 °C of temperature.

Finally, in relation with the films tested for the effects of the matrix modification on the package performance, as well as for some other physicochemical properties, several sheets of PP were pretreated with corona discharge, and subsequently coated with three different EVOH solutions by using the aforementioned automatic coating applicator, equipped and programmed as previously described. In these conditions, one passive and two active multilayer films could be obtained: PP / EVOH + 2 % (w/w) sodium bentonite nanoclay (PP / E + B), PP / EVOH + 7.5 % (w/w) carvacrol (PP / E + CA), and PP / EVOH + 2 % (w/w) sodium bentonite nanoclay + 7.5 % (w/w) carvacrol (PP / E + B + CA), presenting homogeneous and transparent coating layers of approximately 2 µm thick. These two latter materials were employed in the construction of active packages intended to preserve fresh-cut salad products, by following the procedure described in a previous work [23]. In brief, the active films were cut into pieces measuring 25 x 30 cm, and closed in the form of bags with the aid of a 420 SBM impulse heat sealer (Audion Elektro B.V., Weesp, The Netherlands). Prior to applying the final seal, bags were filled with five small cylindrical pieces of gelified water of 10 mL volume, in order to generate and maintain inner relative humidity constant and close to 100 %, and thus to simulate the presence of a high water activity food product. Once bags were hermetically closed, a septum was adhered to their outer face, and 1 L of air at atmospheric pressure was injected into them with the aid of a syringe.

2.3. Determination of the stability of EVOH coatings on pretreated PP and PET substrates: adhesion and thermosealability tests

The adhesiveness of EVOH coatings to PP and PET substrates subjected to different treatments for surface modification was evaluated by means of the well-known Scotch tape test, a qualitative test method based on the ASTM D3359 – 09e2 standard [35]. In detail, two identical pieces of Scotch Magic adhesive tape (3M Corp., St. Paul, MN, USA), of 19 mm wide and 100 mm long, were firmly applied to the front and back surfaces of the films in both transversal and machine directions, left for about 20 s at room conditions (about 23 °C of temperature and 50 % of relative humidity), and stripped off in a 180° angle with one quick peeling. In order to ensure the maximum strength for the anchorages, and thus the optimal testing conditions for the films, essays were performed 24 h after manufacturing, and, for each assayed sample, at least five parallel tests were carried out.

The thermosealability of the multilayer films is closely related to the sealing capabilities of their material layers, just as to the force of adhesion between them. Because of that, several thermosealing tests were performed in parallel with the previous adhesion tests in order to assess the anchorage strength of the EVOH coatings to the diverse pretreated PP and PET substrates more thoroughly. With this objective, several sheets of each manufactured material were placed in pairs between the jaws of the impulse heat sealer described above, to be sealed by their coated face. Immediately afterwards, the timer of the instrument was set to 10, and its jaws were closed to provide a long, continuous, and homogeneous seal. Once sealing area was cooled, films were removed from the instrument and visually examined for faults or imperfections. If no sealing defects were observed, films were pulled apart by applying increasing tensile forces on the seal until causing its detachment or failure. This way, the strength of the seal, and thus the thermosealing characteristics of the assayed material, could be qualitatively evaluated by estimating the magnitude of the tension forces required to break the union between the films, and by the visual inspection of the ripped zones. Furthermore, films which provided the best sealability results were additionally subjected to peeling tests, together with their corresponding substrates, in order to quantitatively determine their sealing strength and to compare it with the values yielded by the original uncoated materials. These essays were performed by following a test procedure based on the ASTM D882 – 12 standard method [36] with the aid of a MultiTest 1-i universal testing machine (Mecmesin Ltd., Slinfold, UK), equipped and programmed as described below in section 2.7. In detail, the sealed films were cut into 1 in. wide strips, their ends were held under 3 bars of pressure with two pneumatic plane grips, and an increasing load was applied

on their seal over time until causing its failure. The load force recorded at the breaking point was then identified as the sealing strength of the assayed sample. Just as for the adhesion tests, both sealing and peeling assays were performed at room conditions the day after film manufacturing, and repeated at least five times for each material sample.

2.4. Determination of the retention of active agents in the coating layers of multilayer films: incorporation efficiencies and partition coefficients

Given that all the active agents incorporated in the multilayer films were volatile compounds, their evaporation losses during the processes of preparation and application of the coating solutions, and thus the retention capabilities of the polymer matrices forming the coating layers, were investigated by measuring the concentrations of these substances remaining in the final active films immediately after being produced at the industrial facilities. These concentrations were determined by thermal desorption and GC analysis, using an 890 thermal tube desorber (Dynatherm Analytical Instruments Inc., Kelton, PA, USA) connected in series to an HP 5890 Series II Plus gas chromatograph (Hewlett Packard Co., Wilmington, DE, USA) equipped with a flame ionization detector (FID) and an Agilent HP-1 semi-capillary column of 30 m length, 0.53 mm internal diameter, and 2.65 µm film thickness (Teknokroma S.C.L., Barcelona, Spain), and following the procedure described in previous works [23, 33].

Since just after the film manufacturing all the retained active molecules were supposed to be contained exclusively in the coating matrices, the amounts of substances detected by the instruments were only attributed to the film mass fraction corresponding to those material layers. This way, the values for the concentrations of each active compound i in the coating matrix of each multilayer film F at the beginning of the material shelf life, $C_{i\,0}^{F}$, were calculated, and then introduced, together with the nominal concentrations detailed in the previous section 2.2, $C_{i\,\mathrm{n}}^{F}$, in the following equation (V.1), in order to determine the percentage efficiency of the incorporation process, E_i^F.

$$E_i^F(\%) = \frac{C_{i\,0}^{F}}{C_{i\,\mathrm{n}}^{F}} \cdot 100 \qquad \text{(V.1)}$$

The retention of the active molecules within the coating layers of the multilayer films after manufacture was also assessed by measuring their tendency to migrate to the substrate layers over time. This tendency is determined by the thermodynamic equilibrium of each substance between both polymer matrices, which can be represented by the partition coefficient corresponding to that system, $K_i^{C/S}$. This thermodynamic parameter can be defined as the ratio between the concentrations at equilibrium of an active compound i in the coating, C_i^C, and in the substrate layers, C_i^S, as equation (V.2) shows:

$$K_i^{C/S} = \frac{C_i^C}{C_i^S} \tag{V.2}$$

In order to properly evaluate these concentrations, the active films were analyzed 6 months after manufacturing, when the thermodynamic equilibrium was assumed to have been reached in the stored reels. All analyses were performed with the same equipment, conditions, and procedure as for the analyses of the initial concentrations described before. However, since in this case the studied compound was distributed between two material phases, which did not allow physical separation, the concentration of the active agent in the coating layer had to be estimated by first measuring the average concentration in the entire film and in the substrate layer, and then by introducing the values obtained in the following equation (V.3), deduced through a mass balance on the two material layers constituting the complete multilayer film:

$$C_i^C = \frac{C_i^F \cdot \rho_F \cdot L_F - C_i^S \cdot \rho_S \cdot L_S}{\rho_C \cdot L_C} \tag{V.3}$$

where L_C, L_S, and L_F, are the thicknesses of the coating and substrate layers, and of the entire film respectively, whereas ρ_C, ρ_S, and ρ_F, are their corresponding densities. Since the active films were manufactured by a coating technology based on gravure printing, and the printed areas did not completely cover the entire film surface, the concentration of the active agent in the substrate layer could be determined by analyzing polymer samples from the film zones that remained uncoated.

2.5. Determination of the surface properties of the multilayer films

The surface properties of the coating and substrate layers of the manufactured films, and, in particular, their wettability, were investigated by measuring static contact angles, in the diverse air / water / polymer systems formed by the films, through the sessile drop method. The studied systems were thus the passive coatings: E and E + B, the active coatings: E + CI, E + MO, E + CO, E + CA, and E + B + CA, and the substrate polymers: PP and PET, as control materials. With this objective, an OCA 15EC goniometer (DataPhysics Instruments GmbH, Filderstadt, Germany) was employed to deposit water droplets on the assayed film surfaces, and its SCA20 software was used for data acquisition and image analysis purposes. Tests were carried out at room conditions in an air atmosphere, by carefully dropping about 8 µL of deionized water with the aid of a dispenser syringe. The static contact angles formed between the water droplets, the film surfaces, and the air atmosphere, were measured 60 s after their deposition, by analyzing the images obtained, and by fitting their shape equations to the Young - Laplace model. Assays were performed on, at least, five different locations of each film sample, and in triplicate for each studied material, in order to ensure the reproducibility of the values obtained and to allow their proper averaging.

2.6. Determination of the optical properties of the multilayer films

The optical properties of the produced films were determined by measuring the material color with a CM-3500D spectrophotometer (Konica Minolta Optics Inc., Tokyo, Japan). The instrument was set to D65 illuminant / 10° observer, equipped with an 8 mm aperture target mask, calibrated with a white calibration plate and a zero calibration box, and programmed to perform three shots in each measurement and subsequently yield the averaged results. The essayed materials were, in this case, the developed active and passive multilayer films, as well as the polymers constituting their substrate layers. Measurements were performed on eight different locations of each film sample, and in triplicate for each studied material; and they were carried out at room conditions of temperature and humidity by placing the film samples onto the device lens and against the surface of a standard white tile. The instrument's software SpectraMagic NX was employed to acquire the color data and to display them in the CIELAB color space. The color coordinates of each film sample: L^* (lightness), a^* (greenness – redness), and b^* (blueness – yellowness), could therefore be obtained, and the corresponding polar

coordinates: C^*_{ab} (chroma or saturation index), and h_{ab} (hue or angle), could easily be estimated from the latter two parameters by introducing them in the following equations:

$$C^*_{ab} = \sqrt{\left(a^*\right)^2 + \left(b^*\right)^2} \quad \text{(V.4)}$$

$$h_{ab} = \arctan\left(\frac{b^*}{a^*}\right) \quad \text{(V.5)}$$

2.7. Determination of the mechanical properties of the multilayer films

The mechanical properties of the diverse manufactured films, and of their substrate polymers, were evaluated by following a test procedure based on the ASTM D882 – 12 standard method [36] with the aid of a MultiTest 1-i universal testing machine (Mecmesin Ltd., Slinfold, UK), equipped with a 100 N static load cell and with small pneumatic plane grips. In detail, the studied materials were cut into strips of 25.4 mm wide and 140 mm long, and the obtained samples were conditioned in climatic chambers at 23 ± 1 °C temperature and 0 ± 5 % of relative humidity for at least 48 h prior to testing. Immediately afterwards, at least 10 specimens of each assayed film were successively extracted from the chambers, inserted between the grips, and firmly held in place with 3 bars of pressure. The instrument's software Emperor was then used to set the grip separation at exactly 100 mm, the cross-head speed at 25 mm/min, and the data sampling rate at 1 kHz. In these test conditions, an increasing load was applied on the film samples over time, causing their elongation, and the corresponding force (F_t) – displacement (ΔL_t) curves were thus obtained. These plots were standardized by transforming them into stress (σ_t) – strain (ε_t) curves with the application of the corresponding definition equations:

$$\sigma_t = \frac{F_t}{A_0} = \frac{F_t}{w_0 \cdot t_0} \quad \text{(V.6)}$$

$$\varepsilon_t = \frac{\Delta L_t}{L_0} \cdot 100 \quad \text{(V.7)}$$

where A_0 is the original cross-sectional area of the tested sample, product of its original width (w_0) and thickness (t_0), and L_0 is the original grip separation. This way, the mechanical properties of the studied materials, namely the ultimate tensile strength, the deformation at break, and the Young's modulus, could be estimated through the graphical assessment of the newly obtained curves.

2.8. Determination of the barrier properties of the multilayer films

The barrier properties of the produced passive films, and of their corresponding substrates, were investigated by measuring their oxygen and carbon dioxide permeances as a function of the relative humidity, following the procedures described in a previous work [33], based in the ASTM D1434 – 82(2009)e1 standard method [37]. Oxygen transport was studied by means of an OX-TRAN model 2/21 ML (Paul Lippke Handels – GmbH, Neuwied, Germany) programmed to measure the oxygen permeance at 23 ± 2 °C and at 0, 35, 50, 75, and 90 ± 0.01 % RH, whereas for carbon dioxide transport, an isostatic permeation apparatus, described in this previous work, was used to measure the gas permeance at 23 ± 2 °C and at 0, 30, 45, 75, 85, and 100 ± 0.1 % RH. In both cases, between two and four film samples were placed in the instrument cells, held in place with high-vacuum silicone, and conditioned for 12 h prior to the permeation tests. The gas permeance was measured every 45 min until constant, and, from that moment, at least three more points were recorded in order to obtain an average value.

2.9. Determination and simulation of the performance of the active packages

Differences in performance between the packages constructed with neat EVOH and those comprising an EVOH / clay nanocomposite were assessed by studying their activity over time in actual working conditions. With this objective, three packages of each type were placed in a climatic room, at 23 ± 1 °C and 30 ± 5 % RH, for one week, and the concentration of carvacrol in their headspace was periodically evaluated. Analyses were performed on a daily basis, by extracting at least three gas samples of 500 µL from their inner atmosphere with the aid of a 1750 Gastight precision syringe (Hamilton Co., Reno, NV, USA), and by injecting them in the inlet port of an HP 5890 Series II Plus gas chromatograph (Hewlett Packard Co., Wilmington, DE, USA). The instrument was equipped with a flame ionization detector (FID) and a 30 m, 0.32 mm, 0.25 µm Agilent HP-5 capillary column

(Teknokroma S.C.L., Barcelona, Spain), programmed in accordance with the procedure described in previous work [23], and calibrated by injecting carvacrol in known concentrations. After averaging the results acquired in each assay period, two experimental curves for the evolution in time of the concentration of carvacrol in the headspace of both studied packages could be obtained.

In order to assess the effects of the EVOH matrix modification on the package performance more thoroughly, as well as to validate the experimental procedure carried out, a mathematical model based on the finite element method was applied to the assayed packages, and the simulation of their activity over time was therefore performed. This model had already been developed specifically for those systems in prior work [23] with the aid of the Chemical Transport of Diluted Species physics interface of the COMSOL Multiphysics 4.2 modeling suite (COMSOL AB, Stockholm, Sweden). In the present case, the model was fed with the fundamental hypotheses and physicochemical properties gathered in the previous studies [23, 33], as well as with the geometric characteristics and integration conditions corresponding to the systems investigated here, further detailed throughout this paper. As a result, two theoretical curves for the evolution in time of the concentration of carvacrol in the headspace of both packages could be obtained, and were then subsequently compared with their experimental counterparts.

2.10. Data analysis

The values for all the parameters and coefficients presented in this work are expressed as "$\left(\bar{x} \pm \varepsilon\right)$ units," where $\bar{x}$ stands for the sample mean of parameter x, and ε stands for its absolute error. This absolute error is equal to the sample standard deviation for the measured variables, and was determined by propagation of uncertainty (partial derivatives method) for the calculated variables.

Statistical analysis of the results obtained for mechanical properties was performed with the aid of IBM SPSS Statistics 21 commercial software (IBM Corp., Armonk, NY, USA). Concretely, a one-way analysis of variance (ANOVA) was carried out, and differences found between mean values for the studied materials were assessed by means of confidence intervals using Tukey's test at a $p \leq 0.05$ level of significance.

3. RESULTS AND DISCUSSION

3.1. Assessment of stability of EVOH coatings on pretreated PP and PET substrates

Although both PP and PET substrates can easily be coated by hydroalcoholic EVOH solutions, yielding highly transparent and homogeneous multilayer films, the large differences in chemical structure and polarity existing between both materials, and thus their low chemical compatibility, prevent them from developing a sufficient anchorage mechanism in their contact interface. This lack of coating adhesiveness leads to film delamination when slight tensile forces are applied between the material layers, such as during the manufacturing of the films or during the formation of the packages, or when external compounds, such as water or plant essential oils, are scalped from the preserved food products [38].

Table V.1. Qualitative results of the adhesion and thermosealability tests for the four anchorage technologies applied on the multilayer films, and sealing strength on uncoated substrates and on those coated with EVOH through the application of corona discharge + PEI-based primer.

Anchorage technology	Adhesion	Thermosealability
UV radiation	weak	none
Corona discharge	moderate	poor
Corona discharge + PU-based primer	none	none
Corona discharge + PEI-based primer	strong	good

Sealed films	Sealing strength (N)	Type of failure
PET // PET	5.7 ± 0.9	Seal opening
PET / E // E / PET	12.1 ± 2.4	Seal opening + delamination
PP // PP	8.0 ± 1.0	Seal opening
PP / E // E / PP	21.6 ± 3.0	Seal opening

Since in this work all the manufactured materials were intended to be employed in the construction of active packages for fresh-cut salad or similar products, containing essential oils or their constituents as natural antimicrobials, the application of an effective anchorage treatment on the PP and PET substrates was indispensable to ensure good stability of the deposited EVOH coatings. With this objective, four different technologies for surface modification, namely UV irradiation, corona discharge, and corona discharge followed by the application of PU or PEI-based primers, were

implemented in the manufacture process of the developed films, and qualitatively evaluated by means of Scotch tape adhesion tests. The results obtained are displayed in **Table V.1** and, as shown, for every applied treatment no distinction is made between both assayed substrates, because no relevant differences were found in their adhesiveness behavior.

With respect to the diverse technologies investigated, UV irradiation failed to produce a satisfactory adhesion on either PP or PET substrates, thus yielding easily delaminable films, although in the former material some peeling resistance was observed during the progression of the tests (weak adhesion). The corona discharge, by contrast, produced reasonably good results in both materials, complicating or even impeding their delamination, although, according to observation during the tests, the surface treatment had not been applied uniformly, and, in consequence, the points of anchorage between layers were heterogeneously distributed (moderate adhesion). Finally, the casting of primers after corona pretreatment yielded very opposite results depending on the substance applied. In this sense, whereas the PEI-based primer produced an excellent adhesion with both the EVOH coatings and the PP or PET substrates, making their detachment absolutely impossible (strong adhesion), the PU-based primer not only failed in providing some adhesion between layers, but, owing to its obstructive location, also prevented the corona-treated surfaces of the substrates from interacting with the coatings, and thus from generating some anchorage points between both (none adhesion). These facts led the corona discharge treatment to reach worse results when followed by a PU-based primer, or better when followed by PEI-based one, than when applied alone.

In addition to the adhesion tests, the stability of the EVOH coatings on the pretreated PP or PET substrates was also assessed by subjecting the manufactured films to thermosealing tests, carried out with the aid of a manual impulse heat sealing machine. The performance of these parallel assays was motivated by two main reasons. Firstly, the thermosealing properties of the studied materials were closely related to the hermeticity attainable in the final targeted packages, key characteristic of their structural design. Secondly, the sealing capabilities of the developed films were also dependent upon the force of adhesion between their material layers and thus their evaluation could contribute to corroborating the results obtained in the former tests. Just as for those essays, the qualitative results of the thermosealability tests are displayed in **Table V.1**, and for every applied treatment no distinction is made between both studied substrates either.

As this table shows, there was a good correlation between the results yielded by both tests for the four different treatments applied on the multilayer films. According to this, materials manufactured with UV-irradiated substrates were not sealable, owing to the low strength of the anchorage points created

between layers, and thus of the final seal formed between films. Materials subjected to corona discharge, in turn, were only sealable to a limited extent, because, although the obtained seal presented quite good appearance and seemed to attach both films firmly, when slight tensile forces (≤ 1 N) were applied on the joint it promptly failed and the films were easily detached again. This phenomenon could be product of an irregular application of the anchorage treatment, as explained above in the results of the adhesion tests. Lastly, films formed through primers application yielded extreme results depending upon the substance employed. In agreement with the adhesion essays, materials containing a PEI-based primer were perfectly sealable, because very strong tensile forces had to be applied to separate the films, and also films were not detached by seal failure but by matrix failure, while the sealing area remained intact. On the contrary, materials containing a PU-based primer could not be assayed because of the absolute lack of adhesion between their layers, as reported before in the previous tests.

Finally, since the substrates coated through the application of a PEI-based primer yielded the best results in both stability tests, the quantitative analysis for the determination of the sealing strength was only carried out on these materials. The values found are also included in **Table V.1,** and compared with those obtained for the uncoated substrates. As can be seen, the EVOH-coated films presented the highest peel strengths, thus confirming the excellent sealability properties of EVOH copolymers, as published elsewhere [30]. Also, the improvement observed with respect to the uncoated films is probably due to the lower melting temperature of EVOH with respect to the substrate polymers, especially to the PET film. Hence, since all the sealing tests were carried out under the same testing conditions, the higher percentage of polymer melted during the essays would be responsible for the stronger sealings.

To conclude, the application of corona discharge followed by a PEI-based primer was definitely the best anchorage technology available to bond EVOH coatings with PP or PET substrates, and it was therefore implemented in the manufacturing process of the active multilayer films. Obviously, the physicochemical assays described below were only performed on such films.

3.2. Assessment of retention of active agents in the coating layers of multilayer films

The retention of a chemical compound in a polymeric matrix is a function of the thermodynamic equilibrium of the substance between the system phases involved, in this case: air, coating and substrate, and of its kinetics within them. Since some of the active agents studied in this work are known to show volatility as well as a considerable solubility in other polymeric materials, and thus to undergo a substantial migration to the adjacent phases over time, especially in highly hot and/or humid conditions [23, 25, 26], the evaluation of their remaining concentration in the coating and substrate layers of the multilayer films, immediately after their manufacturing and after long-term storage in reels, was essential to assess their retention in the original carrier matrices. For this reason, all the concentrations involved were measured at the mentioned moments by thermal desorption and GC analysis, and subsequently introduced in the previous equations (V.1) and (V.2), to finally estimate the percentage efficiency of the incorporation process for the active agent, E_i^F, and its partition coefficient between the film layers, $K_i^{C/S}$. Since both parameters quantify the tendency of the embedded compounds to transfer over time to other system phases, i.e. air or substrates, respectively, they are considered good indicators of their retention in the coating layers.

The results for the incorporation efficiencies of the active agents in the coating layers of the multilayer films, together with their corresponding initial and nominal concentrations, are collected in **Table V.2**, whereas the values estimated for the partition coefficients are detailed in **Table V.3**. As **Table V.2** shows, the efficiencies of the incorporation procedure range, in general terms, between 40 and 60 % for all the materials and compounds essayed. These values mean important losses of activity during the manufacture of the films, probably produced by evaporation during the processes of preparation and application of the coating solutions. This hypothesis can also be reinforced by the fact that all the reported efficiencies show quite high correlation with the volatility of the embedded compounds. In fact, citral, the most volatile substance among the active agents studied in this work, yielded very low efficiencies in both PP and PET-based films, on which grounds it was incorporated with the highest nominal concentration. However, and as can be seen in this **Table V.2**, the performance of a matrix modification in the EVOH coating, by embedding a 2 % of bentonite nanoclay in its structure, resulted in a great enhancement of its retention capacity, with an increase of about 22 % with respect to the original value.

Table V.2. Initial and nominal concentrations of the active agents in the coating layers of the multilayer films, and efficiencies of the incorporation process.

Active multilayer film	$C^F_{i\,0}$ (%)	$C^F_{i\,n}$ (%)	E^F_i (%)
PP / E + CI	4.3 ± 0.4	10	43 ± 4
PP / E + MO	4.6 ± 0.2	7.5	62 ± 3
PP / E + CA	3.8 ± 0.1	7.5	50 ± 1
PP / E + B + CA	4.6 ± 0.2	7.5	61 ± 3
PET / E + CI	4.6 ± 0.3	10	46 ± 3
PET / E + CO	3.0 ± 0.6	7.5	40 ± 8

Table V.3. Equilibrium concentrations of the active agents in the coating and substrate layers of the multilayer films, as derived from the mass balance depicted in equation (V.3), and their partition coefficients between both materials.

Active multilayer film	$K_i^{C/S}$	$C^C_{i\,\infty}$ (%)	$C^S_{i\,\infty}$ (%)
PP / E + CI	1.5 ± 2.1	0.71	0.47
PP / E + MO	42.4 ± 2.9	5.10	0.12
PET / E + CI	1260 ± 240	9.76	0.01
PET / E + CO	6.0 ± 5.6	1.22	0.20

Finally, the partition coefficients of the active agents between the coating and substrate layers, as **Table V.3** shows, are all noticeably higher than the unity, up to three orders of magnitude in some case, and are thus in agreement with the value reported in a previous work for the partition of carvacrol between EVOH and PP, which, at room temperature and dry conditions (23 °C and 0 % RH), was of about 10000 [23]. These results mean that all the investigated compounds, that is, essential oils and their constituents, are far more soluble in EVOH than in PP or PET matrices, which is very advantageous for the retention of the active agents in the coating layers. However, considering that the substrate layers are about 26 times thicker than their corresponding coatings in all cases, the amount of substance finally transferred to the former material after 6 months of storage can become significant in some. In this context, citral is worth mentioning, since it shows extreme behaviors depending upon the substrate employed. Indeed, it undergoes an intense migration towards the PP layer but its lower affinity to the PET matrix makes it attain a high retention in the EVOH coating, which

must be taken into account when it comes to employing these materials in the construction of active packages. In order to better illustrate such behaviors, the expected concentrations at equilibrium of the active agents in the coating, $C_{i\infty}^{C}$, and substrate layers, $C_{i\infty}^{S}$, of the multilayer films, assuming a value of 100 % for the incorporation efficiency, have been estimated from the reported values of the nominal concentrations and the partition coefficients by introducing them in the previous equations (V.2) and (V.3). The results obtained are also displayed in **Table V.3**, and, as shown, in those films presenting lower values of the partition coefficients the greater thickness of the substrate layers with respect to their coatings can lead to the virtual exhaustion of the active agents in the latter materials.

3.3. Assessment of the surface properties of the multilayer films

Because all the multilayer films developed in this work were intended to be used in the construction of active packages for minimally processed vegetables, good optical characteristics, such as high gloss or transparency, were a strong requirement for them. However, the high water content of this foodstuff could saturate their headspace atmosphere with humidity, and subsequently promote its condensation on their inner surfaces, giving them a foggy appearance and thus a limited transparency. The formation of small water droplets on the packaging films, responsible for the light scattering phenomena, is a function of their surface properties, and, in particular, of their wettability. Hence, this property was investigated on the manufactured materials by measuring static contact angles of water droplets on their surface through the sessile drop method with the aid of a goniometer, and the results obtained were plotted in **Figure V.1**.

As this figure shows, contact angles of untreated PP and PET substrates are quite high, of about 98 and 72° respectively, which proves their hydrophobic nature in their original conditions, especially in the former material, owing to its lower polarity. Surprisingly, coatings of neat EVOH, a highly hydrophilic polymer, also show a high value for this parameter, around 99°, very similar to that reported for PP. This result means that, despite its hydrophilicity, EVOH shows a great hydrophobic behavior when its surface chains are not given enough time to interact with the water molecules. In any case, all three polymers seem to be naturally hydrophobic under those experimental conditions, which could pose some difficulties when it comes to fixing inks or to removing fogging in the final packages. However, when an active agent is embedded into the EVOH matrix, the contact angles drop dramatically, between 33 and 46 % from the original value, reaching a minimum at about 53° for the marjoram oil.

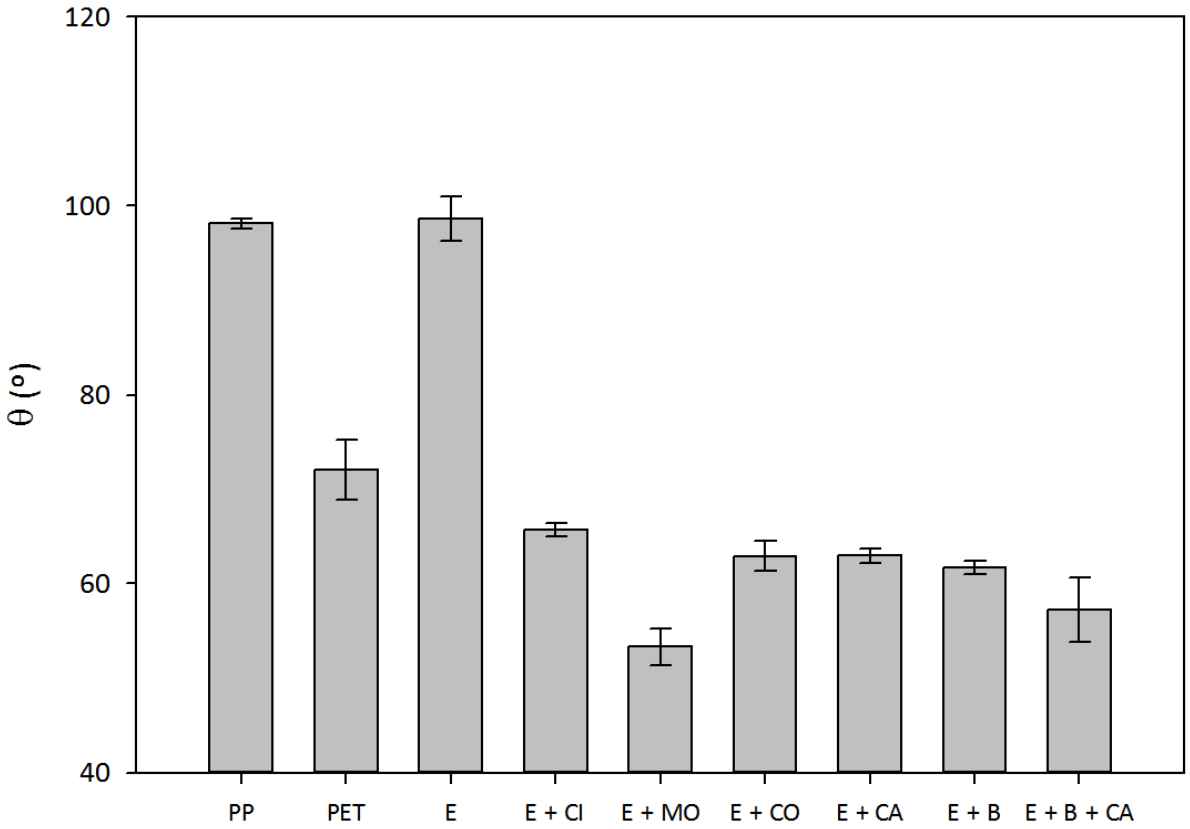

Figure V.1. Static contact angles of water droplets on the surfaces of the multilayer films.

This phenomenon can be due to the presence of active molecules on the material surface, which, owing to their greater polarity, could substantially increase its interactions with water, and thus its wettability. In addition, the incorporation of only 2 % of bentonite nanoclay in its structure is also capable, by itself, of reducing its contact angle by 37 %, and, as a result, of reaching even lower values, up to 57°, when combined with carvacrol as active agent. In this case, the presence of numerous nanometric particles of bentonite, a highly hydrophilic material which can absorb several times its weight in water, in the EVOH surface could also multiply its interactions with the water molecules and, consequently, further enhance its wettability. This result is also in agreement with the findings in a previous study [33], where 2 % of bentonite was reported to increase the hydrophilic behavior of EVOH by 17 %.

3.4. Assessment of the optical properties of the multilayer films

Just as explained in the last section, since the target packages of the materials studied in this paper were hermetic bags intended to preserve ready-to-eat food products, their optical properties had to be as good as possible in order to maintain the appearance of quality of the contained foodstuffs. However, given that all the developed films comprised active compounds or inorganic fillers of natural origin, they could become slightly opacified or colorized by them, thus losing their original aspect. For this reason, the optical properties of all the manufactured active and passive films were studied with a spectrophotometer, by measuring their color coordinates and subsequently displaying the acquired data in the CIELAB color space. The values found for their lightness were plotted in a bar graph in **Figure V.2**, whereas the values obtained for their other color parameters were converted into chroma and hue parameters, through equations (V.4) and (V.5), and plotted in a polar graph in **Figure V.3**.

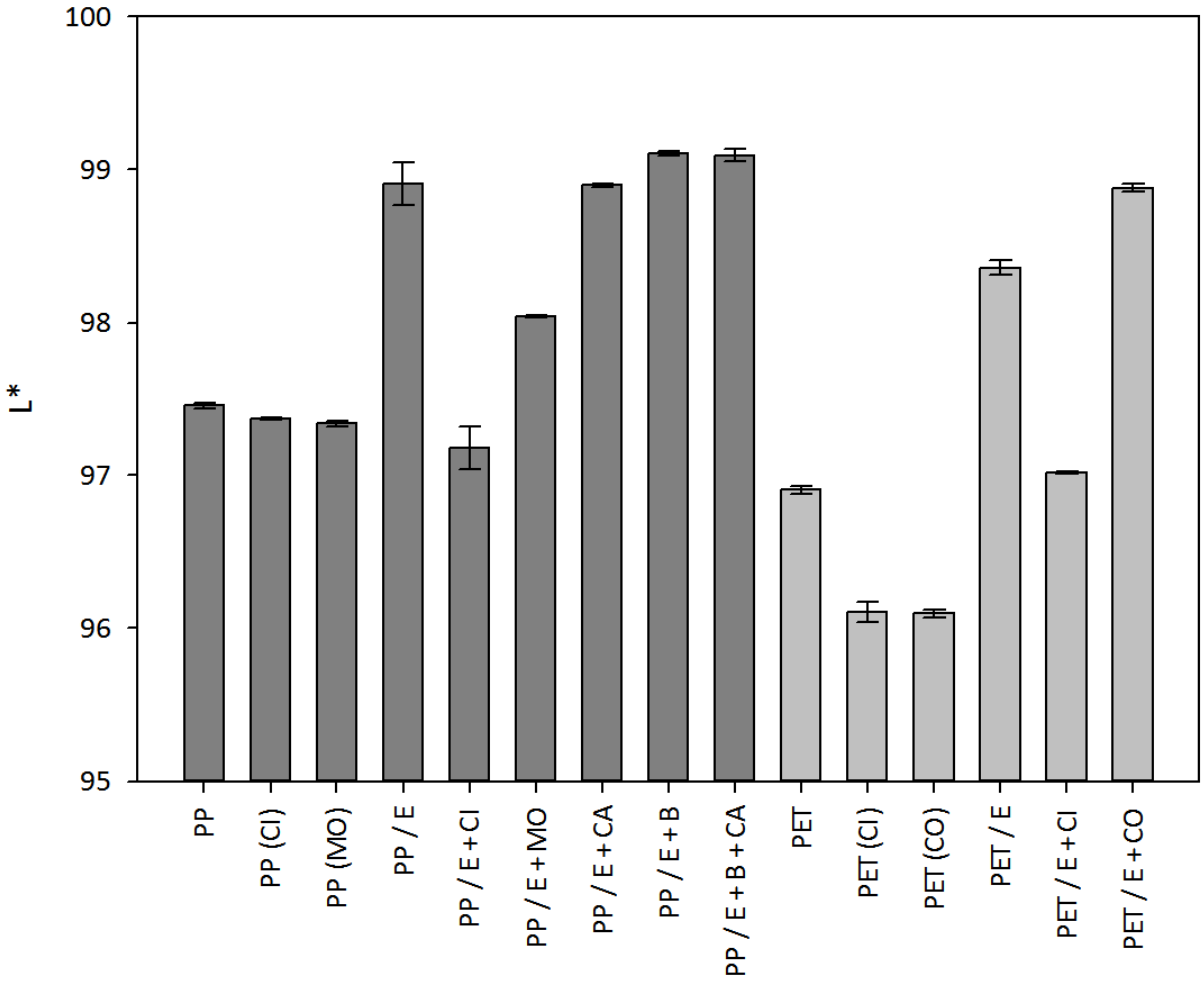

Figure V.2. Lightness of the multilayer films on the CIELAB color space.

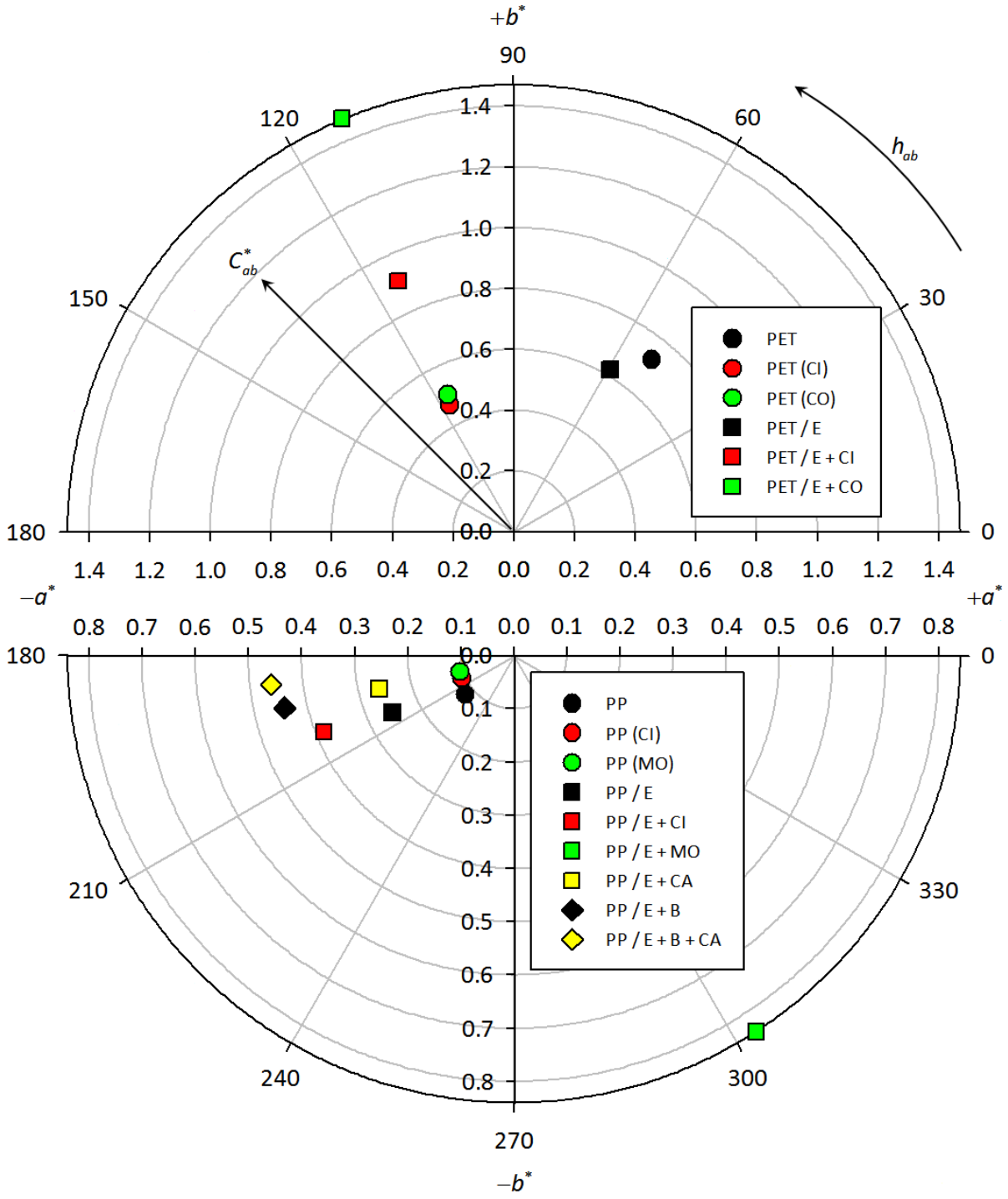

Figure V.3. Chroma and hue of the multilayer films on the CIELAB color space.

With respect to lightness, both PP and PET substrates showed very high values, of about 97, owing to their high purity and homogeneity qualities. However, after being stored for six months in direct contact with active materials their lightness became slightly reduced, probably due to the absorption of active compounds migrating from their EVOH coatings. On the opposite, when both substrates were

coated by neat EVOH their lightness increased significantly, by about a 1.5 %, although when those coatings also included an active agent in their structure the value of this parameter decreased again, between 0.01 and 1.75 %, depending upon the substance incorporated. From a macroscopic inspection of the manufactured films it could be stated that all the EVOH coatings showed a whitish appearance, which could contribute to the higher lightness observed in those materials, and this phenomenon could be due to the fact that, since a coating technology based on gravure printing was employed to apply the EVOH solutions on the substrate polymers, they were not casted as a single film but rather deposited as small individual droplets, therefore yielding highly light scattering polymer coatings. However, when an active compound was embedded in those matrices lightness decreased again by absorption phenomena, just as occurred in the substrate materials. Finally, the effect of the incorporation of a 2 % of bentonite nanoclay in the EVOH coatings was an increase of about a 0.2 % in their lightness, probably due to the additional scattering phenomena introduced by the dispersed particles. In any case, it must be noticed that all the values reported in the graph range only between 96 and 99, so it can be concluded that the lightness of the studied materials can barely be modified by the presence of either active compounds or inorganic fillers.

Regarding the chroma and hue parameters, whereas PP substrates showed almost no coloration, with a chroma value near zero, PET substrates showed a substantial chroma, of about 0.7, with a slight reddish / yellowish tonality. In addition, when both polymers were analyzed after absorbing active compounds from their EVOH coatings, very opposite results were found, unlike for the lightness study. In detail, although both materials reduced their chroma in similar proportions, whereas PP practically conserved its hue, PET substrates moved sharply from a reddish to a greenish tonality, while maintaining their yellow intensity. Furthermore, when both substrates were coated by neat EVOH different behaviors were also observed, concretely, the chroma value was slightly reduced for PET while doubled for PP, although both materials shared a noticeable displacement in the green direction. This movement was further sharpened with the incorporation of active agents to the EVOH coatings, especially in the case of the PET-based films, which reached a deeper yellowish tonality while changing their redness to greenness, thus attaining a higher value for their chroma, between 0.9 and 1.5, depending on the compound embedded. Finally, the addition of a 2 % of bentonite nanoclay to the EVOH matrices of PP-based films again doubled their chroma value, up to 0.45 approximately, also moving them on the way towards the greenish region. To summarize, it can be stated that in general terms, the coating of PP or PET substrates with a neat EVOH layer does not significantly modify their color, but when natural substances, such as active compounds or inorganic fillers, are also present in the polymers, they will produce a considerable increase of the chroma and a substantial displacement

to the greenish and yellowish regions in most cases, probably due to their characteristic and predominant colorations. However, and just as occurred for lightness, it must be remarked that no studied material presented chroma values greater than 1.5, which is quite a low amount. Hence, it can be concluded that all the changes observed in the coloration of the films will not be macroscopically perceptible to the naked eye, and thus will virtually not affect their optical properties in a significant way either.

3.5. Assessment of the mechanical properties of the multilayer films

Among the physical properties of relevance for food packaging applications, the mechanical ones are probably the most important since films must undergo numerous and different strains during their manufacturing, as well as during the filling, transportation, and commercialization of the final packages. In addition, the potential scalping of diverse organic substances from the preserved food products by the packaging materials, such as water or plant essential oils, can deteriorate their polymeric structure and thus reduce their mechanical performance. Because of this, some mechanical properties, namely the ultimate tensile strength, the deformation at break, and the Young's modulus, were determined on the diverse developed active and passive films, by elongating them under increasing load forces in a universal testing machine, and by converting the obtained force – displacement curves into stress – strain curves through the application of equations (V.6) and (V.7). The values finally found for the three mentioned parameters are plotted in bar graphs in **Figure V.4**, together with their corresponding subset tags, according to the grouping of means yielded by the post-hoc statistical test.

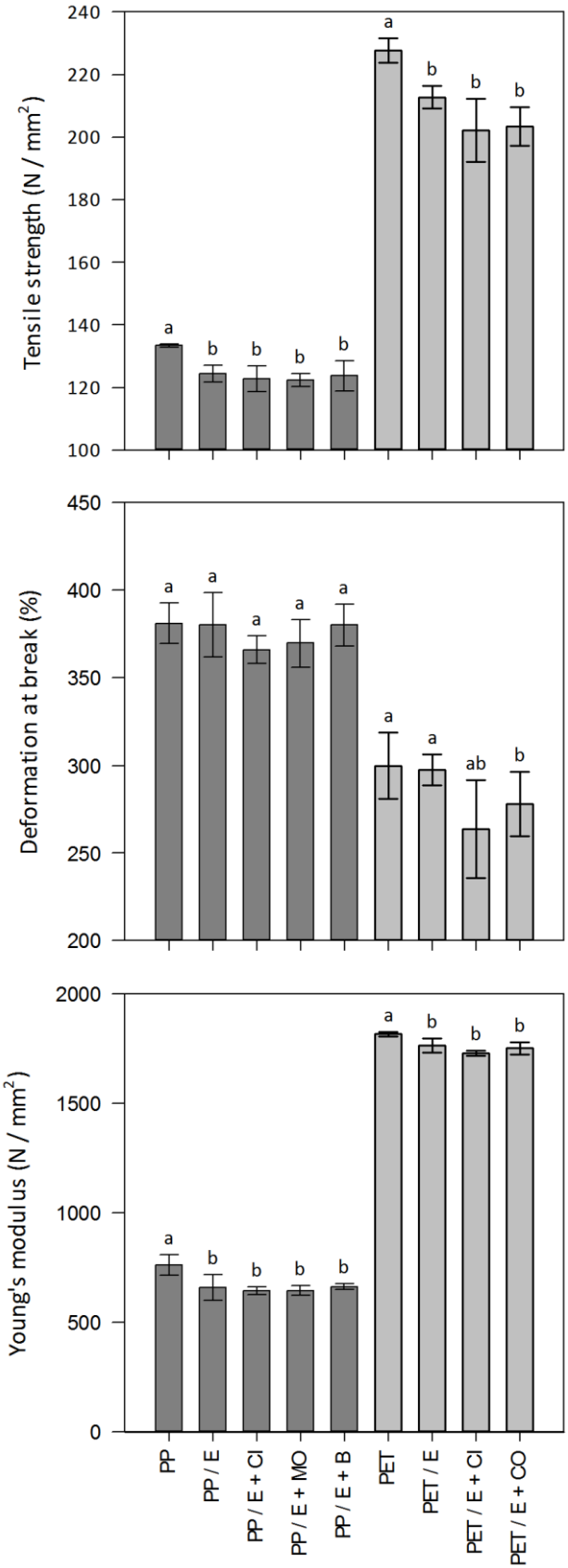

Figure V.4. Ultimate tensile strength, deformation at break, and Young's modulus of the multilayer films. Letters correspond to homogeneous subsets of means with significant differences.

In relation to the ultimate tensile strength, as this figure depicts, PP substrates resisted a considerable level of stress, around 130 N/mm^2, whereas PET materials almost doubled this number, up to 230 N/mm^2, when tested in their original conditions. However, when coated with a layer of EVOH these values decreased significantly, by about 7 %. Furthermore, if this material, in turn, contained an active compound, a further reduction of about 1.6 and 5 %, respectively, was also observed in both types of films with respect to those comprising the neat polymer, although according to the ANOVA test, the differences found were not significant. This slight worsening of the tensile strength in both materials can be attributed to two different facts. Firstly, given that the EVOH coatings were not deposited on the substrates as single layers but as small individual droplets, as explained in the previous section 3.4, they would only increase the thickness of the final films, but could not provide any additional noticeable resistance to the load forces applied. Hence, and according to equation (V.6), the tensile stresses finally obtained would always be lower for them than for their corresponding substrates. Secondly, the scalping of organic substances from these coatings by their substrate materials, such as water or 1-propanol, could also have plasticized them, therefore reducing their ultimate tensile strength, but this phenomenon could even have been aggravated with the absorption of active compounds, since they are known to be good plasticizers of such polymers, and, in addition, their activity could also have promoted some reaction with them, thus somewhat degrading their molecular structure. To end, the presence of 2 % of bentonite nanoparticles in the EVOH matrix produced a slight increase of the tensile strength of about 0.5 % with respect to the unfilled film, which, despite being statistically insignificant, can be indicative of some improvement in its mechanical performance, in agreement with the results reported elsewhere for other clay nanocomposites.

Regarding the deformation at break, in this case both substrates reached high values, around 380 % for PP and 300 % for PET, which were also slightly lower for their EVOH-coated counterparts, by about 0.2 and 0.7 % respectively, although without statistical significance ($p > 0.05$). Equally, in their active equivalents further reductions were also observed with respect to the passive films, up to 3.9 and 12.8 % respectively, which were significant only for the PET-based materials. These results could also be explained by the scalping effect mentioned above, through which the studied substrates would absorb diverse organic substances from their EVOH coatings, and, especially, from the active ones, and consequently undergo some matrix deterioration, such as a weakening or perhaps breaking of its molecular bonds, which, besides leading them to premature failure, would also prevent them from reaching such large deformations. Concerning the modification of the EVOH structure by the addition of bentonite, in this case no differences were found with respect to the neat polymer.

The assessment of the Young's modulus, in turn, yielded similar results to the other two parameters, thus contributing to corroborating the hypotheses posed above. In the case here, PP substrates showed a moderate value for this property, around 760 N/mm^2, whereas PET materials could attain a far higher number, of about 1820 N/mm^2, owing to their greater stiffness. However, the values reported for both polymers were significantly reduced when an EVOH coating was applied, by 13.5 and 2.8 % respectively, and further decreases were observed again with respect to these new materials when active substances were also incorporated, up to 2 % more, depending upon the compound embedded. In addition, and just as for the ultimate tensile strength, the presence of 2 % of bentonite nanoclay increased the value of this parameter by approximately 0.75 %, although this difference once more lacked statistical significance, as the previous results.

In summary, it can be stated that all the variations reported for the three studied parameters are indicative that, in effect, some scalping phenomenon is occurring in the developed multilayer films, especially in the active ones, which, by either plasticization or reaction mechanisms, could be responsible for the softening or degradation of the structure of their substrates, and thus of the lower values found for their ultimate tensile strength, deformation at break, and Young's modulus. This behavior can be partially counteracted by the presence of bentonite nanoparticles in the coating matrix, although, according to the values detailed, only to a low extent. In any case, it must be remarked that none of the properties assessed in the manufactured films was observed to vary by more than 15 % with respect to their corresponding substrates, therefore it can be concluded that their mechanical performance will not become substantially deteriorated in the final packages.

3.6. Assessment of the barrier properties of the multilayer films

Given that the food packages aimed in this work were sealed bags for the preservation of fresh-cut salad or similar products, as mentioned above, all the developed multilayer films had to allow an adequate gas exchange between their inner and outer atmospheres as to properly maintain the quality and sensory characteristics of the contained foodstuffs. However, the simple application of a thin coating of EVOH, a high-barrier polymer, on the original PP films, for example, could lead to a substantial decrease of the gas transmission rate through these packaging materials. Consequently, it could put the preserved food products at risk of developing strange flavors or smells throughout their shelf life, by effect of the excessive accumulation of carbon dioxide in the package headspace, and thus at risk of becoming inedible. For this reason, the barrier properties of all the manufactured passive

films and substrates were studied by measuring their oxygen and carbon dioxide permeances as a function of the relative humidity, in both isostatic permeation instruments, yielding as a result the values collected in **Table V.4**.

Table V.4. Oxygen and carbon dioxide permeances in the passive multilayer films and their substrates as a function of the relative humidity.

Films	$\wp^F_{O_2} \cdot 10^{15}$ (m³ (STP) / (m² · s · Pa))				
	0 % RH	35 % RH	50 % RH	75 % RH	90 % RH
PP	148 ± 2				
PP / E	0.85 ± 0.03	1.49 ± 0.08	3.30 ± 0.13	34.8 ± 0.2	112 ± 2
PP / E + B	0.86 ± 0.05	0.76 ± 0.06	0.79 ± 0.08	12.5 ± 0.1	111 ± 1
PET	4.8 ± 0.2				
PET / E	0.76 ± 0.07	0.84 ± 0.09	1.20 ± 0.09	2.98 ± 0.06	3.83 ± 0.03

Films	$\wp^F_{CO_2} \cdot 10^{15}$ (m³ (STP) / (m² · s · Pa))					
	0 % RH	30 % RH	45 % RH	75 % RH	85 % RH	100 % RH
PP	1170 ± 40					
PP / E	7.8 ± 0.2	9.83 ± 0.08	11.4 ± 0.1	48.8 ± 0.5	146 ± 2	247 ± 2
PP / E + B	7.61 ± 0.19	7.71 ± 0.17	11.0 ± 0.3	30.5 ± 1.0	129 ± 2	234 ± 15
PET	56.3 ± 0.8					
PET / E	9.36 ± 0.18	10.2 ± 0.9	11.2 ± 0.2	30.7 ± 0.4	35.2 ± 0.5	39.4 ± 0.3

As this table shows, for the substrate polymers no distinction is made between the diverse relative humidities assayed in the permeation tests, because, although five or six different conditions were considered, depending upon the compound studied, no relevant differences were found in the gas transmission rates, according to the well-known hydrophobic behavior of those materials. With respect to the values displayed, the oxygen permeance was quite high in both polymers, especially in the PP film, although the transport of carbon dioxide yielded even higher figures for this parameter, about 10 times more on average for both substrates. However, when a thin coating of EVOH was applied on those materials, their permeance dropped dramatically, being able to reach, in dry conditions, about a 1/160 of its original value for the PP-based films, and about a 1/6 for the PET ones, as expected from the high barrier characteristics of such a polymer. Nevertheless, owing to its highly

hydrophilic nature, as reported elsewhere [27 – 29], this barrier effect gradually dissipated as the relative humidity increased, undergoing a sharper change at 75 % RH, probably due to the proximity of the glass transition point [33], and attaining permeance values at 100 % RH somewhat comparable to those reported for the uncoated substrates, mostly between 70 and 80 % of the original values. Finally, the incorporation of 2 % of bentonite nanoclay to the EVOH coatings produced a further decrease of the films' permeances to both gases when they were assayed at moderate relative humidities, up to 76 % with respect to the unfilled materials, whereas at extreme ambient conditions the differences found did not exceed a 5 %. As a conclusion, it could be asserted that, given the highly humid conditions expected in the package headspace during the product preservation time, the presence of a thin coating layer of EVOH or bentonite-filled EVOH on the packaging materials will not affect their gas transport in a substantial way, and thus will neither modify the respiration rate of the contained foodstuffs so much as to significantly deteriorate their quality or sensory characteristics.

3.7. Assessment of the performance of the active packages

In previous works, food packages consisting of EVOH-coated PP films containing essential oils or their constituents as active antimicrobial agents were successfully developed and tested for the preservation of fresh-cut salad and fish products. However, the assays carried out in both systems revealed an unconstrained free release of the active compounds to the headspace of the packages, which induced an early peak of antimicrobial activity at the beginning of the product shelf-life, followed by a rapid decay in a few days. For this reason, a matrix modification based on the incorporation of bentonite nanoclay was assessed on EVOH active films in a subsequent study [33], yielding substantial improvements in the retention capacity and rate of release of the active agents. Hence, following this line, the effects of such modification on the performance of active packages, assayed in actual working conditions, were investigated in the present work, by determining their activity over time with a gas chromatograph, and by simulating it through the application of a mathematical model. Both experimental and theoretical results are displayed in **Figure V.5**, where the evolution in time of the concentration of carvacrol in the headspace of the packages has been plotted for both original and nanocomposite active films.

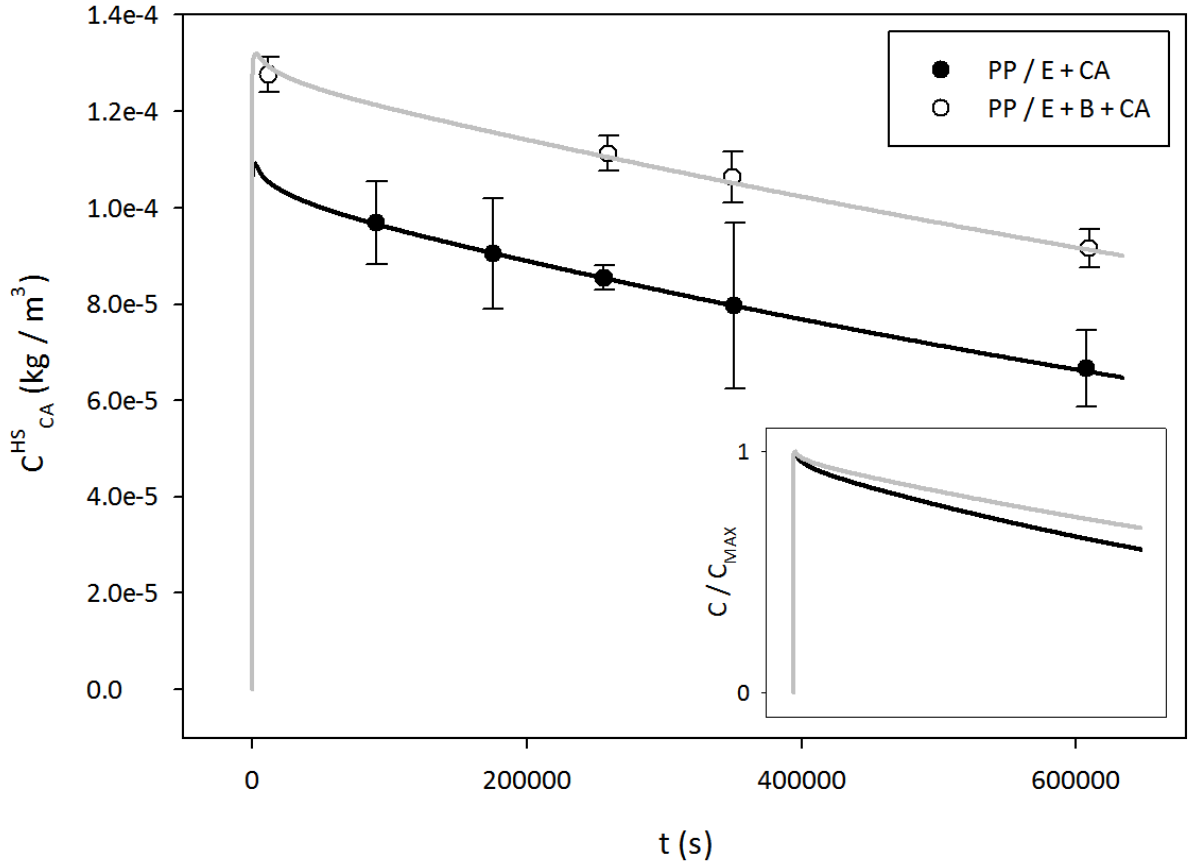

Figure V.5. Evolution in time of the carvacrol concentration in the headspace of packages containing a neat or nanocomposite EVOH active layer. Symbols correspond to experimental values and curves correspond to theoretical performances predicted by the mathematical model. Inset graph: normalized curves of theoretical performances of the active packages in full time scale.

As can be seen in the graph, both theoretical curves describe the experimental behavior of the assayed packages very accurately, meaning that both the test procedure carried out and the mathematical model applied, were perfectly valid for the systems and conditions studied in this work. On another matter, the evolutions in time of the carvacrol concentration described by both curves are analogous to those reported in a previous work for a similar package [23], since they exhibit a maximum value immediately after the beginning of the storage period, followed by a gradual and continuous decline for the remaining days. In this case, neither the initial overshoot nor the subsequent drop of antimicrobial activity are as pronounced as in the previous study, probably owing to the lower relative humidity existing in the storage room (30 % vs. 70 %), although the performance of the active packages still diminishes quite rapidly with the course of the preservation time, in agreement with what was observed in the mentioned work.

Nevertheless, the addition of only 2 % of bentonite nanoparticles into the EVOH active layer noticeably improved both the release rate of the embedded compound and the retention capacity of the carrier matrix. In effect, as **Figure V.5** shows, the peak concentration of carvacrol in the headspace of the packages, which mainly depends upon the amount of substance finally retained in their active layer, is about 21 % higher in those containing the nanocomposite material than in the original ones. In addition, since this difference is maintained or even increased during the preservation time, up to 39 % at the end of the storage period, it means that the release rate of the active compound must also be slower in those systems. This effect can be visualized better in the inset graph, where the theoretical curves for the evolution in time of the carvacrol concentration in the package atmosphere have been normalized to their maximum values, in order to become comparable from a kinetic point of view. As a result, an average reduction of about 23 % in the slope of the nanocomposite curve is finally observed, demonstrating that the incorporation of bentonite nanoclay to the carrier matrix not only increases antimicrobial activity in the package headspace, by reducing its losses to the external atmosphere, but also contributes to maintaining it more constant and stable throughout the product's shelf life.

4. CONCLUSIONS

In this work, diverse passive, active, and nanocomposite multilayer films, selected from the materials developed in previous studies, were subjected to several physicochemical tests in order to demonstrate their suitability for food packaging applications. In detail, the properties investigated were: the stability of EVOH coatings on PP and PET substrates pretreated with different anchorage technologies; the mechanical, optical, surface, and barrier properties of active multilayer films, consisting of EVOH coatings on PP and PET substrates containing essential oils or their constituents as natural antimicrobials, as well as the retention of these compounds in their carrier matrices; and lastly, the effects of a matrix modification, based on the addition of a 2 % of bentonite nanoclay into an EVOH active layer, on the performance of PP / EVOH packages containing carvacrol as active agent, and assayed in actual working conditions.

The results obtained indicated the application of corona discharge followed by a PEI-based primer as the best anchorage technology available to bond EVOH coatings with PP or PET substrates. With respect to the active agents incorporated, their retention into EVOH matrices ranged from low to moderate, depending upon the substance included and upon the substrate employed. Nevertheless, the final manufactured films showed a substantial improvement in their wettability characteristics, and no noticeable or important differences in their mechanical, optical, or barrier properties. The inclusion of bentonite nanoparticles into EVOH active coatings, in turn, considerably enhanced the performance of the preservation system, by increasing its retention capacity for the embedded compounds, while reducing their release rate to the package headspace. In addition, the surface and mechanical properties of these nanocomposite materials were also slightly improved, whereas their optical appearance stayed practically the same.

In conclusion, all the developed active films are perfectly suitable for food packaging applications, and the incorporation of bentonite nanoclay to their carrier layers is strongly recommended, as to improve their physical properties as much as to increase the performance of the targeted packages, although some additional assays might be then necessary to confirm that the current legal thresholds for the migration of inorganic nanoparticles were never exceeded.

ACKNOWLEDGMENTS

The authors thank the Spanish Ministry of Science and Innovation (projects AGL2009-08776 and AGL2012-39920-C03-01), European Comission (Nafispack project 212544), and Generalitat Valenciana (J.P.C. fellowship) for financial support, ITENE (Associated Unit of CSIC) for scientific collaboration and Mr. Tim Swillens for correction services.

REFERENCES

[1] Rooney, M. L. (1995). *Active packaging in polymer films. Active food packaging*, Blackie Academic & Professional, London, UK.

[2] Gerding, T. K., Rijk, M. A. H., Jetten, J., van den Berg, F., de Kruijf, N. (1996). Trends in food packaging: arising opportunities and shifting demands. *Packaging Technology and Science*, 9 (3), 153 – 165.

[3] Ahvenainen, R., Hurme, E. (1997). Active and smart packaging for meeting consumer demands for quality and safety. *Food Additives and Contaminants*, 14 (6 – 7), 753 – 763.

[4] Floros, J. D., Dock, L. L., Han, J. H. (1997). Active packaging technologies and applications. *Food Cosmetics and Drug Packaging*, 20 (1), 10 – 17.

[5] Vermeiren, L., Devlieghere, F., Van Beest, M., de Kruijf, N., De – bevere, J. (1999). Developments in the active packaging of foods. *Trends in Food Science & Technology*, 10 (3), 77 – 86.

[6] Fernández, M. (2000). Review: Active food packaging. *Food Science and Technology International*, 6 (2), 97 – 108.

[7] Gontard, N. (2000). *Panorama des emballages alimentaires actifs.* Gontard, N. (ed.) *Les emballages actifs*, Tech & Doc Lavoisier, France.

[8] Brody, A. L., Strupinsky, E. R., Kline, L. R. (2001). *Active packaging for food applications,* CRC Press LLC, Boca Raton, FL, USA.

[9] Gavara, R., Català, R., Hernández – Muñoz, P. (2009). Extending the shelf – life of fresh – cut produce through active packaging. *Stewart Postharvest Review*, 5 (4), 1 – 5.

[10] Collins – Thompson, D., Hwang, C. – A. (2000). *Packaging with antimicrobial properties.* Robinson, R. K. (ed.) *Encyclopedia of food microbiology*, Academic Press, London, UK.

[11] Català, R., Gavara, R. (2001). Nuevos envases. De la protección pasiva a la defensa activa de los alimentos envasados. *Arbor*, CLXVIII, 661, 109 – 127.

[12] Cooksey, K. (2001). Antimicrobial food packaging materials. *Additives for Polymers*, 2001 (8), 6 – 10.

[13] Appendini, P., Hotchkiss, J. H. (2002). Review of antimicrobial food packaging. *Innovative Food Science & Emerging Technologies*, 3 (2), 113 – 126.

[14] Vermeiren, L., Devlieghere, F., Debevere, J. (2002). Effectiveness of some recent antimicrobial packaging concepts. *Food Additives and Contaminants*, 19 (suppl. 1), 163 – 171.

[15] Suppakul, P., Miltz, J., Sonneveld, K., Bigger, S. W. (2003). Active packaging technologies with an emphasis on antimicrobial packaging and its applications. *Journal of Food Science*, 68 (2), 408 – 420.

[16] Joerger, R. D. (2007). Antimicrobial films for food applications: a quantitative analysis of their effectiveness. *Packaging Technology and Science*, 20 (4), 231 – 273.

[17] Han, J. H. (2013). *10 – Antimicrobial packaging systems.* Ebnesajjad, S. (ed.) *Plastic films in food packaging,* Elsevier William Andrew, USA.

[18] López, P., Sánchez, C., Battle, R., Nerin, C. (2007). Development of flexible antimicrobial films using essential oils as active agents. *Journal of Agricultural and Food Chemistry*, 55 (21), 8814 – 8824.

[19] Kuorwel, K. K., Cran, M. J., Sonneveld, K., Miltz, J., Bigger, S. W. (2011). Essential oils and their principal constituents as antimicrobial agents for synthetic packaging films. *Journal of Food Science*, 76 (9), R164 – R177.

[20] Suppakul, P. (2011). *15 – Natural extracts in plastic food packaging.* Lagarón, J. M. (ed.) *Multifunctional and nanoreinforced polymers for food packaging*, Woodhead Publishing Limited, Cambrigde, UK.

[21] Tyagi, A. K., Malik, A., Gottardi, D., Guerzoni, M. E. (2012). Essential oil vapour and negative air ions: A novel tool for food preservation. *Trends in Food Science and Technology*, 26 (2), 99 – 113.

[22] Sadaka, F., Nguimjeu, C., Brachais, C., Vroman, I., Tighzert, L., Couvercelle, J. (2013). Review on antimicrobial packaging containing essential oils and their active biomolecules. *Innovative Food Science and Emerging Technologies*, (in press).

[23] Cerisuelo, J. P., Muriel – Galet, V., Bermúdez, J. M., Aucejo, S., Català, R., Gavara, R., Hernández – Muñoz, P. (2012). Mathematical model to describe the release of an antimicrobial agent from an active package constituted by carvacrol in a hydrophilic EVOH coating on a PP film. *Journal of Food Engineering*, 110 (1), 26 – 37.

[24] Cerisuelo, J. P., Bermúdez, J. M., Aucejo, S., Català, R., Gavara, R., Hernández – Muñoz, P. (2013). Describing and modeling the release of an antimicrobial agent from an active PP/EVOH/PP package for salmon. *Journal of Food Engineering*, 116 (2), 352 – 361.

[25] Muriel – Galet, V., Cerisuelo, J. P., López – Carballo, G., Lara, M., Gavara, R., Hernández – Muñoz, P. (2012). Development of antimicrobial films for microbiological control of packaged salad. *International Journal of Food Microbiology*, 157 (2), 195 – 201.

[26] Muriel – Galet, V., Cerisuelo, J. P., López – Carballo, G., Aucejo, S., Gavara, R., Hernández – Muñoz, P. (2013). Evaluation of EVOH – coated PP films with oregano essential oil and citral to improve the shelf – life of packaged salad. *Food Control*, 30 (1), 137 – 143.

[27] Aucejo, S., Marco, C., Gavara, R. (1999). Water effect on the morphology of EVOH copolymers. *Journal of Applied Polymer Science*, 74 (5), 1201 – 1206.

[28] Aucejo, S. (2000). *Estudi i caracterització de l'efecte de la humitat en les propietats barrera d'estructures polimèriques hidròfiles.* Tesi doctoral, Universitat de València, València.

[29] Aucejo, S., Català, R., Gavara, R. (2000). Interactions between water and EVOH food packaging films. *Foods Science and Technology International*, 6 (2), 159 – 164.

[30] López – de – Dicastillo, C., Pezo, D., Nerín, C., López – Carballo, G., Català, R., Gavara, R., Hernández – Muñoz, P. (2012). Reducing oxidation of foods through antioxidant active packaging based on ethyl vinyl alcohol and natural flavonoids. *Packaging Technology and Science*, 25 (8), 457 – 466.

[31] López – de – Dicastillo, C., Gallur, M., Català, R., Gavara, R., Hernández – Muñoz, P. (2010). Immobilization of β – cyclodextrin in ethylene – vinyl alcohol copolymer for active food packaging applications. *Journal of Membrane Science*, 353 (1 – 2), 184 – 191.

[32] López – de – Dicastillo, C., Català, R., Gavara, R., Hernández – Muñoz, P. (2011). Food applications of active packaging EVOH films containing cyclodextrins for the preferential scavenging of undesirable compounds. *Journal of Food Engineering*, 104 (3), 380 – 386.

[33] Cerisuelo, J. P., Alonso, J., Aucejo, S., Gavara, R., Hernández – Muñoz, P. (2012). Modifications induced by the addition of a nanoclay in the functional and active properties of an EVOH film containing carvacrol for food packaging. *Journal of Membrane Science*, 423 – 424, 247 – 256.

[34] Cerisuelo, J. P., Gavara, R., Hernández – Muñoz, P. (2015). Diffusion modeling in polymer – clay nanocomposites for food packaging applications through finite element analysis of TEM images. *Journal of Membrane Science*, 482, 92 – 102.

[35] ASTM D3359 – 09e2. Standard test methods for measuring adhesion by tape test. ASTM International, West Conshohocken, PA, USA.

[36] ASTM D882 – 12. Standard test method for tensile properties of thin plastic sheeting. ASTM International, West Conshohocken, PA, USA.

[37] ASTM D1434 – 82(2009)e1. Standard test method for determining gas permeability characteristics of plastic film and sheeting. ASTM International, West Conshohocken, PA, USA.

[38] Pieper, G., Petersén, K. (1995). Free fatty acids from orange juice absorption into laminated cartons and their effects on adhesion. *Food Science*, 60 (5), 1088 – 1091.

VI ANTIMICROBIAL FILMS AND COATINGS FOR FOOD PACKAGES BASED ON CARVACROL AND ETHYLENE COPOLYMERS: STUDY OF MATRIX EFFECTS ON THEIR ACTIVE AND FUNCTIONAL PROPERTIES

Josep Pasqual Cerisuelo [a], Rafael Gavara [a, *], Pilar Hernández – Muñoz [a]

[a] Laboratori d'envasos, Institut d'Agroquímica i Tecnologia d'Aliments, IATA – CSIC.
Av. Agustí Escardino, 7. 46980 Paterna, València.

* Autor de contacte. Tel.: +34 963900022, e-mail: rgavara@iata.csic.es

ABSTRACT

Research into active antimicrobial packaging has experienced a significant increase in the last decade due to its numerous advantages over other traditional technologies, especially when using volatile antimicrobials of natural origin. However, one of the obstacles to overcome in its effective implementation is the difficulty in controlling the retention capacity of the carrier polymer for the embedded compounds, and their rate of release into the package headspace. For this reason, two new matrix modifications have been explored in this work, consisting in the variation of both its chemical affinity for the active agent, i. e. carvacrol, by employing ethylene copolymers of ranging polarity, and its internal structure, through their application in form of latex dispersions. As a result, four new polymeric materials, namely, ethylene-octene copolymer (LLDPE), ethylene-vinyl acetate copolymer (EVA), ethylene-methacrylic acid copolymer (EMA), and ethylene-methacrylic acid salt copolymer (ION), were successfully developed in form of both active films and coatings over polypropylene (PP) sheets, and tested for their active and functional properties.

Results of SEM imagery evidenced an insufficient heat input into the latex films during their drying process, which led to a partially incomplete coalescence of their polymeric particles. Consequently, various film structures of ranging heterogeneity, porosity, and roughness were obtained, with morphologies generally correlated with the melting temperature of the studied polymers, and with their different behavior in most of the active and functional tests carried out. Concretely, LLDPE and EVA, the most heterogeneous polymers, were generally more permeable, less resistant, more deformable, less transparent, and more wettable than EMA and ION, which exhibited a completely coalesced structure. For carvacrol, both LLDPE and EVA yielded higher values for its diffusion coefficient, in agreement with their permeability results, whereas both EMA and ION showed higher solubilities, according to their greater affinity to the active molecule derived from their ionic nature.

***Polymer International*, 2015, (under review).**

1. INTRODUCTION

Antimicrobial packaging is a form of active packaging whose interactions with the product or the headspace are intended to reduce, inhibit, or retard the growth of microorganisms that may be present in the packed food or on the surface of the packaging materials, thus extending the shelf life of the preserved foodstuffs (Appendini & Hotchkiss, 2002). Research into this area has experienced a significant increase during the last decade due to producers, the food industry and governments regarding it as a valuable tool in the fight against most potential food safety hazards, such as the spoilage of food products, food-borne illnesses, or malicious tampering, while also satisfying the increasing quality and convenience standards demanded by consumers, even in the most challenging systems involving fresh, minimally processed, or additive free food products (Collins – Thompson & Hwang, 2000; Cooksey, 2001; Gavara et al., 2009; Han, 2013; Joerger, 2007; Suppakul et al., 2003).

Since much of the microbial contamination and growth affecting packed solid or semisolid foods occurs primarily at the product surface level, especially in the areas in contact with the package where a film of moisture may form between them, antimicrobial activity should be mostly exerted on these zones (Brody et al., 2001; Han, 2013). In this context, antimicrobial packaging is an advantageous technology in comparison with the direct addition of preservatives into the bulk of foodstuffs, or with dipping and spraying techniques. Indeed, these conventional methods usually require the incorporation of large amounts of the active compound into the food matrices, since its performance can be greatly affected by dilution or inactivation phenomena due to its migration towards the food center. By contrast, antimicrobial packages can provide a uniform and constant activity on the product surface without requiring such high concentrations, thanks to their ability to deliver the active agent at a slow and constant pace, therefore preventing potential organoleptic issues or high implementation costs (Appendini & Hotchkiss, 2002; Vermeiren et al., 2002).

The vapor-active concept of antimicrobial packaging is the most suitable for the preservation of such types of foodstuffs, since it is able to gradually release an active volatile compound to the package headspace which can act on the microorganism membrane, either directly from the vapor phase, or through a previous sorption and concentration on the food surfaces, without even needing to be in direct contact with them (Appendini & Hotchkiss, 2002; Català & Gavara, 2001; Cooksey, 2001). In this latter case, the efficiency of the package is strongly related to the balance between the release rate of the active agent from the carrier material, its sorption extent and diffusion rate through the food matrix, and the kinetics of the microbial growth (Han, 2013). The former parameter, in turn, is

dependent, among others, on the nature of both substances involved and the interactions between them (Tunç & Duman, 2011). In this sense, the best efficiency results are usually obtained when using a polymeric matrix with low diffusivity values for the embedded compound as carrier material (Han, 2013) and when forming this active polymer as an inner coating layer in a multilayer packaging structure. This way, the antimicrobial agent can be delivered to the package headspace at a slow and continuous rate. Coating technologies, on the other hand, can effectively prevent the thermal degradations occurring during the polymer extrusion or thermoforming processes, as well as reduce the material losses to the package outside induced by diffusive outflows (Appendini & Hotchkiss, 2002).

In previous works (Cerisuelo et al., 2012a, 2013, 2014; Muriel – Galet et al., 2012, 2013) diverse antimicrobial coatings casted onto bi-oriented polypropylene substrates, consisting of carvacrol, a volatile antimicrobial compound of natural origin, and EVOH, a hydrophilic copolymer of ethylene and vinyl alcohol, were successfully developed and tested for the preservation of fresh-cut salad and fish products. Unfortunately, owing to the high water content of these foodstuffs, and to the highly hydrophilic nature of the carrier material (Aucejo, 2000; Aucejo et al., 1999, 2000), the assayed systems showed an unconstrained free release of the active agents to the package headspace, inducing an early peak of antimicrobial activity at the beginning of the preservation period, followed by a pronounced decline in the subsequent days. Because of this, in later works (Cerisuelo et al., 2012b) a matrix modification based on the addition of bentonite nanoclay was also assessed in EVOH / carvacrol active systems, yielding a considerable enhancement in their diffusivity and solubility parameters for the embedded compound.

Besides these, other authors have also successfully developed diverse antimicrobial materials based on natural essential oils and polyolefins, by mixing their components through melt blending during the extrusion of the active films. However, although not always reported, the processing of essential oils at high temperatures can result in their massive degradation or evaporation, both involving the occurrence of severe agent loss (Suppakul et al., 2008, 2011) and thus the potential creation of an unbreathable and dangerous atmosphere in the processing facility (López – Rubio et al., 2004).

Hence, in the present work two alternative matrix modifications in the carrier material are also explored with the aim of further controlling its retention capacity for the antimicrobial agent, as well as the rate of release of such a compound into the package headspace. Concretely, the assessed modifications consisted in the variation of the matrix compatibility with the active substance, namely carvacrol, through the employment of diverse ethylene copolymers of ranging polarity, together with

the variation of the matrix structure through the application of such materials in the form of latex dispersions. This type of polymer formulation allows the creation of an extensive three-dimensional network of high specific surface area within the formed films (Chen et al., 2011; Keddie, 1997), with great potential for use in the controlled absorption or release of volatile substances (Nestorson et al., 2006, 2007a, 2008), as well as to prevent the mentioned thermal abuse on the embedded compound. The latex dispersions assayed in this work consisted of ethylene – octene copolymer (LLDPE), ethylene – vinyl acetate copolymer (EVA), ethylene – methacrylic acid copolymer (EMA), and ethylene – methacrylic acid salt copolymer (ION), and their matrix effects on the functional and active properties of the formed coatings were also assessed. Specifically, the tested properties were their effective diffusivity and solubility coefficients for carvacrol, as well as their morphological, mechanical, thermal, optical, surface, and barrier characteristics in the final coated PP films.

2. MATERIALS AND METHODS

2.1. Materials

Carvacrol of at least 98 % purity was purchased from Sigma-Aldrich Co. LLC. (St. Louis, MO, USA), as well as reagent-grade magnesium nitrate, sodium nitrite and phosphorus pentoxide. Silica gel was provided by Merck KGaA (Darmstadt, Germany), high-vacuum silicone was supplied by Panreac Química S.L.U. (Barcelona, Spain), and deionized water was obtained from a Milli-Q Plus purification system of EMD Millipore Corp. (Billerica, MA, USA).

Food-contact grade bi-oriented polypropylene (PP) film 30 µm thick was kindly supplied by Envaflex S.A. (Utebo, Spain), whereas latex dispersions of food-contact grade ethylene copolymers, namely, linear low density polyethylene (LLDPE), ethylene-vinyl acetate copolymer (EVA), ethylene-methacrylic acid copolymer (EMA), and its neutralized derivative (ionomer, ION), were kindly provided by Paramelt BV (Heerhugowaard, The Netherlands). All latexes were manufactured following a proprietary high-shear mechanical process developed by Dow Chemical, which yields aqueous dispersions of spherical polymer particles of about 1 µm of diameter, stabilized in water with the aid of anionic surfactants of low molecular weight. All physicochemical data provided by the manufacturer, such as chemical composition, solids content, viscosity, or pH, were collected from the product technical datasheets and summarized in **Table VI.1**.

Table VI.1. Physicochemical data of the latex dispersions employed in this work.

Trade name	Chemical composition	Short name	Solids content (%)	Viscosity at 23 °C (mPa · s)	pH at 20 °C
Aquaseal X 2200	Ethylene – octene copolymer	LLDPE	50	150	10 – 11
Aquaseal X 2235	Ethylene – vinyl acetate copolymer	EVA	45	150 – 200	9.5 – 10
Aquaseal 2093	Ethylene – methacrylic acid copolymer	EMA	25	300	9
Aquaseal X 2280	Ethylene – methacrylic acid salt copolymer	ION	45	700	9

2.2. Preparation of latex films and coatings

All latex films and coatings, both with or without the active agent, were prepared through a casting technique, following the procedure described in a previous work (Cerisuelo et al., 2012a). In this case though, according to the manufacturer, all latex dispersions were ready-to-use just as supplied, as long as sufficient stirring was provided prior to their application to ensure they reached highly homogeneous conditions. Because of this, two 20 mL aliquots of each polymer suspension were simply set out in glass vials and introduced in an Ultrasons ultrasonic bath (J. P. Selecta S. A., Barcelona, Spain) at room temperature for at least 30 minutes. The formulation for the active materials was prepared by only dissolving carvacrol in one of both aliquots during its ultrasonic stirring, at a concentration of 5 % in weight with respect to the nominal dry polymer content.

Regarding film formation, since latex dispersions consisted of small spherical polymer particles suspended in water, once solvent was completely evaporated they had to undergo a sufficient sintering or coalescing process so as to yield a cohesive structure which could allow their extraction in the form of a solid film with good physicochemical properties. According to manufacturer documentation, a complete coalescence of the latex particles could be achieved if the materials reached a dry web temperature between 80 and 100 °C at the end of the drying process. For this reason, the latex dispersions were cast over glass plates with the aid of two Mayer rods, one of 100 µm deep thread for LLDPE, EVA, and ION, and another of 150 µm for EMA (due to is lower solids content), and subsequently placed under the heat radiation source of a 2500 W home-made drying hood, to be dried for 5 minutes at a temperature of at least 80 °C. After manufacturing, all the latex

films obtained were found to be highly homogeneous and translucent, with an average thickness of 35 ± 5 µm, which was individually measured, prior to testing, with an ABSOLUTE Digimatic Indicator ID-C Series 543 digital micrometer (Mitutoyo America Corp., Aurora, IL, USA).

With respect to the coated PP films, in order to ensure a proper anchorage of the latex particles to the surface of the substrate polymer, several PP sheets were subjected to corona discharge by passing them through the plasma region generated by the electrode of a BD-20AC high frequency corona surface treater three times (Electro-Technic Products, Inc., Chicago, IL, USA). Immediately afterwards, the pretreated PP substrates were placed on an Elcometer 4340 automatic coating applicator (Elcometer Ltd., Manchester, UK), equipped with a Mayer rod of 7 µm deep thread, and subsequently coated by the latex dispersions previously prepared. Casting was performed at room temperature with an application velocity of 8 cm/s, and the resulting coated PP films were then introduced in the drying hood described before, and dried for 5 minutes at a temperature of at least 80 °C. After manufacturing, all the multilayer films obtained were found to be highly homogeneous and transparent, with thicknesses approximately in accordance with the solids content of their corresponding latex dispersions, that is, around 3.5, 3.15, 1.75, and 3.15 µm, for LLDPE, EVA, EMA, and ION, respectively.

Lastly, in order to avoid potential contaminations or antimicrobial activity losses in the produced materials, all the dry films obtained were preserved in aluminum hermetic bags, and stored until utilization in freezing chambers at -18 °C of temperature.

2.3. Determination of the microstructural morphology

The microstructural morphology of the produced passive latex films was studied by field emission scanning electron microscopy (FE–SEM), with the aim of checking the degree of coalescence achieved by the particles at the end of the drying process. FE–SEM analysis was carried out in an S–4800 unit (Hitachi Ltd., Tokyo, Japan) equipped with an FEG electron source, a BSE detector and an image capture system, using 10 kV of accelerating voltage. Film samples were prepared by cryofracture under liquid nitrogen, and the fragments obtained were adhered to the faces of a copper cube with double-sided carbon tape and subsequently placed in a desiccator filled with phosphorus pentoxide to be thoroughly dried until their analysis. Samples were also metallized immediately prior to inserting them in the FE–SEM unit, by coating them with gold–palladium nanoparticles under vacuum conditions in a sputter coating unit.

2.4. Determination of the thermal properties

Thermal characterization of the prepared latex films was performed by thermogravimetric analysis (TGA) and differential scanning calorimetry (DSC). With respect to TGA, analyses were carried out in a Q5000 unit (TA Instruments Corp., New Castle, DE, USA) and only on the passive materials, by introducing at least three film samples of each one, weighting approximately 10 mg, in 50 µL platinum pans, and by subsequently heating them from 25 to 900 °C at 10 °C/min under a nitrogen atmosphere. As a result, the TGA instrument yielded diverse weight – temperature curves, which were later assessed with the aid of Universal Analysis 2000 instrument software, included in the Thermal Advantage software suite. Within this data assessment, the percentage weight loss of residual solvents, Δm_s, was estimated from the first signal drop observed in the normal curves, whereas the decomposition temperature, T_d, was determined from the second signal maximum appearing in their corresponding derivative curves.

Regarding DSC, analyses were carried out in a Q2000 unit (TA Instruments Corp., New Castle, DE, USA), programmed to perform a three – cycle thermal analysis, consisting of a first heating from -60 to 200 °C, followed by a cooling down to -60 °C and by a second heating up to 200 °C, all ramps being of 10 °C/min. In this case, both types of materials, active and passive, were analyzed by the instrument, and a minimum of three film samples of each one, weighting approximately 8 mg, were cut and subsequently introduced in 40 µL T-zero aluminum hermetic pans prior to undergoing the thermal treatment. The thermograms thus obtained were again processed with Universal Analysis 2000 instrument software, and, within the assessment performed, the melting point temperature, T_m, range, R_m, and enthalpy, ΔH_m, of the studied materials could be determined from the signal minimum, and from the width at half height, and area, of their melting endotherm, respectively.

2.5. Determination of the barrier properties

The barrier properties of the manufactured passive latex films were investigated by measuring their oxygen, carbon dioxide, and water vapor permeabilities in controlled conditions of temperature and relative humidity, following the procedures described in a previous work (Cerisuelo et al., 2012b).

In brief, the oxygen transport was analyzed at 23 ± 1 °C and at 50 ± 0.01 % RH with an OX-TRAN model 2/21 ML permeation system (Paul Lippke Handels – GmbH, Neuwied, Germany). The transport of

carbon dioxide was studied at 23 ± 1 °C and at 50 ± 0.1 % RH by means of an isostatic permeation cell and a GC-TCD, detailed in the mentioned paper. In both cases, four film samples of each assayed material were placed in the instrument cells and conditioned for at least 8 h prior to the permeation tests. Then, the gas transmission rates were measured every 45 min until constant, and, from that instant, at least five more points were acquired in order to obtain good average values for the gas permeabilities. Active films could not be measured since volatile organic compounds would be massively released from the film samples during the conditioning period and, furthermore, they are known to poison the OX-TRAN sensor.

With respect to the transport of water vapor, permeation tests were carried out employing several Elcometer 5100 Payne permeability cups (Elcometer Ltd., Manchester, UK) made up of anodized aluminum, in compliance with the ISO 2528:1995 standard method. In short, each cup was filled with approximately 10 g of silica gel, their rims were coated with high-vacuum silicone, and the tested film was held in place with the aid of a flat Viton ring, an aluminum ring, and three press-screws. Once cups were properly mounted they were placed in a climatic chamber, filled with a saturated solution of sodium nitrite and conditioned at 23 ± 1 °C and at 64 ± 5 % RH for at least 48 h prior to the experimentation, in order to generate a sufficient humidity gradient through the tested films, and thus a sufficient mass transport of water molecules, as to induce a noticeable weight gain by water absorption in the permeation cups. This weight gain was monitored on a daily basis until depletion of the drying agent, and subsequently plotted versus the elapsed time to obtain the permeation curves. The values for the water vapor permeability were estimated from the slope of the straight part of the curves (dm/dt), the sample thickness (L), the permeation area (A), and the difference of water vapor pressure between the inner and the outer face of the film (Δp_w) through the following equation:

$$P_w = \frac{dm}{dt} \cdot \frac{L}{A \cdot \Delta p_w} \qquad \text{(VI.1)}$$

In order to verify the repeatability of the results obtained each studied material was tested in quadruplicate.

2.6. Determination of the mechanical properties

Differences in the mechanical behavior of the latex-coated PP films with respect to the uncoated substrate were assessed by means of a MultiTest 1-i universal testing machine (Mecmesin Ltd., Slinfold, UK), equipped with a 100 N static load cell and with small pneumatic plane grips, and programmed to perform a tensile test based on the ASTM D882 – 12 standard method. Specifically, the studied films were cut with a laboratory guillotine into a minimum of 10 strips per material, measuring 1 in. width and 140 mm long, and the resulting samples were placed in a climatic chamber, filled with a saturated solution of magnesium nitrate, to be conditioned at 23 ± 1 °C and at 54 ± 5 % RH for at least 48 h prior to their trial. Once samples were properly equilibrated they were consecutively extracted from the chamber, placed between the grips, and tightly held with 3 bars of pressure. Then, Emperor instrument software was employed to set the separation between grips at 100 mm, the cross-head velocity at 25 mm/min, and the data sampling frequency at 1 kHz, before being ordered to start the test. Under such conditions, film samples were subjected to an increasing load over time and thus underwent an increasing elongation, yielding force (F_t) – displacement (ΔL_t) curves which were standardized to the corresponding stress (σ_t) – strain (ε_t) curves by application of the following equations:

$$\sigma_t = \frac{F_t}{A_0} = \frac{F_t}{w_0 \cdot t_0} \qquad \text{(VI.2)}$$

$$\varepsilon_t = \frac{\Delta L_t}{L_0} \cdot 100 \qquad \text{(VI.3)}$$

where A_0 is the initial cross-sectional area of the tested sample, product of its initial width (w_0) and thickness (t_0), and L_0 is the initial separation between grips. Thereby, the mechanical properties of the studied materials, i.e. the ultimate tensile strength, the deformation at break, and the Young's modulus, could finally be estimated through the graphical assessment of the transformed curves.

2.7. Determination of the optical properties

The optical properties of the produced passive latex films, and their variation with the addition of active agent, were evaluated by measuring the material color with the aid of a CM-3500D spectrophotometer (Konica Minolta Optics Inc., Tokyo, Japan). Prior to optical characterization, the instrument was set to D65 illuminant / 10° observer, provided with a target mask of 8 mm aperture, calibrated with a zero calibration box and a white calibration plate, and programmed to acquire three spectra in each color analysis and afterwards display the averaged results. Color measurements, in turn, were carried out under room conditions (about 23 °C of temperature and 50 % of relative humidity), by placing the film samples onto the device lens and against the surface of a standard white tile. Then, SpectraMagic NX instrument software was used to execute the shots, after previously being configured to collect and present the color data in the CIELAB color space. Thereby, the color coordinates of each film sample: L^* (lightness), a^* (greenness – redness), and b^* (blueness – yellowness), were finally obtained, and their polar counterparts: C^*_{ab} (chroma or saturation index), and h_{ab} (hue or angle), were then calculated from the latter two parameters through the application of the corresponding definition equations:

$$C^*_{ab} = \sqrt{\left(a^*\right)^2 + \left(b^*\right)^2} \tag{VI.4}$$

$$h_{ab} = \arctan\left(\frac{b^*}{a^*}\right) \tag{VI.5}$$

Reproducibility of the results found was checked by performing the color measurements on eight different locations of each film sample, and in triplicate for each assayed material.

2.8. Determination of the surface properties

The surface characteristics of the passive latex films and coatings, and, particularly, their wettability, were studied by measuring static contact angles through the sessile drop technique. With this aim, an OCA 15EC goniometer (DataPhysics Instruments GmbH, Filderstadt, Germany) was utilized to deposit water droplets on the surface of the tested films, whereas the data acquisition and image analysis procedures were carried out with SCA20 instrument software. Assays were performed in an air

atmosphere at room conditions (23 °C and 50 % RH), by gently dropping 8 µL of deionized water with a dispenser syringe. The static contact angles formed between the water droplets, the film surfaces, and the air atmosphere, were measured 60 s after the deposition, by assessing the images collected, and by fitting their shape equations to the Young - Laplace model. Tests were carried out on a minimum of five different positions of each film sample, and in quadruplicate for each studied material, in order to allow a good averaging of the values obtained and to ensure the repeatability of the final results.

2.9. Determination of the active properties

2.9.1. Carvacrol solubility

The chemical compatibility of the active substance with the diverse latex matrices obtained was investigated by determining its solubility coefficients under controlled conditions of temperature and relative humidity. For this purpose, several film samples of each studied material were cut into small disks of 4 cm diameter, and subsequently introduced into a hermetic glass container together with two small and open vials, one with pure carvacrol and the other containing a saturated solution of magnesium nitrate. In order to avoid any direct contact between the four materials assayed, or between them and the liquid vials or the inner glass walls, samples were properly separated with several pieces of filter paper prior to their introduction in the jar. Once the container was hermetically closed, the substances included allowed its inner atmosphere to become completely saturated with the active agent while simultaneously maintaining its relative humidity constant and close to 54.4 %, the critical relative humidity of the salt employed. In these conditions, the complete system was stored in a dark room at 23 ± 1 °C of temperature for approximately six months, in order to give it enough time to attain its equilibrium state.

Once this period had passed, the assayed film samples were successively extracted from the glass container and immediately introduced in a 890 thermal tube desorber (Dynatherm Analytical Instruments Inc., Kelton, PA, USA) connected in series to an HP 5890 Series II Plus gas chromatograph (Hewlett Packard Co., Wilmington, DE, USA), equipped with a flame ionization detector (FID) and with a 30 m, 0.53 mm, 2.65 µm Agilent HP-1 semi-capillary column (Teknokroma S.C.L., Barcelona, Spain), in order to be analyzed for the determination of their final carvacrol concentration, according to the procedure described in previous works (Cerisuelo et al., 2012a, 2012b). In this way, the equilibrium

concentration of the active agent in the polymeric matrix of each studied material, C_c^P, could finally be obtained, and, by introducing it in equation (VI.6), together with the equilibrium concentration in the jar headspace, C_c^{HS}, (i.e. the saturation concentration of carvacrol derived from its vapor pressure), the corresponding values of the carvacrol solubility coefficient could also be estimated.

$$S_c^P = \frac{C_c^P}{C_c^{HS}} \qquad \text{(VI.6)}$$

2.9.2. Carvacrol effective diffusivity

The rate of release of the active compound from the four developed latex materials was determined by measuring its diffusion coefficient through the different carrier matrices, under controlled conditions of temperature and relative humidity. With this aim, one active film of each studied material was placed on a gridded metal support and stored in a climatic room for 10 days. The atmosphere of the room was previously conditioned at 23 ± 1 °C of temperature and at 50 % ± 5 % of relative humidity, and was also continuously renewed during the course of the experimentation in order to avoid any carvacrol accumulation. During that time, the concentration of carvacrol remaining in the tested films was monitored by periodically extracting samples of about 20 mg and subsequently analyzing them by thermal desorption and gas chromatography, following the procedure described in the above section.

The pairs of experimental data for time, t, and carvacrol concentration, C_c^P, thus obtained were then introduced in the analytical solution of Fick's law for a process of desorption from a sheet of infinite length (Crank, 1975):

$$\frac{C_c^P}{C_{c0}^P} = \frac{2}{\pi^2} \cdot \sum_{\nu=1}^{\infty} \frac{1}{\left(\nu - \frac{1}{2}\right)^2} \cdot \mathrm{e}^{\frac{-\pi^2 \cdot \left(\nu - \frac{1}{2}\right)^2 \cdot D_c^P \cdot t}{L_P^2}} \qquad \text{(VI.7)}$$

together with the corresponding values of the film thickness, L_P, and of the initial concentration of carvacrol in the essayed film, C_{c0}^P. This way, by fitting the previous equation (VI.7) to the mentioned experimental points an estimated value for the carvacrol diffusion coefficient through each studied material, D_c^P, could finally be obtained.

2.10. Data analysis

The values for all the parameters and coefficients presented in this work are expressed as "$(\bar{x} \pm \varepsilon)$ units," where $\bar{x}$ stands for the sample mean of parameter x, and ε stands for its absolute error. This absolute error is equal to the sample standard deviation for the measured variables, and was determined by propagation of uncertainty (partial derivatives method) for the calculated variables.

Statistical analysis of the results obtained for mechanical properties was performed with the aid of IBM SPSS Statistics 21 commercial software (IBM Corp., Armonk, NY, USA). Concretely, a one-way analysis of variance (ANOVA) was carried out, and differences found between mean values for the studied materials were assessed by means of confidence intervals using Tukey's test at a $p \leq 0.05$ level of significance.

3. RESULTS AND DISCUSSION

3.1. Film appearance and microstructural morphology

After manufacturing, all the prepared latex films were found to be colorless and highly homogeneous, given that no particles, agglomerates, or any other defects were visible to the naked eye. Nevertheless, only the EMA and ION latex dispersions yielded completely transparent and glossy films, whereas the EVA and LLDPE ones produced translucent or opaque materials, depending upon their final thickness, with a matte surface and a dull whitish coloration. This last phenomenon is a common optical effect occurring on multiphasic systems, where a finely dispersed phase scatters the incident light in all directions, giving a cloudy or milky appearance to the macroscopic system. Given that all the developed materials were prepared from aqueous dispersions of spherical micrometric polymer particles, the mentioned phenomenon occurring in the EVA and LLDPE latex films could be explained by an incomplete particle sintering or coalescence during their manufacturing process.

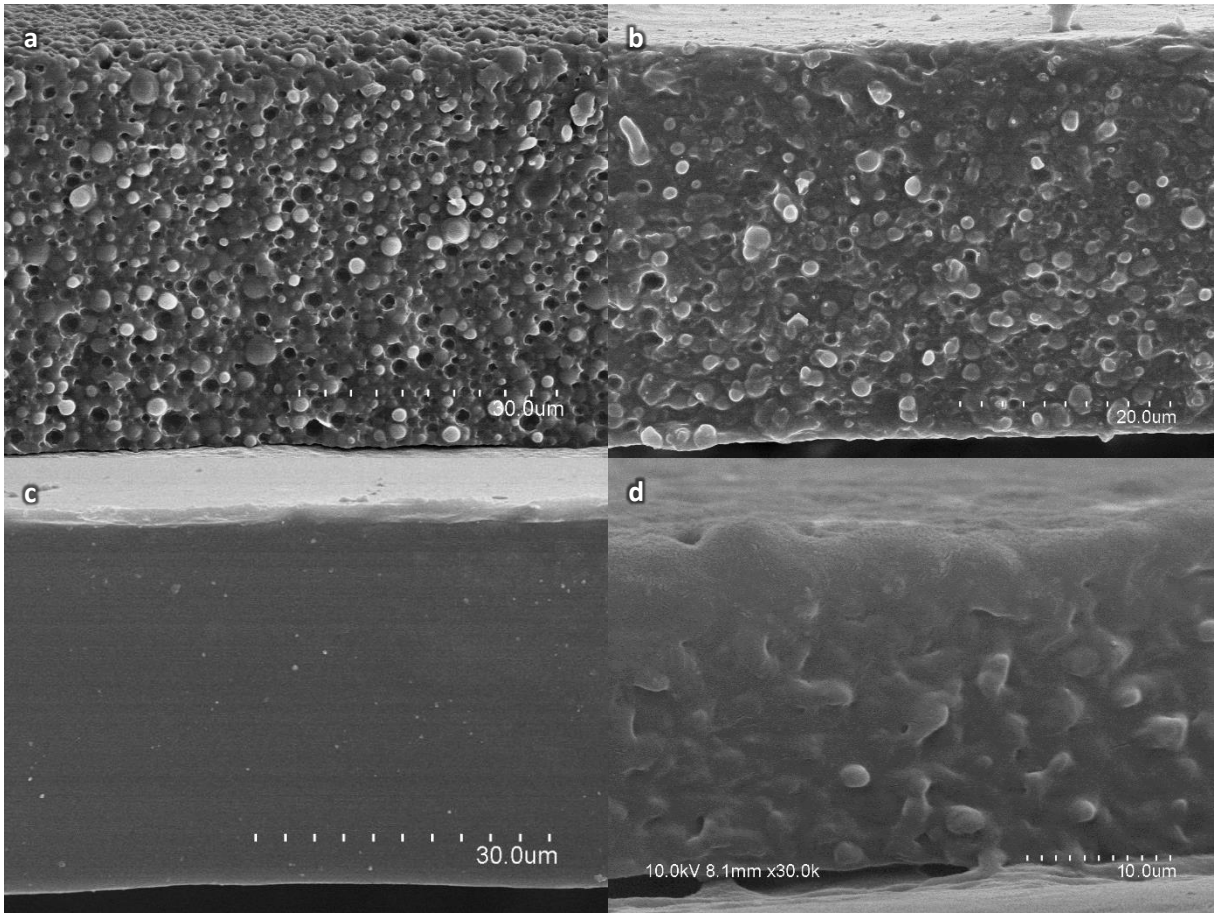

Figure VI.1. FE-SEM micrographs of the cryofractured surface of the four studied passive latex films: (a) LLDPE, (b) EVA, (c) EMA, and (d) ION.

These macroscopic observations could also be confirmed when assessing their internal structure through the cross-sectional images obtained by cryofracture and FE-SEM analysis, depicted in **Figure VI.1**. As can be seen, whereas the EMA latex film shows a uniform and homogeneous monophasic structure with a flat and clean cryofractured section, all the remaining materials still show vestiges of their prior particulate structure. This fact is most evident in the LLDPE film whose sintering process seems to have stopped in its first stages, yielding an extensive three-dimensional network of micrometric spherical particles and pores resembling a sponge. Such particles are only bonded among themselves through some molten polymer formed during the heat-drying of the films, although not enough liquid was generated during such a process so as to fill the pores existent between them, thus leading to a highly heterogeneous and light-scattering film structure. Regarding EVA, some differences with respect to LLDPE can quickly be noticed. In this case, the sintering process kept advancing and, as a consequence, the polymer particles remaining in the film clearly became smaller and more irregular than those of LLDPE, owing to their further melting. In parallel, the higher amount of formed liquid

phase could completely fill a greater number of pores, especially in the lower part of the film due to the effect of gravity. As a result, the remaining pores were also fewer, smaller and more irregular than those of LLDPE, and, therefore, the internal film structure became more compact and homogeneous, with a smoother surface, although not enough so as to completely prevent the light scattering phenomena. Finally, the ION film micrograph shows a particle sintering process in a much more advanced stage, which has led to a monophasic and rather homogeneous film structure where almost all pores have been collapsed by the molten polymer and most particles have completely disappeared, only leaving behind some small vestiges of their former structure. In addition, and just as in the case of the EVA film, the coalescence of the ION particles has taken place to a greater extent in the lower part of the film, in contact with the casting glass plate, therefore achieving an almost perfectly homogeneous and uniform microstructure in such regions, resembling that of the EMA film, which is responsible for its aforementioned good optical properties.

In conclusion, it can be stated from the results presented above that the drying temperature range recommended by the manufacturer of the latex dispersions was only adequate to EMA and to ION, whereas both LLDPE and EVA clearly required a greater heat input, either in form of longer drying time or higher temperature, to achieve a completely coalesced film structure.

3.2. Thermal properties

The developed latex films, with and without carvacrol, were thermally characterized by means of TGA and DSC analysis. This characterization comprised the determination of the percentage weight loss of residual solvents, the decomposition temperature, and the melting temperature, range, and enthalpy of the manufactured films, whose final values are collected in **Table VI.2**. As can be noticed, the mentioned table does not include any data related to the studied active films, since they did not show any significant differences in terms of thermal behavior with respect to their passive counterparts, with the exception of the loss of carvacrol, which was reflected as a signal drop in the TGA analyses. In order to illustrate this statement, the DSC thermograms of the LLDPE passive and active films, obtained during their first heating cycles, are depicted as an example in **Figure VI.2**. As figure shows, the only perceptible difference between both curves is perhaps a slightly deeper endothermic valley between 50 and 90 °C in the active LLDPE curve, probably due to the evaporation of the active agent inside the DSC sample pan. Hence, it is safe to state that the presence of carvacrol in the polymeric matrix of any of the latex materials studied in this work does not affect their thermal performance in a significant way.

Table VI.2. Percentage weight loss of residual solvents, decomposition temperature, and melting temperature, range, and enthalpy of the passive latex films as obtained by TGA and DSC analysis.

Material	Δm_s (%)	T_d (°C)	T_m (°C)	R_m (°C)	ΔH_m (J/g)
LLDPE	1.77 ± 0.01	480.5 ± 0.2	124.2 ± 0.1	9.4 ± 0.7	39.6 ± 1.8
EVA	2.34 ± 0.03	482.9 ± 0.3	68.0 ± 0.5	68 ± 2	73.8 ± 0.9
EMA	2.55 ± 0.02	474.0 ± 0.2	86.0 ± 0.5	53.4 ± 1.1	73.9 ± 1.2
ION	0.97 ± 0.01	490.1 ± 0.3	99.8 ± 0.2	16 ± 1.5	84.6 ± 1.4

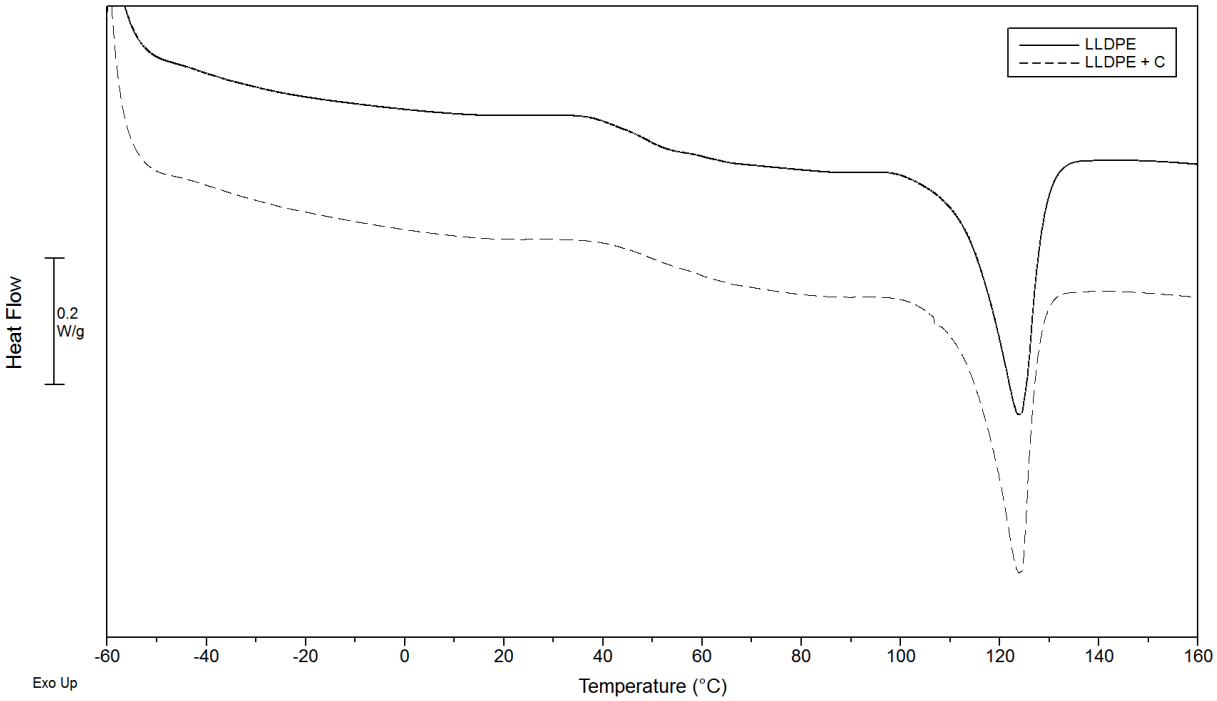

Figure VI.2. DSC thermograms of the LLDPE passive and active films corresponding to their first heating cycle.

With respect to the thermal properties displayed in the table, some important differences can be observed between the values belonging to the different tested materials. For example, the percentage weight loss of residual solvents ranged from approximately 1 % for ION to about 2.5 % for EMA. Although all the reported values are quite low, they mean that all the studied polymers contained a certain amount of volatile organic compounds (VOCs) as stabilizing agents for their water-based dispersions, or as coalescing agents for their film-forming particles. In particular, the relatively high value for EMA can be related to its content in ammonia, a pH-controlling additive, and thus a dispersion stabilizing agent, reflected in the material safety data sheet. Regarding the melting endotherm, both

its temperature and enthalpy also showed great differences between polymers, although their final values were situated within the usual range for this type of materials. Among the obtained results, it is worth mentioning the uncommonly low melting enthalpy, and thus crystallinity, exhibited by LLDPE in comparison with EVA, a highly amorphous polymer. In contrast, the higher values of this parameter were correctly found in ION, whose ionic nature facilitated the generation of large crystals. In addition, it is also worth mentioning the general correspondence between the melting temperature of the studied materials and their microstructural morphology. This is especially remarkable in the case of LLDPE, whose highly uncoalesced structure can be now explained by the insufficient drying temperature reached during its manufacturing process. On the contrary, EVA showed unexpected and contradictory results, given that it presented the widest melting range and the lowest melting point of all polymers, both located around 68 °C according to its DSC thermogram, and well below the temperature of the drying hood, it nonetheless yielded a partially uncoalesced considerably heterogeneous film structure. This suggested that the kinetics of the sintering process was also highly determining for the final morphology of the latex materials, and thus that small differences in their drying time could entail great differences in the finally obtained film structure. To finish, the decomposition temperature did not show any significant differences between all the tested materials, taking a high value of approximately 480 °C for all of them, although an earlier and smaller secondary transition was also found at about 360 °C for EVA, probably due to the prior release, and subsequent degradation, of its substituent acetate groups.

3.3. Barrier properties

Since the four developed latex materials possessed a ranging matrix polarity and microstructural morphology, in order to assess the influence of both factors on the transport of water vapor, oxygen, and carbon dioxide through them, the corresponding permeability coefficients were measured on the passive films under controlled conditions of temperature and relative humidity. The values thus obtained are displayed in **Table VI.3** and, as can be noticed, although they are generally comparable to those reported in the literature (Marais et al., 2000; Massey, 2003), some interesting observations can be made.

Table VI.3. Permeabilities of the passive latex films to water vapor, oxygen and carbon dioxide.

Material	$P_w \cdot 10^{14}$ ($g \cdot m / m^2 \cdot s \cdot Pa$)	$P_{O_2} \cdot 10^{18}$ ($m^3 \cdot m / m^2 \cdot s \cdot Pa$)	$P_{CO_2} \cdot 10^{18}$ ($m^3 \cdot m / m^2 \cdot s \cdot Pa$)
LLDPE	16 ± 4	6.5 ± 1.3	11.4 ± 0.3
EVA	1.8 ± 0.6	5 ± 2	11.0 ± 0.5
EMA	6.7 ± 1.1	2.7 ± 0.5	6.7 ± 0.1
ION	2.7 ± 0.5	2.6 ± 0.6	8.7 ± 0.4

First, LLDPE yielded the highest value for the water vapor permeability while having a very similar hydrophobic nature to EVA, the less permeable material. This phenomenon could easily be explained by the microstructural morphology of the LLDPE films, assessed above, whose highly porous structure, resembling a sponge, would allow gas molecules to more rapidly diffuse through the spaces between particles, and thus to compensate the lack of chemical compatibility, and thus solubility, between both substances. In contrast, EVA showed a low value of this parameter, properly in accordance with its high hydrophobicity, despite the remaining presence of some pores and heterogeneities in its incompletely coalesced internal structure. The two other polymers, EMA and ION, in turn, were more permeable to water vapor than EVA, in spite of their almost perfectly homogeneous and uniform film structure, although this behavior can clearly be attributed to their higher polarity, and thus hydrophilicity, derived from their acid or ionic chain segments.

With respect to the permeability to oxygen and carbon dioxide of the tested materials, the values finally obtained followed the expected trends better, with LLDPE being the most permeable polymer to both gases, followed by EVA, and then by EMA or ION. This sequence of materials is very logical and easily explainable, given its high agreement with their order in terms of polarity, microstructural morphology, and crystallinity. In this sense, and as can be seen in the presented tables and figures, the permeability of the studied polymers to such permanent gases grew as the porosity or heterogeneity of their matrix increased, and as its polarity and crystallinity decreased. Another relevant aspect reflected in the mentioned **Table VI.3** is the ratio between the carbon dioxide and the oxygen permeabilities, whose values range between approximately 1.75 and 3.35, also in good agreement with the data reported in the literature.

3.4. Mechanical properties

After discovering a ranging microstructural morphology in the developed latex materials by FE-SEM analysis, attributable to the different levels of progress of their incomplete sintering process, the determination of their mechanical behavior became of great interest to investigate the degree of cohesion finally reached in their polymeric matrices. This determination was performed by assessing the potential improvements, or deteriorations, experimented by the latex-coated PP films in the ultimate tensile strength, deformation at break, and Young's modulus, with respect to the neat uncoated substrate, and the results obtained from those measurements are detailed in **Figure VI.3**.

As this figure shows, all the polymers which underwent an incomplete coalescence of their particles, and thus which developed some heterogeneous internal structure, namely, LLDPE, EVA, and ION, had a noticeable and significant decrease of about 7 % in the ultimate tensile strength of PP films when they were applied as their coating layers. In contrast, when these coatings consisted of EMA, the only polymer with a completely coalesced and perfectly homogeneous internal structure, the value of this parameter increased 0.5 % with respect to that of the substrate material, although not in a significant amount. This same behavior was also observed in the Young's modulus chart, where the EMA-coated film yielded a value 4 % higher than the uncoated substrate for such a parameter, whereas the coatings constituted by any other latex material were responsible for reductions of between 2 and 3 % of the reference value for PP. Although all the differences mentioned in this graph were not significant either, they meant, together with those observed above in the tensile strength graph, that the mechanical performance of the tested films was highly dependent on the particle sintering process, and, in particular, on the level of cohesion finally achieved by their internal structure.

Regarding the results for the deformation at break, the incorporation of a coating layer of any latex material to the PP substrate produced a substantial and significant increase in the value of such a parameter, from about 36 % for EMA up to 79 % for ION. In this case, the observed variation cannot be attributed to the presence of a thin coating layer attached to the substrate polymer, regardless of its internal structure, but can still be related with a certain plasticization of this latter material caused by the absorption of organic solvents or additives from the latex dispersions during their deposition. In addition, this possible plasticization effect on the substrate material could also have contributed to the decrease in the values of the ultimate tensile strength and the Young's modulus, thus also helping to explain the small improvements or even deteriorations exhibited by the final multilayer films when a latex coating was applied on their PP substrates.

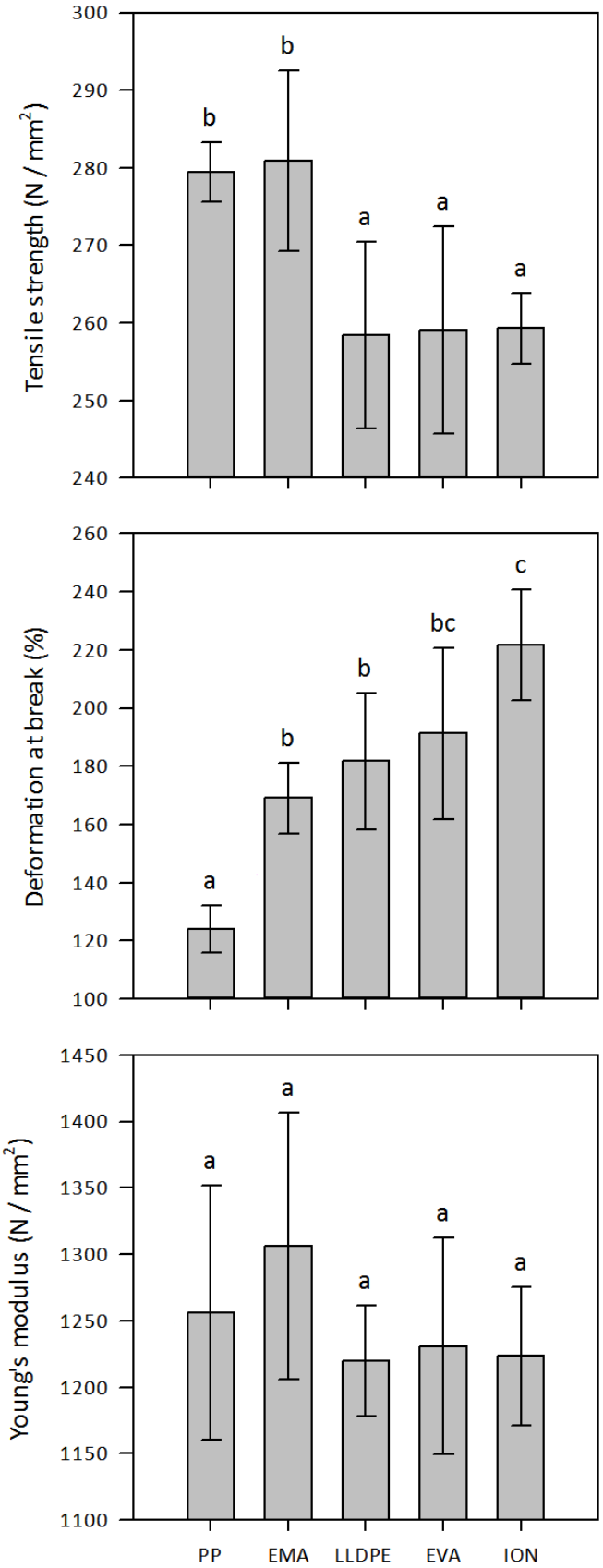

Figure VI.3. Ultimate tensile strength, deformation at break, and Young's modulus of the uncoated and latex-coated PP films. Letters correspond to homogeneous subsets of means with significant differences.

3.5. Optical properties

Just as explained in section 3.1, all the prepared passive films were found to be, immediately after their manufacture, highly homogeneous and colorless to the naked eye. With respect to the active films, they apparently shared, from a macroscopic point of view, the same optical characteristics as their passive counterparts, despite their high content in carvacrol, an antimicrobial compound with a deep orange-red coloration. However, during the preparation of the active latex dispersions, it was also observed that carvacrol could interact with EMA, given that, if left resting overnight after its incorporation to the mixture, it acquired a purplish coloration, therefore yielding purple films when casted over glass plates. In consequence, and in view of the mentioned optical phenomena, all the studied latex films, passive as well as active, were subjected to an optical analysis some days after their manufacture, in order to investigate the potential effects of the addition of the active agent, as well as the development of unexpected colorations which could be indicative of incipient chemical reactions or degradations occurring within their internal structure.

Such optical analysis was carried out by measuring the material color with the aid of a spectrophotometer, which yielded the color data as Cartesian or polar color coordinates on the CIELAB color space**.** Regarding the first analyzed parameter, lightness, its complete dataset was depicted in a bar chart in **Figure VI.4** in order to better compare the results obtained for both types of materials. As this figure shows, lightness was very high in all the studied polymers and very similar among them, especially in those presenting some heterogeneous internal structure, with values ranging from 94.76 of EMA to 98.82 of ION. However, when carvacrol was incorporated to their polymeric matrix at a concentration of 5 % in weight, the value of such a parameter decreased in a small, although significant amount of between 0.3 and 1.4 %, depending on the carrier material. This reduction was as expected, given the high color depth, and thus high light dulling capabilities, of the active agent.

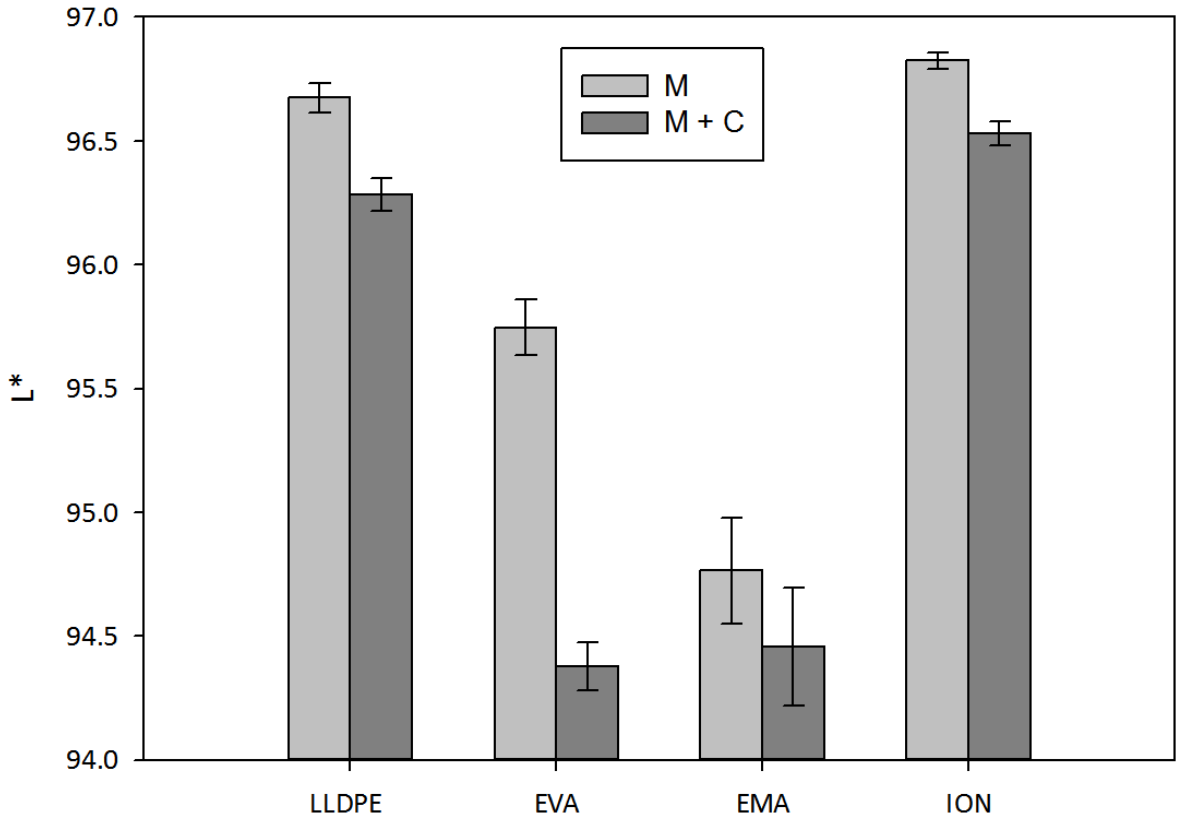

Figure VI.4. Lightness of the active and passive latex films on the CIELAB color space.

With respect to the two remaining color parameters, chroma and hue, their full datasets were plotted in a polar graph, depicted in **Figure VI.5**, in order to better perceive the differences in color existing among the studied materials. As can be seen in the figure, the chroma values were very low in all the tested polymers, below 0.4 in all cases, and even below 0.2 in those materials presenting a highly homogeneous internal structure, and thus higher transparency and gloss, in agreement with their macroscopic colorless appearance. Nevertheless, all these chroma values were even further reduced with the addition of carvacrol, given that, according to the detailed graph, the green-turquoise hue shown by all the passive materials could have been partially neutralized by the orange-reddish coloration provided by the active compound, placed just at the opposite quadrant of the polar graph. Finally, concerning this latter parameter, a considerable shift to the right can also be observed in the color of all the active materials with respect to the passive ones, mostly in the direction of the first quadrant, just towards the point where the carvacrol color would be located.

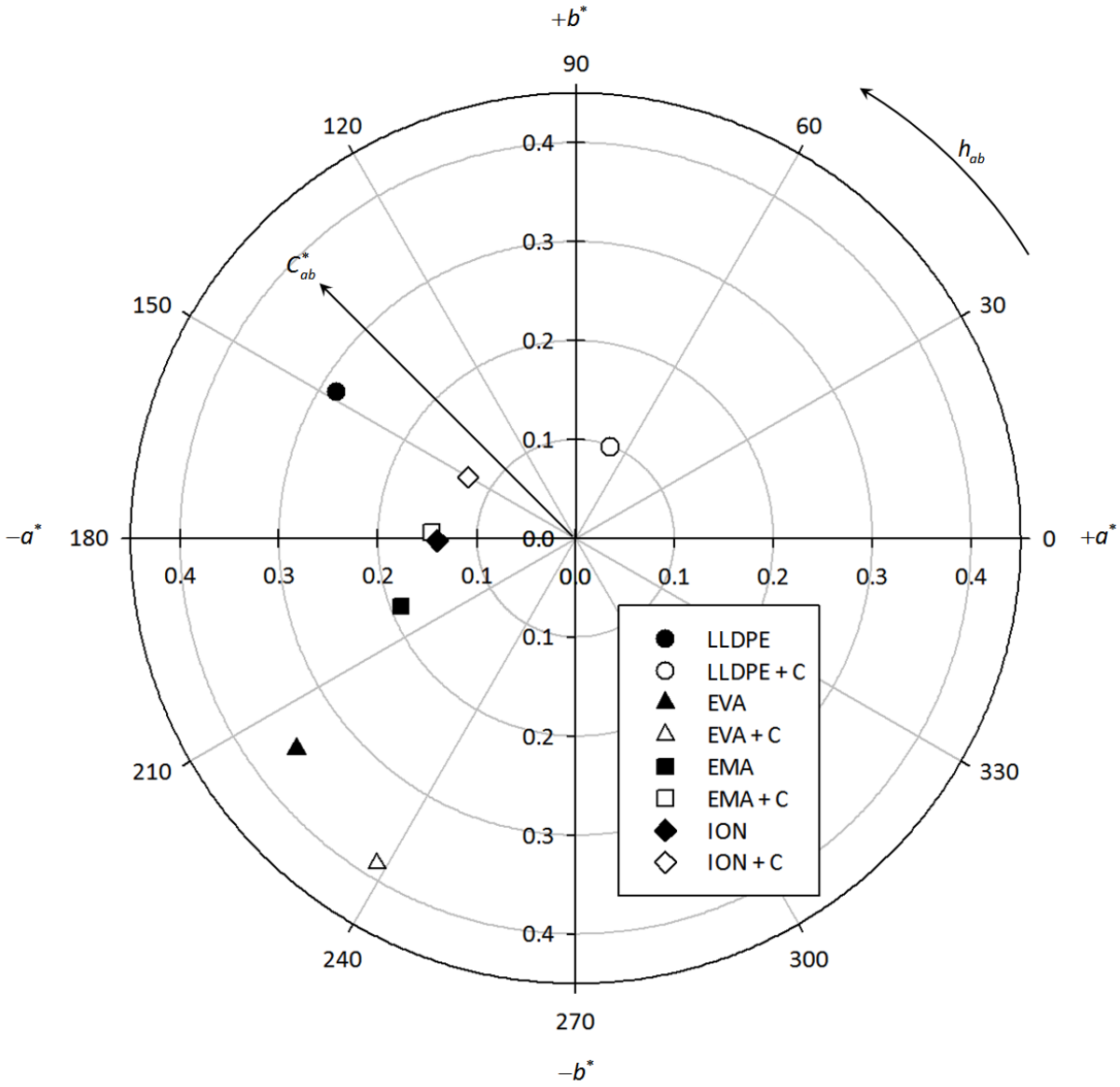

Figure VI.5. Chroma and hue of the active and passive latex films on the CIELAB color space.

In conclusion, the lack of color developments or alterations in the active materials, with the exception of those expected by the incorporation of a highly colorful substance, could be interpreted as an evidence of absence of chemical reactions or degradations.

3.6. Surface properties

All the polymers studied in this paper are common packaging materials, whose surface characteristics have already been the object of thorough investigation in the past, given their great importance for numerous industrial applications, and can thus easily be found in the literature (Doganci et al., 2012; España et al., 2012; Jitianu et al., 2008; Meiron & Saguy, 2007). However, most of the properties reported in such works are usually determined on ideal, chemically homogeneous and topographically smooth, polymer surfaces, since both these factors, surface roughness and chemical heterogeneity, can greatly affect the measured values of the static contact angle, and thus the surface wettability. This relationship between wettability and roughness was mathematically defined by Wenzel in 1936, and by Cassie and Baxter in 1944, who demonstrated that the wettability caused by the chemistry of a surface could be enhanced by adding further surface roughness when the tested liquid effectively penetrated its roughness grooves (Wenzel, 1936), or rather deteriorated when the surface was chemically heterogeneous or such penetration was impeded by the presence of partially trapped air pockets (Cassie & Baxter, 1944). Since most of the materials developed in this work were ethylene copolymers, i. e. polymers of a dual chemical nature, and some of them also yielded an extensive three-dimensional network of micrometric spherical particles and pores when forming a film, as displayed in **Figure VI.1**, their lateral surfaces could present a considerable chemical heterogeneity and porosity, just as their internal structure, as well as an important surface roughness in agreement with the cross-sectional topography of their cryofractured section. Therefore, in order to properly assess the influence of all these parameters on the surface properties of the studied materials, and, particularly, on their wettability, the static contact angles formed by water droplets on all the developed passive latex films and coatings were measured through the sessile drop method with the aid of a goniometer, and the results obtained were depicted in **Figure VI.6**.

As figure shows, the four investigated polymers yielded contact angles of similar values, all located between 70 and 90° in both their film and coating configurations, which evidenced a certain hydrophilic behavior of their lateral surfaces. However, differences from 4.4 up to 22° in the value of such a parameter were also observed between both forms of the same material, which could only be related to the different thermal treatment undergone by each one as a consequence of their different thickness. Indeed, whereas the produced latex films were very thick, 35 ± 5 µm, and thus the provided heat was not sufficient so as to completely coalesce their internal structure, the applied coatings, with nominal thickness between 1.75 and 3.5 µm, were much thinner, and, therefore, they could have achieved a perfectly homogeneous and uniform microstructure during their drying process. As a

consequence, in this latter case, the values obtained for the static contact angle should be close, or, at least, comparable, to those reported in the literature for ideal films of such polymers, as observed in the presented results, whereas the angles yielded by the corresponding films should mainly be dependent on the combination of porosity, roughness, and chemical heterogeneity exhibited by their lateral surfaces. This behavior is clearly the case for LLDPE and EVA, the most heterogeneous materials in their film conformation, whereas for EMA and ION the differences found between both structures were not significant, due to their higher homogeneity, lower porosity, and smoother surfaces. Regarding LLDPE, the higher porosity, and thus greater water sorption capacity, of its internal structure could be responsible for the low values of the static contact angle observed in the tested films with respect to the corresponding coatings, in agreement with Wenzel's theoretical approach. In contrast, the EVA copolymer showed the opposite effect, with angles 10° higher in its film configuration than in the coating one, in agreement with the model of Cassie and Baxter and with the values reported in the literature (Doganci et al., 2012), probably due to its dual chemical nature and to its lower porosity, consisting of numerous isolated pores embedded in its microstructure and becoming roughness grooves with trapped air in the proximities of the film surfaces.

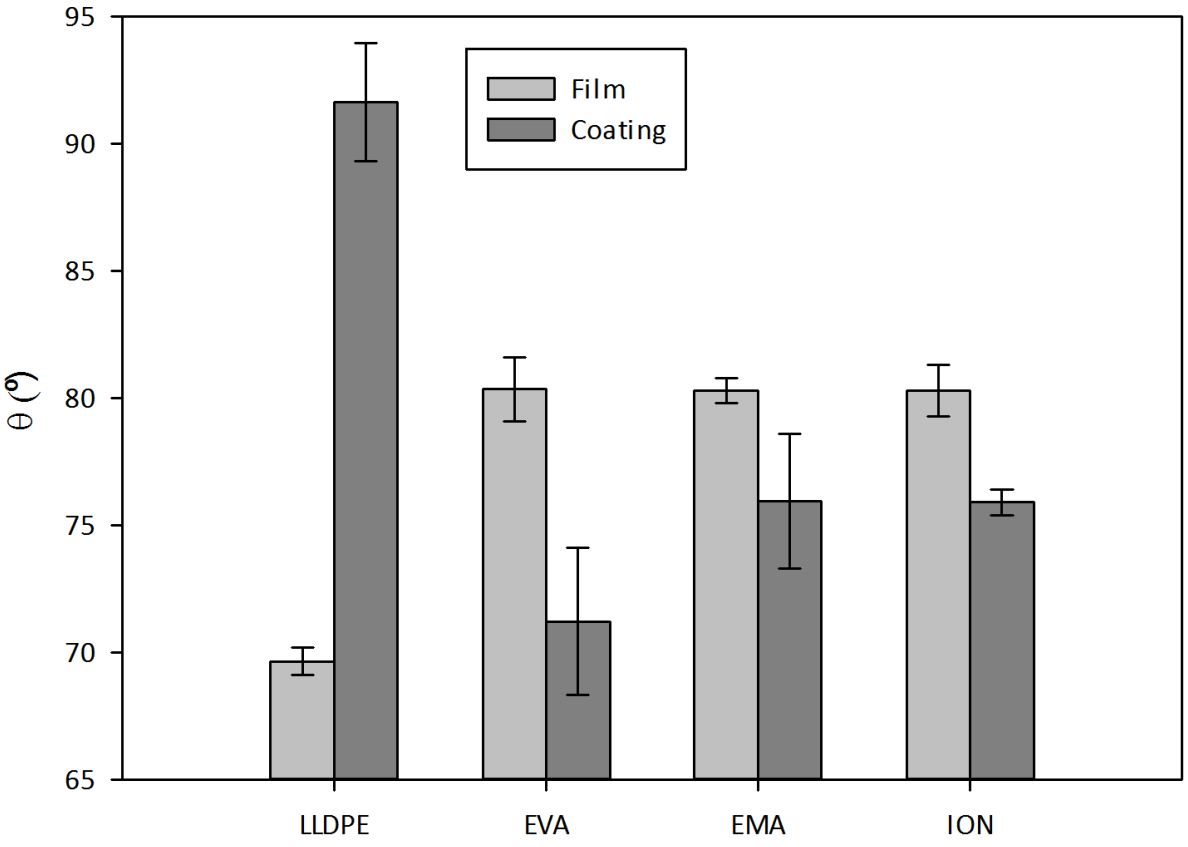

Figure VI.6. Contact angles of water droplets on the surface of the passive latex films and coatings.

3.7. Active properties: carvacrol solubility and effective diffusivity

Just as explained in the introductory section, the main objective of this research work was to enhance the performance of polymeric materials intended to carry antimicrobial agents in active packages, by further controlling their retention capacity for the embedded compounds as well as their rate of release to the package headspace. With this purpose, two new matrix modifications were explored in the carrier material, consisting of the variation of its chemical compatibility with the active substance through the employment of alternative polymers of diverse polarity, together with the variation of its internal structure through their application in the form of latex dispersions. As a result, four new packaging materials exhibiting different combinations of polarity and microstructure were finally developed, and the effects induced in their active properties were also assessed by measuring the corresponding effective diffusivity and solubility coefficients in their polymeric matrix, which yielded the results collected in **Table VI.4**.

Table VI.4. Carvacrol effective diffusivity and solubility coefficients in the active latex films.

Material	$D_c \cdot 10^{16}$ $\left(m^2/s\right)$	$S_c \cdot 10^{-3}$
LLDPE	50 ± 3	6.98 ± 0.07
EVA	7.0 ± 0.5	10.98 ± 0.11
EMA	4.4 ± 0.4	10.5 ± 1.0
ION	5.8 ± 0.3	22.1 ± 1.6

With respect to the carvacrol effective diffusivity, the sequence of values obtained for the tested polymers was in high agreement with their order in terms of microstructural morphology and matrix crystallinity, just as occurred for their permeability coefficient to oxygen and carbon dioxide. As table shows, the diffusion of the active molecule through LLDPE was about 10 times faster than through EMA, owing to its particular combination of high porosity, involving numerous interconnected pores which formed an extensive network of traversing channels, and high content of amorphous phase. EVA, in turn, allowed carvacrol to only diffuse about 60 % faster than EMA, mainly due to its higher crystallinity and lower porosity, consisting of fewer, smaller, and more isolated pores. In contrast, the carvacrol effective diffusivity in ION was very close to that of EMA, which can be explained by the great chemical, thermal, and structural similarities shared by both ionic copolymers. The abovementioned sequence of polymers can also be better observed in the graph of **Figure VI.7**, where the carvacrol

release kinetics has been illustrated by plotting the evolution in time of the experimental normalized concentration of each studied material, together with the corresponding theoretical curves predicted by equation (VI.7).

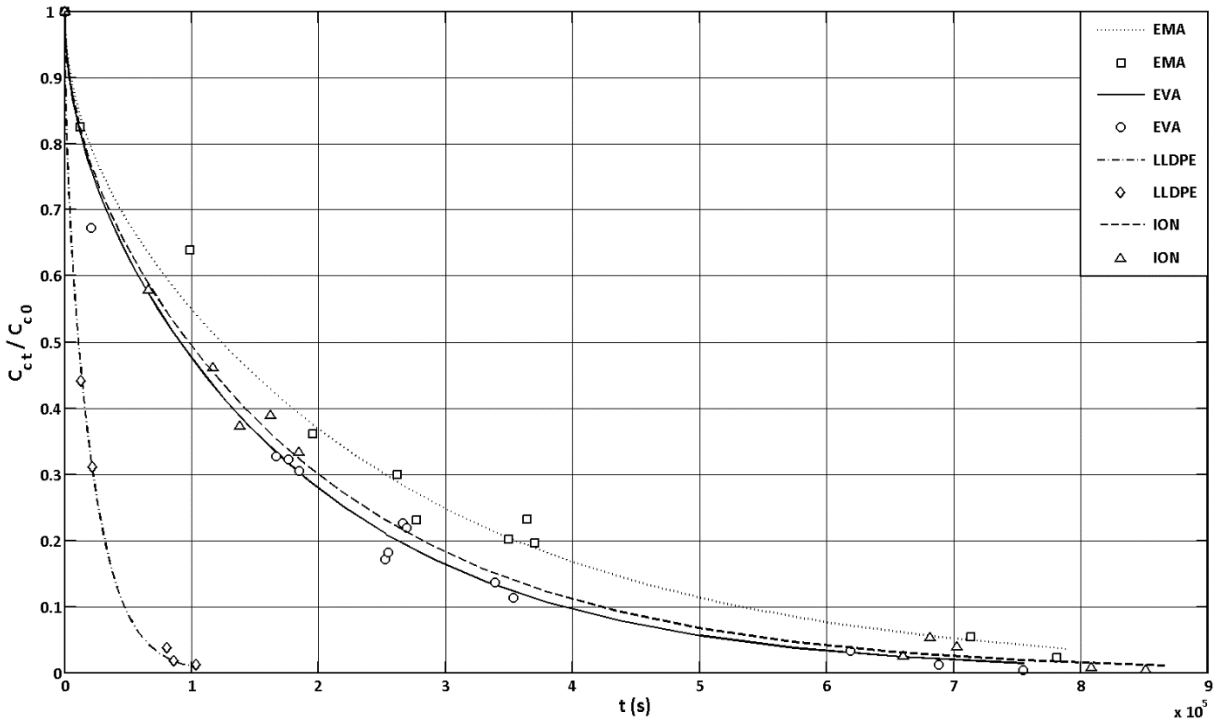

Figure VI.7. Evolution in time of the normalized carvacrol concentration in the polymeric matrix of the active latex films. Symbols correspond to experimental values and curves correspond to the theoretical release kinetics predicted by equation (VI.7).

In general, the results presented here are in agreement with some values reported in the literature for similar cases. Specifically, Nestorson et al. prepared styrene-acrylate latex films with 1-hexanol and limonene at low temperature (50 °C), obtaining diffusivities of about 4 and $7.5 \cdot 10^{-15}$ m^2/s, respectively (Nestorson et al., 2007b), very nearby to that reported here for carvacrol in LLDPE, of $5 \cdot 10^{-15}$ m^2/s. In addition, these results also demonstrate that the latex materials developed in this work generally exhibit better active properties than their melt-processed counterparts. Indeed, conventional packaging polymers, such as polypropylene (PP) or low density polyethylene (LDPE), tend to show invariably high values of the carvacrol diffusion coefficient in their extruded or compression molded forms, of about $3 \cdot 10^{-15}$ m^2/s for both materials (Cerisuelo et al., 2012a; Rupika, 2010), which involve a rapid and unconstrained free release of the active agent to the package headspace, and thus a reduction of its antimicrobial effectiveness (Han, 2013). On the contrary, most of the latex materials studied in this paper yielded quite low values of such parameter, of between 4.4 and $7 \cdot 10^{-16}$ m^2/s, in

spite of their higher porosity, heterogeneity, and thus permeability to water vapor and permanent gases. This particular characteristic is of great interest for the design of active packages intended to preserve highly breathing foods, such as fresh vegetables or ready-to-eat salad products, since it allows a slower release of the active compound, a longer microbial inhibition period and thus a higher antimicrobial effectiveness (Han, 2013), without significantly impairing their gas exchange through the package walls, and thus their cellular respiration. Furthermore, such carvacrol diffusivities can be easily modified through the variation of the manufacturing conditions of the latex films to properly match the growth kinetics of the target microorganisms, and thus to also maximize the antimicrobial effectiveness of the active package.

Regarding the carvacrol solubility, the values found for this parameter could not be clearly related with either the crystallinity of the tested polymers, or the characteristics of their internal structure. Instead, they were in agreement with the polarity of their polymeric matrix, in a direct proportional relation, as can be evidenced from the results displayed in **Table VI.4**. In effect, since the carvacrol molecule is quite amphiphilic, due to its hydrophobic monoterpenic body and to its hydrophilic OH group (Peltzer et al., 2009), it could show more chemical affinity for polymeric matrices exhibiting two different chemistries, and thus dual polarities, such as those of the ionic ethylene copolymers, than for monopolar matrices characteristic of simple homopolymers or of copolymers constituted by monomers of similar chemical nature, such as LLDPE or EVA. Concretely, in the case of the former materials, the development of dipole-dipole interactions, as well as hydrogen bonds, between their carbonyl groups and the hydroxyl group of the carvacrol molecule could probably be responsible for the high values obtained. In any case, all the values finally found for such parameter, ranging between 7 and $22 \cdot 10^3$, are in good agreement with the results reported by Nestorson et al. for the solubility of diverse aroma compounds in styrene-acrylate and styrene-butadiene latex films at room temperature, located between 1 and $20 \cdot 10^3$ (Nestorson et al., 2006, 2007b). However, this author also concludes that the uptake of aroma compounds cannot be related solely with the polarity of the latex films, but also with their internal structure, yielding lower solubilities in the less coalesced materials, which could also contribute to explain the unusual low values found for LLDPE in the present study.

Finally, it is worth to mention the high retention capacity of the latex films for the active agent, which ranged from 74 ± 6 % for LLDPE to 81 ± 7 % for EMA, and thus the percentage efficiency of the incorporation process, was considerably higher than previous reported retain-abilities of similar compounds in extruded polymer matrices. Indeed, owing to the high volatility of some active substances of natural origin and to the high temperatures reached during the melt processing of the

carrier polymers, important losses of agent by evaporation phenomena, and thus of antimicrobial activity, are frequently observed in the processing facilities (Suppakul, 2011). In this sense, and as example, Suppakul et al. reported losses of about 96.5 % for linalool and methyl chavicol in extruded LLDPE films (Suppakul et al., 2002), and of about 66 % in extruded films of LDPE and EVA blends (Suppakul et al., 2008), whereas Efrati et al. reported losses of between 55 and 64 % for thymol in extruded LLDPE films (Efrati et al., 2014), and Kuorwel et al. reported losses of about 70.5, 72 and 74 % for thymol, carvacrol, and linalool, respectively, in starch-based films formed by heat pressing (Kuorwel et al., 2013). All these losses which results in elevated processing costs, in addition, usually translate into large emissions of compound vapors to the internal atmosphere of the processing or packaging facilities, and thus into strong contamination of nearby products, equipment, and potential health issues to operators (López – Rubio et al., 2004). Hence, the active latex materials developed in this work mean a substantial improvement in matters of production costs and safety risks with respect to their melt-processed counterparts.

4. CONCLUSIONS

In this paper, two new matrix modifications performed on polymeric materials intended to carry antimicrobial agents in active packages, consisting in the variation of both their internal structure and their chemical affinity for the active substance, were investigated with the aim of further controlling their retention capacity for the embedded compound as well as its rate of release into the package headspace. As a result, four new polymeric materials based on latex dispersions of ethylene copolymers, concretely, ethylene – octene copolymer (LLDPE), ethylene – vinyl acetate copolymer (EVA), ethylene – methacrylic acid copolymer (EMA), and ethylene – methacrylic acid salt copolymer (ION), were successfully developed, in form of both active films and coatings over polypropylene sheets, and tested for their active and functional properties, in particular, for their microstructural morphology and for their mechanical, thermal, optical, surface, and barrier properties.

The results obtained evidenced that the thermal treatment undergone by the latex films during their drying process was not sufficient so as to completely coalesce their polymeric particles, therefore leading to various internal structures of ranging heterogeneity, porosity, and surface roughness, depending upon the degree of coalescence finally achieved. This varying microstructural morphology was generally correlated with the melting temperature of the studied polymers, and was also responsible for their different performance in most of the active and functional tests carried out. In

this sense, LLDPE and EVA, those polymers presenting a partially coalesced and highly heterogeneous film structure, were generally more permeable, less resistant, more deformable, less transparent, and more wettable than EMA and ION, those exhibiting a completely coalesced internal structure and thus a higher homogeneity, which obviously showed the opposite behavior. With respect to their active counterparts, LLDPE and EVA, they yielded higher values for the carvacrol diffusion coefficient, in high agreement with the results obtained for their permeability to permanent gases, whereas EMA and ION showed higher carvacrol solubilities, owing to their greater affinity to the active molecule as derived from their ionic nature. Finally, it must be also mentioned that the incorporation of carvacrol to the developed latex films did not involve any noticeable deterioration of their polymeric matrices, given that it did not alter their thermal or optical properties in a significant way.

In conclusion, this work presents an innovative and almost unexplored manner of manufacturing antimicrobial films exhibiting controlled and tailor-made active properties. Customized diffusivities, solubilities, and retainabilities of the carrier materials for the active compound, which are structure and polarity-dependent, can be easily modified during their manufacture to fit the requirements imposed by target food packages without significantly altering their other functional properties, especially if applied as active coatings onto functional films made up of conventional polymers. In addition, those modifications in the structure and polarity of the carrier materials are not induced by means of additives or other embedded compounds, but only through the employment of diverse latex dispersions of ethylene copolymers in their manufacture, which also constitutes an advantageous alternative to the conventional melt blending and extrusion methods in matters of safety risks and production costs.

ACKNOWLEDGMENTS

The authors wish to thank the contribution made by Rosa Luz Parada Díaz, the financial support provided by the Spanish Ministry of Science and Innovation (projects AGL2009-08776, AGL2012-39920-C03-01) and the Generalitat Valenciana (J.P.C. fellowship), as well as the English correction performed by Mr. Tim Swillens and the collaboration of ITENE (CSIC associated unit).

REFERENCES

Appendini, P., Hotchkiss, J. H. (2002). Review of antimicrobial food packaging. *Innovative Food Science & Emerging Technologies*, 3 (2), 113 – 126.

ASTM D882 – 12. Standard test method for tensile properties of thin plastic sheeting. ASTM International, West Conshohocken, PA, USA.

Aucejo, S. (2000). *Estudi i caracterització de l'efecte de la humitat en les propietats barrera d'estructures polimèriques hidròfiles. Tesi doctoral*, Universitat de València, València.

Aucejo, S., Marco, C., Gavara, R. (1999). Water effect on the morphology of EVOH copolymers. *Journal of Applied Polymer Science*, 74 (5), 1201 – 1206.

Aucejo, S., Català, R., Gavara, R. (2000). Interactions between water and EVOH food packaging films. *Foods Science and Technology International*, 6 (2), 159 – 164.

Brody, A. L., Strupinsky, E. R., Kline, L. R. (2001). *Active packaging for food applications.* CRC Press LLC, Boca Raton, FL, USA.

Cassie, A. B. D., Baxter, S. (1944). Wettability of porous surfaces. *Transactions of the Faraday Society*, 40, 546 – 551.

Català, R., Gavara, R. (2001). Nuevos envases. De la protección pasiva a la defensa activa de los alimentos envasados. *Arbor*, CLXVIII, 661, 109 – 127.

Cerisuelo, J. P., Muriel – Galet, V., Bermúdez, J. M., Aucejo, S., Català, R., Gavara, R., Hernández – Muñoz, P. (2012a). Mathematical model to describe the release of an antimicrobial agent from an active package constituted by carvacrol in a hydrophilic EVOH coating on a PP film. *Journal of Food Engineering*, 110 (1), 26 – 37.

Cerisuelo, J. P., Alonso, J., Aucejo, S., Gavara, R., Hernández – Muñoz, P. (2012b). Modifications induced by the addition of a nanoclay in the functional and active properties of an EVOH film containing carvacrol for food packaging. *Journal of Membrane Science*, 423 – 424, 247 – 256.

Cerisuelo, J. P., Bermúdez, J. M., Aucejo, S., Català, R., Gavara, R., Hernández – Muñoz, P. (2013). Describing and modeling the release of an antimicrobial agent from an active PP / EVOH / PP package for salmon. *Journal of Food Engineering*, 116 (2), 352 – 361.

Cerisuelo, J. P., Gavara, R., Hernández – Muñoz, P. (2014). Natural antimicrobial – containing EVOH coatings on PP and PET films: Functional and active property characterization. *Packaging Technology and Science*, 27 (11), 901 – 920.

Chen, X., Fischer, S., Men, Y. (2011). Temperature and relative humidity dependency of film formation of polymeric latex dispersions. *Langmuir*, 27 (21), 12807 – 12814.

Collins – Thompson, D., Hwang, C. – A. (2000). *Packaging with antimicrobial properties.* Robinson, R. K. (Ed.) *Encyclopedia of food microbiology*, Academic Press, London, UK.

Cooksey, K. (2001). Antimicrobial food packaging materials. *Additives for Polymers*, (8), 6 – 10.

Crank, J. (1975). *The mathematics of diffusion*, Clarendon Press, London, UK.

Doganci, M. D., Cansoy, C. E., Ucar, I. O., Erbil, H. Y., Mielczarski, E., Mielczarski, J. A. (2012). Combined XPS and contact angle studies of flat and rough ethylene – vinyl acetate copolymer films. *Journal of Applied Polymer Science*, 124 (3), 2100 – 2109.

Efrati, R., Natan, M., Pelah, A., Haberer, A., Banin, E., Dotan, A., Ophir, A. (2014). The combined effect of additives and processing on the thermal stability and controlled release of essential oils in antimicrobial films. *Journal of Applied Polymer Science*, 131 (15), 40564.

España, J. M., García, D., Sánchez, L., López, J., Balart, R. (2012). Modification of surface wettability of sodium ionomer sheets via atmospheric plasma treatment. *Polymer Engineering & Science*, 52 (12), 2573 – 2580.

Gavara, R., Català, R., Hernández – Muñoz, P. (2009). Extending the shelf – life of fresh – cut produce through active packaging. *Stewart Postharvest Review*, 5 (4), 1 – 5.

Han, J. H. (2013). *10 – Antimicrobial packaging systems.* Ebnesajjad, S. (Ed.) *Plastic films in food packaging*, Elsevier William Andrew, USA.

ISO 2528:1995. Sheet materials. Determination of water vapour transmission rate. Gravimetric (dish) method. International Organization for Standardization, Geneva, Switzerland.

Jitianu, A., Amatucci, G., Klein, L. C. (2008). Organic – inorganic sol – gel thick films for humidity barriers. *Journal of Materials Research*, 23 (8), 2084 – 2090.

Joerger, R. D. (2007). Antimicrobial films for food applications: a quantitative analysis of their effectiveness. *Packaging Technology and Science*, 20 (4), 231 – 273.

Keddie, J. L. (1997). Film formation of latex. *Materials Science and Engineering: R: Reports*, 21 (3), 101 – 170.

Kuorwel, K. K., Cran, M. J., Sonneveld, K., Miltz, J., Bigger, S. W. (2013). Migration of antimicrobial agents from starch – based films into a food simulant. *LWT – Food Science and Technology*, 50 (2), 432 – 438.

López – Rubio, A., Almenar, E., Hernández – Muñoz, P., Lagarón, J. M., Catalá, R., Gavara, R. (2004). Overview of active polymer – based packaging technologies for food applications. *Food Reviews International*, 20 (4), 357 – 386.

Marais, S., Nguyen, Q. T., Devallencourt, C., Metayer, M., Nguyen, T. U., Schaetzel, P. (2000). Permeation of water through polar and nonpolar polymers and copolymers: determination of the concentration – dependent diffusion coefficient. *Journal of Polymer Science. Part B: Polymer Physics*, 38 (15), 1998 – 2008.

Massey, L. K. (2003). *Permeability properties of plastics and elastomers. A guide to packaging and barrier materials. 2nd edition.* Plastics Design Library / William Andrew Publishing, NY, USA.

Meiron, T. S., Saguy, I. S. (2007). Wetting properties of food packaging. *Food Research International*, 40 (5), 653 – 659.

Muriel – Galet, V., Cerisuelo, J. P., López – Carballo, G., Lara, M., Gavara, R., Hernández – Muñoz, P. (2012). Development of antimicrobial films for microbiological control of packaged salad. *International Journal of Food Microbiology*, 157 (2), 195 – 201.

Muriel – Galet, V., Cerisuelo, J. P., López – Carballo, G., Aucejo, S., Gavara, R., Hernández – Muñoz, P. (2013). Evaluation of EVOH – coated PP films with oregano essential oil and citral to improve the shelf – life of packaged salad. *Food Control*, 30 (1), 137 – 143.

Nestorson, A., Leufvén, A., Järnström, L. (2006). Interactions between aroma compounds and latex films: partition coefficients and influence on latex film formation. *Packaging Technology and Science*, 19 (2), 71 – 82.

Nestorson, A., Forsgren, G., Leufvén, A., Järnström, L. (2007a). Multivariate analysis of retention and distribution of aroma compounds in barrier dispersion coatings. *Packaging Technology and Science*, 20 (5), 345 – 358.

Nestorson, A., Leufvén, A., Järnström, L. (2007b). Control of aroma permeability in latex coatings by altering the vinyl acid content and the temperature around T_g. *Polymer Testing*, 26 (7), 916 – 926.

Nestorson, A., Neoh, K. G., Kang, E. T., Järnström, L., Leufvén, A. (2008). Enzyme immobilization in latex dispersion coatings for active food packaging. *Packaging Technology and Science*, 21 (4), 193 – 205.

Peltzer, M., Wagner, J., Jiménez, A. (2009). Migration study of carvacrol as a natural antioxidant in high – density polyethylene for active packaging. *Food Additives & Contaminants: Part A: Chemistry, Analysis, Control Exposure and Risk Assessment*, 26 (6), 938 – 946.

Rupika, L. A. (2010). *Development and evaluation of low density polyethylene – based antimicrobial food packaging films containing natural agents.* PhD dissertation, Victoria University, Melbourne, Australia.

Suppakul, P. (2011). *15 – Natural extracts in plastic food packaging.* Lagarón, J. M. (ed.) *Multifunctional and nanoreinforced polymers for food packaging.* Woodhead Publishing Limited, Cambridge, UK.

Suppakul, P., Miltz, J., Sonneveld, K., Bigger, S. W. (2002). Preliminary study of antimicrobial films containing the principal constituents of basil. *Proceedings of the 13th IAPRI World Packaging Conference*, 834 – 839.

Suppakul, P., Miltz, J., Sonneveld, K., Bigger, S. W. (2003). Active packaging technologies with an emphasis on antimicrobial packaging and its applications. *Journal of Food Science*, 68 (2), 408 – 420.

Suppakul, P., Sonneveld, K., Bigger, S. W., Miltz, J. (2008). Efficacy of polyethylene – based antimicrobial films containing principal constituents of basil. *LWT – Food Science and Technology*, 41 (5), 779 – 788.

Suppakul, P., Sonneveld, K., Bigger, S. W., Miltz, J. (2011). Diffusion of linalool and methylchavicol from polyethylene – based antimicrobial packaging films. *LWT – Food Science and Technology*, 44 (9), 1888 – 1893.

Tunç, S., Duman, O. (2011). Preparation of active antimicrobial methyl cellulose / carvacrol / montmorillonite nanocomposite films and investigation of carvacrol release. *LWT – Food Science and Technology*, 44 (2), 465 – 472.

Vermeiren, L., Devlieghere, F., Debevere, J. (2002). Effectiveness of some recent antimicrobial packaging concepts. *Food Additives and Contaminants*, 19 (suppl. 1), 163 – 171.

Wenzel, R. (1936). Resistance of solid surfaces to wetting by water. *Industrial and Engineering Chemistry*, 28 (8), 988 – 994.